Exhumation of ultrahigh-pressure metamorphic oceanic crust from Lago di Cignana, Piemontese zone, Western Alps

Dissertation
zur Erlangung des Grades eines
Doktors der Naturwissenschaften der
Fakultät für Geowissenschaften an
der Ruhr-Universität Bochum

vorgelegt von
Sebastiaan Nicolaas Gerardus Cornelis van der Klauw
aus Gouda (Niederlande)

Bochum 1998

Als Dissertation genehmigt von der Fakultät für
Geowissenschhaften der Ruhr-Universität Bochum

Tag der Disputation: 11. Mai 1999

Promotionskomission:

Vorsitzender:	Prof. Dr. Dr. h.c. L. Dresen
Erster Gutachter:	Prof. Dr. B. Stöckhert
Zweiter Gutachter:	Prof. Dr. W. Schreyer
Fachfremder Gutachter:	Prof. Dr. B. Marschner

Kurzfassung

Zur Entschlüsselung der Exhumierungsgeschichte ehemaliger ozeanischer Kruste im Gebiet des Lago di Cignana, Valtournanche, in den Westalpen wurden die hier vorkommenden ultrahochdruckmetamorphen Coesit-führenden Basalte und Sedimentgesteine untersucht. Unter Einbeziehung von Altersbestimmungen aus der Literatur werden mögliche Exhumierungsprozesse eingegrenzt.

In den metabasischen Gesteinen ist folgende Geschichte aufgezeichnet: Unter ultrahochdruckmetamorphen Bedingungen (ca. 600 °C, 2,7 GPa) wurden die Eklogite durch Versetzungskriechen von Omphacit verformt**.** Scherbänder belegen eine Lokalisierung der Verformung. Für die ersten 50 km der Exhumierung existieren keine Aufzeichnungen, was suggeriert, dass die Verformung außerhalb des Aufschlussbereiches lokalisiert war. Bei Druck- und Temperaturbedingungen von 1,2 GPa und 500 °C wurde ein kleiner Teil der ultrahochdruckmetamorphen Minerale statisch ersetzt. Weitere statische Ersetzungen benötigte Fluid-Infiltration entlang von Zugrissen, die jetzt als Quarzgänge vorliegen. Form und Orientierung der verschiedenen Generationen von Quarzgängen deuten auf niedrige Differentialspannungen hin. Die Ganggenerationen können mit den Stadien des Ersatzes der ultrahochdruckmetamorphen Minerale korreliert werden. So kann eine Änderung in der Orientierung des Spannungsfeldes und eine Zunahme der Differentialspannung bei Temperaturen um 500 °C und Drücken um 0,8 GPa abgeleitet werden.

Bei Druck- und Temperaturbedingungen von unter 0,6 GPa und 450 °C wurden die metasedimentären Gesteine durchgreifend verformt, wobei sämtliche früher angelegten Strukturen überprägt wurden. In den Eklogiten fand die Verformung lokal statt und führte zur Bildung von Grünschiefern. Mikrostrukturen in den Quarzgängen belegen für dieses Ereigniss eine Verformung durch Versetzungskriechen von Quarz. Weitere Verformung war lokalisiert und fand bei Temperaturen um 350 °C und höheren Differentialspannungen statt. Die Dichte von Fluideinschlüssen belegt eine Abkühlung unter 300 °C bei Drücken zwischen 0,2 und 0,4 GPa. Eine spätere spröde Verformung konnte mit dem Druck-Temperatur-Pfad nicht in Bezug gesetzt werden.

Der Vergleich von publizierten radiometrischen Altersbestimmungen mit der Entwicklungsgeschichte zeigt, dass die Exhumierung in zwei Phasen ablief. Die Exhumierung aus einer Tiefe von etwa 90 km bis auf etwa 25 km fand innerhalb weniger Millionen Jahre bei niedrigen Differentialspannungen statt. Das Model eines Subduktionskanals mit einer Zone entgegengesetzt gerichteten Flusses passt zu dieser Entwicklungsgeschichte. Die Exhumierung von etwa 25 km bis auf etwa 10 km Tiefe fand langsamer und bei höheren Differentialspannungen statt. Dieser Teil der Entwicklungsgeschichte wird im Einklang mit Konzepten zur regionalen Geologie wie folgt interpretiert. Auf eine Stapelung von Decken folgte die Exhumierung durch Extension der verdickten Kruste an flach einfallenden Abschiebungen.

Abstract

The metamorphic and structural history of coesite-bearing ultra high pressure metamorphic oceanic crust at Lago di Cignana, Valtournanche, Western Alps, recorded during exhumation has been resolved. The record of metamorphic oceanic crust consisting of metabasalts and metasedimentary rocks combined with geochronologic data from the literature is used to constrain possible exhumation mechanisms.

In the metabasic rocks following history has been recorded: At ultra high pressure metamorphic conditions (ca. 600 °C, 2.7. GPa) the eclogites were deformed by dislocation creep of omphacite. The deformation was progressively localised into shearbands. A gap in the record for the first 50 km of subsequent exhumation suggests that any deformation during this time was localised outside the outcrop area. At pressure and temperature conditions of 1.2 GPa and 550 °C the record shows static replacement of a minor part of the ultra high pressure metamorphic mineral assemblage in small scale closed systems. Further static replacement required fluid infiltration, concentrated along tensile fractures now represented by veins. Shape and orientation of the several vein generations indicate relatively low differential stresses. The vein generations can be correlated with replacement stages of the ultra high pressure metamorphic minerals. In this way, a change in the orientation of the stress field and an increase of the differential stress can be inferred at a temperature of around 500 °C and a pressure of 0.8 GPa.

At pressure and temperature conditions below 0.6 GPa and 450 °C intense deformation wiped out all structures that might have formed earlier in the metasedimentary rocks. Localised ductile deformation transformed part of the eclogites to greenschists. Microstructures of quartz veins deformed during this stage indicate deformation by dislocation creep of quartz. This was followed by a period of low differential stress. Localised deformation occurred at temperatures of ca. 350 °C and at higher differential stresses. The densities of fluid inclusion suggest cooling to below ca. 300 C° at pressures between 0.2 and 0.4 GPa. Later deformation that occurred in the brittle field could not be correlated with the pressure and temperature path.

The combination of this pressure-temperature-deformation-record with published geochronologic data indicates a two stage exhumation. Exhumation from depths of approx. 90 km to depths of approx. 25 km took place in at maximum a few million years and with low differential stresses in the rock. For this exhumation stage the concept of a subduction channel with a zone of reverse flow remains within the constraints posed by the record. Exhumation from depths of approx. 25 km to approx. 10 km was slower and differential stresses were higher. This part of the record is in conjunction with the regional geologic framework interpreted to represent the stacking of thrust slices, followed by extension along low angle normal faults to explain exhumation.

Acknowledgments

This study became possible due to financial support from the German Science Foundation as part of the Research group „High-pressure metamorphism in nature and experiment“ at the Ruhr-University Bochum. This study was initiated by Prof. Dr. Bernard Stöckhert and Dr. Thomas Reinecke, who both through numerous discussions and critical comments focused my thinking about exhumation of high pressure metamorphic rocks. I must also thank numerous other persons at the Institute of Geology and the Institute of Mineralogy and will risk to forget more than a few by mentioning some.

I will start with Mr Gilsing and Mr Eickhoff, who prepared, usually in remarkably short time, a large number of thin sections for me. Next on the list are Dr. Bernhardt and Mr Köhler-Schnettger who kept the electron microprobe in running order. For SEM and CL photographs I have to thank Dr. Rolf Neuser and Dirk Habermann. Dirk and Peter Wagner-Zweigel are also thanked for the good time we had in the Alps. Thanks are also due for Mr Reß and Mrs Aschenbrenner for numerous quickly delivered photographs.

The many computerprograms written by Klaus Röller made data interpretation much easier. I should not forget to thank all the colleagues who introduced me to different analytical methods.

I like to thank my former roommates at the institute Petra Heckhoff, Sybille Schwarz and Andreas Toetz for their introduction to the Ruhr-University. Finally, all colleagues from Bochum and Jena, who spent time for discussions with beer, coffee, etc., are also thanked.

Contents

List of abbreviations

°	degree
°C	degree Celsius
α	angle between surface of the orogenic wedge and the horizontal
β	angle between the basal decollement of the orogenic wedge and the horizontal
Δ-velocity	difference between the velocity of the downgoing plate and the material in the subduction channel close to the plate-channel interface
θ	frontal angle of the orogenic wedge
μ	shear modulus
μm	micrometer, 10^{-6}m
μm^2	square micrometer
ρ	density
σ	sigma, standard deviation
σ_1	largest principal stress
σ_3	smallest principal stress
τ_b	shear stress along the basal decollement of the orogenic wedge
A&E87	Anovitz & Essene, 1987
A94	Ai, 1994
ab	albite
acm	acmite, or acmite component in clinopyroxene
adr	andradite, or andradite component in garnet
ae	aegerine, or aegerine component in clinopyroxene
aggr.	aggregate
alm	almandine, or almandine component in garnet
amp gln	rims of blue-green amphibole around glaucophane
amp grt	discontineous overgrowth of blue-green amphibole on garnet
amp	amphibole
an	anorthite, or anorthite component in plagioclase
ap	apatite
app	appendix
approx.	approximately
arg	aragonite
b	burgers vector
B88	Berman, 1988
biot	green brown mica
BSE	back scattered electron
c	core position
ca.	circa
cal	calcite
cf.	confer
chl	chlorite
CL	cathodoluminescence
cm	centimeter
cm^3	cubic centimeter
cpx	clinopyroxene
cs	coesite
czo	clinozoisite

D	deformation
d	grain size
D_{1e}	first deformation stage in eclogites
D_{2g}	second deformation stage in the greenschists
D_{2s}	second deformation stage in the metasedimentary rocks
D_{3e}	third deformation stage in the eclogites
D_{3g}	third deformation stage in the greenschists
D_{3s}	third deformation stage in the metasedimentary rocks
D_{4e}	fourth deformation stage in the eclogites
D_{4e1}	number one shearzone of the fourth deformation stage in the eclogites
D_{4e2}	number two shearzone of the fourth deformation stage in the eclogites
D_{4g}	fourth deformation stage in the greenschists
D_{4s}	fourth deformation stage in the metasedimentary rocks
D_{5g}	fifth deformation stage in the greenschists
D_{5s}	fifth deformation stage in the metasedimentary rocks
DEDM	Digital Element Distribution Map
diop	diopide, or diopside component in clinopyroxene
dol	dolomite
Dr.	Doctor
E	east
$_{e}$	in eclogite
E&G79	Ellis & Green, 1979
e.c.c.	extensional crenulation cleavage
e.g.	example given
ENE	east-north-east
eq.	equivalent
exhum.	exhumation
Fig.	figure
g	gravity
gln	glaucophane
GPa	giga Pascal (10^9 Pascal, 10 kilobar)
gr	gramm
grs	grossular, or grossular component in garnet
grt	garnet
h	thickness of the orogenic wedge
H&B94	Holland & Blundy, 1994
H79	Holland, 1979
hed	hedenbergite, or hedenbergite component in clinopyroxene
HP	high pressure
HPM	high pressure metamorphic
ilm	ilmenite
J&P71	Johannes & Puhan, 1971
jd	jadeite, or jadeite component in clinopyroxene
K	Kelvin
K88	Krogh, 1988
km	kilometer
K_n	constant in the recrystallised grain size paleopiezometer
kV	kilovolt

L_{1e}	stretching lineation of the first deformation stage in eclogites
L_{2s}	stretching lineation of the second deformation stage in the metasedimentary rocks
l-ab	low albite
m	meter
m.y.	million years
m^2	square meter
Ma	million years before present
max.	maximum
mc	microcline
min.	minimum
mm	millimeter, 10^{-3} m
MORB	mid ocean ridge basalt
MPa	mega Pascal, (10^6 Pascal, 0,1 kbar)
n	constant in the recrystallised grain size paleopiezometer
N	north
NE	north-east
NNE	north-north-east
NNW	north-north-west
NW	north-west
omp	omphacite, or omphacite component in clinopyroxene
P	pressure
P&N89	Pattison & Newton, 1989
P85	Powell, 1985
Pa	Pascal
P_f	pore fluid pressure
pfu	per formula unit
pg	paragonite
phe	phengite
pl	plagioclase
prp	pyrope, or pyrope component in garnet
PT	pressure and temperature
qtz	quartz
quad	quadrilateral pyroxene
r	rim position
rt	rutile
$_s$	in metasedimentary rock
s	second
S	south
s^{-1}	per second
S_{1e}	foliation of the first deformation stage in eclogites
S_{1g}	foliation of the first deformation stage in the greenschists
S_{2e}	foliation of the second deformation stage in eclogites
S_{2g}	foliation of the second deformation stage in the greenschists
S_{2s}	foliation of the second deformation stage in the metasedimentary rocks
S_{3e}	foliation of the third deformation stage in the eclogites
S_{3s}	foliation of the third deformation stage in the metasedimentary rocks
SE	south-east
SEM	scanning electron microscope

sps	spessartine, or spessartine component in garnet
SSW	south-south-west
SW	south-west
sympl	symplectite
T	temperature
t	time
Te	tensile strength
T_{eut}	eutectic temperature
T_{hom}	homogenisation temperature
tlc	talc
T_m	melting temperature
tot	total
ttn	titanite
UHP	ultra high pressure
UHPM	ultra high pressure metamorphic
V	volume
vol.%	volume percent
W	west
WNW	west-north-west
WSW	west-south-west
wt.%	weight percent
X	maximum principal strain axis
Y	intermediate principal strain axis
Z	minimal principal strain axis
zoi	zoisite
Z-S	Zermatt Saas

List of Tables

Appendix B

Appendix C

List of Photographs

Table of figures

Appendix A

1 Introduction

Ultrahigh pressure metamorphic (UHPM) rocks have been described from a number of localities (for reviews, see Schreyer, 1995; Harley & Carswell, 1995; Coleman & Wang, 1995). These crustal rocks underwent metamorphism at depths well above the thickness of present-day crust, at temperature-pressure ratios below 50 °C/100 MPa. The processes, during which such high pressures at relatively low temperatures are produced, are generally accepted and a subduction mechanism with thickening through thrusting in the overlying crust is usually postulated (e.g., Chopin, 1984; Schreyer, 1995). The processes that returned UHPM rocks to the surface are still under discussion, however (e.g., Platt, 1993; Harley & Carswell, 1995). Understanding of these processes constrains kinematics and dynamics of convergent plate boundaries and several kinematic exhumation models have been proposed (e.g., Platt, 1993; Chemenda et al., 1995; Davies & von Blanckenburg, 1995; Thomson et al., 1998). To distinguish between these models, accurate information on P(ressure), T(emperature), and structural evolution as well as unambigeous geochronological data for the UHPM rocks must be available. For most UHPM rocks the outlines of the PT-paths are principally known and continually improved (see Schreyer, 1995; Harley & Carswell, 1995), although the reconstruction of complete PT-paths is hampered by the discontinuous record preserved in the rocks and the common failure of rocks at attaining even small scale heterogeneous equilibrium during exhumation. Data for the structural evolution of most UHPM terrains are scarce (see Michard et al., 1995), because UHPM deformation fabrics and structures formed on the earlier part of the exhumation path are seldom preserved, owing to intense distributed deformation under greenschist facies conditions. The structural record acquired on the way to the surface provides vital information about the exhumation process, however, and every proposed exhumation scenario should be based on an analysis of this record (e.g., Wheeler, 1991; Henry et al., 1993; Michard et al., 1993 in Dora Maira and Andersen et al., 1991, in south Norway). Geochronological data from several localities, indicate that UHPM at depths of 100 km or more and a return to shallower crustal levels may take place in a few million years (e.g., Tilton et al., 1991; Gebauer et al., 1997 in Dora Maira; Barnicoat et al., 1995; Amato et al., 1999, in Zermatt Saas; Ames et al., 1996; Hacker & Wang, 1995 in Dabie Shan; Shatsky et al., 1999 in Kazachstan).

This study concentrates on the exhumation of a small occurrence of UHPM oceanic crust at Lago di Cignana, Valtournanche, Western Alps (Reinecke, 1991; Reinecke et al., 1994). Part of this study, which deals with the petrologic, structural, and microstructural record of the metabasic rocks at Lago di Cignana, was published in van der Klauw et al. (1997). The record of the metabasic rocks will be correlated with the PT-record (Reinecke, 1995; 1998), and the (micro-)structural record of the metasedimentary rocks and discussed in terms of state of stress, and mechanical behaviour during successive stages of exhumation. These data provide the boundary conditions for a tentative exhumation model for the UHPM rocks of Lago di Cignana.

2 Regional geology

The Alps are traditionally subdivided in four domains (Fig. 1A); the Helvetic and Penninic domains both with mainly north vergent structures, derived from the European continent, respectively, the European continent and oceanic crust; and the Austroalpine and Southalpine domains both derived from the southern continent and with mainly north, respectively, south vergent structures (e.g., Heim, 1922; Debelmas & Lemoine, 1970). The arrangement of these domains, with the Austroalpine domain thrust on the Penninic domain and both thrust on the Helvetic domain, indicate that convergence of the European plate and the Adriatic plate and SE directed subduction of intervening oceanic crust, followed by continent-continent collision during the Cretaceous and Tertiary, formed the Alps (e.g., Coward & Dietrich, 1989; Dewey et al., 1989; Polino et al., 1990).

Lago di Cignana is situated in the northern part of the Western Alps (Fig. 1B). The UHPM rocks are part of the Penninic, Piemontese zone - a remnant of the former ocean. The Piemontese zone is divided in the Combin zone, consisting mainly of calcschists (e.g., Deville et al., 1992) and in the Zermatt Saas zone - a dismembered ophiolitic sequence - that is built up by peridotites, metabasalts and subordinate oceanic metasedimentary rocks (e.g., Bearth, 1952; Barnicoat & Fry, 1986). The UHPM rocks are part of the Zermatt Saas zone.

The mineral assemblages in the rocks of the Zermatt Saas zone reflect an eclogite facies metamorphic imprint of Early Tertiary age (52 ± 18 Ma, Bowtell et al., 1994; 40.6 ± 2.6 Ma, Amato et al., 1999; 44.1 ± 0.7 Ma, Rubatto et al., 1998). The PT-conditions for this eclogite facies metamorphism have been estimated by several authors (Table 1). The large differences in the estimated PT-conditions may reflect real differences in the metamorphic evolution of different parts of the Zermatt Saas zone, but the discrepancies are for the earlier studies (Ernst & Dal Piaz, 1978; Oberhänsli, 1980) certainly also due to the lack of well calibrated geothermobarometers at that time. The eclogite facies mineral assemblages were partly reequilibrated during cooling and decompression (e.g., Meyer, 1983; Barnicoat & Fry, 1989). Locally an intense greenschist facies overprint developed (Ernst & Dal Piaz, 1978; Barnicoat, 1988b). The K-Ar, Ar-Ar, and Rb-Sr ages of white micas range from 45 to 30 Ma (Hunziker, 1974; Barnicoat et al., 1995). The oldest ages are interpreted as

Table 1

Pressure and temperature estimates of different authors for the high pressure metamorphism and later reequilibration (exhum. P1; T1, exhum. P2; T2) of rocks from the Zermatt Saas zone.

UHPM Minerale	Authors	P(GPa); T(°C)	exhum. P1; T1	exhum. P2; T2
Breuil-St. Jacques	Ernst & Dal Piaz, 1978	0.8-1.2; 420-530		0.1-0.5; 350-450
Zermatt	Oberhänsli, 1980	1.4; 600		
Zermatt	Barnicoat & Fry, 1986; 1989; Barnicoat, 1988b	1.8-2.0; 550-600	1.2-1.6; 500-550	0.1-0.6; 400-500
Saas-Fee	Bucher & Frey, 1994; Meyer, 1983	2.5; 650	1.6; 500	0.4-0.5; 400-450
Lago di Cignana	Reinecke, 1991	2.6-2.8; 590-630	1.3-1.5; 490-510	0.4-0.6; 360-430

cooling ages below the closure temperature of white mica (ca. 350 °C, Hodges, 1991). The younger ages are interpreted as reset during later localised deformation (Barnicoat et al., 1995).

The rock units in the northern part of the Western Alps can be subdivided in units that experienced an eclogite facies metamorphism (Zermatt Saas, Monte Rosa and parts of the Sesia zone) and units

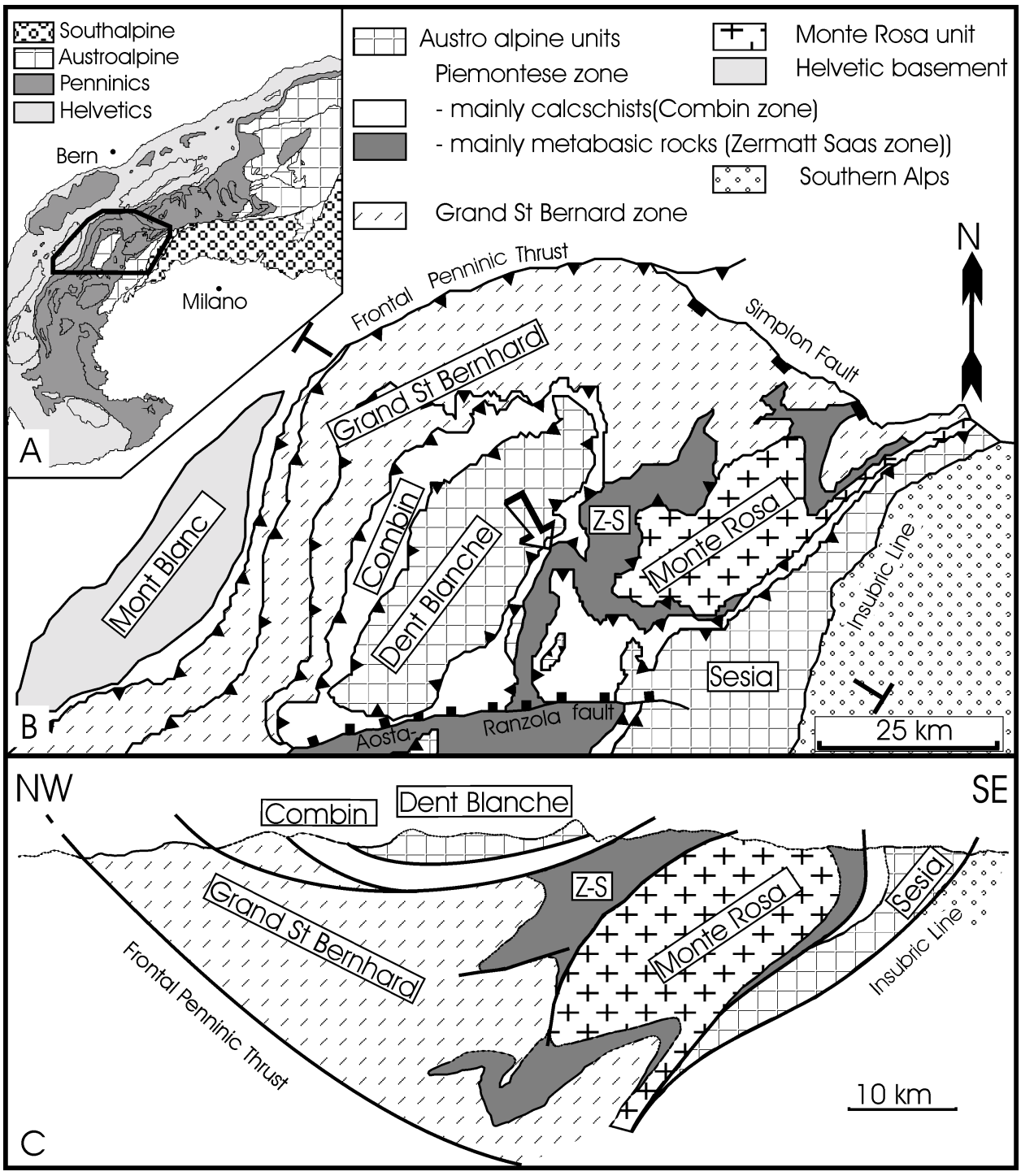

Figure 1

A Simplified geological map of the Central and Western Alps.

B Simpflied geological map of the northern part of the Western Alps (modified after Ballèvre & Merle, 1993). The arrow shows the approximate position of Lago di Cignana. Z-S = Zermatt-Saas.

C Simplified cross section through Figure 1B (modified after Ballèvre & Merle, 1993).

that experienced maximum pressures (< 1.4 GPa) of blueschist facies metamorphism (Grand Saint Bernhard, Dent Blanche and Combin), during the alpine orogeny. In these last units, an early blueschist facies metamorphic imprint (e.g., Ayrton et al., 1982; Desmons, 1992) is almost completely obliterated by a greenschist facies overprint, associated with an usually penetrative ductile deformation (e.g., Wüst & Baehni, 1986; Dal Piaz & Ernst, 1978). Only for the Grand Saint Bernhard unit an age estimate for the blueschist facies metamorphism is known (< 54 Ma, Monié, 1990). The later greenschist facies overprint is estimated for all units to have occured between 45 - 35 Ma (Hunziker, 1986; Hunziker et al., 1989). Structures at the contacts between the blueschist units, indicate juxtaposition of these units by NW-ward directed thrusting under greenschist facies conditions (Mazurek, 1986; Wüst & Baehni, 1986; Ellis et al., 1989). The units with eclogite facies metamorphism experienced different maximum pressure and temperature conditions (e.g., Table 1; Chopin & Monié, 1984) at different times. This shows that juxtaposition of these units did not occur at high pressure conditions, as also suggested by the greenschist facies shearzones at the contacts between the units (Ellis et al., 1989). A greenschist facies metamorphic overprint, estimated to have occurred between 40 and 35 Ma (Chopin & Monié, 1984; Barnicoat et al., 1995; Inger et al., 1996), is locally developed, often accompanied by penetrative ductile deformation (e.g., Williams & Compagnoni, 1983; Frey et al., 1976; van der Klauw et al., 1997).

The present day configuration, with the blueschist to greenschist facies metamorphic rocks on top of the eclogite facies metamorphic rocks (Fig. 1C), developed between 36 and 30 Ma (Barnicoat et al., 1995; Freeman et al., 1997), by SE directed thrusting of the blueschist facies rocks over the eclogite facies metamorphic units, under lower greenschist facies conditions (Wheeler & Butler,

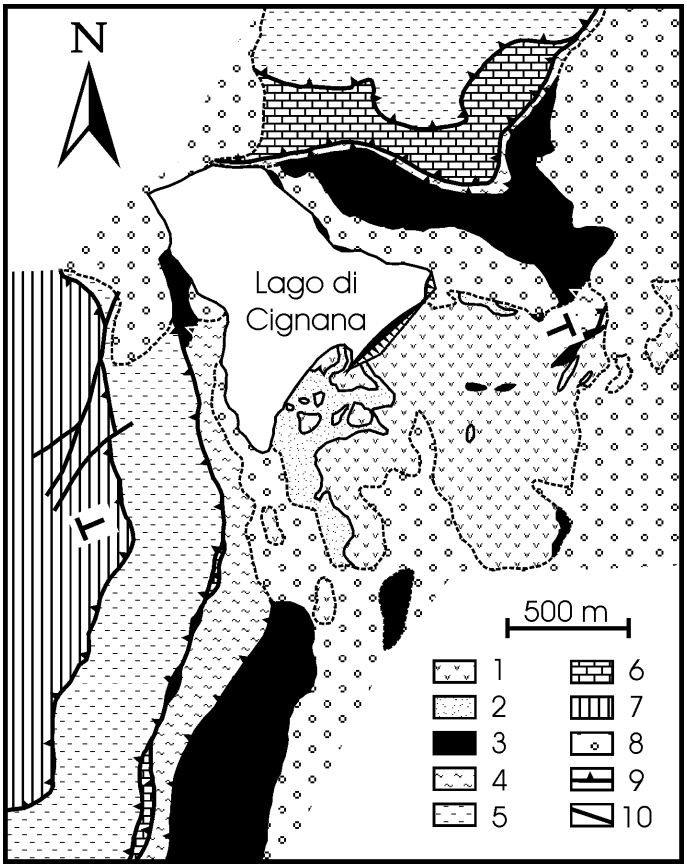

Figure 2

Simplified geological map of the vicinity of Lago di Cignana, based on 1.10000 mapping by Habermann (1992) and Wagner-Zweigel (1993).

Key: (1) eclogites and derived greenschists (Zermatt Saas zone), (2) UHPM metasedimentary rocks (Zermatt Saas zone), (3) serpen-tinised ultramafic rocks, (4) greenschists with minor calcschists (Combin zone), (5) calc- schists with minor greenschists and marbles (Combin zone), (6) dolomite-calcite marbles (exotic decollement sheet, cf. Dal Piaz, 1988), (7) Austroalpine (undifferentiated), (8) scree, moraine deposits and wetlands, (9) tectonic contact, (10) normal faults.

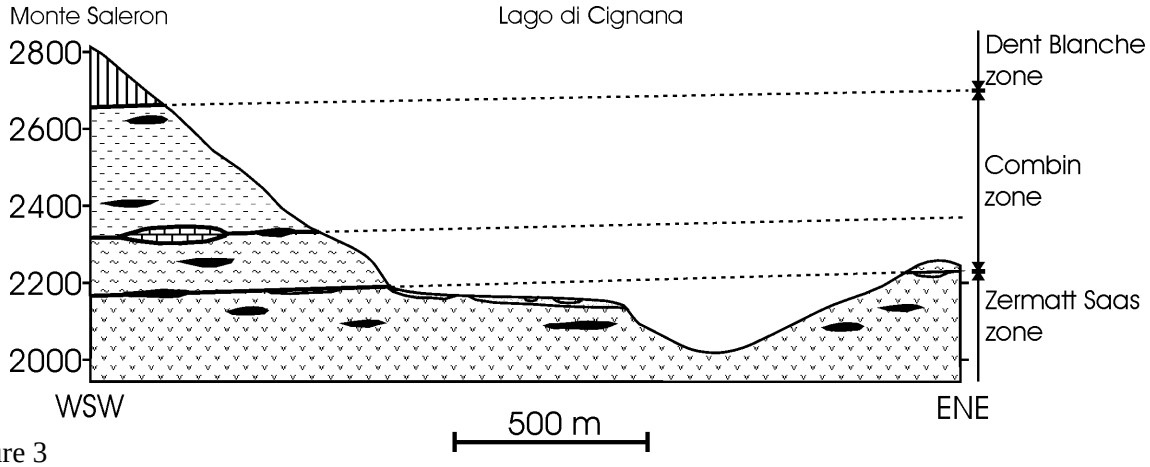

Figure 3

Simplified geological cross section through figure 2, showing the structure of the studied area. Key as in figure 2.

1993). The zircon fission track ages of approx. 33 Ma observed in all rock units in this part of the Alps indicate that at this time all units exposed at the surface today were at temperatures of ca. 225 °C (Hurford et al., 1991). The different apatite fission track ages within some units, suggest differential uplift and cooling histories for parts of these units between the Oligocene and the present (Hurford et al., 1991).

2.1 The studied area

The studied area is situated south of Lago di Cignana, Valtournanche. The rocks in this area belong to the Zermatt Saas zone, the Combin Zone, and the Dent Blanche zone. A simplified geologic map of the area (Habermann, 1992; Wagner-Zweigel, 1993) and a simplified section are shown in figures 2 and 3. The lithological divisions are comparable to those proposed by other authors in this area (Dal Piaz, 1988; Marthaler & Stampfli, 1989; Vannay & Allemann, 1990).

In the area, the lowermost rocks are serpentinites of the Zermatt Saas zone. The serpentinites are overlain by eclogites with a strong greenschist facies metamorphic overprint, usually, without preservation of the eclogite facies mineral assemblage (Habermann, 1992). The top of these overprinted eclogites consists of well preserved coesite bearing eclogites and metasedimentary rocks of the Zermatt Saas zone. Most of the work was done on these eclogites, which were extremely well exposed at the southern shore of the lake.

The rocks of the Zermatt Saas zone are overlain by the rocks of the Combin zone that can be divided in three parts. The lowermost part of the Combin zone consists of greenschists with minor amounts of calcschists. The upper part of the Combin zone is dominated by calcschists with only minor amounts of greenschists and dolomitic marbles. Between these parts, locally dolomitic and calcitic marbles occur that are considered a separate unit by Dal Piaz (1988). The uppermost rocks in the studied area are the gneisses and schists of the Dent Blanche zone.

The occurence of serpentinites as small lenses within all units and as large lenses at the contacts between the units, suggests that not only the contacts between the units are tectonic, but that also within the units tectonic contacts occur.

3 The record in the metabasic rocks

In this chapter the record preserved in the metabasic rocks will be presented in two parts, first the petrological part and second the structural part. The record preserved in the veins of the metabasic rocks will be presented in chapter 5.

3.1 Petrology of the metabasic rocks - eclogites and greenschists

The metabasic rocks are presumed to be derived from basalts of former oceanic crust. This interpretation is supported by bulk rock analyses of seven samples with different degrees of lower PT-replacement (Table C2 in app. C) that invariably indicate MORB affinity, and by relic pillow structures. This was already established for other localities in the Zermatt Saas zone (Dal Piaz et al., 1981; Beccaluva et al., 1984; Pfeifer et al., 1989 and Bearth, 1959; Oberhänsli, 1982).

Two principal types of metabasic rocks can be distinguished. The first type comprises eclogites and transformed eclogites, where the original eclogitic microstructure is still discernable owing to pseudomorphic replacement. This holds true, even where the replacement to a lower PT-paragenesis has gone to completion. The second type is represented by schistose metabasic rocks devoid of high-pressure relics and is subsequently called greenschist. Greenschists constitute the minor portion (estimated < 5 vol.%) of the metabasic rock in the studied area. They occur frequently at the contacts between metasedimentary rocks and eclogite bodies and as m-sized lenses in both eclogitic and metasedimentary rocks.

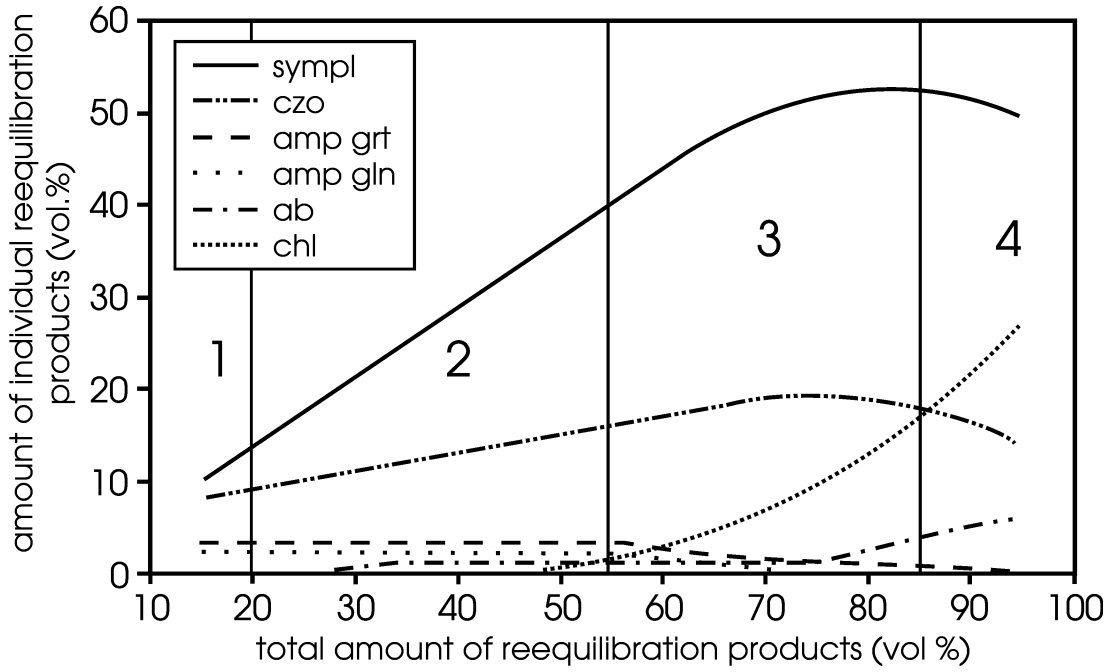

Figure 4

The amount of individual reequilibration products plotted against the total amount of reequilibration products in group 1 to 4 eclogites. Minor amounts (< 2 vol.%) of titanite (± ilmenite) rims around rutile in all eclogites are omitted. Key: sympl = symplectite of blue-green amphibole and albite, czo = clinozoisite, amp grt = discontineous overgrowth of blue-green amphibole on garnet, amp gln = rims of blue-green amphibole around glaucophane, chl = chlorite, and ab = albite.

Table 2

The UHPM mineral assemblage and the lower PT-replacement products formed at their expense in the different eclogite groups. sympl. = symplectite, aggr. = aggregate.

UHPM minerals	new minerals in group 1 eclogites	new minerals in group 2 eclogites	new minerals in group 3 eclogites	new minerals in group 4 eclogites
omphacite	sympl. of magnesio-/ actinolitic-horn-blende, albite	sympl. of actinolitic-hornblende, albite	sympl. of actinolitic-hornblende/actinolite, albite	
garnet	ferroan-pargasite to edenitic-hornblende		chlorite, biotite, epidote, albite aggr.	chlorite, biotite, epidote, albite aggr.
glaucophane	barroisite	sympl. of actinolitic-hornblende, albite	sympl. of actinolitic-hornblende/actinolite, albite	
zoisite clinozoisite	clinozoisite	clinozoisite		
paragonite	clinozoisite	clinozoisite	chlorite	albite
rutile	ilmenite/titanite	titanite	titanite	
apatite				
phengite I/II	phengite II			
dolomite	calcite	calcite		
coesite	quartz			
		sympl.	albite, actinolite	albite, actinolite chlorite

The eclogites can be classified in 5 groups, based on the degree of their lower PT-replacement (Fig. 4 and Table 2):

Group 0 eclogites represent an idealised eclogite with perfectly preserved UHPM paragenesis. In fact, such eclogites lacking any lower PT-replacement have not been found.

Group 1 eclogites appear macroscopically fresh, but a moderate amount (estimated 15-20 vol.%) of replacement products is visible under the microscope.

Group 2 eclogites appear macroscopically darker green, because of partial replacement of omphacite by a symplectite of amphibole and albite. Garnet is macroscopically still fresh, however. Under the microscope between 20 and 55 vol.% of lower PT-replacement products are visible.

In group 3 eclogites the replacement of garnet through an aggregate of biotite, chlorite, and epidote is macroscopically visible. Between 55 and 85 vol.% of replacement products are visible under the microscope.

In group 4 eclogites the replacement reactions have gone to completion and the amount of replacement products reaches up to 100 vol.%.

For all eclogite groups, appearence and compositions of its minerals will be presented, followed by a discussion of potential equilibrium paragenesis and PT-estimates. The minerals of the green-schists will be treated together with group 4 eclogites.

3.1.1 Group 0 eclogites

In group 0 eclogites, clinopyroxene (omphacite), garnet, blue amphibole (glaucophane), clinozoisite I, zoisite, white mica, rutile, coesite, and apatite occur in all samples, whereas dolomite occurs only in a few samples. Because no group 0 eclogites have been found, the mineral compositions given are of minerals of group 1 eclogites, that are not in contact with lower PT-replacement products.

3.1.1.1 Mineral compositions

omphacite (omp)

The amount of omphacite ranges from 50 to 80 vol.% of the rocks. The omp grains are anhedral; their shape preferred orientation partly defines the foliation. The grain size ranges from ca. 40 μm for matrix grains, to ca. 400 μm for grains in strain shadows and along shearbands. The matrix omp often shows a patchy extinction due to compositional inhomogenities. Grain boundaries between omp grains are serrated. Some of the larger grains have slightly blueish anomalous interference colours.

The omp composition in all samples (Fig. 5, Table C3 in app. C) and within a single sample varies between $Na_{(0.4\text{-}0.6)}Ca_{(0.4\text{-}0.6)}Mg_{(0.28\text{-}0.48)}Fe^{2+}_{(0.03\text{-}0.14)}Al_{(0.36\text{-}0.56)}Fe^{3+}_{(0\text{-}0.14)}Si_2O_6$. Mean composition for all samples is close to $Na_{0.53}Ca_{0.47}Mg_{0.38}Fe^{2+}_{0.09}Al_{0.47}Fe^{3+}_{0.06}Si_2O_6$. The composition appears to be unrelated to the kind of adjacent mineral. Individual grains are homogeneous or consists of an irregular patchwork of domains with slightly different composition, but generally, do not show a regular zoning pattern. The boundaries between these domains are sharp. Commonly, omp inclusions in garnet have similar compositions as matrix omp. Only in samples Bk 39 and Cig 91/40, the

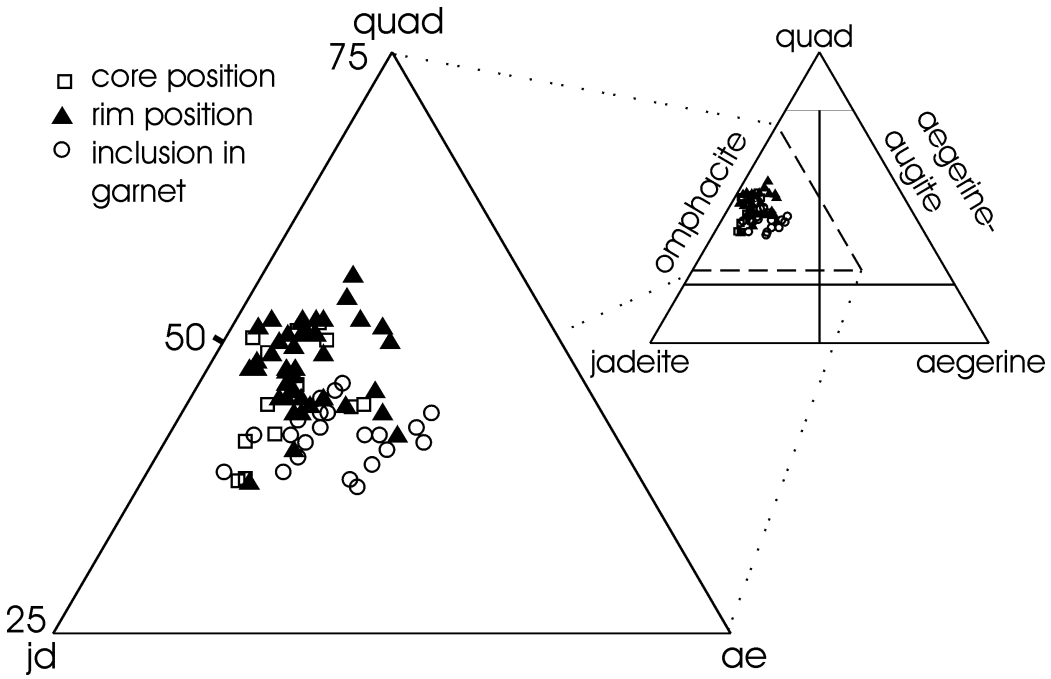

Figure 5

Compositions of clinopyroxene in eclogites from Lago di Cignana. Only analyses from sample Bk 39 are shown; the core and rim analyses of Bk 39 are representative for omphacites from all samples studied. Key: ae = aegerine, jd = jadeite, quad = quadrilateral pyroxene.

aegerine content in inclusions is slightly larger and the jadeite content in the inclusions is slightly smaller than in the matrix (Fig. 5).

garnet (grt)

Garnet occurs as euhedral porphyroblasts of up to 1 cm in diameter. The amount of grt ranges from 10 to 20 vol.% of the rock. The cores of garnets contain abundant inclusions of omp, quartz single crystals, and composite clinozoisite/epidote; paragonite; and titanite inclusions - pseudomorphs after lawsonite (Bearth, 1959). In the rim of grt inclusions occur less frequently and are smaller. They consist of omp, rutile and rarely very small (< 10 μm) quartz pseudomorphs after coesite.

Garnets are almandine rich (50-65 mol%), with appreciable amounts of pyrope (10-35 mol%) and grossular components (10-35 mol%) and only minor (< 5 mol%) amounts of spessartine and andradite components (Table C4 in app. C). Between the samples, compositions differ mainly in the amounts of pyrope and grossular component (Fig. 6). The compositional zoning pattern of garnets from different samples is similar (Fig. 6). The core of grt is relatively grossular rich. Towards the rim the grossular component decreases and the pyrope and almandine components increase. The compositional trend changes abruptly in the outer rim, with a relative decrease in almandine component and an increase in pyrope component. The highest pyrope content occurs in the grt rim. This change in composition trend, coincides with the change from inclusion rich core to inclusion poor rim (Photo 3, Fig. 12).

glaucophane (gln)

The amount of gln ranges between 5 to 15 vol.%. The grains are subhedral; their shape preferred orientation partly defines the foliation and stretching lineation. Grain sizes range from 50 μm in

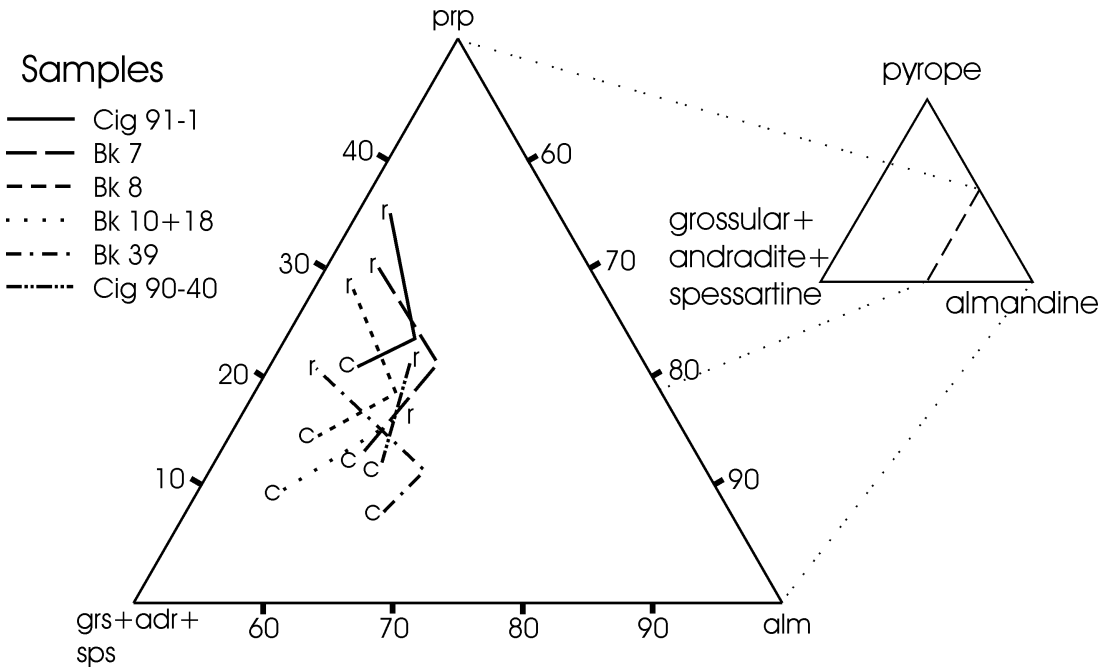

Figure 6

Compositional trends of zoned garnets in different eclogitic samples from Lago di Cignana. Key: c = core position, r = rim position, adr = andradite, alm = almandine, grs = grossular, prp = pyrope, sps =spessartine.

sections perpendicular to c-axis to 500 μm parallel to c-axis. The composition (Table C5 in app. C) differs slightly between the samples, varying between
$(Na_{0\text{-}0.1},K_{0\text{-}0.1})(Na_{1.55\text{-}1.90},Ca_{0.10\text{-}0.45})(Fe^{2+}_{0.55\text{-}1.00},Mg_{2.00\text{-}2.45},Al_{1.60\text{-}1.85},Fe^{3+}_{0.10\text{-}0.30})2(Si_{7.70\text{-}7.95},Al_{0.05\text{-}0.30})O_{22}(OH)_2$.
Within a sample, the compositional variation is small and gln grains have a homogeneous composition.

clinozoisite I (czoI)

Clinozoisite I amounts to < 10 vol.% of the rock. The grains size is up to 200 μm, the grains are subhedral and their shape preferred orientation partly defines foliation and stretching lineation. The composition lies between $Ca_2Fe^{3+}_{(0.26\text{-}0.50)}Al_{(0.50\text{-}0.74)}Al_2Si_3O_8(OH)$ with the smallest Al_2Fe^{3+} epidote component in the cores of larger grains, increasing towards the rim (Table 6C in app. C). Differences in Al_2Fe^{3+} epidote component in relation to the adjacent mineral are not observed. Between samples, the range in Al_2Fe^{3+}epidote component differs slightly (Table C6 in app. C).

zoisite (zoi)

The amount of zoi is in the order of 3 vol.% of the rock. It is present as large (up to 3 mm) anhedral grains with a patchy extinction and as smaller (< 50 μm) subhedral grains with a homogeneous extinction. The shape preferred orientation of the zoi aggregates partly defines foliation and stretching lineation. Large grains have numerous randomly orientated white mica inclusions. Composition varies between $Ca_2Fe^{3+}_{(0.10\text{-}0.15)}Al_{(0.85\text{-}0.90)}Al_2Si_3O_8(OH)$ (Table C7 in app. C), with the higher Al_2Fe^{3+} epidote component in contact with czoI.

white mica

The white micas in group 0 eclogites are paragonite (pg) and phengite (phe) and usually cannot be distinguished optically. The presence of pg or phe was established with powder X-ray diffraction. In most samples pg is the only white mica, in some samples powder X-ray diffraction showed the presence of both pg and phe, however. Further investigation with the electron microprobe, indicated that in these cases the white mica generally consists of pg with phe intergrowths; the width of the phe layers is below the beam size of the microprobe (about 5 μm). Only a few samples have phe as the only white mica.

paragonite (pg)

The amount of pg ranges from 4 to 8 vol.% of the rock. Pg grains are subhedral and their shape preferred orientation partly defines the foliation. Grain size is about 40 μm. The composition varies slightly around $(Na_{1.9},K_{0.1})Al_4[Si_6Al_2O_{20}](OH)_4$. Pg in phe bearing samples can have up to 15 mol% of phe solid solution (Table C8 in app. C).

phengite (phe)

The amount of phe can amount to ca. 10 vol.% of samples, where it is only white mica. Phe is present as small (< 40 μm) grains in the matrix and as large (about 400 μm) porphyroblasts. The grains of both varieties are subhedral and their shape preferred orientation partly defines the foliation. The large phe have compositions (Fig.7, Table C9 in app. C) varying between

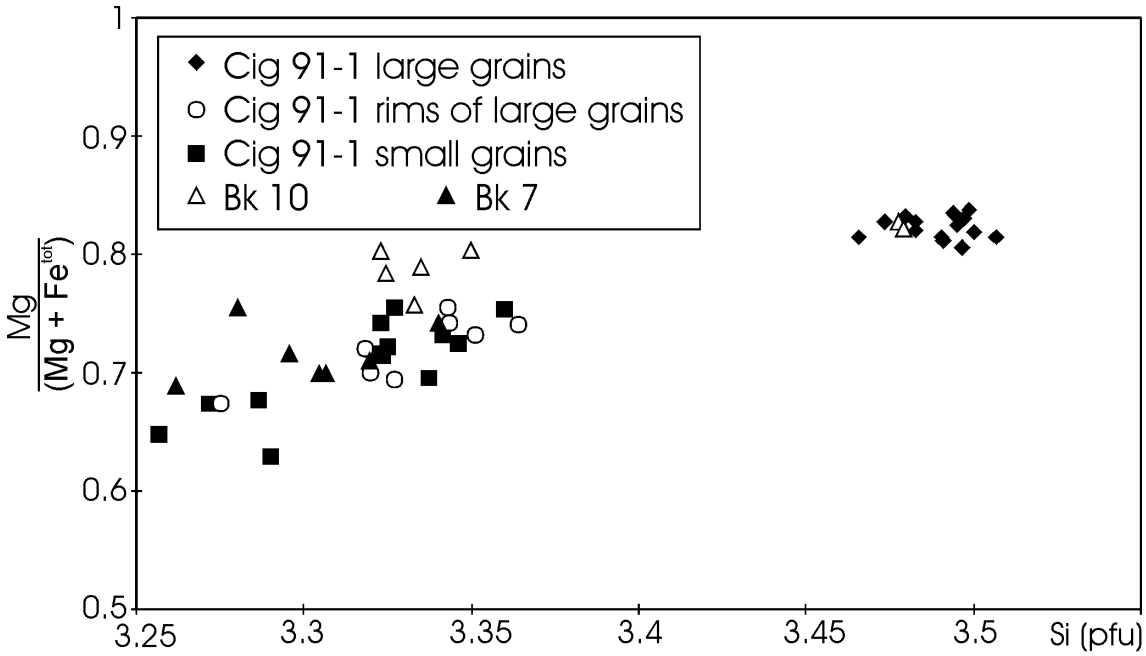

Figure 7

Differences in phengite compositions in relation to grain size and position of the analyses in the grain for sample Cig91-1 and the compositions of phengites from other samples.

$(K_{0.94\text{-}0.98},Na_{0.03\text{-}0.05})(Mg_{0.40\text{-}0.47},Fe^{2+}_{0.02\text{-}0.07})(Al_{1.40\text{-}1.46},Fe^{3+}_{0.03\text{-}0.08})(Si_{3.45\text{-}3.51},Al_{0.49\text{-}0.55})O_{10}(OH)_2$. Similar composition are found in a few small matrix phe. Most small matrix phe and the rims of the large phe have compositions (Fig.7, Table C9 in app. C) varying between $(K_{0.89\text{-}0.94},Na_{0.08\text{-}0.12})(Mg_{0.29\text{-}0.35},Fe^{2+}_{0\text{-}0.04})(Al_{1.50\text{-}1.56},Fe^{3+}_{0.08\text{-}0.14})(Si_{3.28\text{-}3.38},Al_{0.62\text{-}0.72})O_{10}(OH)_2$. Which phe composition belongs to the UHPM mineral paragenesis is not clear, because phe of both compositions occurs in contact with UHPM minerals as well as with late PT-replacement products.

rutile (rt)

Rutile amounts to up to 2 vol.% of the rock. The grains are anhedral, rounded and about 30 µm in size. In one sample (Bk 8) mm-sized anhedral rt grains occur. Composition is TiO_2 without significant amounts of other elements (Table C10 in app. C).

apatite (ap)

Apatite amounts to 0.5 vol.% of eclogitic rocks and is present as anhedral rounded grains. Its grainsize is up to 50 µm, in some quartz veins large 5 mm sized ap grains occur, however. Ap compositions were not analysed.

dolomite (dol)

Dolomite occurs only in metabasic rocks that are rich in gln and white mica and are considered to be derived from pillow rims or interpillow material (e.g., Oberhänsli, 1982; Barnicoat, 1988a). The amount of dol is below 4 vol.% of the rock. Dol is present as small (< 40 µm) anhedral grains. and often occurs in elongated aggregates of max. 0.5 cm in length. The shape preferred orientation of these aggregates partly defines the foliation. It also occurs as approximately equidimensional aggregates in strain shadows at grt. Dol is easy distinguished optically from late calcite, due to

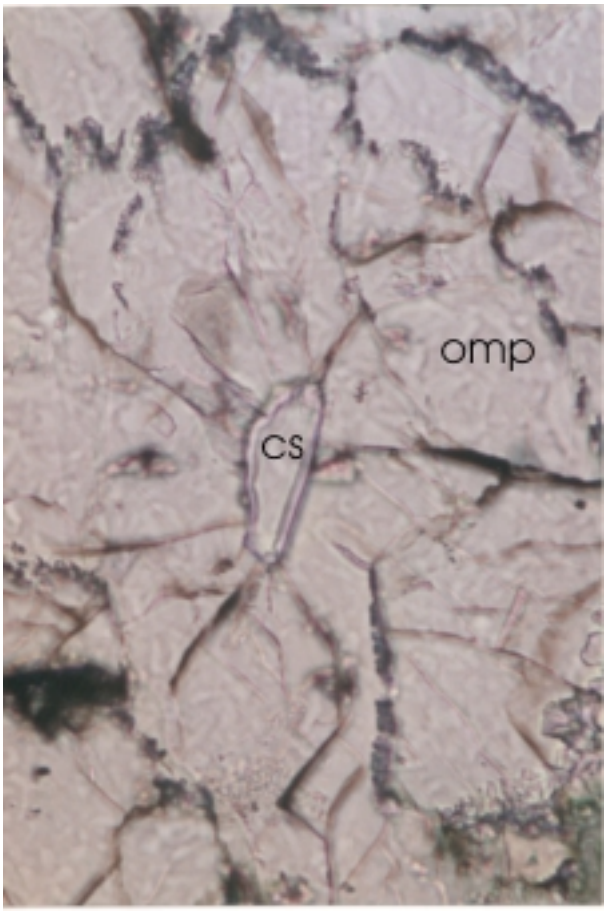

Photo 1

Typical coesite inclusion in omp with a small rim of quartz between omp and cs. Note the cracks in omp, radiating away from the inclusion. Plane polarised light, length of photograph 1.4 mm.

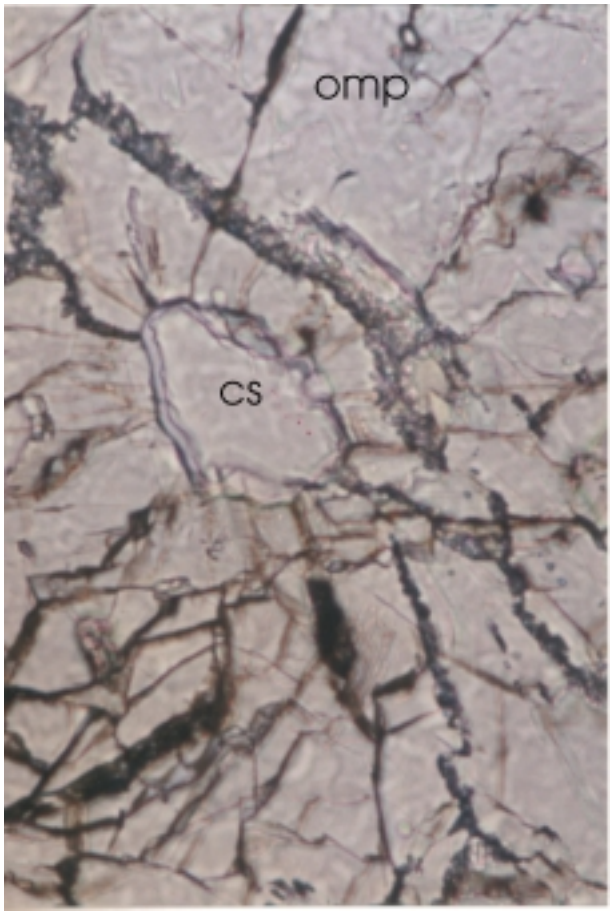

Photo 2

Coesite inclusion in omp, with a small rim of quartz between cs and omp. Note, that the diameter of the inclusion is more than half the diameter of the including omp grain. Plane polarised light, length of photograph 1.4 mm.

numerous fine grains of an opaque mineral, resulting from the oxidation of the ankerite component in dol, that are present along its cleavage planes. Dol is considered part of the UHPM mineral assemblage, because it occurs in contact with all other UHPM minerals and has inclusions of gln and rt. The composition varies between $Ca(Mg_{0.75\text{-}0.80}Fe_{0.25\text{-}0.20})(CO_3)_2$, with minor (< 2 mol%) amounts of Mn substituting for Mg and Fe (Table C11 in app. C).

coesite (cs)

Coesite is found as inclusions in omp (up to 30 μm) and possibly in grt rims (< 10 μm). The cs inclusions have the typical characteristics described by Chopin (1984) with radial cracks in the host mineral and a rim of columnar quartz between cs and the host mineral (Photos 1, 2). Cs occurs as colourless to slightly greenish grains with higher relief as the surrounding quartz. In several inclusions in omp, the presence of cs was unequivocally proven with the electron microprobe, that showed a SiO_2 composition for phases in the inclusions and, respectively, blue and yellow luminesence colours for cs and quartz (Schulze & Helmstaedt, 1988). The cs in the two small inclusions in grt could not unequivocally be identified.

3.1.1.2 Mineral paragenesis and PT-estimates

All minerals of group 0 eclogites (omp, grt, gln, czoI, pg, zoi, cs, rt, and ap, with in some samples that will not be discussed, dol and phe), with exception of gln and zoi, can be found occuring in mutual contact, although lower PT-replacement products always occur at contacts between some minerals (e.g., blue-green amphibole between grt and gln). Paragonite is considered part of the UHPM mineral paragenesis of group 0 eclogites, although experimental investigations (e.g., Holland, 1979), indicate that pg is not stable at the PT-conditions of UHPM (2.7 GPa at 625 °C, Reinecke 1991; 1995). At these conditions, pg should have reacted to jadeite (jd component in cpx) and kyanite (Holland, 1979). However, kyanite has not been observed in the metabasic rocks at Lago di Cignana and pg occurs without UHPM reaction textures in direct contact with the other minerals of the UHPM paragenesis. Furthermore, pg occurs as inclusions in omp, that has the same composition as omp with cs inclusions. Similar observations of the persistence of pg outside its stability field are known from Dora Maira (Schertl et al., 1991) and from Dabie Shan (Okay, 1995).

That gln and zoi do not occur in mutual contact, but are always separated by other UHPM minerals, suggests that in group 0 eclogites two local equilibrium assemblages, with slightly different bulk rock compositions, occur. The first and most abundant assemblage consists of omp, grt, gln, pg, czoI, cs, rt, and ap, the second assemblage consists of omp, grt, zoi, pg, czoI, cs, rt, and ap. These assemblages are coupled by the reaction (in mol):

$$0.25\ \text{gln} + 0.29\ \text{zo} = 0.87\ \text{omp} + 0.07\ \text{grt(rim)} + 0.08\ \text{czoI} + 0.14\ \text{pg} + 0.07\ \text{cs/qtz} + 0.22\ H_2O$$

calculated with the mineral compositions of sample Bk 39, which is representative for group 0 eclogites. Rutile and ap are the only Ti-, respectively, P-bearing minerals and, therefore, do not appear in this reaction. A similar reaction is given by Reinsch (1977) and Ridley (1984), as the reaction, that marks the temperature dependent transition from blueschist to eclogite in metabasic rocks. This indicates that mm-scale compositional inhomogenities (the size of the smallest gln or zoi domains) that were present in the blueschist precursor of the eclogite, were preserved during UHPM.

The inhomogeneous composition of grt, czoI, and omp can be explained with partial equilibrium that assummes that reaction with a disequilibrium phase is kinetically inhibited. The equilibrating bulk composition is the original bulk composition minus the composition of the disequilibrium phase (Loomis, 1983). In the case of the more or less concentrically zoned grt and czoI, it can be argued that only the outer rim is in equilibrium with the other phases, and that the core region is no longer part of the system, because of relatively slow intracrystaline diffusion in grt (e.g., Chakraborty & Ganguly, 1990) and czoI at the temperature of 625 °C during UHPM. The variable omp compositions cannot be attributed to partial equilibrium, however. Omphacite grains are either homogeneous, or consist of irregular domains with different compositions. The formation of these domains is attributed to localised compositional reequilibration during grain boundary migration (chapter 3.2), due to deformation under changing PT-conditions. This process makes it impossible to identify the omp composition in equilibrium with the other phases.

PT-estimates

Equilibration temperatures for the UHPM mineral assemblage were obtained with garnet-clinopyroxene Fe^{2+}-Mg exchange thermometry (see appendix B for a discussion of the different calibrations of the thermometer). The presence of cs inclusions in matrix omp and of small inclusions of quartz (pseudomorphs after cs) in grt rims, indicates that grt rims must be combined with matrix omp to obtain temperatures for the UHPM. The Powell (1985) calibration gives temperatures of 595 ± 35 °C (1 σ) for 27 grt (rim)-omp pairs from five samples, calculated at a pressure of 2.7 GPa. The variation in exchange temperatures is larger within one sample (Table 3, Table B2 in app. B), than between the samples. This large variation might have several causes:

* Analytical erors, that influence the calculation of the Fe^{2+} and Fe^{3+} content in grt and omp.
* The incomplete zoning pattern of grt. The Mg-richest rim of the normal zoned grt is often missing, for example, where grt partly embays a matrix omp.
* The inhomogeneous omp composition in contact with the grt rim. As discussed earlier, it is not possible to unequivocally determine the omp composition, that is in equilibrium with the grt rim.

Analytical errors were minimised by measuring each mineral at least two times in direct contact and by comparing these single analyses. Deviating analyses were discarded and temperatures were calculated with the mean of the remaining analyses for every grt-omp pair.

To solve the other problems, digital element distribution maps (DEDM, Bernhardt et al., 1995) were made of all garnets used for geothermometry. These maps show that a compositionally homogeneous omp can be embayed in a zoned grt (Photo 3) and therefore, occurs in contact with a range of grt compositions. The DEDM do not show a reversal of the prograde compositional zoning trend in grt at grt-omp interfaces. Therefore, reequilibration of the Fe^{2+}-Mg exchange on the exhumation path and diffusive relaxation in grt rim and omp rim can be excluded. The impossibility to define unique grt and omp equilibrium compositions, indicates that during UHPM Fe^{2+}-Mg exchange equilibrium between grt and omp was not reached at all grt-omp interfaces.

Table 3

Temperatures (at 2.7. GPa) calculated with different calibrations of the grt-cpx thermometer for some representative grt and omp combinations. Key: E&G79 = Ellis & Green (1979), P85 = Powell (1985), K88 = Krogh (1988), P&N89 = Pattison & Newton (1989) and A94 = Ai (1994)

Sample	Pair	X^{grt}_{Mg}	X^{grt}_{Ca}	X^{cpx}_{Mg}	E&G79	P85	K88	P&N89	A94
Bk 7	B2	0.293	0.177	0.828	616 °C	591 °C	545 °C	514 °C	594 °C
Bk 7	D1	0.322	0.177	0.801	685 °C	661 °C	618 °C	582 °C	678 °C
Bk 39	A1	0.205	0.268	0.821	595 °C	572 °C	548 °C	440 °C	567 °C
Bk 39	C1	0.249	0.247	0.810	644 °C	621 °C	597 °C	507 °C	626 °C
Bk 39	C4	0.259	0.251	0.872	568 °C	544 °C	517 °C	420 °C	536 °C

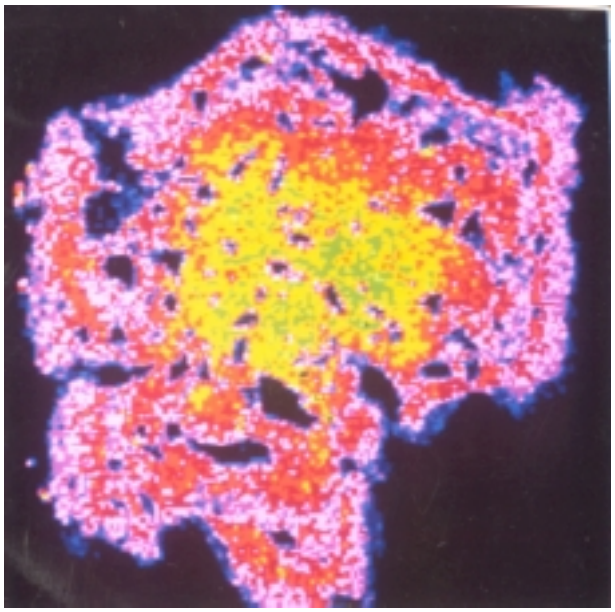

Photo 3

A digital element distribution map for Mn in grt. Mn-content decreases from green-yellow in the core over orange to pink and blue in the rim. Black islands in garnet are mostly omp inclusions. Note in the lower right and upper left corner of the grt, omp inclusions in contact with grt core composition and grt rim composition. Length of the picture ca. 5 mm.

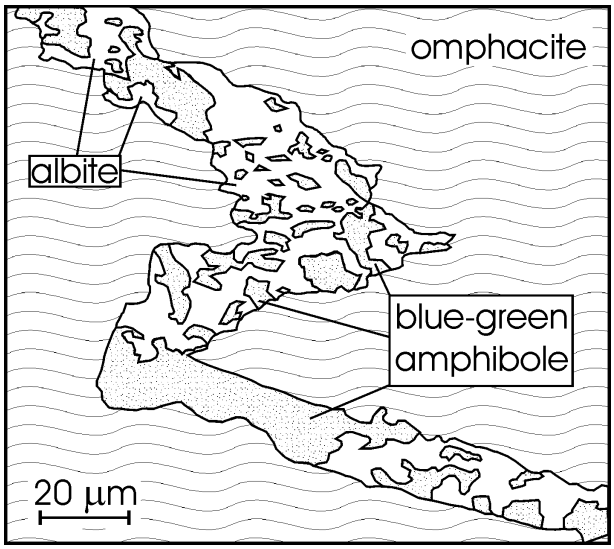

Figure 8

Drawing after a SEM image of a blue-green amp, ab symplectite at an omp-omp grain boundary.

3.1.2 Group 1 eclogites

In group 1 eclogites several minerals have formed as partial replacement products of the UHPM mineral assemblage (Table 2). These replacement minerals are restricted to specific UHPM minerals and microstructural sites. A symplectite of albite and blue-green amphibole often replaces omp along cracks and grainboundaries (Fig. 8). Blue-green amphibole develops as rims around gln (Photo 4), at contacts of grt with pg and gln and is often also present at grt in contact with other UHPM minerals and along cracks in grt. In phe-bearing samples a green-brown mica occurs as lower PT-replacement product between grt and phe. Rims of ilmenite and/or titanite develop around rt. Clinozoisite II partly replaces zoi and pg. Quartz replaces cs and in dol bearing samples, calcite partly replaces dol.

The relative amounts of these replacement products are similar in all group 1 samples (Fig. 4). Only during this replacement stage irregular overgrowths of blue-green amphibole formed around grt and gln. During later replacement stages, the amount of these amphiboles remained constant, as long as these could be recognised from their microstructural position (Fig. 4). Therefore, this replacement stage is considered common to all eclogite groups.

3.1.2.1 Mineral compositions

albite (ab)

Albite amounts to between 50 and 70 vol.% of the symplectite that replaces omp. This symplectite amounts to between 8 and 12 vol.% of group 1 eclogites. Albite forms grains of up to 50 µm in

diameter that include the smaller amphibole grains. The anorthite (an) component of ab is below 5 mol% (Table C13 in app. C).

blue-green amphibole (amp)

Blue-green amphibole in group 1 eclogites can be divided in three groups with different micro-structural positions and compositions (Fig. 9):

1. amphibole rims around garnet
2. amphibole rims around glaucophane
3. amphibole in symplectite

1. amphibole rims around garnet.

The amount of this amp ranges from 2 to 3 vol.% in group 1 and 2 eclogites. In group 3 and 4 eclogites with partly replaced grt, the amp around garnet is difficult to distinguish from other amphiboles and its amount becomes less. This amp is present as thin (max. 30 µm) discontinuous rims around grt and along fractures in grt. The grains are anhedral and up to 100 µm in length. The

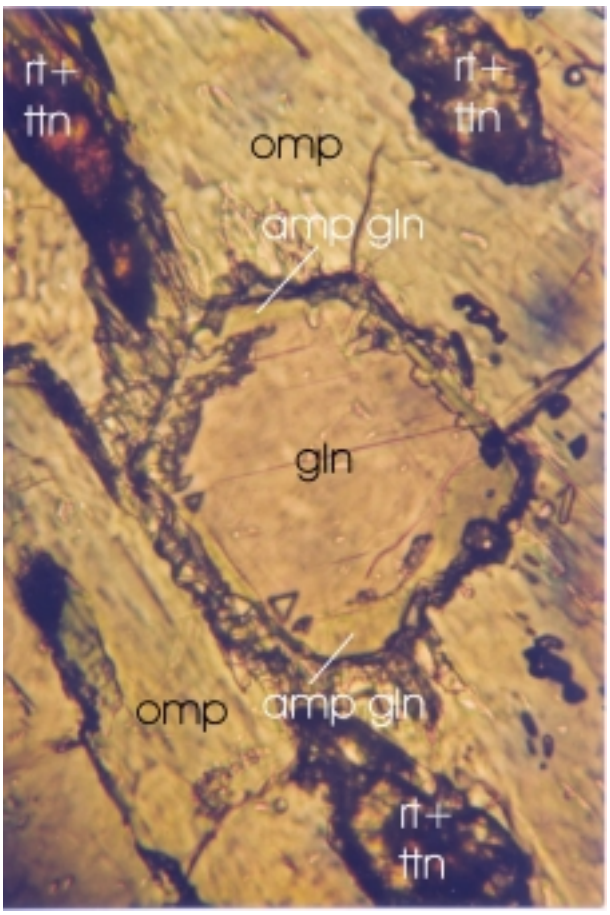

Photo 4

Glaucophane rimmed by blue-green amp (amp gln) in a matrix of omp and rt with titanite (ttn) rims. Plane polarised light, long side of the photograph is 1.4 mm.

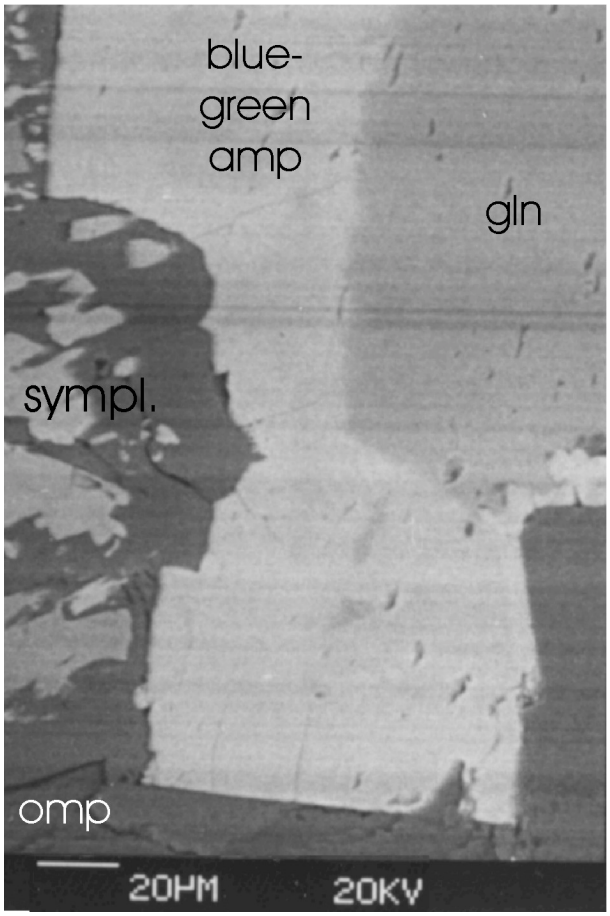

Photo 5

B(ack)S(cattered)E(lectron) photograph of the rim of blue- green amp around gln. Different shades of gray in the rim suggest slight compositional differences in the blue-green amp.

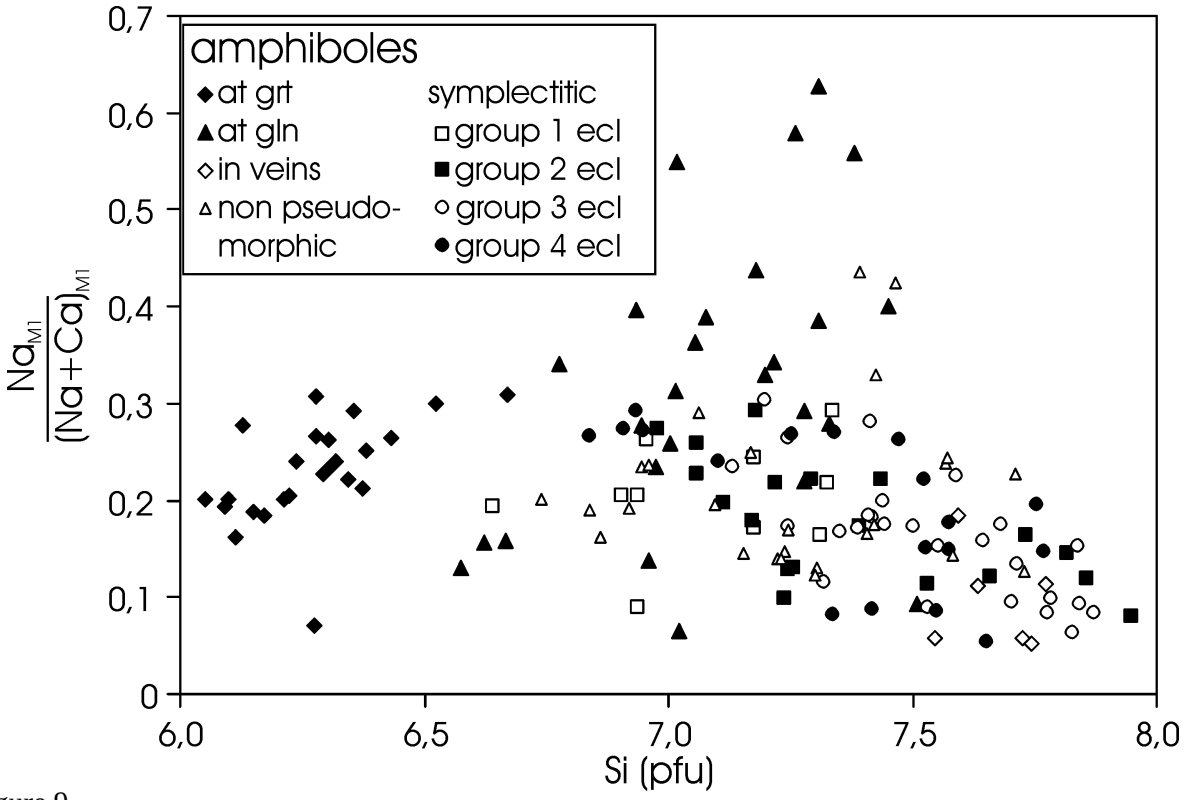

Figure 9

Compositional differences of amphiboles in different textural position for all eclogite groups. Amp at grt and at gln only occur in group 1 and 2 eclogites, non pseudomorphic amphiboles and vein amphiboles only occur in group 3 and 4 eclogites. Na_{M1} is Na in the M1-position, pfu is per formula unit.

composition (Table C14 in app. C) ranges between magnesian-hastingite and magnesian-hastingitic-hornblende (amp names after Leake, 1978).

2. amphibole rims around glaucophane

The amount of this amp ranges from 2 to 3 vol.% in group 1 and 2 eclogites. In group 3 and 4 eclogites, gln is completely transformed, and this amp cannot be identified. At grt-gln contacts a transition in composition from amp around gln to the amp around grt is found. Back scattered electron (BSE) images of amp rims indicate that these rims consist of patches (few μm^2 in size) with different compositions (Photo 5). The size of these patches is close to the beam size of the microprobe and this is reflected by the highly variable measured compositions (Fig. 9, Table C15 in app. C) for these amphiboles, between barroisite, actinolite and magnesio-hornblende (amp names after Leake, 1978).

3. amphibole in symplectite (ampI)

The ampI comprises between 30 and 50 vol.% of the ab-amp symplectites (Fig. 8) that are the lower PT-replacement products of omp. The grains are subhedral and small (< 20 μm). The composition (Table C16 in app. C) ranges from magnesian-hornblende to actinolitic-hornblende (amp names after Leake, 1978). In direct contact with quartz, ampI is always actinolite. This suggests that after formation of the symplectite from omp, the ampI in contact with quartz has reequilibrated according to the simplified reaction:

edenite + quartz = tremolite + albite (Holland & Blundy, 1994).

This is supported by the observations that i) symplectites after omp in quartz veins comprise a larger amount of ab and ii) ampI adjacent to quartz aggregates is an actinolite at the symplectite-quartz contact, but an actinolitic hornblende at the symplectite omp contact.

titanite (ttn)

Titanite amounts to up to 1.5 vol.% of group 1 eclogites. It forms anhedral grains up to 50 μm in size, often with minor rt and ilmenite preserved in its core and also occurs as composite inclusions with pg and czo in the core of garnets. Its composition is approximately $Ca(Ti_{0.95}\ Al_{0.05})[SiO_4](O,OH,F)$ (Table C17 in app. C).

ilmenite (ilm)

Ilmenite amounts to 0.5 vol.% of the rock. It forms small (< 20 μm) anhedral grains that usually occur as discontinuous rims around rt. Ilmenite has also rarely been observed along cracks and as inclusions in grt. The ilm composition in contact with rt is $(Mg_{0.2}, Mn_{0.03}, Fe^{2+}_{0.95})TiO_3$, in grt its composition $(Mg_{0.01}, Mn_{0.1}, Fe^{2+}_{0.89})TiO_3$ is similar along cracks and in inclusions (Table C18 in app. C).

clinozoisite II (czoII)

Clinozoisite II amounts to up to 3 vol.% of group 1 eclogites. It occurs as discontinuous rims around large czoI grains in contact with lower PT-replacement products and as small (about 20 μm) euhedral grains in aggregates of white mica. The composition of czoII (Table C6 in app. C) lies between $Ca_2Fe^{3+}_{(0.40\text{-}0.55)}Al_{(0.45\text{-}0.60)}Al_2Si_3O_8(OH)$. Between samples, the range in Al_2Fe^{3+}epidote component differs slightly.

quartz (qtz)

Quartz amounts to up to 2 vol.% of metabasic rocks. It is present as anhedral grains of max. 40 μm or as aggregates of several grains of up to 100 μm in size. It is also present as small (< 30 μm) grains along shearbands and as vein filling material. Quartz is always completely surrounded by lower PT-replacement products. Quartz also occurs as monomineralic inclusions in grt and seldom in omp.

calcite (cal)

Calcite is present in only few samples of the metabasic rocks. In one group 1 eclogite, cal occurs as a rim around dol grains and it amounts to < 2 vol.% of the rock. The composition varies slightly between $(Fe, Mg, Mn)_{<0.1}Ca_{>0.9}CaCO_3$ (Table C12 in app. C). Cathodoluminesence (CL) investigations of cal, have shown that the CL colours depend on the relative amounts of Mn and Fe (Marshall, 1988). High Mn- and low Fe-contents result in bright yellow CL colours; High Fe- and low Mn-contents result in a dark CL colour. In the group 1 eclogites, the Mn-content of cal is almost constant at approx. 1 mol% (Table C12 in app. C). The Mg- and Fe-content is positively correlated. Therefore, the CL colours of cal give an indication of the relative amounts of Mg and Fe in calcite. Dark

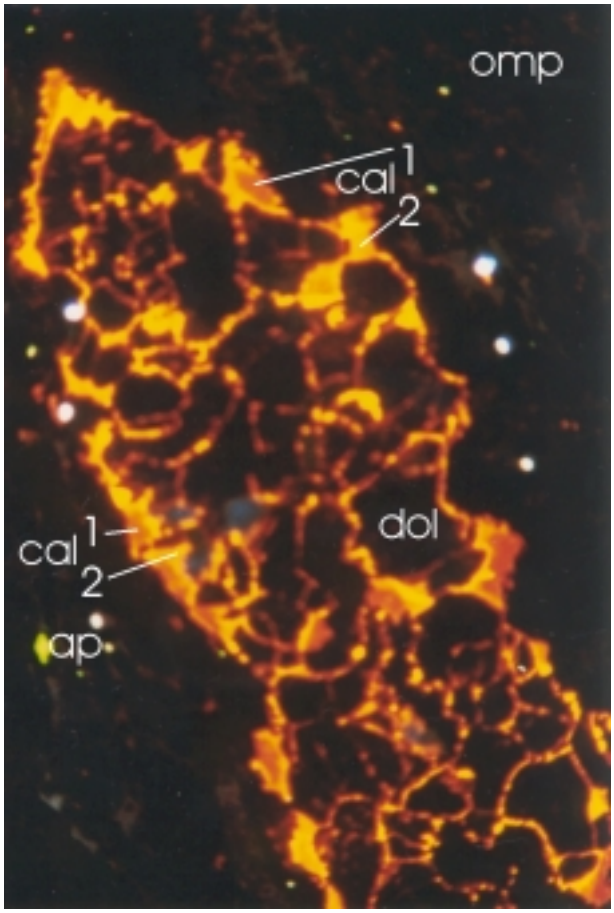

Photo 6

Cathodoluminescence photograph of cal in a dolomite domain. Different shades of orange (cal1, cal2) represent cal with different amounts of Mn, Mg and Fe. Long side of the photograph is 3.8 mm.

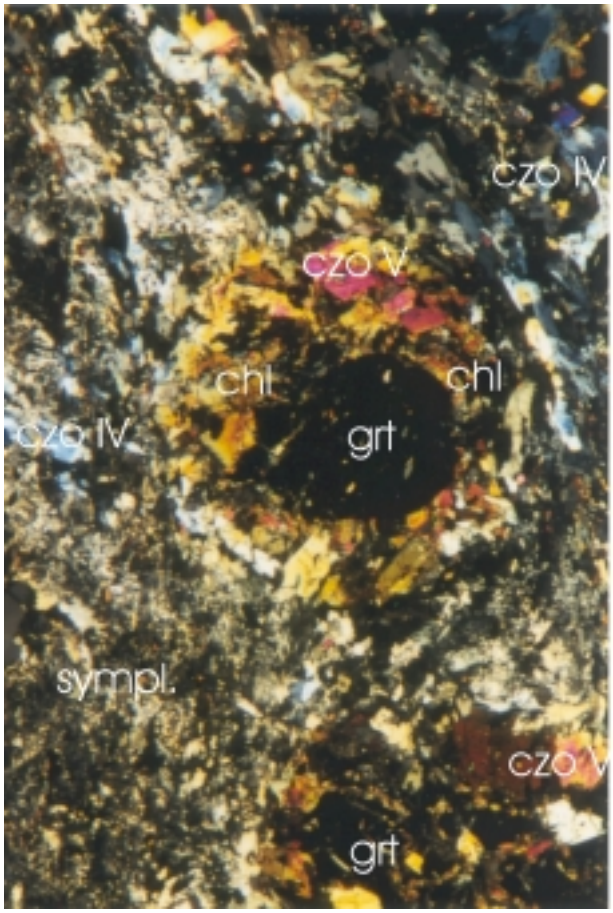

Photo 7

Late replacement of grt by chl and epidote (czoV). Crossed polars, long side of the photograph is 7 mm.

orange-red CL colours (high Mg- and Fe-contents) occur at the rim zone away from dol in the cal overgrowths on dol, whereas towards dol the cal becomes brighter orange (Photo 6). In contact with dol, cal has yellow-orange CL colours (low Mg- and Fe-contents). This change in CL colours is present in all carbonate aggregates, but the absolute amounts of Mg and Fe differ slightly between the aggregates.

green-brown mica

This green-brown mica occurs as small anhedral grains between phe and grt. It amounts to < 1 vol.% and its composition is approximately $(Na_{0.06}K_{0.94})(Mg_{1.23}Fe_{1.18})Al_{1.8}Si_{2.67}O_{10}(OH)_2$ (Table C19 in app. C).

3.1.2.2 Mineral paragenesis and PT-estimates

In the group 1 eclogites several minerals have formed as partial replacement products of minerals of the UHPM assemblage. The amount of these replacement products is similar in all group 1 eclogites, independent of the relative amounts of the UHPM minerals. This suggests that these replacement products formed simultaneous. However, the minerals of this first replacement stage

are not an equilibrium paragenesis, because three amp at different textural sites have different compositions. The observation, that the lower PT-replacement products are restricted to specific minerals of the UHPM mineral assemblage (Table 2), suggests local equilibrium. The local equilibrium domains were defined by the different chemical compositions of the UHPM minerals and the size of the domains was the grain size of the UHPM minerals.

PT-estimates

Pressures and temperatures for the onset of this lower PT- replacement can be obtained from two independent domains: the omp (symplectite) domain present in all samples and the carbonate domain present in one sample only.

The omphacite domain

The reaction inferred for this domain is:

omphacite = amphibole + albite

This reaction can be used to calculate temperatures and pressures according to partial reactions (discussion of these thermo-barometers in Appendix B):

jadeite (in omp) + quartz = albite (barometer, Holland, 1980)

edenite (in amp) + quartz = tremolite (in amp) + albite (thermometer, Holland & Blundy, 1994).

A prerequisite, to obtain equilibrium temperatures and pressures with these reactions for omp decomposition, is that qtz and omp occurred in mutual contact. Quartz is only seldom found in partly replaced eclogites and never in mutual contact with omp. Therefore, the calculated pressures of 1.2 to 1.3 GPa (Table 4, Table B6 in app. B) and temperatures of 525-575 °C (Fig. 9A, Table B3 in app. B) are maximum pressures and temperatures for the omp decomposition reaction. When qtz is present, it occurs in veins or it is completely surrounded by lower PT-replacement products. This

Table 4

Pressures (at 550 °C) calculated with the jd (in omp)+qtz=ab barometer of Holland (1980), using the method of Holland (1990) for the calculation of jadeite activity in omp, for extreme omp compositions. Key: X(jd,acm,diop,hed) = resp. jadeite, acmite, diopside and hedenbergite component in cpx, a(jd) = jadeite activity, max. X(xx) = cpx analysis with highest xx component, min. X(xx) = cpx analysis with lowest xx component, the analyses with min. X(jd) and min. X(diop) have also, resp., max. X(diop) and max. X(hed).

	sample, analysis, date	X(jd)	X(acm)	X(diop)	X(hed)	a(jd)	P (GPa)
max.X(jd)	Bk 8, 12, 29.01.93	0.58	0.02	0.32	0.08	0.63	1.32
min. X(jd)	Bk 7, 41, 27.08.92	0.34	0.10	0.54	0.03	0.49	1.22
max. X(acm)	Bk 39, 11, 28.08.92	0.41	0.17	0.34	0.08	0.47	1.20
min. X(acm)	Cig 91-1, 11, 28.11.93	0.53	0	0.32	0.15	0.64	1.32
min. X (diop)	Bk 39, 9, 23.03.92	0.49	0.06	0.27	0.17	0.54	1.26
min. X(hed)	Bk 39, 8, 23.03.92	0.41	0.15	0.42	0.02	0.48	1.21
mean (n = 95)	all omp rim positions	0.45	0.07	0.40	0.08	0.56	1.27
sigma		0.05	0.03	0.05	0.02	0.03	0.02

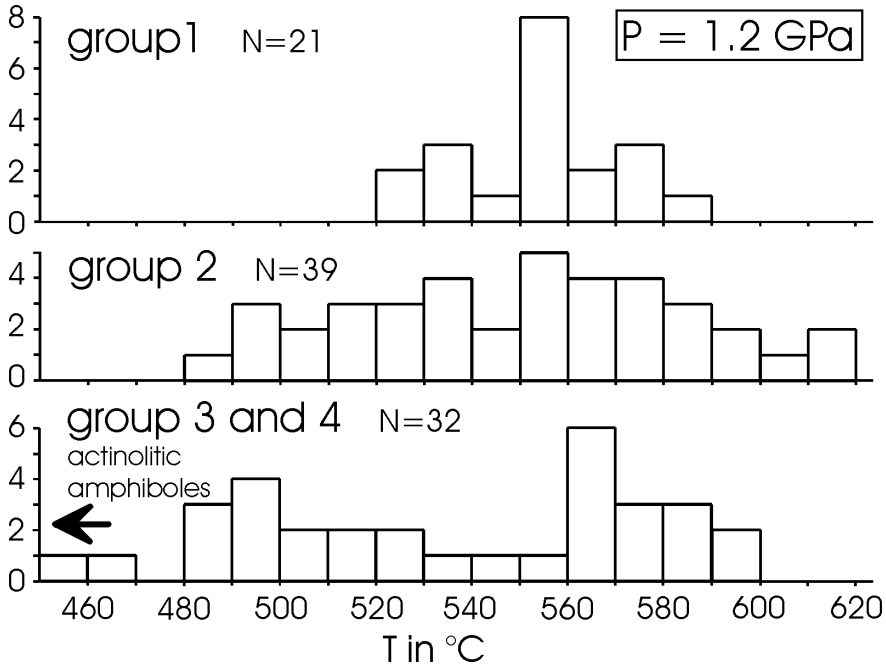

Figure 10

Histogram of temperatures calculated with the plagioclase-amphibole thermometer of Holland & Blundy (1994) for ab-amp symplectites in group 1 to 4 eclogites, calculated at a pressure of 1.2 GPa. N is number of samples

suggest that the decomposition reaction ceased, when all qtz present in the reaction domain was used up. Another suggestion is that the reaction ceased, when qtz was no longer available in the reaction domains due to its rim of lower PT-replacement products.

The large range of temperatures (Fig. 10, Table B3 in app. B), partly results from the inhomogeneous compositions of educt and product phases. Omphacite has $0.6 > X_{jd} > 0.45$ and, therefore, the onset of symplectite formation will occur at different pressures and temperatures. Consequently, the varying ampI compositions reflect different formation temperatures. The varying ampI compositions could also result from contamination of the analyses of these fine grained ampI with ab, resulting in higher Si, Al and Na content in the ampI and in a lower calculated formation temperature.

The carbonate domain

Pressure and temperature estimates for this domain are obtained with the cal-dol solvus thermometer (Anovitz & Essene, 1987, see Appendix B for discussion), from calcite in contact with dolomite, which shows temperatures of 575-450 °C for cal in aggregates with dol (Table 5, Table B5 in app. B). Combined CL and electron microprobe investigations of the carbonate aggregates, show that the calculated temperature depends on the position in the carbonate aggregate (Photo 6). This suggests that the reaction of dol to cal started at the rim of the dol grain and that the earliest cal formed in equilibrium with dol was relatively Mg and Fe rich (dark orange-red CL colours). Further reaction of dol to cal occurred at the interface between the earlier formed cal and dol. This new cal, which formed in equilibrium with dol, was less Mg and Fe rich (orange CL colours). Again further reaction occurred at the interface between the younger cal and dol. The cal formed at this stage in equilibrium with dol, was relatively Fe and Mg poor (yellow-orange CL colours). This zoning trend

Table 5

Temperatures calculated with the calcite-dolomite thermometer of Anovitz & Essene (1987) for some representative cal analyses in domains with different cl colours. T1 and T2 are, resp., calculated for system Ca^{2+}-Mg^{2+} and Ca^{2+}-Mg^{2+}-Fe^{2+}.

cl colour	sample, analysis, date	Ca(mol)	Mg(mol)	Fe(mol)	Mn(mol)	T1(°C)	T2 (°C)
brown-red	Bk 7 , 8, 26.04.93	0.895	0.062	0.033	0.009	572	577
	Bk 7 , 21, 26.04.93	0.903	0.059	0.030	0.008	560	568
orange-red	Bk 7th, 7, 11.06.94	0.918	0.047	0.025	0.010	515	533
	Bk 7th, 28, 11.06.94	0.914	0.045	0.032	0.009	506	530
orange-yellow	Bk 7 , 64, 26.04.93	0.937	0.033	0.022	0.008	445	475
	Bk 7th, 24, 11.06.93	0.930	0.036	0.026	0.008	465	495

is contrary to a trend expected for diffusional reequilibration for cal in contact with dol. This means that temperatures calculated with the compositions of cal with dark orange-red CL colours (575-525 °C) mark the upper limit for the onset of the reaction of dol to cal.

Because aragonite does not contain appreciable amounts of Mg, Fe and Mn, the Mg-Fe-Mn rich cal must have formed in the stability field of cal. Therefore, the maximum pressure for the onset of the reaction of dol to cal at 550 °C, is limited to 1.1-1.2 GPa by the aragonite-calcite univariant equilibrium (Johannes and Puhan, 1971).

The PT-conditions for the onset of lower PT-replacement in group 1 eclogites obtained from two independant domains are estimated at P < 1.2 GPa and T < 550 °C.

3.1.3 Group 2 eclogites

In group 2 eclogites the mineral assemblage is the same as in group 1 eclogites, but the amounts of ab-amp symplectites, czo and ttn formed at the expense of omp and gln, pg and rt, respectively, are increased. In carbonate bearing samples, cal is the only carbonate mineral present.

3.1.3.1 Mineral compositions

albite (ab)

In group 2 eclogites ab is present in symplectite that amounts to up to 45 vol.% of group 2 eclogites. The only difference from ab in group 1 eclogites is the grain size of up to 80 μm.

amphibole in symplectite II (ampII)

Amphibole II occurs in the ab-amp symplectites, that are the lower PT-replacement products of omp and gln. The ampII grains are subhedral and often slightly larger (< 30 μm) than ampI grains in group 1 eclogites. However, it is not unequivocally possible in a group 2 eclogite to distinguish between ampI and ampII. The composition of amphibole (ampI + ampII) in group 2 eclogites (Fig. 9, Table C16 in app. C) ranges from magnesio-hornblende to actinolite (amp names after Leake, 1978).

clinozoisite III (czoIII)

Clinozoisite III amounts to up to 3 vol.% of group 2 eclogite and occurs as discontinuous rims around large czoI and czoII grains in contact with lower PT-replacement products, and as rims around the smaller euhedral czoII grains in aggregates of white mica. The composition (Table C6 in app. C) lies between $Ca_2Fe^{3+}_{(0.45\text{-}0.60)}Al_{(0.40\text{-}0.55)}Al_2Si_3O_8(OH)$.

titanite (ttn)

Titanite amounts to up to 2 vol.% of the rock in group 2 eclogites. The ttn formed during this stage of lower PT-replacement has the same composition as earlier formed ttn and can not be distinguished from earlier formed ttn.

calcite (cal)

Calcite occurs as untwinned anhedral grains of up to 4 mm in their longest dimension, interpreted to be pseudomorphs after dol aggregates and as small (< 30 μm) anhedral grains along shearbands. Calcite in group 2 and later eclogites has lower amounts of Mn, Fe and Mg substituting for Ca than cal in group 1 eclogites (Table C12 in app. C), but because of the differing amounts of Mn in the cal, the CL colours can no longer be directly correlated with the amount of Mg and Fe in cal.

3.1.3.2 Mineral paragenesis and PT- estimates

In the group 2 eclogites the mineral assemblage is similar to the assemblage in group 1 eclogites. Some of the lower PT-replacement products that formed during this stage, however, have compositions different from similar replacement products in group 1 eclogites. The replacement minerals that formed earlier did not change their composition in these samples. Therefore, the compositional range of lower PT-replacement products is larger in group 2 eclogites than in group 1 eclogites. The localised occurrence of the newly formed minerals, suggest that similar to group 1 eclogites, the reaction products were in local equilibrium only. Therefore, the size of the equilibrium domains is still similar to the grain size of the UHPM minerals.

PT-estimates

In group 2 eclogites dol is no longer present and therefore, the cal-dol thermometer cannot be applied. Temperatures for this lower PT-replacement stage can be obtained from the omp (symplectite) domain with the Holland & Blundy (1994) plagioclase-amphibole-quartz-thermometer. Temperatures range from 500 to 575 °C (Fig. 10, Table B3 in app. B). This large range in calculated temperatures is due to the presence in group 2 eclogite samples of 2 generations of symplectitic amp (Fig. 9). Higher temperatures are calculated with amphiboles inherited from the earlier lower PT-replacement stage and lower temperatures (500-525 °C) are calculated with newly formed more actinolitic amphiboles. Because ampII is coarser grained than ampI, contamination of these analyses with albite is improbable. Therefore, the higher Si-content in ampII compared to ampI suggests decreasing temperatures (500 -525 °C) during later replacement in group 2 eclogites. A pressure estimate for this stage is not possible.

3.1.4 Group 3 eclogites

In group 3 eclogites the replacement of gln and omp through ab-amp symplectites is completed. The remaining pg is partly replaced by chlorite. Garnet is partly decomposed to an aggregate of chlorite, dark mica, epidote (czoIV) and ab (Photo 7). Symplectitic amp partly grows to a coarser amphibole.

3.1.4.1 Mineral compositions

albite (ab)

Albite occurs in two textural positions in group 3 eclogites. It occurs in symplectites that amount to up to 55 vol.% of group 3 eclogites. This ab differs only in its grain size of up to 120 μm from earlier formed ab in symplectite. Albite also occurs in the aggregates of several minerals replacing grt. This ab forms anhedral grains of up to 100 μm in size and has between 8 and 10 mol% an (Table C13 in app. C).

amphibole in symplectite III (ampIII)

The ampIII grains are subhedral with a grainsize larger (< 50 μm) than ampI and ampII in group 1 and 2 eclogites. In a group 3 eclogite, it is not unequivocally possible to distinguish between ampIII and earlier ampI and ampII. The composition of amphibole (ampI + ampII + ampIII) in group 3 eclogites ranges (Fig. 9, Table C16 in app. C) from magnesio-hornblende to actinolite (amp names after Leake, 1978), with a larger number of actinolites than in group 2 eclogites.

coarse amphibole

This amphibole forms large (up to 100 μm) subhedral grains and amountsto up to 5 vol.%. It develops at the cost of small symplectitic amphiboles and has inclusions of ab, czo and ttn. The composition (Table C20 in app. C) varies from actinolitic hornblende to actinolite (names after Leake, 1978).

clinozoisiteIV (czoIV)

Clinozoisite IV amounts to nearly 3 vol.% and occurs in two textural positions. It occurs as discontinuous rims around earlier czo grains with a composition (Table C6 in app. C) between $Ca_2Fe^{3+}_{(0.50\text{-}0.70)}Al_{(0.30\text{-}0.70)}Al_2Si_3O_8(OH)$ and also as large, up to 80 μm, anhedral grains in mineral aggregates replacing grt, with a composition between $Ca_2Fe^{3+}_{(0.62\text{-}0.78)}Al_{(0.22\text{-}0.38)}Al_2Si_3O_8(OH)$.

chlorite (chl)

Chlorite amounts to up to 5 vol.% of group 3 eclogites. It is present as randomly oriented stacks in large (up to 1 cm) aggregates. The aggregates are approximately circular for chl formed at the expense of grt and “stick” like for chl formed at the expense of white mica. The composition varies between $(Mg_{4.5\text{-}6.5},Fe^{2+}_{1.7\text{-}4.0},Fe^{3+}_{0.80\text{-}0.95},Al_{2.1\text{-}2.5})(Si_{5.3\text{-}5.6},Al_{2.4\text{-}2.6})(OH)_{16}$ (Table C21 in app. C) and depends on textural position. The chl formed at the expense of white mica has X_{Mg}, $Mg/(Mg+Fe^{2+})$ between 0.7-0.8, whereas chl formed at the expense of grt has X_{Mg} between 0.5-0.6 (Fig. 11). In the matrix chl, that cannot be attributed to white mica or grt, has intermediate X_{Mg}.

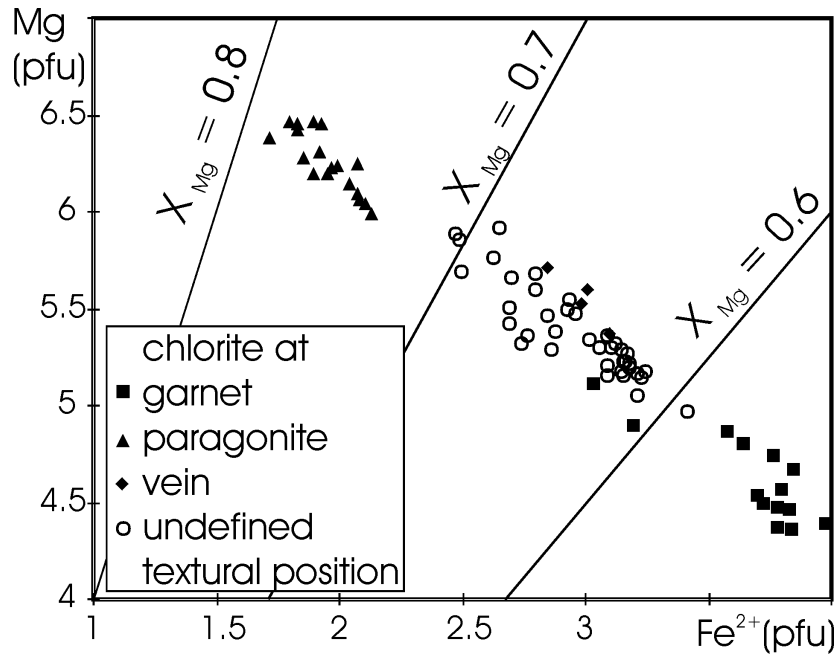

Figure 11

The composition of chlorite in relation to its microstructural position. pfu, per formula unit.

dark mica

This dark mica amounts to up to 1.5 vol.% of the rock and occurs as a fine grained intergrowth with chlorite in aggregates replacing garnet. It was not possible to obtain reliable analyses of this dark mica.

3.1.4.2 Mineral paragenesis and PT-estimates

In the group 3 eclogites the mineral assemblage is the assemblage of group 1 and 2 eclogites with chlorite and a dark mica added. Some of the replacement products formed during this stage have a different composition from similar, earlier formed, replacement products. However, the minerals that formed during these earlier stages retained their composition (e.g., Fig. 9). The localised occurrence of the newly formed minerals, suggest that similar to group 1 and 2 eclogites, the reaction products were in local equilibrium only. However, the presence of chlorite with intermediate composition and the growth of large amphiboles, indicate that at least locally the size of the equilibrium domains was larger than the grain size of the original UHPM minerals.

PT-estimates

Temperatures for this replacement stage can be obtained from the omp (symplectite) domain with the Holland & Blundy (1994) plagioclase amphibole thermometer. Calculated temperatures range from 475 to 575 °C (Fig. 11, Table B3 in app. B). Some of the ampIII has a composition with Si > 7.7 per formula unit (pfu) and is outside the compositional limit of the thermometer (Holland & Blundy, 1994). These compositions, however, still point to formation temperatures below 475 °C. The large range in calculated temperatures is, as in group 2 eclogites, due to preservation of earlier formed amp(I and II). Therefore, a temperature below 500 °C is a reasonable estimate for stage 3 replacement. A pressure estimate for this stage is not possible.

3.1.5 Group 4 eclogites and greenschists

In group 4 eclogites the replacement of the UHPM mineral assemblage goes to completion and a new paragenesis comprising chl, green amp, czoV, ttn, and ab has formed. The earlier replacement products that formed pseudomorphs after the UHPM paragenesis and thereby, preserved the original microstructure, are partly replaced by the new paragenesis; hence, the original microstructure is largely obscured. The greenschists are rocks, where replacement and recrystallisation have gone to completion. The composition of the greenschist minerals is the same as the minerals of the group 4 eclogites.

3.1.5.1 Mineral compositions

albite (ab)

Albite amounts to < 50 vol.% of the rock. It occurs in symplectite, in the aggregates replacing grt, and as latest replacement product of remaining white mica. Locally, cm-sized poikiloblasts of ab occur. In symplectite ab has < 5 mol% an, in other position an contents are between 5 and 10 mol% (Table 13C in app. C).

coarse amphibole

This amphibole forms large (up to 100 μm) subhedral grains and amounts to up to 10 vol.%. It develops at the cost of small symplectitic amphiboles and has inclusions of ab, czo and ttn. The composition (Table C20 in app. C) varies from actinolitic-hornblende to actinolite (names after Leake, 1978).

epidote (czoV)

Clinozoisite V and czoIV amount to up to 5 vol.% of the rocks and have the same composition. Clinozoisite V occurs as large up to 100 μm anhedral grains in the mineral aggregates replacing garnet.

chlorite (chl)

Chlorite amounts to up to 10 vol.% in group 4 eclogites. Composition, distribution and textural position are the same as in group 3 eclogites. The difference between group 3 and 4 eclogites lies mainly in the larger amount of chl that cannot be attributed to grt or pg in group 4 eclogites.

titanite (ttn)

Titanite amounts to nearly 4 vol.% of group 4 eclogites. It occurs as anhedral grains of up to 100 μm in size, often with some rt or ilm in its core. It also occurs as euhedral (up to cm-sized) grains in the host rock of some ttn-bearing quartz veins. Its composition (Table C17 in app. C) is $Ca(Ti_{0.95}\ Al_{0.05})[SiO_4](O,OH,F)$.

3.1.5.2 Mineral paragenesis and PT-estimates

In the group 4 eclogites the mineral assemblage is ab, green amp, chl, czoV, and ttn. Green amp, chl, and CzoV still have large variations in their compositions, partly due to formation at different

textural sites and partly inherited from earlier replacement stages. However, compared to group 3 eclogites the amount of these two minerals with intermediate compositions has increased. This indicates that the size of the local equilibrium domains has increased, but is still below the size of a thin section. In the greenschists, the size of the equilibrium domains is larger than the thin section.

PT-estimates

No reliable geothermobarometers exist for this low temperature mineral assemblage (e.g. Essenne, 1989; Evans, 1990) and one has to rely on petrogenetic grids to obtain pressure and temperature estimates for these rocks. In the petrogenetic grid of Evans (1990), for a similar bulk rock composition as the Lago di Cignana metabasic rocks (Table 6), the assemblage actinolitic amphibole, albite, epidote, chlorite and quartz is stable at pressures below 0.7 GPa, relatively independant of temperature. A reliable temperature for this replacement stage cannot be obtained with the Holland & Blundy (1994) plagioclase amphibole thermometer, because even more amphiboles than in group 3 eclogites have compositions with Si > 7.7 pfu and are outside the compositional limit of the thermometer (Holland & Blundy, 1994). These amphiboles, however, indicate formation at temperatutes below 475 °C. Consequently, the mineral paragenesis of group 4 eclogites and the greenschists probably formed at temperatures below 475 °C and pressures below 0.7 GPa.

3.2 Structures in the eclogites

The only primary structures discernible in the metabasic rocks from Lago di Cignana are deformed pillows, which have been described from many locations within the Zermatt Saas zone (e.g., Bearth, 1959; Oberhänsli, 1982). Where preserved, they consist of omp-rich cores grading into gln-rich rims. The interstices between individual pillows are filled by a gln-rich matrix with qtz and carbonate. In most cases, however, the group 1 eclogites reveal a compositional banding of alternating gln- and omp-rich layers. This banding, presumably, originated from extreme flattening of pillows. This interpretation is supported by the observation of structures resembling isoclinal fold hinges in gln-rich layers, always with gln poorer eclogite in the core, as well as by the discontinuous compositional banding and the gradual changes in gln-content.

Table 6

Mineral compositions of the minerals used by Evans (1990) to construct his petrogenetic grid and the composition of these minerals in the metabasic rocks at Lago di Cignana.

Model	Na-amphibole		Ca-amphibole	chlorite	garnet	epidote	pumpellyite		omphacite
	Mg	Al	Mg	Mg	Mg	Al	Al	Mg	X^{m1}_{Mg}
Evans 1	0.75	0.85	0.834	0.738	0.22	0.82	0.98	0.88	0.43
Evans 2	0.50	0.85	0.625	0.483	0.086	0.82	0.98	0.70	0.33
Evans 3	0.75	0.70	0.834	0.738	0.22	0.78	0.97	0.88	0.43
Evans 4	0.50	0.70	0.625	0.483	0.086	0.78	0.97	0.70	0.33
Cignana	0.75	0.88	0.753	0.644	0.27	0.77	-	-	0.37
2σ	0.08	0.09	0.074	0.056	0.12	0.04	-	-	0.10

The compositional banding, together with a shape preferred orientation of omp, gln, pg, and elongated (clino-)zoisite aggregates (Fig. 12) defines the foliation (S_{1e}) that strikes approximately NE and dips with an angle between 20 and 50° towards the NW (Fig. 13). The orientation of S_{1e} varies between different outcrops, but the spread usually overlaps. On this foliation, a stretching lineation (L_{1e}) is defined by the long axes of gln crystals and elongated aggregates of (clino-)zoisite. The stretching lineation plunges with around 15° to the WNW (Fig. 13). The foliation S_{1e} flows around garnets with symmetric strain shadows filled with coarse-grained (400 µm) omp (Fig. 12). This shows that grt had grown before deformation D_{1e}. The finer grained (40 µm) matrix omp has serrated grain boundaries. This indicates that omp deformed plastically by a combination of dislocation creep and dynamic recrystallisation by grain boundary migration (Buatier et al., 1991; Godard & van Roermund, 1995). In rocks completely transformed to a lower grade paragenesis, the compositional banding is no longer discernible. The foliation S_{1e} is, however, preserved due to pseudomorphic replacement of the UHPM minerals by lower PT-replacement products (Fig. 14). The czo aggregates after zoi and pg, and the symplectites of ab and blue-green amp after omp and gln, preserve the shape of the precursor mineral grains and, in this way, the foliation.

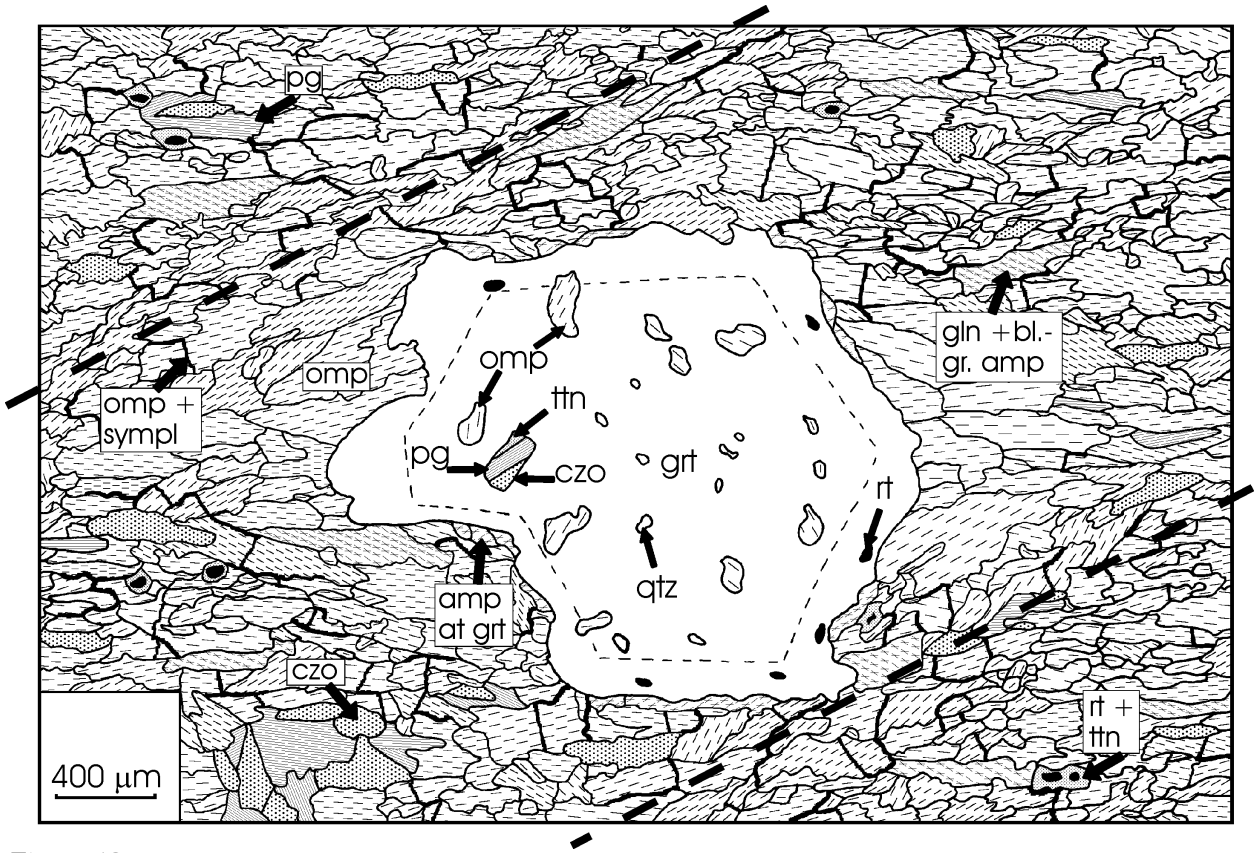

Figure 12

Microstructure of a group 1 eclogite: Grt poikiloblast in a matrix of omp, gln with rims of blue-green amp, rt with ttn rim, czo and pg. Strain shadows at grt filled with omp. The foliation S_{1e}, defined by the shape preferred orientation of omp, gln, pg and czo aggregates lies horizontal. Shear bands S_{2e} (indicated by dashed lines) follow the boundaries of the strain shadows. Note the irregular, patchy distribution of blue-green amp-ab symplectites on intergranular fractures and along omp high-angle grain boundaries and amp overgrowths on grt. The thin dashed line in grt indicates the change of the trend in compositional zoning (Fig. 6). Grt contains inclusions of omp, rt and box-shaped czo-pg ± ttn pseudomorphs after lawsonite.

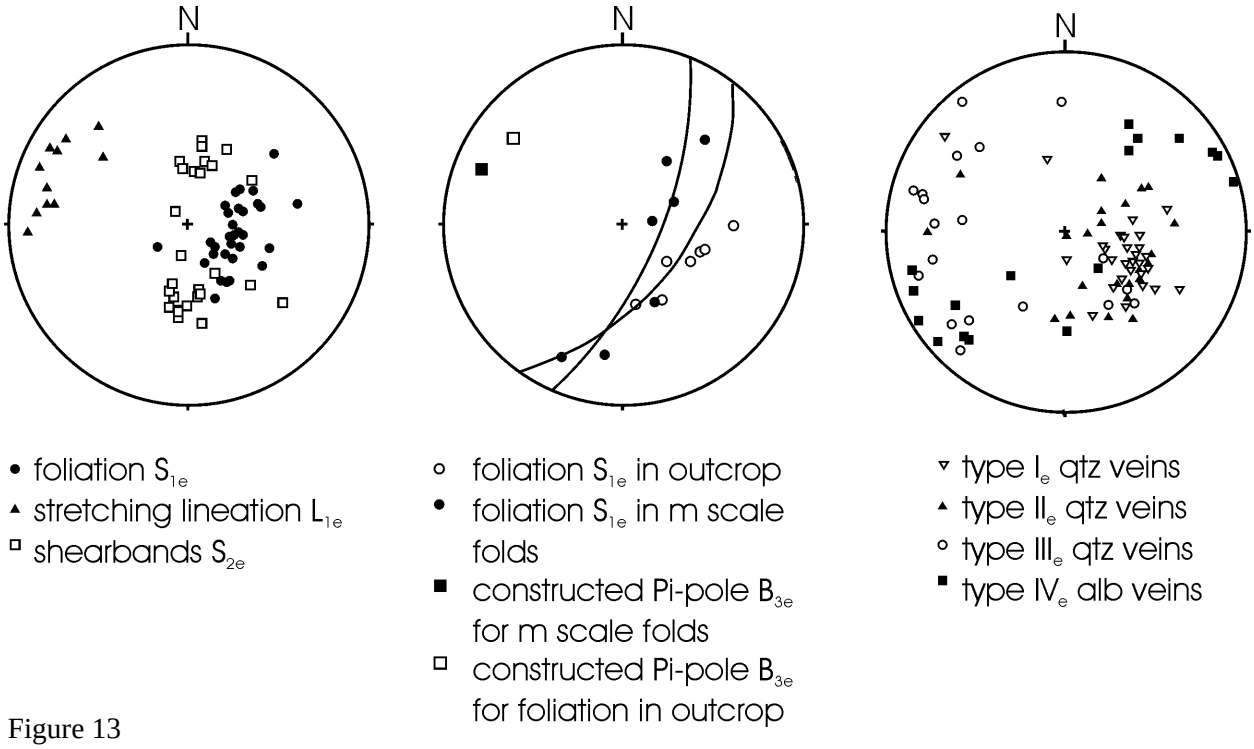

Figure 13

Orientation of structural elements in eclogites, depicted in stereographic projections (lower hemisphere, equal area). Left: foliation S_{1e}, lineation L_{1e} and shearbands S_{2e}. Center: π-pole construction of D_{3e} open folds. Right: orientation of veins.

Locally, S_{1e} is crosscut by extensional shearbands (e.c.c.´s = extensional crenulation cleavage, S_{2e}) (Figs. 12, 13). The distribution of S_{2e} is heterogeneous. Zones with closely spaced shearbands alternate with zones were they are rare. Orientation of S_{2e} varies between the outcrops, as does the foliation S_{1e}. Usually, two sets of shearbands form a conjugate system with one of the orientations dominating in one outcrop. Shearbands nucleated at garnets following the S_{1e} strainshadow interface and developed by coalescence of these domains. S_{2e} is defined by a shape preferred orientation of omp. The coarser grainsize (up to 400 µm) of omp along S_{2e} compared to the matrix, indicates that S_{2e} had formed before transformation of the eclogite to a lower grade mineral paragenesis had started. There is no systematic difference in compositions between matrix omp and coarse grains in S_{2e}. Furthermore, a quartz pseudomorph after coesite has been found in one of the coarse omphacites. All these evidences suggest that S_{2e} (e.c.c.) formed under UHP metamorphic conditions. In eclogites transformed to lower grade paragenesis, S_{2e} was preserved, because symplectites of ab and blue-green amp preserve the shape of precursor omp grains. The frequently observed concentration of minerals formed during lower PT-replacement along S_{2e} is attributed to later fluid infiltration focused along these discontinuities. Fluid infiltration is also suggested by the relative abundance of quartz and calcite along S_{2e} compared to the host rocks.

Later localisation of deformation in the eclogites is revealed by several generations of veins of various kind and scale and by other structures. Veins will be presented first, because they can be used as a reference frame for later deformation stages. The microstructures, fabrics, and fluid inclusions data from veins will be presented in chapter 5. Veins in the eclogites can be classified into four groups (Fig. 15).

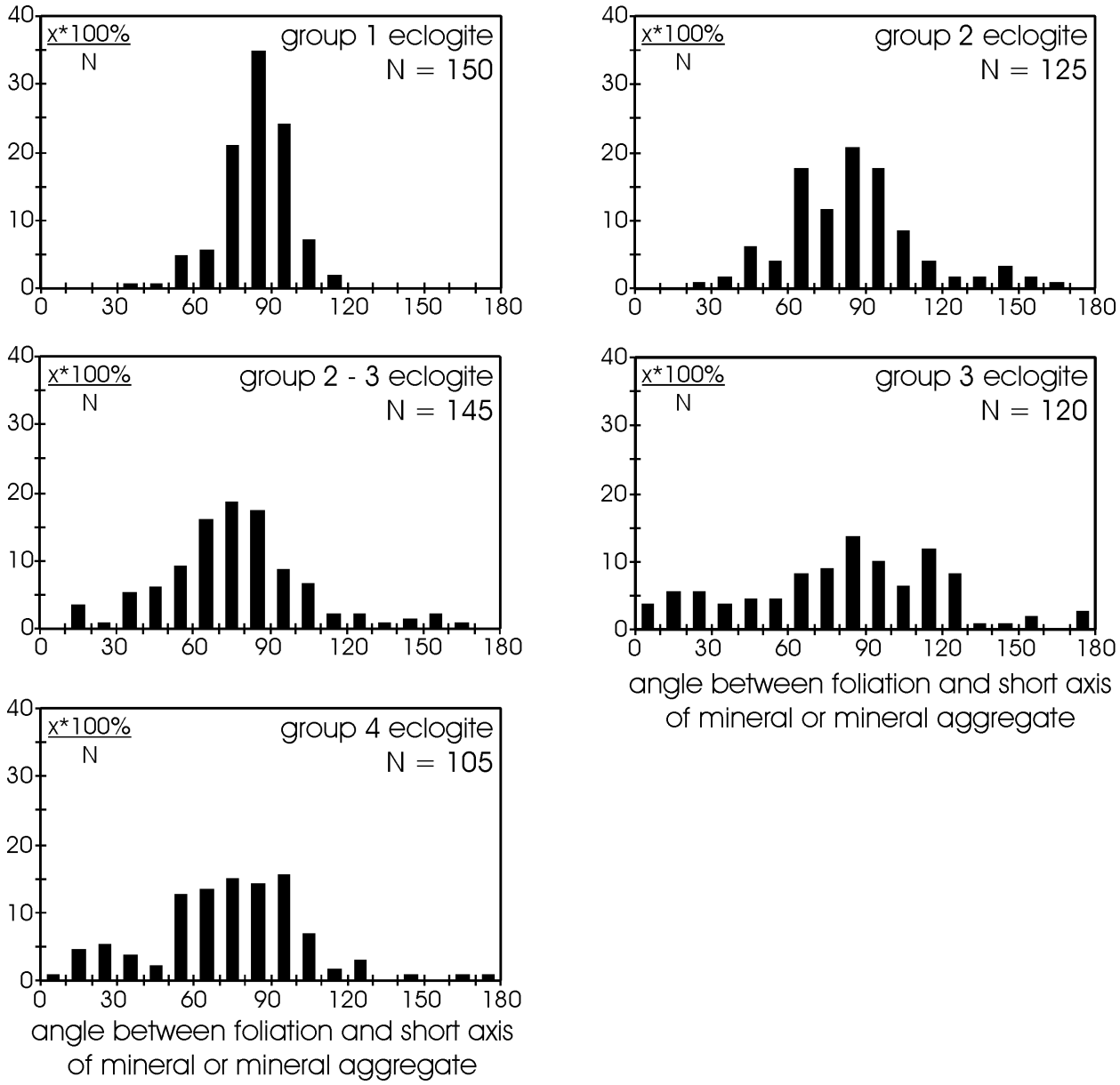

Figure 14

Histograms showing the abundance of measured angles between foliation and shortest dimension of minerals or mineral aggregates for eclogites with different amounts of lower PT-replacement products. Mineral aggregates that formed at the expense of UHP minerals approximately preserve the shape preferred orientation of this mineral and in this way the foliation. In group 3 and 4 eclogites, growth of a amphibole at the expense of symplectitic amphibole partly destroys this pattern.

Type I_e veins are orientated sub-parallel to the foliation S_{1e} (Fig. 13, 15). They exhibit low aspect ratios (< 5) and the opposing flanks do not fit. The vein mineralisation is composed of czo or qtz often accompanied by minor amounts of omp, gln, ap, and rt, or by minor amounts of ttn, and czo. Quartz in these veins is completely recrystallised. Other minerals are usually subhedral, without any obvious lattice or shape preferred orientation. Where abundant, czo forms fibers perpendicular to the vein flanks. The least transformed host rocks of type I_e veins are the group 1 eclogites.

Type II_e veins are orientated sub-parallel to the foliation S_{1e} or sub-parallel to the shearband foliation S_{2e} (Fig. 13, 15). Their aspect ratio ranges up to 10. There is no fit between the

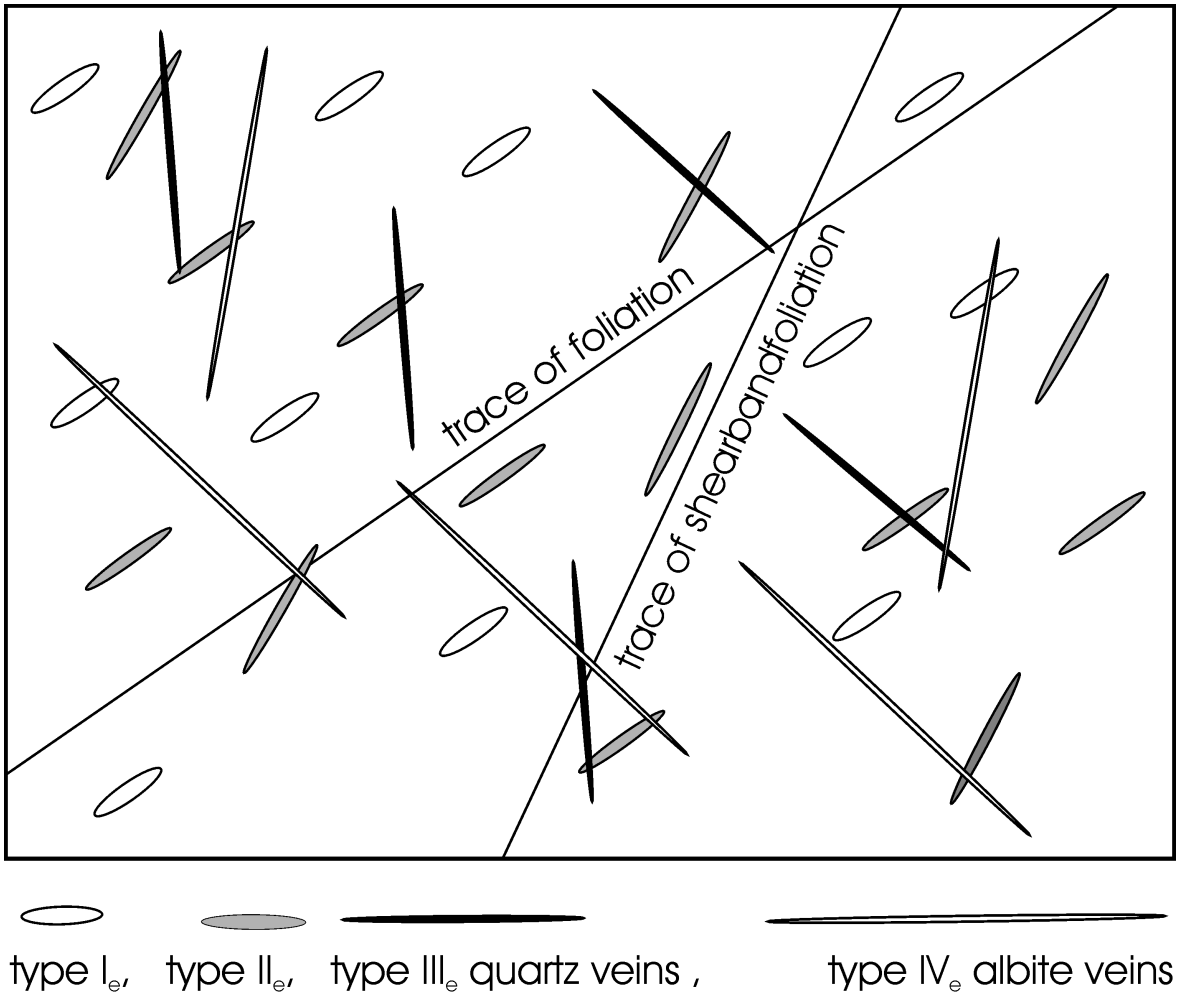

Figure 15

Schematic diagram (not to scale) depicting orientation, crosscutting relations and aspect ratios of the different vein types and their relation to orientation of foliation $S1_e$ and shearbands $S2_e$ as seen on a horizontal plane. Chronological relations between type I_e and type II_e veins could not be deduced. Strike of the foliation is NE with 20-50° dip to the NW. The trace of UHPM extensional shearbands cuts the foliation at a low angle. Late shear zones possibly synchronous with type IV_e veins are not shown.

opposing flanks. The vein mineralogy is qtz, often associated with czo or ttn. The qtz is partly to completely recrystallised. Other minerals present in these veins occur as subhedral grains without shape preferred orientation. The least transformed host rocks of type II_e veins are the group 2 eclogites.

Type III_e veins are orientated at a higher angle (> 30°) to the foliation S_{1e} and the shearbands S_{2e} (Fig. 13, 15). They have aspect ratios up to 40. Usually, there is no fit between the opposing flanks. Their mineralogy is qtz with green amp, with ttn or with czo. The qtz is partly to completely recrystallised. Other minerals present in these veins occur as subhedral grains, without obvious shape preferred orientation. The host rocks of type III_e veins are mainly the group 3 and 4 eclogites.

Type IV_e veins are also orientated at a high angle to foliation S_{1e} and shearbands S_{2e} (Fig. 13, 15). These veins have a high (> 30) aspect ratio and the opposing flanks fit. Their mineralogy is ab, often with green amp and rarely epidote. The primary vein filling structure is preserved,

with fibrous ab, amp and epidote, oriented perpendicular to the vein flank. Crosscutting relations between ab veins, indicate that at least three generations of ab veins exist. The host rock of type IV_e ab veins are the group 4 transformed eclogites.

Locally, foliation S_{1e} is folded on an m to 10 m scale, clearly discernible on stereographic projections of the foliation poles (Fig. 13). On the outcrop scale, open folds with a corresponding orientation (E-W trending fold axes) and a wavelength in the dm- to cm-range are observed. Initial stages of an axial plane crenulation cleavage (S_{3e}) are developed in places. The fold limbs of these microfolds are enriched in amphibole when compared to the fold hinges, indicating that dissolution precipitation creep was involved. A type I_e or II_e qtz vein has also been folded. The folding of foliation S_{1e} in some group 4 transformed eclogites, suggest that deformation D_{3e} took place at T < 475 °C and P < 0.7 GPa.

Late shear zones (D_{4e1}) occur in an eclogitic lens within the metasedimentary rocks. The continuation of the shear zones into the metasedimentary rocks is not exposed. The shearzones strike between E-W and NE-SW and dip with 60° NNW. They acted as normal faults with a dextral strike slip component. Each zone is 30 to 40 cm wide; with the spacing in between ranging from 1.5 to 3 m. The displacement across each individual shear zone is in the order of a few cm as indicated by displaced early albite veins. These shearzones are crosscut by late ab veins.

Another shear zone (D_{4e2}) occurs in a qtz-ab vein in eclogite. Deformation concentrated in the 10-15 cm wide vein, with the wall rock of the vein, consisting of group 4 transformed eclogite,

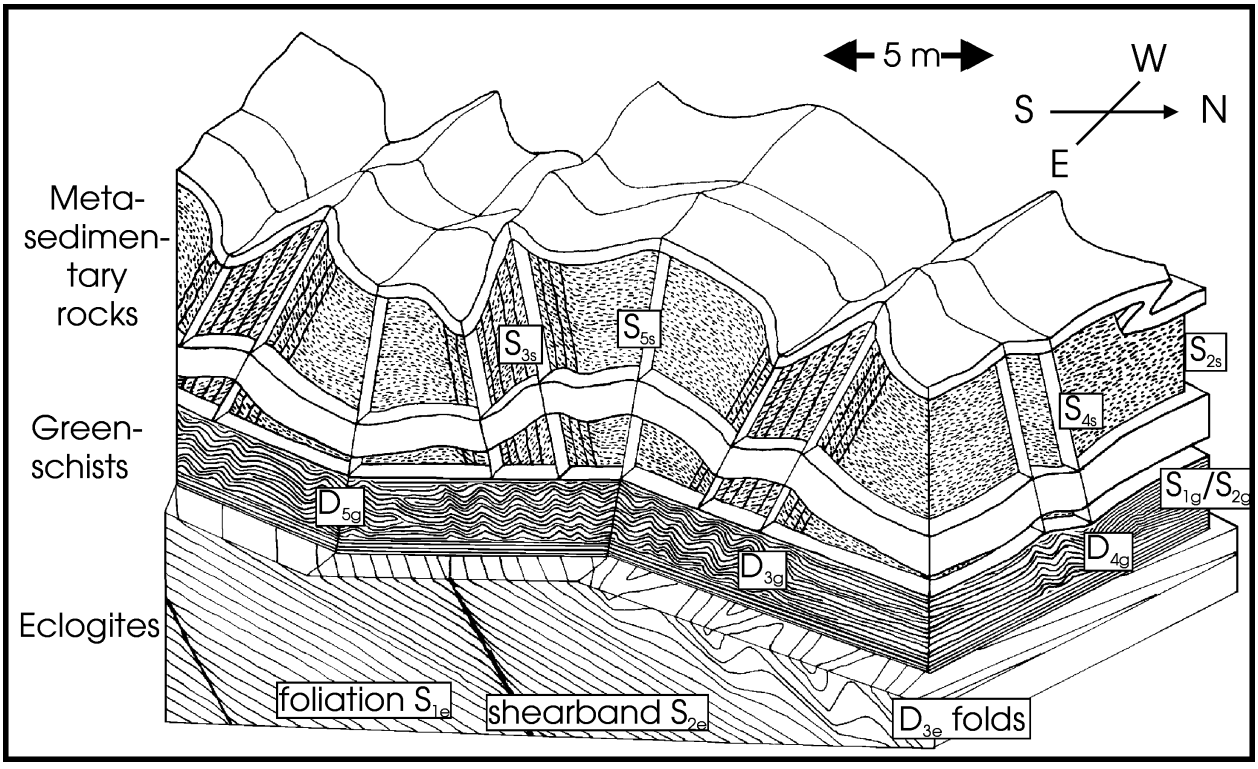

Figure 16

Schematic sketch of mesoscopic structural relations between eclogites, greenschists and metasedimentary rocks at Lago di Cignana. Late shearzones in eclogite (D_{4e1}, D_{4e2}) and veins in eclogites and metasedimentary rocks are not shown.

remaining undeformed. The vein strikes NNE-SSW and dips with 60° W. The exposed length is approx. 10 m; the magnitude of displacement is unknown. The sheared vein is crosscut by late ab veins.

3.3 Structures in the greenschists

More intensive deformation led to the transformation of the pseudomorphically replaced group 4 eclogite into a true greenschist. Therefore, deformation of the greenschists must have occurred at T < 475 °C and P < 0.7 GPa. The foliation of the greenschists (S_{1g}, strike NE, dip 30° NW) is defined by alternating layers of amp or ab and by a shape preferred orientation of green amp (grainsize ca. 100 µm) and epidote, and developed out of S_{3e}. The main foliation is isoclinally folded (D_{2g}), with transposition of S_{1g} to S_{2g}, but without development of a new foliation in the fold hinges. Amphibole has partly recrystallised in the fold hinges. Locally, this foliation (S_{1g}/S_{2g}) is folded on an m- to cm-scale around E-W trending fold axes with a steep axial plane striking approximately E-W (D_{3g}). Furthermore, open folds with vertical N-S (D_{4g}) and E-W (D_{5g}) striking axial planes occur. The orientation of the folds in the greenschists is similar to the orientation of the folds in the metasedimentary rocks (Fig. 16, 17). The greenschists are devoid of veins.

4 The record of the metasedimentary rocks

In this chapter the petrologic and structural records of the metasedimentary rocks will be presented. The record preserved in the veins of the metasedimentary rocks is presented in chapter 5.

4.1 Petrology of the metasedimentary rocks

The petrology of the metasedimentary rocks is a summary of the results of Reinecke (1991; 1995; 1998). The metasedimentary rocks are mainly garnet-phengite-quartz-schists, with variable amounts of dolomite, calcite, paragonite, and epidote. Subordinately, garnet-clinopyroxene-quartzites and piemontite-phengite-quartz-schists occur. The bulk rock composition is very heterogeneous and often changes on a cm-scale. Some samples show up to three stages of garnet growth, associated with varied low-variance inclusion assemblages as well as compositionally zoned phases (e.g., phengite, dolomite, calcite) and distinct reaction textures in the matrix. These rocks provide ample information for the reconstruction of their PT-path. Combining results derived by methods of absolute (geo-Calc-Software: Brown et al., 1988, database of Berman, 1988) and relative thermobarometry (Spear, 1988; Spear & Menard, 1989; Spear, 1993) from three different bulk rock compositions, Reinecke (1995; 1998) has produced a well constrained PT-path of the metasedimentary rocks at Lago di Cignana. The principal results are given below:

Maximum pressures of about 2.8-3.0 GPa were attained at about 600 °C. The thermal peak was reached at 30-45 °C higher temperatures and 0.2-0.3 GPa lower pressures.

Early denudation to approx. 2.3 GPa, into the stability field of quartz, was accompanied by a significant (about 50 °C) temperature decrease.

Decompression from 1.7-1.9 GPa to 1.1-1.2 GPa was almost isothermal (at 500-550 °C).

Further decompression from about 1.1 GPa to 0.6 GPa was accompanied by a temperature decrease from 550 to 450 °C.

A late greenschist facies overprint occurred at 350-420 °C and 0.2-0.5 GPa.

4.2 Structures in the metasedimentary rocks

The compositional banding in the metasedimentary rocks is interpreted as bedding. Sub-parallel to this banding a foliation is developed. Isoclinal folds in compositional bands and foliation prove that the dominant schistosity is at least the second foliation (S_{2s}, strike NE, dip 20° SE, Fig. 17). The foliation is defined by alternating layers rich in quartz and mica, and by the shape preferred orientation of phengite, clinozoisite/epidote, and albite-amphibole symplectites. The stretching lineation (L_{2s}, trend WNW, plunge subhorizontal, Fig. 17) is defined by the shape preferred orientation of clinozoisite/epidote. Boudins of metabasic and quartzitic rocks in a matrix of mica rich rocks are observed in this foliation. The width of the boudins is up to 30 cm and their length up to 40 cm. The boudin necks are filled with quartz and clinozoisite. The quartzitic boudins are slightly rotated along N-S striking, 20° E dipping shearzones. The asymmetric strain shadows at the eclogitic boudins suggest non coaxial deformation and top to the N displacement (Photo 8). Because S_{2s} always flows

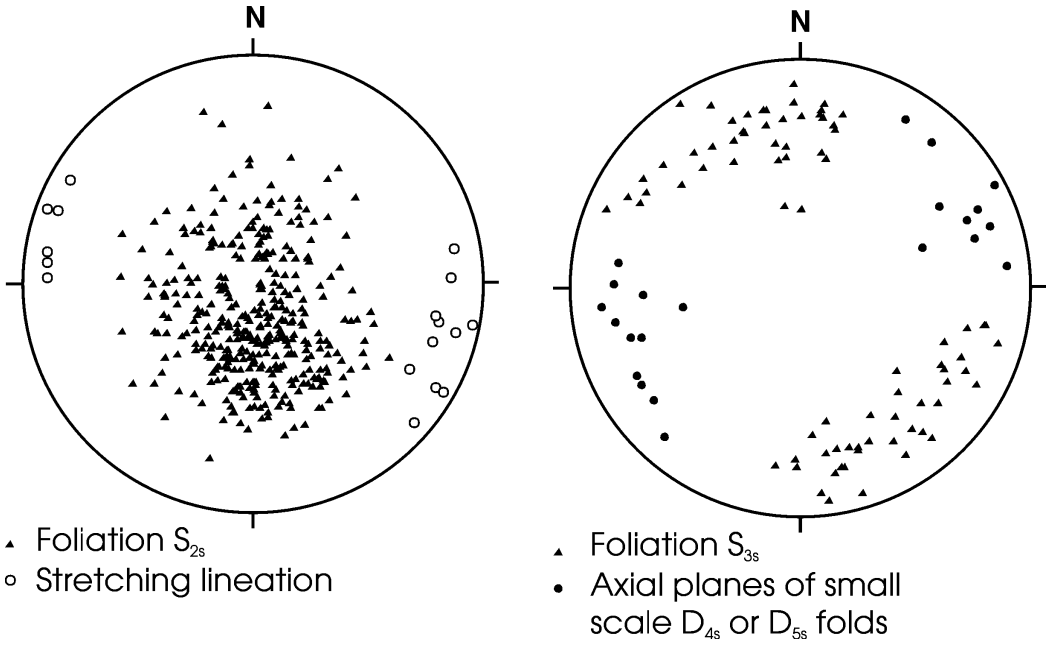

Figure 17

Orientation of structural elements in the metasedimentary rocks, depicted in stereographic projections (lower hemisphere, equal area). Left: Poles of foliation S_{2s} and stretching lineation L_{2s}, Right: Poles of foliation S_{3s} and axial planes to smal scale $D_{4s\ or\ 5s}$ folds

around garnets, these must have been mechanically effective during formation of foliation S_{2s}. Reinecke (1995) calculated the PT-path of the metasedimentary rocks from profiles of zoned garnets. Therefore, S_{2s} must have formed after the last garnet growth at T < 450 °C and P < 0.6 GPa (Reinecke, 1995). In some rock types, the foliation S_{2s} is partly defined by the shape preferred orientation of fine grained aggregates of tremolite + microcline + albite + hematite ± jadeite poor aegerineaugite, that replace UHPM aegerineaugite with $jd_{26\text{-}37}$ (Reinecke, 1995). These fine grained aggregates are undeformed, indicating that the replacement occurred after formation of the foliation. Therefore, S_{2s} must have formed before the late greenschist reequilibration at 350-420 °C and 0.2-0.5 GPa inferred by Reinecke (1995) from these aggregates.

Locally, the foliation S_{2s} is folded on a mm- to 10-m scale (figure 19). A first generation of approximately N-verging folds (D_{3s}) developed an axial plane crenulation cleavage (S_{3s} strike E-W, dip vertical) in mica rich layers. Foliation S_{3s} is defined by a shape preferred orientation of mica and clinozoisite. Foliation S_{2s} and S_{3s} are locally folded on a cm- to m-scale. The relative timing of formation of the later generations of open folds (D_{4s} and D_{5s}) is unclear, because an axial plane cleavage has not developed. Axial planes of D_{4s} and D_{5s} folds strike approximately NE-SW and N-S, respectively, and are almost vertical. Distinction between small scale D_{3s} and $D_{4s\ or\ 5s}$ folds is only possible, when both generations occur in close contact and can be correlated with m-scale folds. These deformation phases could not be correlated with petrologic observations.

In the metasedimentary rocks, veins can be classified into four groups using their relation to foliations S_{2s} and S_{3s}, vein mineralogy and microstructure. The deformation microstructures and fabrics of veins will be presented in chapter 5.

Photo 8

A lens of high viscous eclogite in a matrix of low viscous metasedimentary rocks. The assymmetric structure suggests a high degree of non coaxial deformation. N is up, length of eclogitic lens is ca. 0.5 m.

Photo 9

Dust trails in vein albite, define an older growth structure. Long side of photograph is 7 mm.

Type I_s veins are oriented sub-parallel to the foliation S_{2s}. They often form lenses in the foliation that are the hinges of (refolded) isoclinal folds. The veins are mineralised with quartz, often associated with garnet and white mica. In some veins, garnet is the main vein filling mineral. Quartz in the veins is completely recrystallised. Garnet and white mica are euhedral and white mica has a shape preferred orientation parallel to the foliation outside the vein. In one garnet from these veins, an inclusion of coesite was unequivocally identified. This suggests that at least some of the earliest veins were formed at UHPM conditions or prior to UHPM and recrystallised during UHPM.

Type II_s veins are oriented at an angle (> 10°) to foliation S_{2s} and are sometimes folded by D_{3s}. Aspect ratios of unfolded veins are high (> 20) and opposing vein flanks fit. These veins are mineralised with quartz and clinozoisite. Quartz in those veins is partly recrystallised. Clinozoisite grains are subhedral and often broken.

Type III_s veins crosscut S_{2s} and (where present) S_{3s}. These veins have high aspect ratios (> 30) and opposing flanks fit. They are mineralised with quartz and clinozoisite and/or green amphibole. A vein filling structure is preserved with large (cm-sized) quartz grains, that often

enclose mm-sized amphibole needles. When clinozoisite is present, it forms cm-sized, subhedral grains.

Type IV_s veins are oriented at an angle to S_{2s} and (where present) S_{3s}. These veins have high aspect ratio (> 30) and opposing flanks fit. They are mineralised with albite. A vein filling structure is preserved, with mm-sized subhedral albite grains, that extend from the vein flanks to the vein centre. The centre of the vein is often an open cavity. Fine dust trails in the albite grains trace the outlines of older minerals (Photo 9).

5 Quartz veins (microstructures, fabrics and fluid inclusions)

Microstructure and fabrics of the veins give information about the stress and strain history of the host rock after vein formation and are presented first. Fluid inclusions in the veins can give thermobarometric information (e.g., Sheperd et al., 1985) and are presented at the end of the chapter.

5.1 Microstructures of vein quartz

In most quartz veins in the eclogites and the metasedimentary rocks, the primary microstructure is destroyed due to subsequent deformation by dislocation creep, that caused partial to complete recrystallisation. Locally, relic grains with a diameter of up to several millimetres are preserved in the veins; they are composed of subgrains (Photo 10).

Most quartz veins in eclogite and type I_s veins in the metasedimentary rocks have a recrystallised grain size ranging from 70 to 125 μm. The presence of other minerals, especially of white mica in some veins in the metasedimentary rocks, locally influenced size and shape of the recrystallised grains. Usually, the recrystallised grains are elongated and have a slight shape preferred orientation.

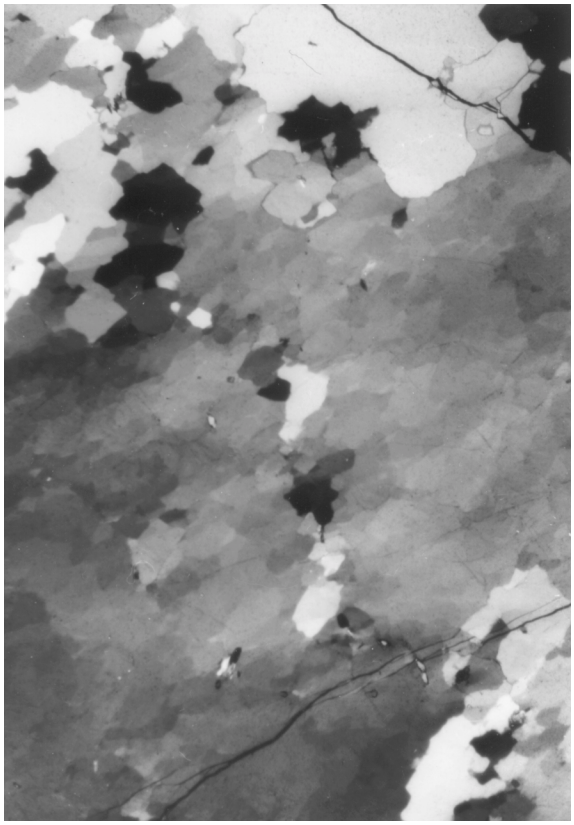

Photo 10

Microstructure of a type II_e quartz vein close to a late shearzone. The polygonisation and subgrain formation of the large grain and the recrystallisation at its rim are inferred to be due to an earlier deformation stage. Sutured grain boundaries and undulatory extinction in the recrystallised grains are due to an overprint at lower temperatures. Crossed polars, long side of the photograph is 7 mm.

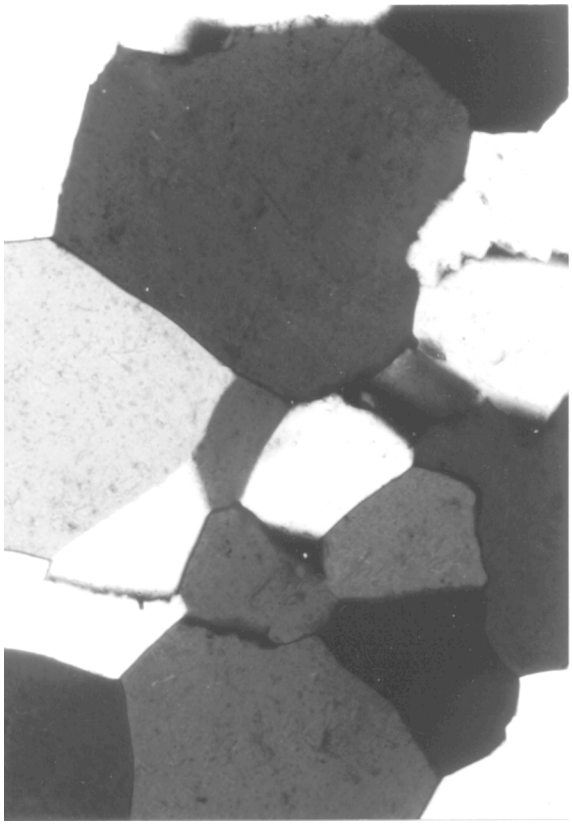

Photo 11

Microstructure of quartz in a deformed type II_e vein. The straight grain boundaris and the 120° angle at the grain edges indicate that recrystallisation was followed by grain growth under low differential stress. Crossed polars, long side of the photograph is 1.4 mm.

The grain boundaries are straight and meet with angles near 120° at grain edges (foam structure, Photo 11), indicating that the deformation was followed by normal grain growth under low differential stress.

This foam microstructure has been overprinted near the later shear zones in the eclogites (D_{4e}) and in type I_s and II_s veins in the metasedimentary rocks folded during D_{3s}(Photos 10, 12, 13). Deformation by dislocation creep under lower temperatures and higher differential stress is reflected by undulatory extinction and irregularly serrated high angle grain boundaries and small recrystallised grains. The recrystallised grain size is around 40 µm in shearzone 1 (Photo 12) and the folded veins in the metasedimentary rocks and around 10 µm in shearzone 2 (Photo 13).

5.2 Paleopiezometry

In the material science, it was noted early that the differential stress during steady state creep of metals and alloys could be related to the recrystallised grain size (e.g., Bird et al., 1969; Luton & Sellars, 1969; Glovers & Sellars, 1973). This relation was later applied to geological materials, mainly quartz and olivine (e.g., Mercier et al., 1977; Twiss, 1977; 1986). Derby & Ashby (1987) and Derby (1991) propose that the steady state grain size at constant differential stress results from

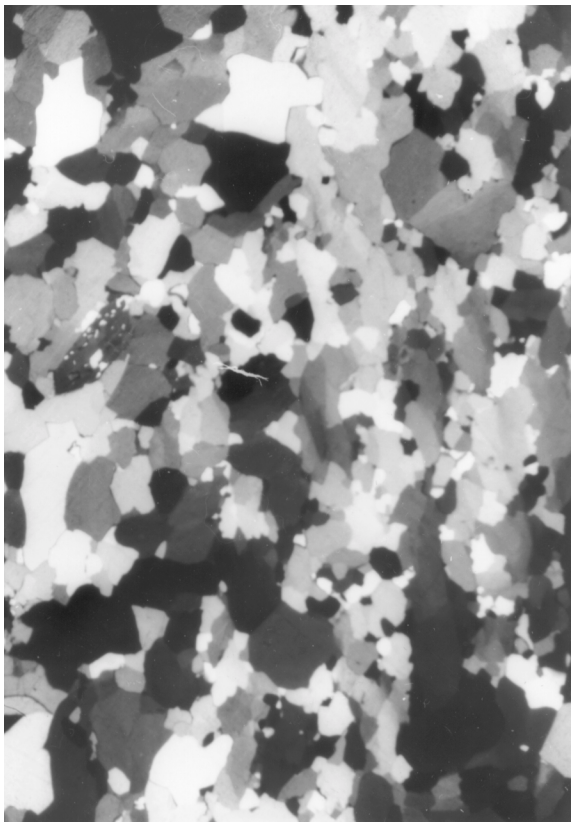

Photo 12

Microstructure of a quartz vein in a small shearzone (D_{4e1}) in an eclogite lens. Note the bimodal grain size distribution. In the upper right of the picture a glaucophane with small quartz inclusions occurs. Crossed polars, long side of the photograph is 7 mm.

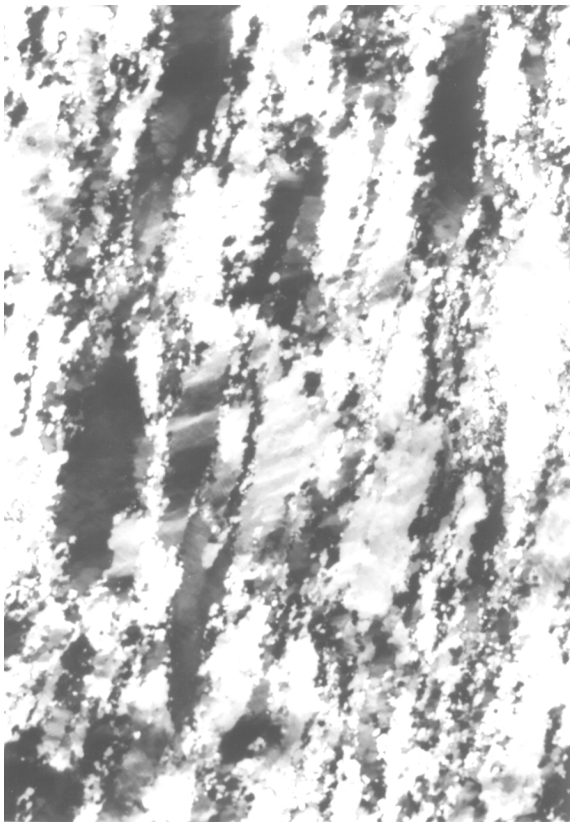

Photo 13

Core and mantle structure in a late intensively deformed quartz vein (D_{4e2}). Crossed polars, long side of the photograph is 7 mm.

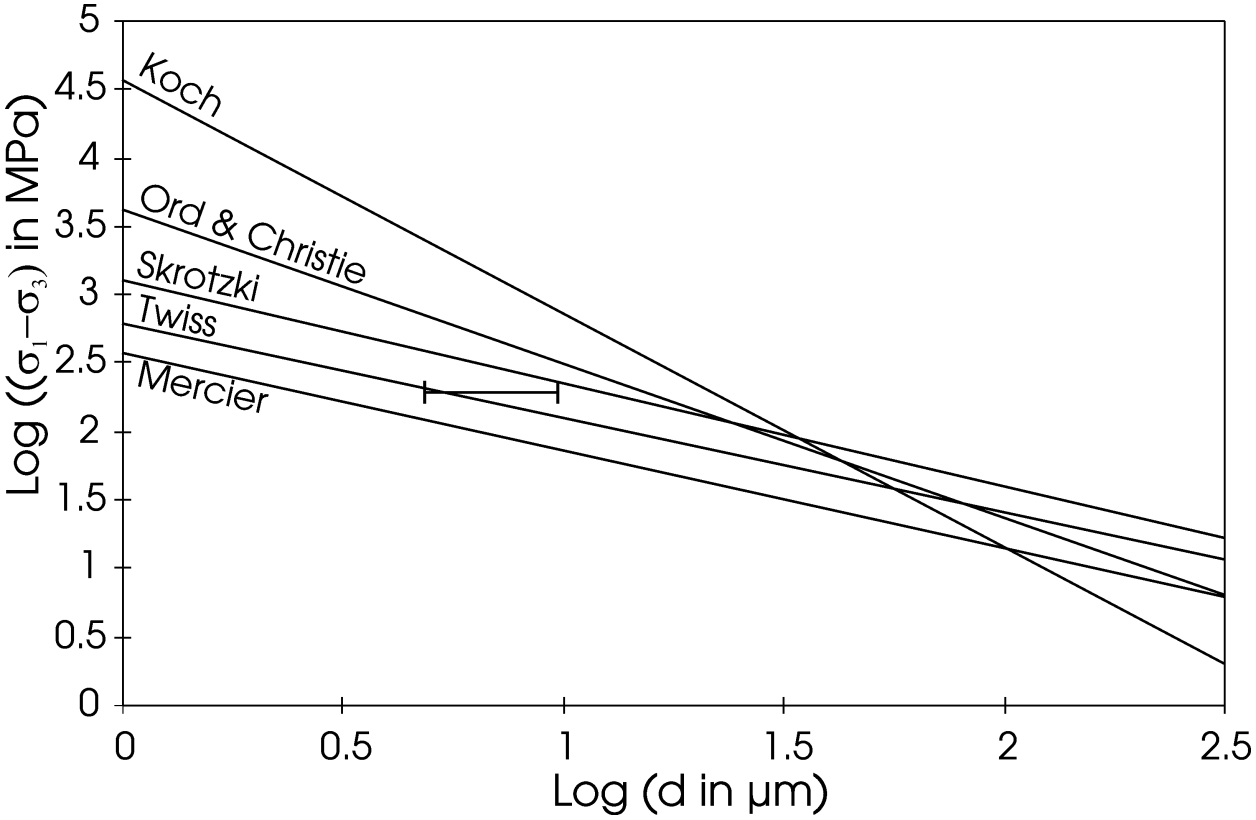

Figure 18

Several calibrations of the dynamically recrystallised grain size paleopiezometer for quartz, from Twiss (1977), Mercier et al. (1977), Koch (1983), Ord & Christie (1984), Skrotzki (1992). The barred line represents the range of recrystallised grain sizes found in a completely recrystallised sample deformed at ca. 200 MPa by Gleason et al. (1993).

a balance between the speed of recrystallisation and the rate of nucleation of new grains. This theory explains the general relation between differential stress and recrystallised grain size:

$$d/b = K_n ((\sigma_1 - \sigma_3)/ \mu)^{-n},$$

with d grainsize, b burgers vector, $(\sigma_1 - \sigma_3)$ differential stress, µ shear modulus and K_n and n constants. Twiss (1977), derived values for these constants theoretically. Other authors determined these constants by fitting the general relation to experimental data. This can be done by inserting b and µ values for one mineral (e.g., quartz) in the formula and fitting this formula to data from experiments on this mineral (e.g., Mercier et al., 1977; Koch, 1983; Ord & Christie, 1984), or by normalising the experimental data from several minerals and metals (d/b and $(\sigma_1 - \sigma_3)/\mu$) and fitting the normalised formula to the data (e.g., Skrotzki, 1992). The various calibrations of the recrystallised grainsize paleopiezometer for quartz (e.g., Twiss, 1977; Mercier et al., 1977; Koch, 1983; Ord & Christie, 1984; Skrotzki, 1992), yield highly differing results (Fig. 18). The calibrations based on experiments, yield for a given grainsize the highest differential stresses. These experiments were performed in a Griggs-Blacic solid-medium deformation apparatus (Griggs, 1967; Blacic, 1972), with either talc, pyrhophyllite, AlSiMag or copper as confining medium (e.g., Koch et al., 1989). Green & Borch (1989; 1990) showed that the strength of the materials used as confining medium could result in a large overestimate of the flow stress and recommended the use of salt as confining medium to

minimise this problem. The experiments of Gleason et al. (1993) using salts as confining medium, provide independent data to check the different calibrations. These authors report for one sample with a pre-deformation grain size of about 50 µm, a recrystallised grain size between 5 and 10 µm after 75 % shortening. The differential stress in this experiment was ca. 200 MPa (Gleason et al., 1993). This data point corresponds very well with the calibration of Twiss (1977) (Fig. 18). Therefore, the Twiss (1977) calibration of the recrystallised grainsize paleopiezometer will be used in this study.

In veins in eclogites and metasedimentary rocks, where the recrystallised grains show indications of normal grain growth, the recrystallised grain size ranges between 70 and 125 µm. The microstructure changed after deformation and does not reflect the differential stresses during deformation any longer. However, the preservation of a shape preferred orientation, suggests that the increase in grainsize was only moderate. The paleopiezometer of Twiss (1977) indicates minimal differential stresses for this deformation of 25 to 35 MPa. In the group II_s veins in the metasedimentary rocks and the veins deformed during D_{4e1}, quartz is only partly recrystallised with grain sizes ranging from 20 to 40 µm. In this case, the paleopiezometer should not be used, because it is not certain that a steady state microstructure is reached. The recrystallised grain sizes of ca. 10 µm of completely recrystallised veins deformed during D_{4e2}, points to differential stresses of ca. 125 MPa.

5.3 C-axis fabrics in quartz veins

For all recrystallised quartz veins, the c-axis fabrics were measured with standard universal stage techniques (e.g., Turner & Weiss, 1963).

5.3.1 Eclogites

The development of foliation and lineation in the eclogitic host rock predated formation and deformation of the quartz veins. Thus, these structural elements cannot be used as kinematic framework. Therefore, the textures are referred to the finite strain axes, assumed to be parallel and normal to the foliation and lineation defined by the shape preferred orientation of the recrystallised grains (Price, 1985). The measured c-axis fabrics range from point maxima, to single girdles, and weakly developed type I cross girdles (Lister, 1977), oriented at a high angle to this foliation (Fig. 19). Owing to the isolated position of the veinlets in essentially undeformed eclogites, accumulation of a large strain is precluded. Hence, the lattice preferred orientation developed during deformation is probably influenced by the orientation of the pre-existing grains. In fact, point maxima are characteristic for veins with mm-sized relic grains and better defined c-axis girdles occur in completely recrystallised veins. As such, the variation in lattice preferred orientation seemingly reflects the intensity of deformation.

For a vein deformed in shear zone 1 (D_{4e1}) the shear zone boundaries are taken as the kinematic framework. The c-axis fabric is diffuse (Fig. 19, Bk 119). Taking into account the small amount of displacement along this shearzone and the bimodal recrystallised grainsize distribution, the diffuse c-axis fabric probably reflects the overprinting of two stages of low finite strain deformation.

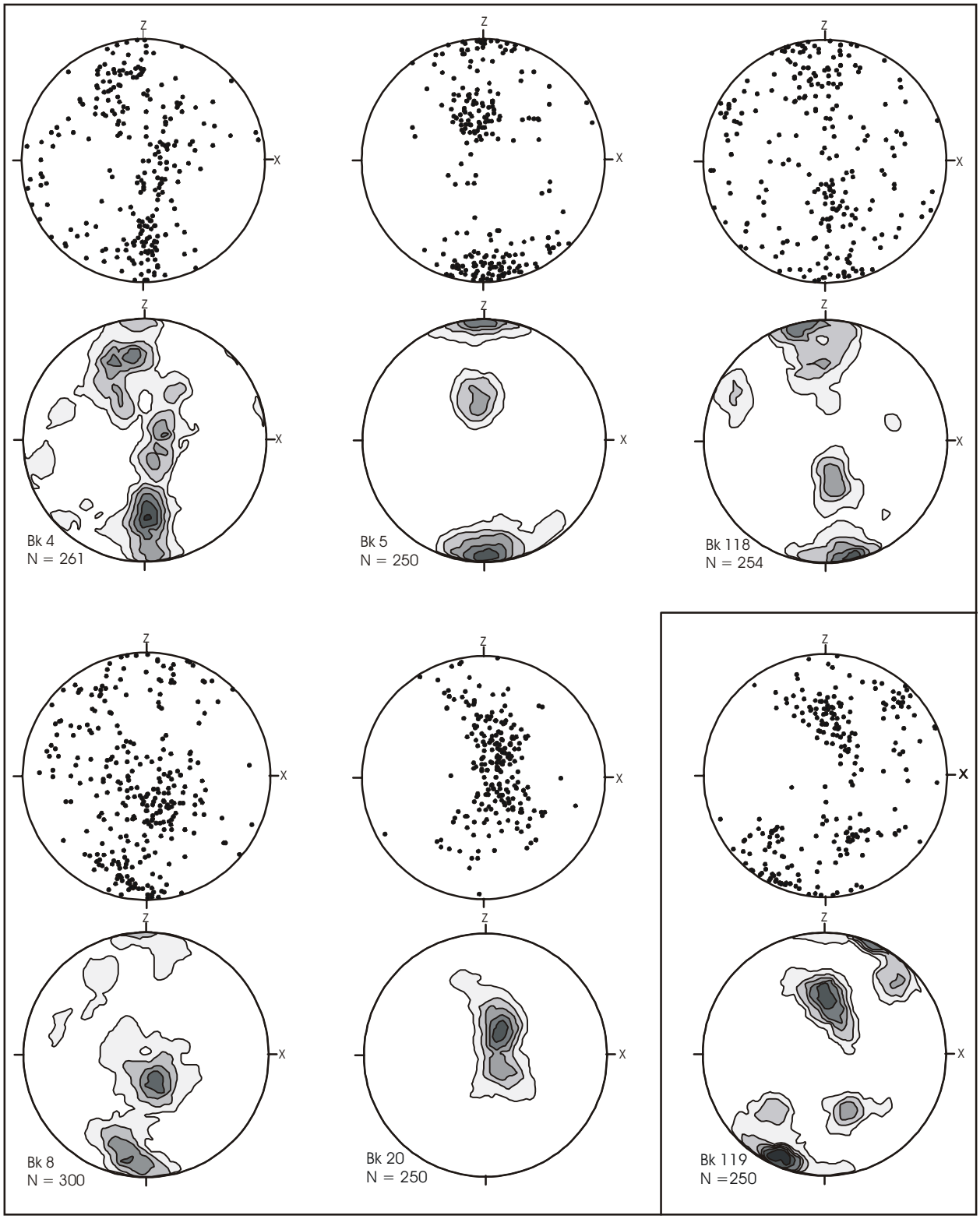

Figure 19

Lattice preferred orientation of quartz (c-axes) in selected veins in eclogite, that underwent grain growth under low differential stress after deformation (Bk 4,5,8,20,118) and a vein that deformed during D_{4e1} (Bk 119). Data are presented as scatter plots and contour plots. The orientation with respect to mesoscopic structures is for all veins only approximate. Bk 5 and Bk 8 are type I_e veins, Bk 4 and Bk 20 are type II_e veins and Bk 118 is a type III_e vein. See text for discussion.

For the veins deformed during D_{4e2}, the shear zone boundaries are not found and the textures are referred to the finite strain axes, assumed to be parallel and normal to the foliation and lineation

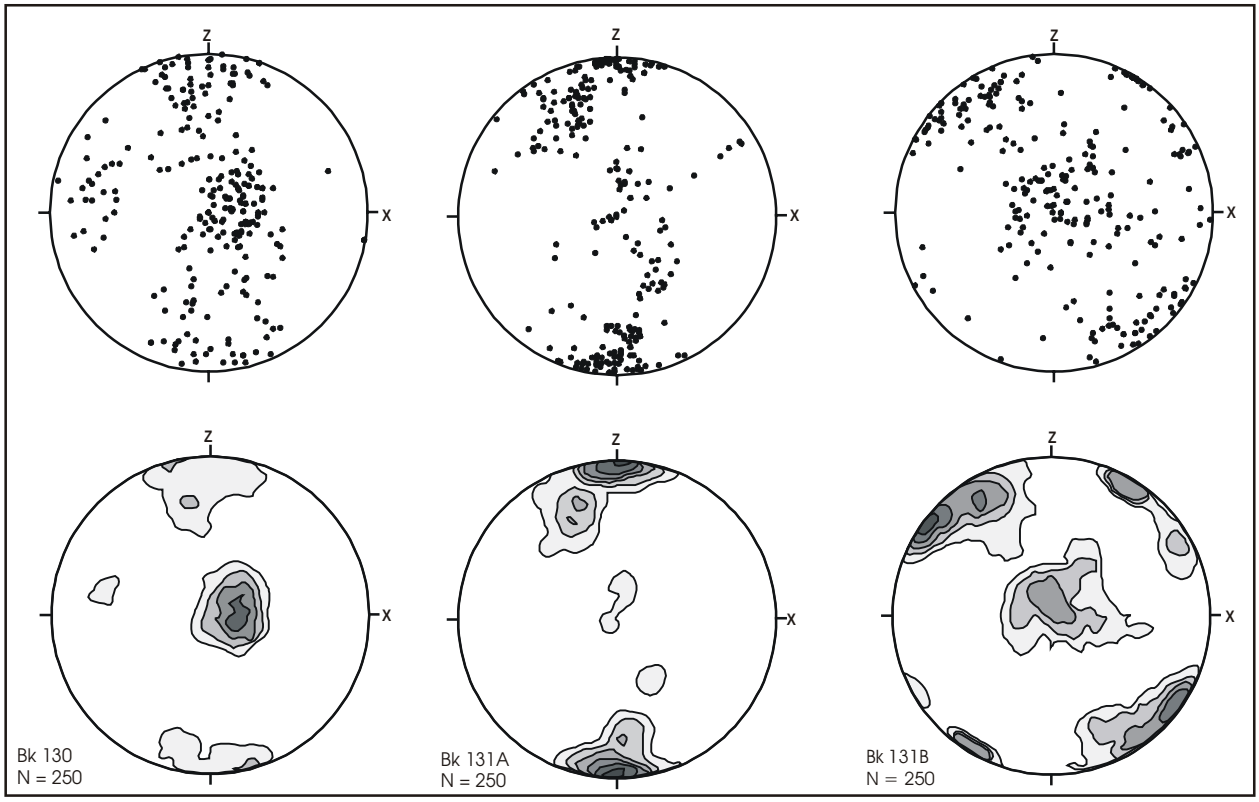

Figure 20

Lattice preferred orientation of quartz (c-axes) of veins deformed during D_{4e2}. Data are presented as scatter plots and contour plots. The orientation with respect to mesoscopic structures is for all veins only approximate.

defined by the shape preferred orientation of the recrystallised grains (Price, 1985). The c-axis fabrics for these veins are single girdles, tending towards type I crossed girdles (Fig. 20).

5.3.2 Metasedimentary rocks

For type I_s veins the foliation S_{2s} and the stretching lineation were taken as kinematic framework. The c-axis fabrics of the type I_s veins (Fig. 21) are double point maxima with one maximum approximately normal to X and Z and the other maximum at a high angle to X and Y. These could be interpreted as single girdles at a high angle to the foliation. Sample Bk 77 has large variations in c-axis orientations. This sample is from an isoclinally folded quartz vein that was refolded by D_{3s}. The large spread in c-axes reflects an overprinting of an earlier fabric by a stage of low finite strain deformation.

For type II_s veins the foliation S_{3s} and the direction normal to the fold axis were taken as kinematic framework, where S_{3s} had developed. In the other cases (Bk 46, Bk 99) the textures are referred to the finite strain axes that are assumed to be parallel and normal to the foliation and lineation defined by the shape preferred orientation of the recrystallised grains (Price, 1985). The c-axis fabrics of the type II_s veins (Fig. 22) are broad point maxima tending to weakly developed single girdles. The broad point maxima probably reflect the influence of the orientation of the large pre-existing grains on the developing lattice preferred orientation. It seems, that D_{3s} deformation of the veins was not intense enough to produce a complete new c-axis fabric. This is supported by sample Bk 77, where the earlier c-axis fabric is only slightly modified by later D_{3s} deformation.

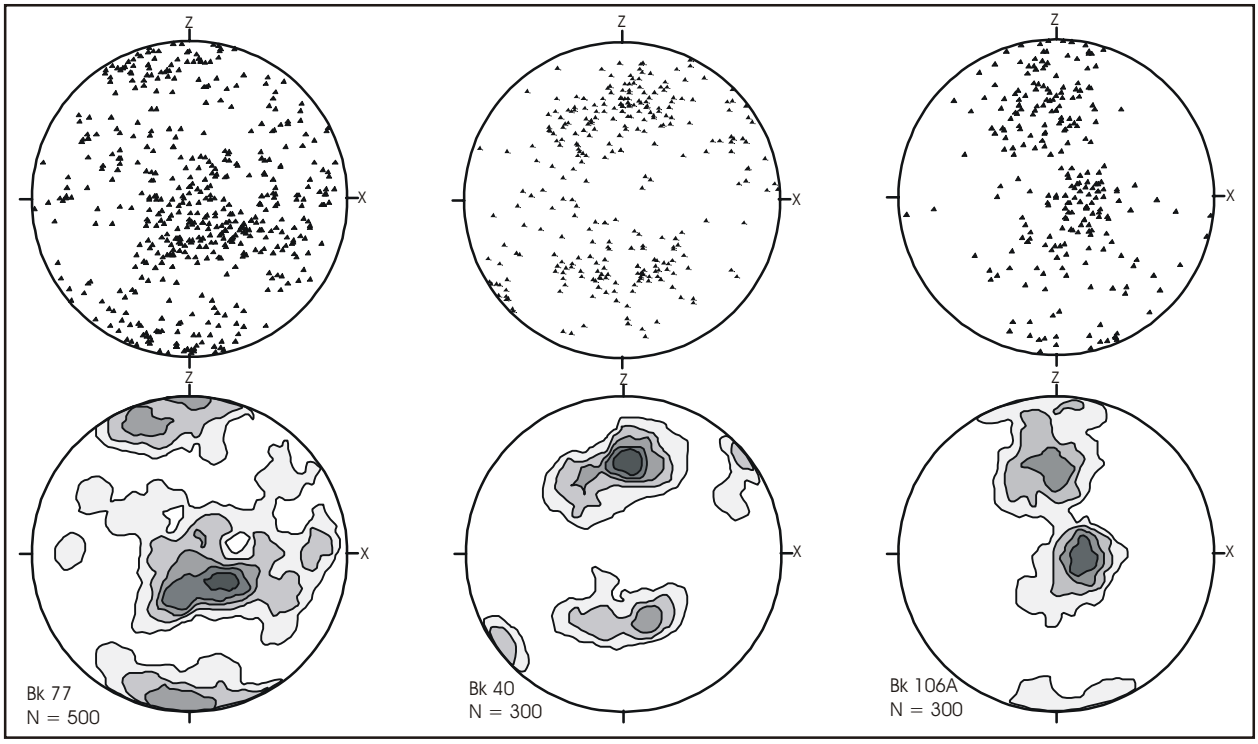

Figure 21

Lattice preferred orientation of quartz (c-axes) in veins subparallel to foliation S_{2s}. Data are presented as scatter plots and contour plots.

5.3.3 Summary

The c-axis fabrics for most veins in eclogites and metasedimentary rocks are not well enough developed to estimate strain ratios or sense of shear from these fabrics (e.g., Price, 1985). Only veins deformed in shear zone (D_{4e2}) have well-developed c-axis fabrics that suggests non coaxial deformation in this shearzone with a dextral sense of shear (Price, 1985). The c-axis girdles approximately normal to the foliation, indicate that <a> glide on various lattice planes (e.g., Schmid & Casey, 1986) was the predominant deformation mechanism. The predominance of <a> glide on various lattice planes, suggests deformation at relatively low temperatures (Hobbs, 1985).

5.4 Fluid inclusions in vein quartz

Fluid inclusions are samples of a fluid phase that may be present during a certain moment in the history of the rock. They are the only direct evidence for the presence of a fluid phase and the only possibility to physically analyse the composition of this fluid phase (e.g., Roedder, 1984). In this study, it is more important that under certain conditions thermobarometric data can be obtained from these inclusions (e.g., Roedder, 1984; Shepherd et al., 1985). Fluid inclusions can be used as thermobarometer, when their composition and density can be determined and when P(ressure)-V(olume)-T(emperature)-data for this composition are available. If the composition and volume of the inclusion did not change after formation, PT-conditions for the formation of the fluid inclusion can be inferred (e.g., Roedder, 1984).

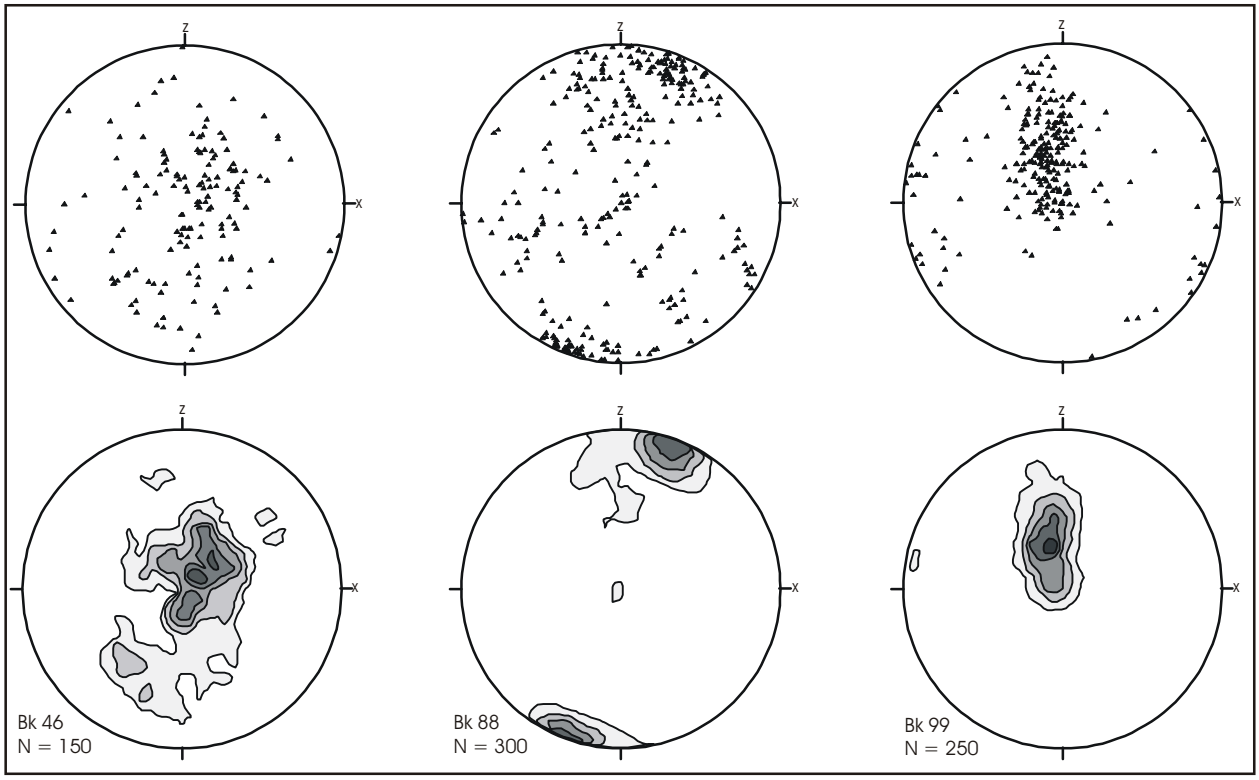

Figure 22

Lattice preferred orientation of quartz (c-axes) in veins deformed in D_{3s}. Data are presented as scatter plots and contour plots.

To interpret these PT-data the origin of the fluid inclusion must be known. Usually, a distinction between primary inclusions that formed during the growth of the host mineral and secondary inclusions that formed after the growth of the host mineral is made (Roedder, 1972).

Fluid inclusions were studied in partly to completely recrystallised type I_e and II_e quartz veins. The arrangement of the high angle grain boundaries of the recrystallised grains in these samples suggests late grain growth under low differential stress. In the recrystallised and relic grains four types of fluid inclusions are recognised:

1. Single fluid inclusions in the recrystallised grains are considered to have formed during recrystallisation (e.g., Wilkins & Barkas, 1978).
2. Fluid inclusions arranged along irregular planes in the recrystallised grains (Photo 14) are interpreted as relics of a grain boundary porosity in an originally finer grained microstructure and thus must have formed during recrystallisation (e.g., Wilkins & Barkas, 1978).
3. Fluid inclusions arranged along planes delineating subgrainboundaries in the relic grains are considered to have formed during polygonisation (e.g., Wilkins & Barkas, 1978).
4. Fluid inclusions arranged along planes that crosscut grain boundaries are interpreted as healed microcracks (e.g., Sprunt & Nur, 1979) and considered to have formed after recrystallisation.

This allows subdivision of the fluid inclusions in two main groups:

Early inclusions of the type 1, 2, and 3 that formed during deformation and recrystallisation of the original vein filling material and are secondary inclusions after Roedder (1972) with

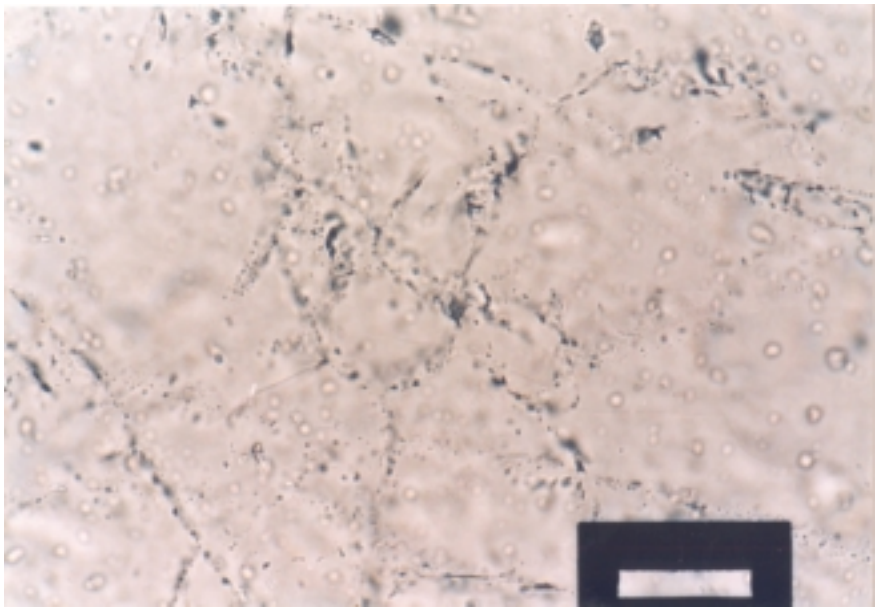

Photo 14

Fluid inclusions arranged along irregular planes in a recrystallised grain, are interpreted as relics of a grain boundary porosity in an originally fine grained structure. In the lower left corner of the photograph a trail of secondary inclusions occurs. Plane polarised light, length of scale bar 125µm.

respect to the relic grains. These inclusions, however, formed during the formation of the recrystallised grains and are, therefore, primary inclusion for the recrystallised grains.

Late inclusions of type 4, that formed after formation of the recrystallised grains are true secondary inclusions after Roedder (1972).

The composition of fluid inclusions is determined through observation of phase transitions at low temperatures. Most fluid inclusions at Lago di Cignana can be described in the relative simple system H_2O-salt and only the phase transformations, that are observed upon heating of a frozen inclusion in this system, will be described.

The first phase transition upon heating after cooling, which is only sometimes observed, is the onset of melting (temperature of eutectic between solid and liquid phase). This temperature indicates which cations might be dissolved in the fluid phase (e.g., Hollister & Crawford, 1981). Because the amount of first melt is very small, the temperature at which this transition is observed will always be higher than the real temperature of eutectic (Küster, 1994).

The next phase transition that occurs in this system, is the melting of the last ice. From the freezing point depression the salinity of the fluid can be calculated (Roedder, 1984).

The density of a fluid inclusion of known composition is determined by measuring the homogenisation temperature. Homogenisation occurs when the vapour bubble in the inclusion disappears. In the fluid inclusions from Lago di Cignana homogenisation was always in the fluid phase (inclusions have a supercritical density); upon heating the vapour bubble becomes smaller and finally disappears (Roedder, 1984). With these observations and if P-V-T-data for these compositions are known, the positions of isochors in the PT-field can be determined (e.g., Haas, 1976; Potter & Brown, 1977).

The temperatures determined for all observed phase transitions must be corrected according to the calibration curve for the heating-freezing stage used (Roedder, 1984). Compositions and densities can then be calculated with the program FLINCOR 1.2.1. using the corrected T_m H_2O and T_{hom} H_2O. The position of the isochores in the PT-field was calculated with the equation of state of Brown & Lamb (1989) in the system H_2O-NaCl. Other equations of state for this system (e.g., Haas, 1976; Potter & Brown, 1977; Zhang & Frantz, 1987) give similar results. Graphical representation of the isochores in a PT-diagram was facilitated with the program FCP of Dr. Röller.

A problem is that the composition (salinity) of the inclusion is inferred from the freezing point depression. The depression depends on the amount and on the kind of anions and cations in the solution. The eutectic temperature suggests which cations might be solved. It gives, however, no indication of the amounts of these cations in the solution. Furthermore, P-V-T-data are not known for more complex salts solved in a fluid phase. Therefore, the salinity of the fluid is approximated in wt.% NaCl-equivalent, because Na^+ and Cl^- are usually the dominant ions in the fluid phase (Roedder, 1962). Because the eutectic temperature of the H_2O-NaCl system is -20.8 °C, fluid inclusions with melting temperatures below this temperature cannot be processed. Melting temperatures at Lago di Cignana were, however, all above this temperature.

5.4.1 Compositions and densities of the fluid inclusions

Fluid inclusions were analysed in three quartz veins that are partly to completely recrystallised. Bk 20 is a type II_e quartz clinozoisite vein in a group 3 eclogite. Bk 100 is a type I_e quartz omphacite segregation in a group 1 eclogite. Bk 101 is a type II_e quartz vein in a group 3 eclogite that is part of a swarm of veins parallel to the foliation in eclogite, that occur within 0.5 m from the contact between eclogite and metasedimentary rock.

All measured inclusions in these quartz veins were at room temperature 2-phased and contained an aqueous fluid of low salinity. At room temperature single phase inclusions were not measured, while even at very low temperatures, usually, no phase transformations were observed. These inclusions contain a low density vapour or a high density fluid phase. The absence of a vapour bubble in a fluid phase could also be due to metastable behaviour of the inclusion (Roedder, 1967). Metastable behaviour was observed in several inclusions that were initially 2-phased, but were single phase after one or more cooling and heating cycles.

For the early inclusions, observed temperatures of eutectic range between -30 and -25 °C, indicating the presence of other cations besides Na^+ in the solution (Hollister & Crawford, 1981). The temperatures of melting range from -1 to -11 °C (between 1.6 and 15 wt.% NaCl-equivalent). Temperatures of homogenisation (in the fluid phase) range from 80 to 190 °C, corresponding to densities between 0.94 and 1.07 gr/cm^3 (equation of state of Brown & Lamb, 1989) (Table 7, Fig. 23).

For the late inclusions, observed temperatures of eutectic are also ca. -30 °C, indicating the presence of other cations besides Na^+ in the solution (Hollister & Crawford, 1981). The temperatures of melting range from -1 to -11 °C (between 1.6 and 15 wt.% NaCl-equivalent). Temperatures of

Table 7

Temperature ranges for observed phase transformations and inferred composition and densities of early and late fluid inclusions from the investigated samples.

	Bk 20		Bk 100		Bk 101	
	early	late	early	late	early	late
T_{eut} (°C)	-30	-30			-25	
T_{melt} (°C)	-1 to -5	-3 to -8	-2 to -9.5	-4 to -10	-2 to -11	-1 to -11
NaCl-eq. (wt.%)	1.6 to 7.8	1.8 to 9.8	4.1 to 13.4	6.3 to 13.9	3.2 to 15	1.6 to 15
T_{hom} (°C)	80 to 120	100 to 160	95 to 160	150 to 240	80 to 190	110 to 250>
density (gr/cm^3)	0.97 to 1.03	0.93 to 1.03	0.94 to 1.02	0.87 to 0.99	0.96 to 1.07	<0.89 to 1.05

homogenisation (in the fluid phase) range from 100 to > 250 °C, corresponding to densities between < 0.87 and 1.05 gr/cm^3 (equation of state of Brown & Lamb, 1989) (Table 7, Fig.23).

The large spread in homogenisation temperatures found in sample Bk 101 can, perhaps, be explained by necking down of larger inclusions (Lemmlein & Kliya, 1952). In this sample fluid inclusions were observed consisting of two spheres connected by a thin tube, indicative for necking down. Because necking down changes the density of the fluid inclusions, only the data of samples Bk 20 and Bk 100 are interpreted. The isochores for the fluid inclusions in these samples are depicted in figure 24.

The thermobarometric interpretation of the fluid inclusion data assumes constant volume (density) and constant composition for the inclusion. Several studies have shown that fluid inclusions that from geological reasoning formed at peak metamorphic conditions, have densities and compositions,

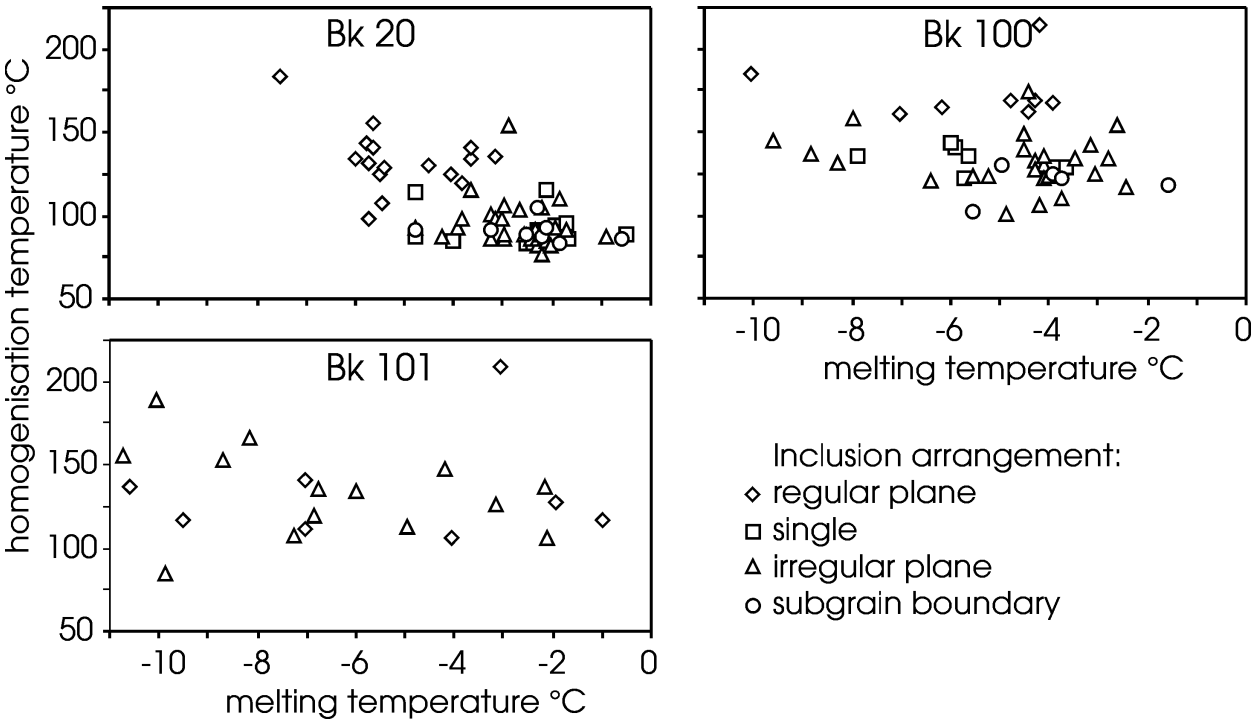

Figure 23

Melting temperatures against temperature of homogenisation for the fluid inclusions in the investigated samples differentiated for the arrangement of the fluid inclusions.

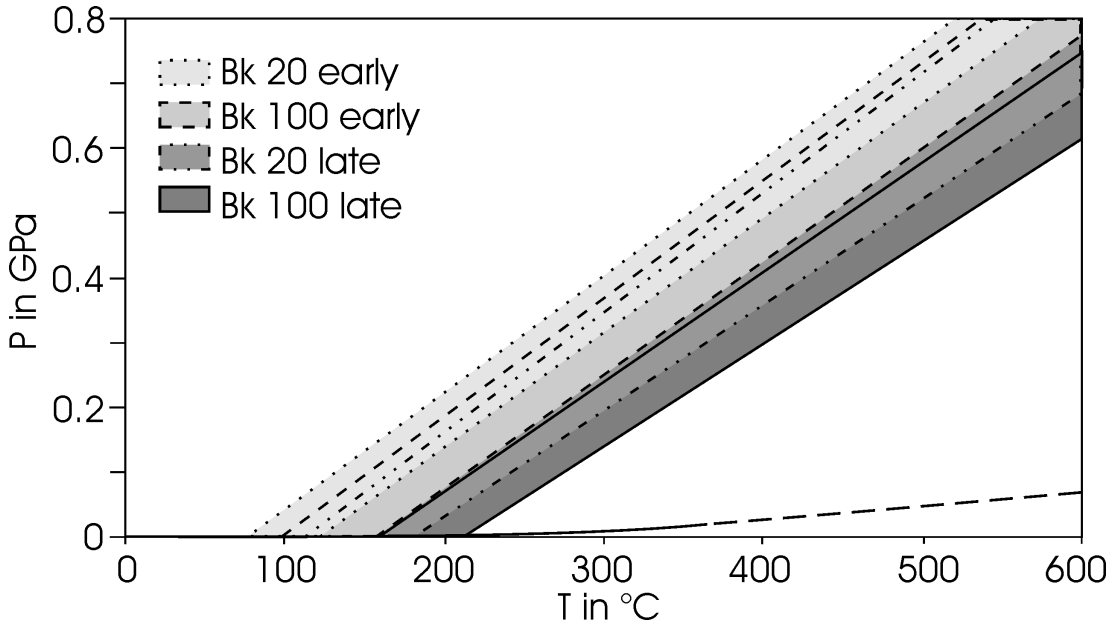

Figure 24

Position of the isochores (equation of state of Brown & Lamb (1989)) for the early and late fluid inclusions from samples Bk 20 and Bk 100.

that suggest pressures and temperatures of formation below these conditions (e.g., Hollister et al., 1979; Küster, 1994 on Crete; Swanenberg, 1980, in Rogaland; Kreulen, 1980 on Naxos). Therefore, the fluid inclusions changed after formation, either their density, or their composition. Experimental investigations on fluid inclusions in quartz have also shown that fluid inclusions can change their density and/or their composition (e.g., Pecher, 1981; Pecher & Bouillier, 1984; Sterner & Bodnar, 1989; Bouillier et al., 1989; Bakker & Janssen, 1990; Bakker, 1994). Compositional changes in fluid inclusions can be explained with diffusion of material out of the inclusion at relatively high (T > 600 °C) temperatures (e.g., Bakker, 1994). A theory, that explains the density decrease observed for fluid inclusions in quartz at lower temperatures (T > 300 °C), has been proposed by Küster (1994) and Küster & Stöckhert (1997). They show that at the low rate of change in P and T in metamorphic rocks, very low strain rates are sufficient for volume adaptation of the inclusions by dislocation creep of the host quartz. Dislocation creep is driven by the differential stresses, that develop in the host mineral around the inclusions, when cooling and decompression does not follow the isochor of the fluid inclusion. Therefore, they suggest that as long as the host mineral behaves ductile, fluid inclusions will change their volume. The density of the fluid inclusions reflects the PT-conditions at which plastic stretching of the host mineral is no longer possible. Experimentally derived flow laws for quartz (e.g., Paterson & Luan, 1990; Koch et al., 1989) suggest that for relevant strain rates (10^{-15}, 10^{-16} s^{-1}, Küster & Stöckhert, 1997) the flow stress drastically increases at temperatures of about 300 °C or somewhat below.

Following the model of Küster & Stöckhert (1997), the densities of the early fluid inclusions measured in two quartz veins at Lago di Cignana suggest a pressure between 0.2 and 0.4 GPa at temperatures around 300 °C (Fig. 24).

6 The exhumation record of the rocks

Metamorphic rocks are sometimes thought of as flight recorders, black boxes recovered from the wreckage of an orogen, that tell us something of that orogens history (Haugerud & Zen, 1991). They differ, however, from flight recorders in that the recording is not continuous and that often parts of the recordings are erased. The record preserved in the rock, generally depends on an incomplete and spatially distributed response of the rock to the changing conditions. During large parts of the exhumation history the rocks have remained essentially passive, without undergoing discernible modification and the exhumation history is, therefore, only partly recorded.

Two general remarks can be made concerning the record found in the rocks:

1. All orientations and directions mentioned in the text are as they occur today. During later deformations earlier structures have been rotated.
2. Uncertainties of absolute PT-estimates pertaining to some well-calibrated geothermobarometers are on the order of 50 K (1 σ) and 500 MPa (Kohn & Spear, 1991a). Differences in P and T, however, calculated with the same thermobarometer from different samples have much smaller uncertainties, that are commonly about a few tens of Kelvin and tens of MPa (Kohn & Spear, 1991a; 1991b; Hodges & McKenna, 1987). This means that absolute PT-conditions mentioned in this study have uncertainties of at least 50 K and 500 MPa, whereas relative changes in PT-conditions are relatively well constrained, but the exact positions of these segments of the PT-path are subject to similar errors as the absolute thermobarometry.

The metabasic and the metasedimentary rocks preserved different parts of the exhumation history. The petrological record (Fig. 25) is nearly complete in the metasedimentary rocks (e.g., Reinecke, 1998) and a similar, but more fragmentary record is found in the metabasic rocks (this study). A comparison of the structural records shows that in the metasedimentary rocks only the last part of this record is preserved, but that the metabasic rocks preserved the UHPM and later parts of the record (Fig. 25). The records of both rock types will now be combined and discussed for several intervals.

6.1 The record during UHPM and early exhumation

In the metabasic rocks deformation under UHPM conditions (Fig. 25; T 575-625 °C; P 2.5-2.8 GPa) is indicated by the foliation (S_{1e}) defined by omphacite. This deformation was heterogeneous, as evident by the variable distortion of pillow structures. The bulk rock rheology was controlled by omp, with the other minerals essentially acting as rigid bodies. This interpretation is supported by the irregulary distributed composition domains found in individual omp grains, attributed to compositional reequilibration during grain boundary migration (e.g., Buatier et al., 1991; Godard & van Roermond, 1995), that contrast with the compositional homogeneity of other minerals and the regular zoning pattern in garnet. Differential stresses must have been high enough to drive deformation by dislocation creep in omphacite at temperatures of about 600 °C. Extrapolation of laboratory data on diopside (e.g., Boland & Tullis, 1986), assumming geological relevant strain

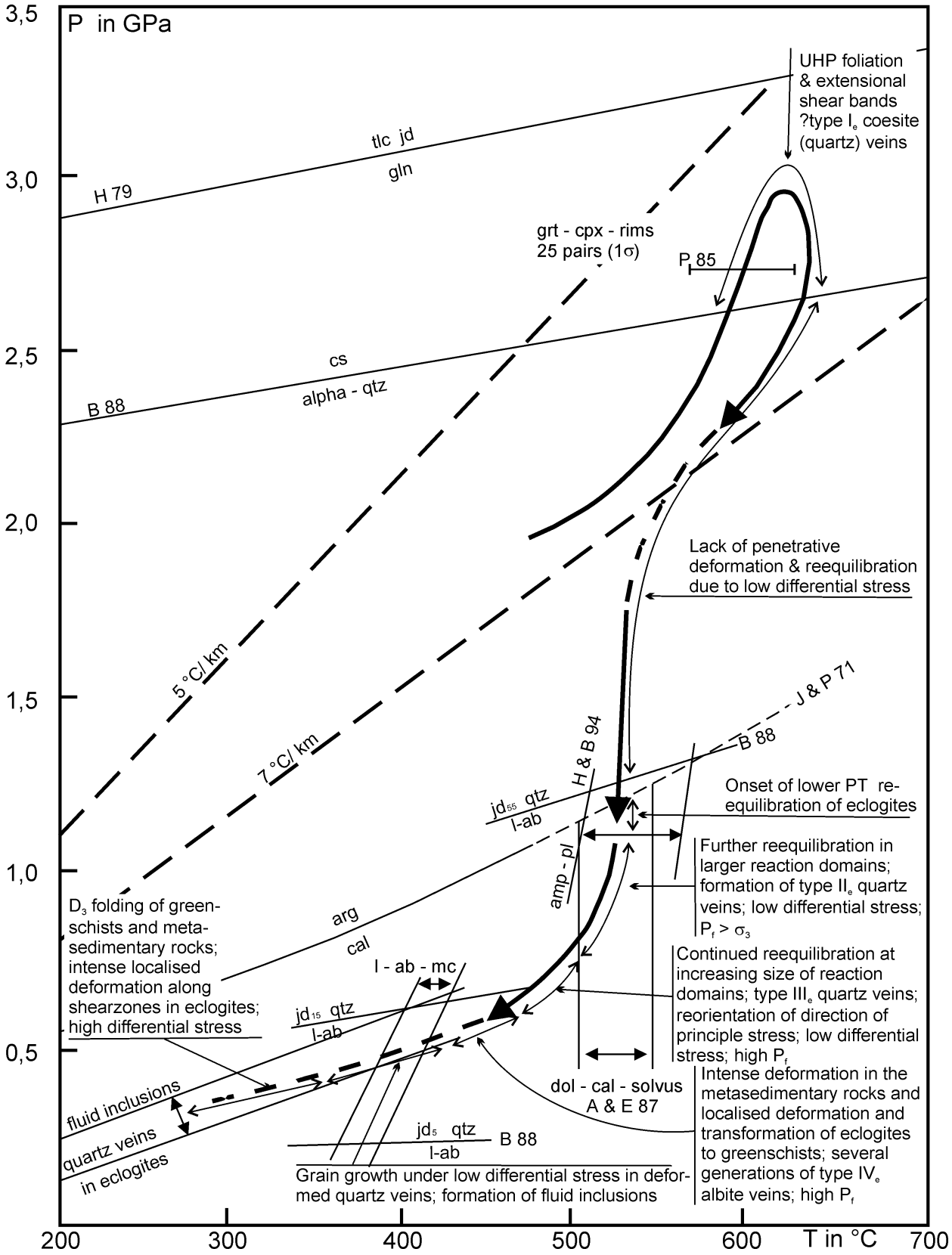

Figure 25

PTD-path for the exhumation of UHPM rocks of Lago di Cignana, Western Alps, Italy, modified after van der Klauw et al., (1997). The continuous segments of the PT-path were derived by Reinecke (1995; 1998) from absolute and relative thermobarometric methods applied to compositional zoning and inclusion patterns in garnet, combined with compositional information from other zoned matrix phases of the metasedimentary

rates (10^{-14}–10^{-16} s^{-1}), provides an upper limit of about 200-250 MPa for the differential stress to drive steady state creep of diopside at these conditions. Preliminary results on the deformation behaviour of jadeite (Stöckhert & Renner, 1998) suggest that at ca. 600 °C and a strain rate of 10^{-14} s^{-1}, the flow stress may be as low as a few MPa. The strength of omp is probably not the same as that of jadeite at these conditions, but possibly well below that of diopside.

The extensional shearbands (S_{2e}) in the metabasic rocks indicate localisation of deformation. Quartz pseudomorphs after coesite in omp grains on these bands, suggest that S_{2e} formed as the rocks were in the stability field of coesite. The shearbands are inferred to have nucleated at the interface between strain shadows at garnets and matrix, and thus result from the contrasts in mechanical properties of the rock forming minerals.

Subsequent to the formation of S_{2e} at P > 2.7 GPa and T > 575 °C, no further deformation and mineral reactions took place in the metabasic rocks prior to the onset of the replacement of the UHPM mineral assemblage at 1.2 GPa and 550-575 °C. Net-transfer and exchange reactions are probably not detected, because the mineral assemblage omp + grt + rt + gln/zoi + czoI is stable over a large range of PT-conditions and minor possible relaxation of Fe-Mg exchange between ferro-magnesian minerals was impeded by slow rates of volume diffusion, due to the relatively low temperatures. Veins parallel to the foliation may have formed, but cannot be distinguished from other vein types. Along this part of the PT-path, the differential stress remained too low to allow for notable deformation of the metabasic rocks. Any deformation during this stage must have been localised into weak shearzones that were not observed or located in the overlying metasedimentary rocks. The metasedimentary rocks preserved the UHPM and early exhumation PT-record, as minerals included in garnet, as minerals in strain shadows or as zoned minerals (Reinecke, 1995; 1998). All structures that might have formed under these conditions were either completely transposed, or wiped out by intense later deformation and the structural record was not preserved. The structural record in the metasedimentary rocks starts at T > 450 °C and P > 0.6 GPa.

6.2 The record between 575 and ca. 450 °C

In the metasedimentary rocks the PT-record of Reinecke (1995; 1998) shows a change from almost isothermal decompression to pronounced cooling with decompression in this temperature interval (Fig. 25). In the metabasic rocks, omp in contact with qtz became unstable at PT-conditions below ca. 1.2 GPa and 575 °C and recording resumed, showing similar PT-changes as the metasedimentary rocks.

The spatial and implied temporal relationship between the late vein types and the extent of lower PT-replacement in the metabasic rocks (Table 8), allows the reconstruction of the trend in the evolution of relative fluid pressures P_f and differential stress on this part of the exhumation path (Fig. 25).

Type I_e qtz veins were formed before or during UHPM and deformed together with their metabasic host rock, probably as coesite veins. Therefore, they give no information about the exhumation history, apart from structures superimposed during post UHPM deformation. According to the

Table 8

Correlation between the degree of lower PT-replacement and the number of veins present in a rock volume.

	group 1 eclogite	group 2 eclogite	group 3 eclogite	group 4 eclogite
number of type I_e and II_e quartz veins	3	21	13	36
number of type III_e quartz veins	0	5	4	17
number of type IV_e albite veins	0	0	2	15
area (m^2) (total ca. 80 m^2)	6	25	12	37
type I_e and II_e quartz veins per m^2	0.5	0.84	1.08	0.97
type III_e quartz veins per m^2	0	0.2	0.33	0.46
type IV_e albite veins per m^2	0	0	0.17	0.41
total veins per m^2	0.5	1.04	1.58	1.84

correlation with the type of lower PT-replacement, type II_e qtz veins were formed at temperatures of about 550 to 500 °C and type III_e qtz veins at T < 500 °C. Shape and aspect ratio of type II_e and III_e qtz veins, and the lack of fit between the vein flanks, indicate that the host rock deformed plastically at the time of vein formation. In contrast, the shape of most type IV_e ab veins, formed at temperatures below ca. 475 °C, indicates that the host rocks exhibited brittle behaviour at the time of vein formation.

The orientation of the veins with respect to pre-existing structures and discontinuities can be used to place some qualitative constraints on the magnitude of differential stress (Etheridge, 1983; Sibson, 1985). Type II_e qtz veins are oriented parallel to foliation S_{1e} or S_{2e}; these are interpreted to represent planes of low tensile strength. Differential stress was too low to allow formation of new cracks in other orientations. Hence, σ_3 was oriented at a large angle, but not necessarily normal to the veins. Furthermore, formation of veins in these orientations requires that P_f exceeded the normal stress acting across these planes; hence, P_f was larger than σ_3. This limits the magnitude of the differential stress to very low values (Jaeger & Cook, 1979). The later formation of type III_e qtz veins at a high angle to the pre-existing discontinuities, requires a reorientation of the principal stress directions to prevent cracks following pre-existing discontinuities. The three generations of type IV_e ab veins, indicate that conditions favouring the formation of open cracks at a high angle to pre-existing discontinuities, were realised several times during later deformation history.

An upper limit for the magnitude of the differential stress during formation of tensile fractures is given by Jaeger & Cook (1979) as σ_1-σ_3 < 4Te, where Te denotes the tensile strength of the rock. For this, Etheridge (1983) proposes 10 MPa as an upper limit in unfractured rocks under metamorphic PT-conditions. It is expected that this magnitude is drastically reduced along pre-existing discontinuities. According to these considerations, the magnitude of differential stress during formation of type III_e and IV_e veins is limited to less than 40 MPa, and may have been significantly lower for the formation of type II_e veins.

6.3 The record between ca. 450 and 300 °C

In the metasedimentary rocks the PT-record (Reinecke, 1995; 1998) shows a slight decompression with decreasing temperature from ca. 0.6 GPa at 450 °C to 0.2-0.5 GPa at 350-420 °C (Fig. 25). This fits well with the PT-estimate of 0.2–0.4 GPa at around 300 °C, inferred with the method of Küster & Stöckhert (1997) from fluid inclusions in quartz veins in the metabasic rocks.

The structural record in the metabasic rocks shows localised folding of foliation S_{1e} in pseudomorphic replaced eclogite with a greenschist facies mineral assemblage at T < 475 °C and P < 0.7 GPa. Localisation and more intense deformation led to the development of the foliated (S_{1g}/S_{2g}) greenschists. Lenses of metabasic rocks in the metasedimentary rocks have their foliation (S_{1e}, S_{2e}) at varying angles to foliation S_{2s} of the metasedimentary rocks, if they consist of (pseudomorphic) eclogite; the foliation (S_{2g}) is parallel to S_{2s}, if they consist of greenschists, indicating that S_{2g} and S_{2s} formed during the same deformation event. At this stage, also the quartz veins in the metabasic rocks and type I_s veins were deformed by dislocation creep of quartz. The recrystallised grainsize in those veins ranges between 70 and 125 µm, indicating minimal differential stresses of 25 and 35 MPa (Twiss, 1977) for this deformation. In combination with experimentally determined "best choice 2" flow law of Paterson & Luan (1990), these differential stresses indicate for assumed strain rates of 10^{-14}-10^{-16} s^{-1} temperatures between 400 and 450 °C during deformation (Fig. 26). These temperatures are in good accordance with temperatures for D_{2s} inferred from petrologic observations.

The arrangement of high angle grain boundaries in the quartz veins indicates interfacial free energy control. This microstructure can only be attained, if no driving force for grain boundary migration is exerted by contrasting dislocation densities. Different dislocation densities are produced during dislocation creep deformation, that at these temperatures requires only low differential stresses (e.g., Stöckhert et al., 1997). Consequently, the magnitude of differential stress must have been low subsequent to this (D_{2s}, D_{2g}, D_{3e}) deformation event.

After this period of low differential stress, only localised deformation occurred, suggesting a heterogeneous stress field. Similarities in microstructures of quartz veins folded in D_{3s}/D_{3g} and deformed in D_{4e} shearzones suggest that they were deformed under similar conditions. The weakly developed lattice preferred orientation and incomplete recrystallisation in most veins deformed during this stage suggest that a steady state microstructure had not developed. Only one quartz vein in eclogite deformed in a shear zone (D_{4e2}) shows irregular serrated grain boundaries of quartz and a strong lattice preferred orientation, suggesting development of a new steady state microstructure during this deformation. The 10 µm recrystallised grain size indicates a differential stress of ca. 125 MPa (Twiss, 1977) during deformation of this vein. In combination with the "best choice 2" flow law of Paterson & Luan (1990), this suggests, for the assumed geological strain rates of 10^{-14}-10^{-16} s^{-1}, temperatures between 325 and 375 °C (Fig. 26). The localised more intense deformation (D_{4e2}), however, could indicate that the deformation was strongly localised (e.g., Küster & Stöckhert, 1999) and the rock deformed with a faster strain rate. This would require higher temperatures

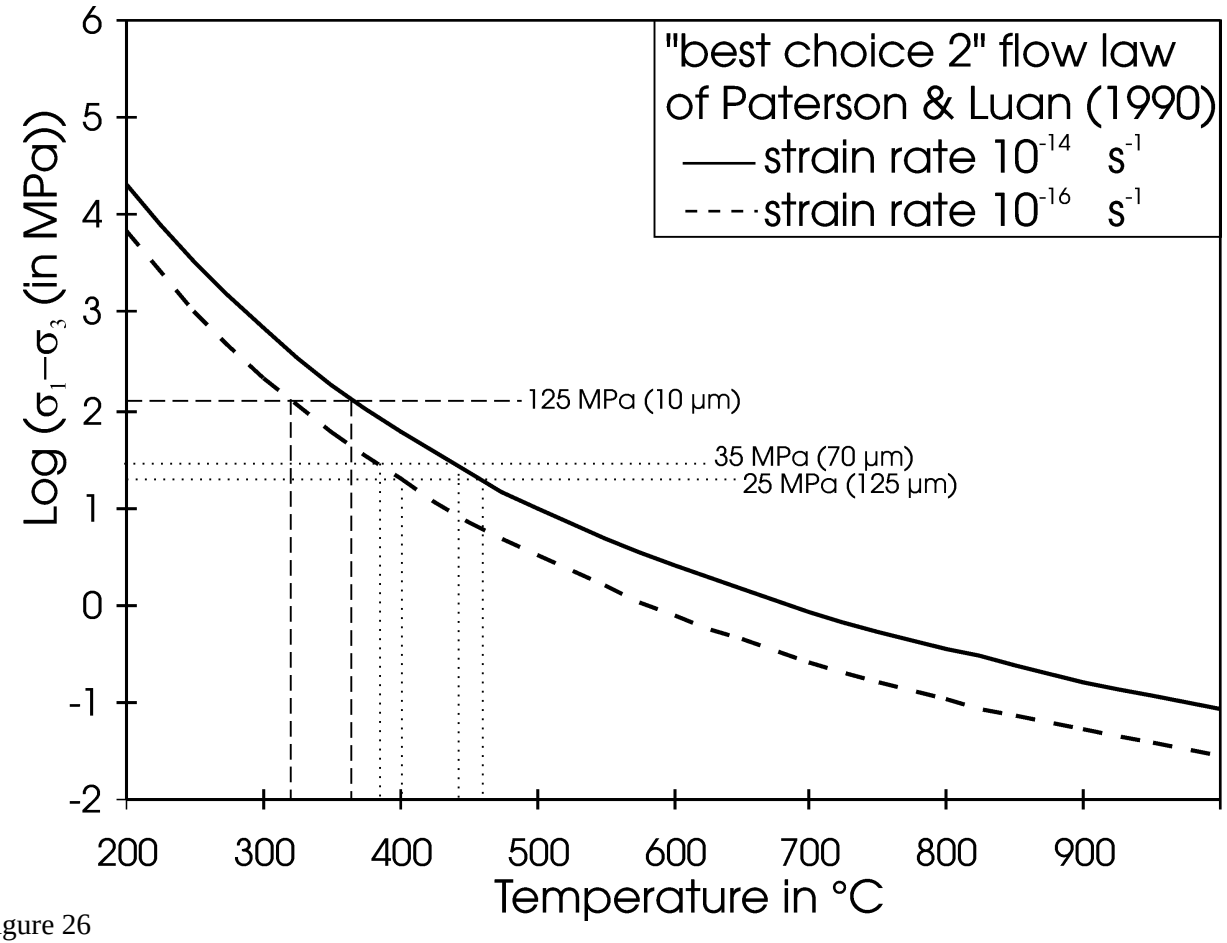

Figure 26

Flow law „best choice 2“ of Paterson & Luan (1990) for dislocation creep in synthetically prepared wet quartzite for geological relevant strain rates of 10^{-14} and 10^{-16} s^{-1}. Also depicted are differential stress estimates for quartz veins deformed during D_{2s} and D_{4e}, as determined with the Twiss (1977) quartz recrystallised grainsize paleopiezometer. This suggests temperatures between 375 and 450 °C during D_{2s} and of ca. 330 °C during D_{4e}.

during deformation. There is no independent evidence for the temperature during this deformation stage.

The later deformation stages in the metasedimentary rocks and greenschists (D_{4s-g} and D_{5s-g}) could not be correlated with deformed veins or petrologic information and inferences about PT-conditions during these deformations are not possible.

6.4 Synthesis: A two stage exhumation for the UHPM rocks of Lago di Cignana

A combination of the PT-path with published geochronological data allows an approximate reconstruction of the PTt-evolution (Fig. 27). An Sm-Nd garnet age of 40.6 ± 2.6 (2 σ) Ma is given by Amato et al. (1999) for the eclogitic rocks of Lago di Cignana. The closure temperature of the Sm-Nd system in garnet is ca. 600 °C (Hodges, 1991) and the age of 41 Ma can be considered to date the UHPM. A similar age, 44.1 ± 0.7 (95 % confidence interval) Ma was obtained with SHRIMP, U-Pb dating of zircons (closure temperature > 700 °C, Hodges, 1991) in the eclogites (Rubatto et al., 1998). The later greenschist facies overprint was dated between 40 and 45 Ma with Rb-Sr in

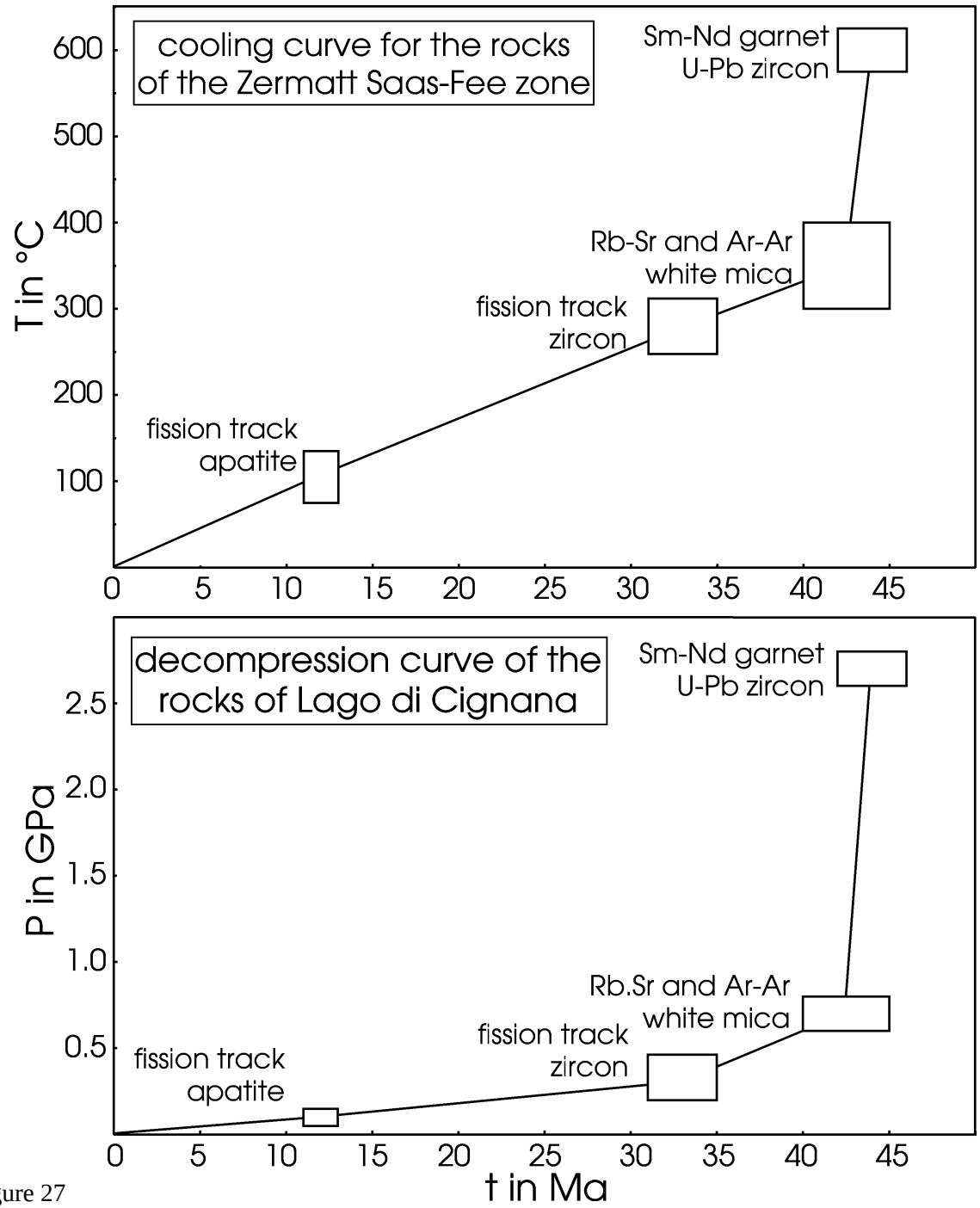

Figure 27

Above: Cooling curve calculated for rocks of the Zermatt Saas-Fee zone, calculated with the published ages of Amato et al., (1999), Rubatto et al., (1998), Barnicoat et al., (1995) and Hurford et al., (1991), with closure temperatures of Hodges (1991).

Below: Decompression curve for the rocks of Lago di Cignana calculated by combining the cooling curve of the Zermatt Saas-Fee zone and the PT-path of the rocks fom Lago di Cignana.

newly grown phengites and with U-Pb in titanite by Barnicoat et al. (1995). The fission track ages in the units above and below the Zermatt Saas eclogites indicate cooling to below 300 - 250 °C (Tagami & Dumitru, 1996; Wagner et al.,1997) at ca. 33 Ma and cooling to below ca. 125 °C (Hodges, 1991) at ca. 12 Ma (Hurford et al., 1991).

The earliest exhumation from 2.6 to ca. 0.8 GPa occurred in at maximum 4 m.y. and the minimal time for this exhumation can be < 1 m.y., because the ages for UHPM and greenschistfacies

metamorphism are identical within the limits of error. This results in a minimum average decompression rate of 450 MPa/m.y. (ca. 15 mm/year for a mean rock density of 3 gr/cm^3) and a maximum average decompression rate of > 1800 MPa/m.y. (> 54 mm/year). The second part of the exhumation path requires decompression from 0.8 to 0.3 GPa in, at maximum 11 and, at minumum 7 m.y. and results in a minimum average decompression rate of 45 MPa/m.y. (1.3 mm/year) and a maximum average decompression rate of 70 MPa/m.y. (2.1 mm/year) (Fig. 27).

The large change in decompression rate at pressures around 0.8 GPa, that coincides with a reorientation of the stress field, indicates a change in the exhumation mechanism at a depth of ca. 25 km for the UHPM rocks of Lago di Cignana. The first exhumation mechanism brings the rocks very fast (> 8 mm/year) from depths of ca. 90 km to depths of ca. 25 km and with a small decrease in temperature and low differential stresses. The transition to a different exhumation mechanism occurs at depths of around 25 km. At this depth, stages with high pore fluid pressures and low differential stresses alternated with stages with low pore fluid pressures and differential stresses of up to 40 MPa. The second exhumation mechanism brings the rocks slower (ca. 1-2 mm/year) from depths of ca. 25 km to depths of ca. 10 km. During this part of the exhumation path the stress field was very heterogeneous and periods with relatively high (40 to 125 MPa) differential stresses and low pore fluid pressures alternated with stages with almost lithostatic pore fluid pressure and low differential stress, as indicated by several generations of late albite veins. For the last part of the exhumation path, from depths of ca. 10 km to surface conditions, this study provides no constraints.

7 Discussion and Exhumation concepts

In this chapter concepts for the exhumation of HPM rocks to normal crustal levels will be introduced and compared to the constraints obtained for the first part of the exhumation path. On this basis, a tentative scenario for the the two stage exhumation from 90 to ca. 10 km depth of the UHPM rocks of Lago di Cignana will be proposed.

7.1 Exhumation theories

Before introducing exhumation concepts, some terms must be defined, because exhumation and uplift are often used in a confusing way in the geological literature (e.g., Behrmann & Ratschbacher, 1989). In this study, exhumation means the vertical movement of rocks with respect to the Earth's surface, whereas uplift is vertical movement of rocks or surface with respect to the Geoid (England & Molnar, 1990). In principle, there are three possible ways to bring rocks closer to the surface:

1. removal of the overburden by erosion,
2. removal of the overburden by extensional tectonic processes,
3. transport of the rocks to the surface in a flowing matrix.

These three exhumation principles are used in all exhumation concepts for HPM rocks and will be discussed, where relevant, with concepts proposed for the Western Alps as illustration.

7.1.1 Exhumation through erosion

Erosion is an important exhumation process. It is, however, difficult to quantify the effect of erosion on exhumation. Recent erosion rates are locally upto 13 mm/year, but over a larger area maximum rates are usually not above 2 mm/year (Allen, 1997). Erosion rates are controlled by surface elevation and by climate (rainfall) (England & Molnar, 1990; Koons, 1990). The last factor is often ignored, but may influence erosion rates by one order of magnitude. Surface elevation is dependent on surface uplift and a high erosion rate can only be maintained, when erosion rate is approximately balanced by the rate of surface uplift. Therefore, postulation of exhumation through erosion should always be accompanied by a hypothesis that explains the continuous surface uplift.

Older literature about exhumation in the Western Alps (e.g., Dal Piaz et al., 1971; Hsü, 1991; Gillet et al., 1985; 1986), usually combines erosion with thrusting, to provide the continuous surface uplift. These concepts rely heavily on a ca. 100 Ma old ultra high pressure metamorphism at depths of 80 km or more and a return to midcrustal levels of these HPM rocks at ca. 40 Ma, to be able to exhume these rocks with reasonable erosion rates. The 41 Ma age for UHPM at Lago di Cignana (e.g., Amato et al., 1999) requires for the first part of the exhumation path a minimum decompression rate of 15 mm/year. Therefore, exhumation through erosion is not feasible for the first part of the exhumation path. It might, however, be important for the second part of the exhumation path with decompression rates between 1 and 2.1 mm/year.

The concept of Chemenda et al. (1995) differs from the standard concepts, in that it combines normal faulting with localised erosion and thrusting and only requires locally high erosion rates,

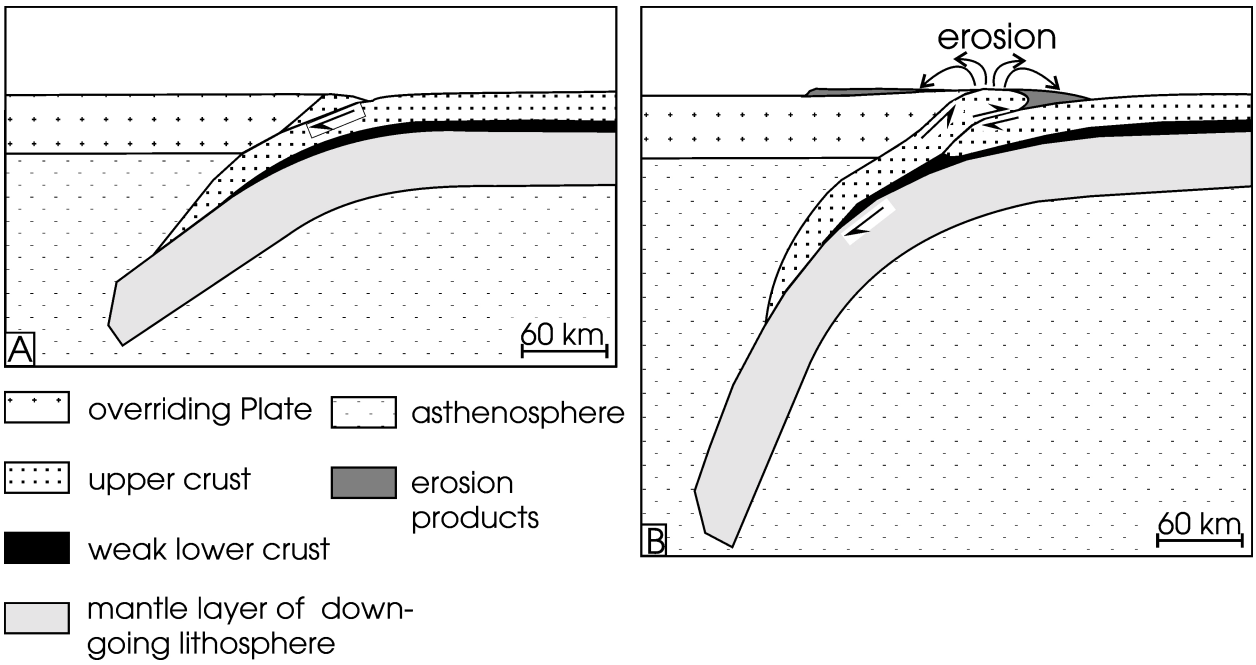

Figure 28

Schematic sketches illustrating the exhumation concept of Chemenda et al. (1995). See text for discussion.

but has not yet been applied to the Alps. Chemenda et al. (1995) assume subduction of the continental crust. When the crust is subducted to depths of approx. 250 km, the buoyant upper crust "delaminates" from the weak lower crust and is thrusted on the foreland (Fig. 28A). Ongoing subduction will further underthrust the continental crust and result in isostatic uplift of this thrust stack and concomitant erosion. The delaminated upper crust is bounded by two relatively weak zones; the upper weak zone is the former subduction channel and the lower weak zone is the weak lower crust or the new subduction channel. The erosional unloading causes this buoyant segment of subducted upper crust to move upward along the weak lower crust (Fig. 28B). This movement results in faster movement along the lower thrust and produces normal movement and exhumation along the upper surface of the slice. However, the low strength of the continental material at UHPM conditions (Stöckhert & Renner, 1998) precludes the exhumation of large coherent slices of UHPM material as suggested by Chemenda et al. (1995). Hence, this concept appears unrealistic.

7.1.2 Exhumation by extension tectonics

Exhumation by extension tectonics brings rocks with different metamorphic grade in contact or will result in large changes of pressure and temperature over a small area. This situation is often observed in orogens like the Alps (e.g., Selverstone, 1985; Ratschbacher et al, 1989; Blake & Jayko, 1990), the Franciscan, (Harms et al., 1992), Betics, (Platt & Behrmann, 1986), the Aegean (e.g., Jolivet et al., 1996; Thomson et al., 1998). This observation alone is not necessarily an indication for extensional tectonics, because a similar configuration can be obtained by reimbrication of a nappe pile, or by juxtaposition of rocks that experienced metamorphism at different times (e.g., Wheeler & Butler, 1994).

For extensional tectonics to take place one has to postulate a period of plate divergence or a concept to explain extension in a convergent plate tectonic setting. Three concepts exist at present to explain extension in a convergent plate tectonic setting:

1. the critical wedge (Platt, 1986; 1987).
2. lithospheric extension through gravitational collapse (e.g., Dewey, 1988; England & Houseman, 1989; Lister & Davis, 1989).
3. subduction roll back (e.g., Royden, 1993; Thomson et al., 1998).

These three concepts will be introduced first and concepts that postulate a period of divergence will be discussed at the end of this section.

7.1.2.1 The critical wedge concept

This concept of Platt (1986; 1987) is based on the work of Chapple (1978), Davis et al. (1983), and Dahlen et al. (1984) on thrust belts. Platt (1987; 1986) gives a general analysis of an orogenic wedge with only one rheological assumption, viz. that in a orogenic wedge temperatures and fluid content will be high enough for ductile flow to occur and to prevent build up of a high stress (e.g., Rutter, 1976; 1983; Etheridge, 1983; Atkinson, 1980). Assuming a wedge that has achieved a dynamic equilibrium, the stable form of the wedge is described by:

$$\tau_b = \rho\ g\ h\ \alpha$$

with τ_b shear stress along the basal decollement, ρ density, g gravity, h thickness of the wedge and α surface slope (Fig. 29). The significance of this formula is, that it allows to predict the reaction of the wedge to external modification of its geometry.

If the values of α and/or h are decreased the basal traction exerted by τ_b (unchanged) is no longer compensated by the gravity sliding (ρ g h α) and the wedge will shorten. If the wedge shortens α and h become larger and a stable configuration is restored. The values of α and h can be decreased by erosion at the rear of the wedge or by frontal accretion.

If the values of α and/or h are increased the gravity sliding force (ρ g h α) becomes larger than the drag force exerted by τ_b and the wedge will extend. Extension occurs by brittle normal faulting close to the surface and by horizontal ductile extension at depth. This extension decreases the values of α and/or h and a stable wedge configuration is restored. The values of α and h can be increased by underplating at the rear of the wedge or by sedimentation on the wedge.

The combination of underplating below the wedge, with extension in the upper part of the wedge, elegantly explains formation, preservation and exhumation of HPM rocks. Scenarios for the exhum-

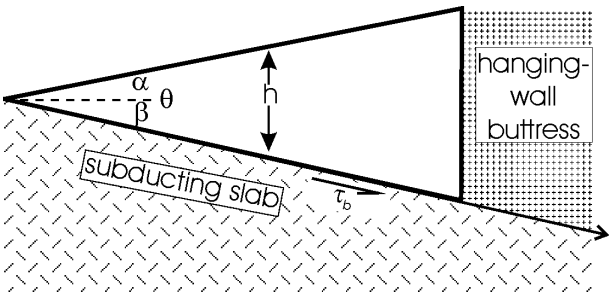

Figure 29

The plastic or Coulomb wedge in the concept of Platt (1986, 1987), with terms that describe the geometry of a steady state wedge (modified after Platt, 1993).

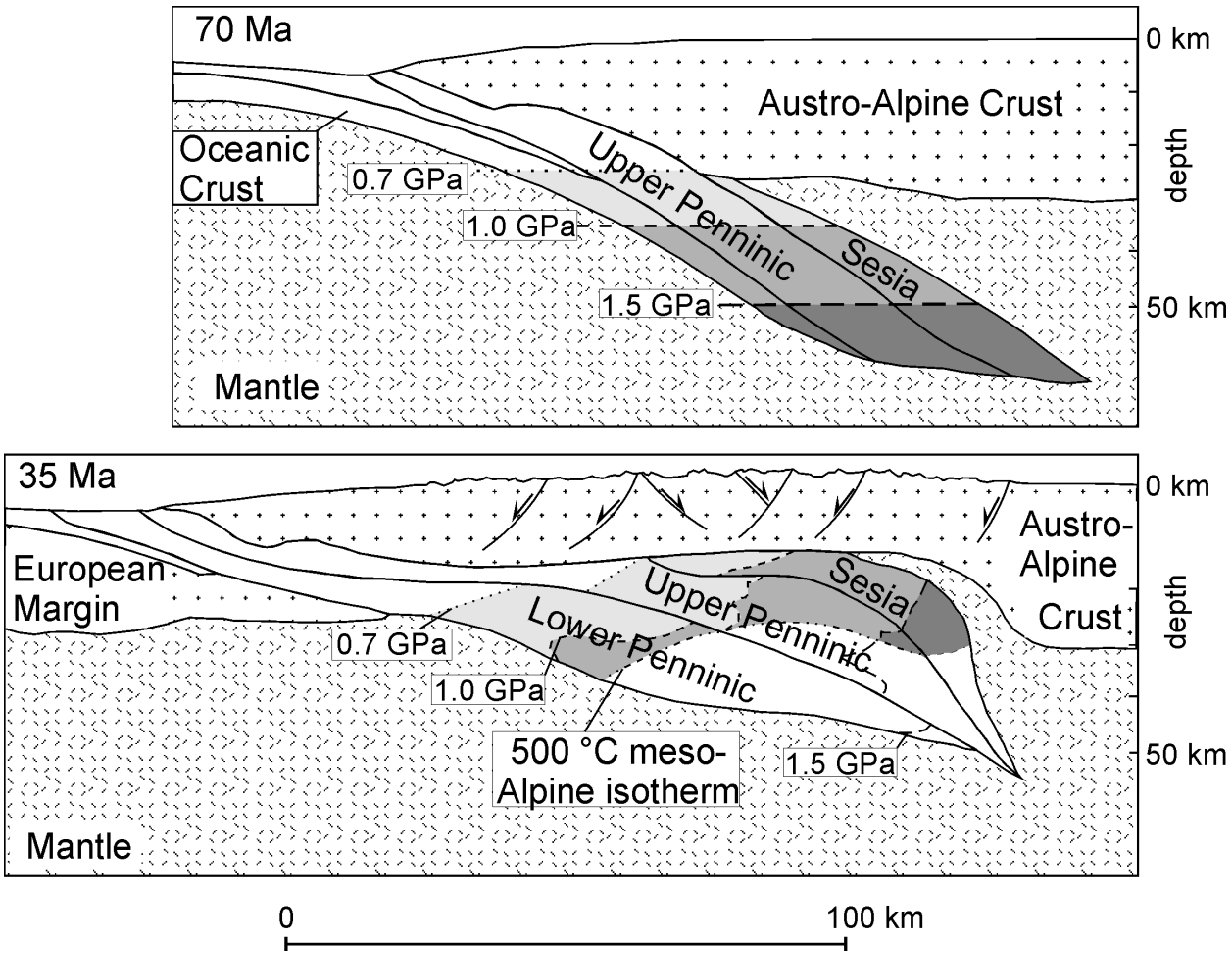

Figure 30

Tectonic evolution of the Western Alps after Platt (1987). In the late Cretaceous (70 Ma) upper Penninic and Sesia zone rocks have been subducted and experienced HP metamorphism, ongoing subduction of oceanic crust keeps temperature in these rocks low. Continued underplating till early Oligocene (35 Ma) of lower Penninic rocks resulted in oversteepening of the wedge and in extension in the overlying Austro-Alpine and upper Penninic rocks, allowing the HPM rocks to rise towards the surface.

ation of the HPM rocks of the Western Alps using this concept are given by Platt (1986) (Fig. 30) and Polino et al. (1990).

7.1.2.2 The lithospheric extension concept

This is derived from the metamorphic core complex concept (e.g., Lister & Davis, 1989). It suggests that metamorphic rocks are exhumed through lithospheric extension, involving low-angle (listric) normal faults (e.g., Lister & Davis, 1989). The concept requires thickening of the continental lithosphere and isostatic uplift of the surface. The vertical stress generated through this topographic elevation is balanced by a horizontal stress through continuing convergence. Upsetting of this force balance in favour of the vertical stress will result in horizontal extension with the development of low-angle normal faults (e.g., England & Houseman, 1986). The force balance can be disturbed through removal of a gravitational unstable high density lithospheric root (e.g., England & Houseman, 1989; Dewey, 1988). A variant of this concept is the slab breakoff concept of Davies & von Blanckenburg (1995), that results in a localised disturbance of the force balance.

These concepts, however, cannot be used for the exhumation of the HPM rocks of the Western Alps, because replacement of the relatively cold material at the base of the crust by relatively hot asthenosphere results in a temperature increase at the base of the crust (e.g., Sonder et al., 1987; Davies & von Blanckenburg, 1995). The HPM rocks in the Western Alps do, however, not reflect a significant temperature increase prior or during exhumation (e.g., Schertl et al., 1991, this study).

7.1.2.3 The subduction zone roll back concept

This concept suggests that extension in the upper plate occurs when the subduction rate exceeds the convergence rate of the plates (Fig. 31). The high subduction rate is thought to be caused by the slab pull exerted by the sinking of heavy oceanic lithosphere in the mantle (Royden, 1993). Typical features expected in this situation are, regional extension in the overriding plate, topographical low mountains and a low erosion rate, low grade to no metamorphism, almost no involvement of crystalline basement in thrusting and continuous flysch sedimentation (Royden, 1993; Thomson et al., 1998). The Western Alps clearly do not display these features and therefore, this concept cannot be used to explain the exhumation of HPM rocks in the Western Alps.

7.1.2.4 Concepts that require a period of divergence

Several authors have attributed exhumation of HPM rocks in the Western Alps through extension, to a period of divergence between the European and African plates (e.g., Butler, 1986; Ballevre & Merle, 1993). These scenarios require a middle to late Cretaceous (100- 80 Ma) HP metamorphism and a period of extension sometime between 80 and 60 Ma (e.g., Butler, 1986; Ballevre & Merle,

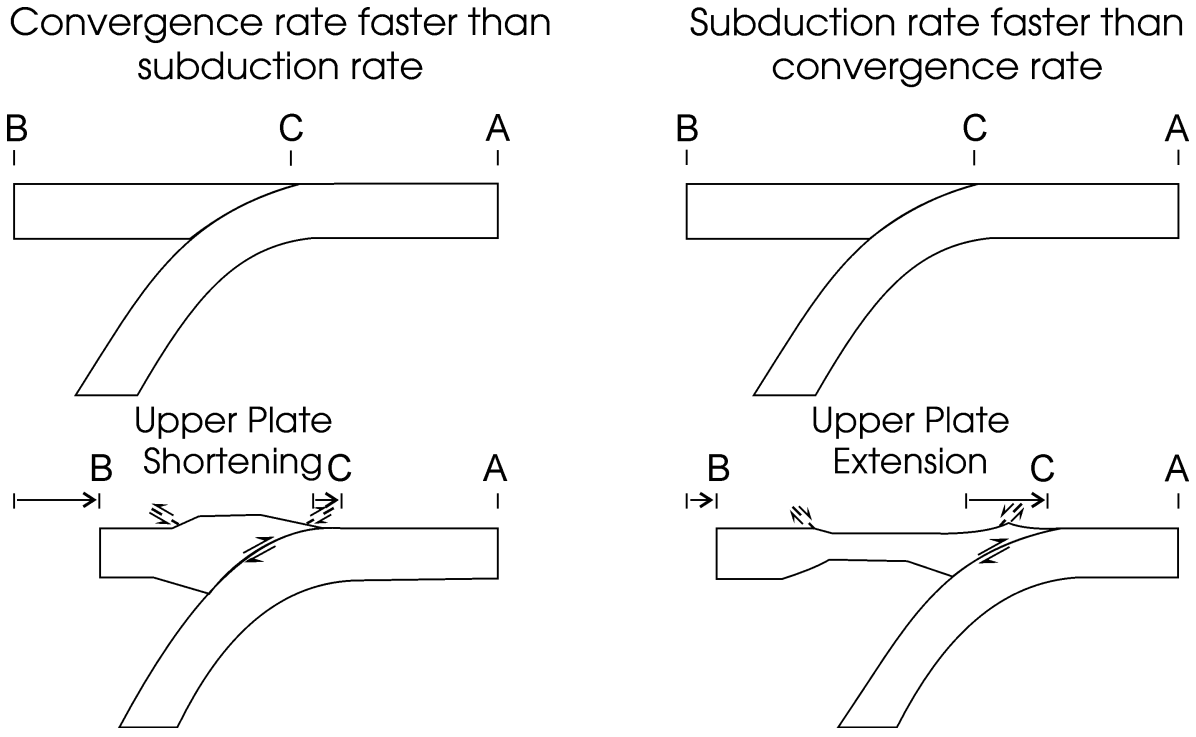

Figure 31

Schematic diagramm after Royden (1993) showing the response of the upper plate to different relative velocity configurations of the subducting and overriding plate.

1993) to partly exhume these HPM rocks. The newer radiometric ages between 70 and 35 Ma (e.g., Inger et al., 1996; Gebauer et al., 1997) for the UHP metamorphism leave, however, not enough time for a period of plate divergence to exhume HPM rocks.

7.1.3 Upflow concepts

Exhumation by upflow requires the high pressure metamorphic rocks to be embedded in a low viscosity matrix (Cloos, 1982; Emerman & Turcotte, 1983; Platt, 1993). The HPM rocks themselves cannot have a low viscosity, because the intense deformation that low viscous rock would experience during exhumation, would probably result in complete reequilibration of the mineral paragenesis (e.g., Rutter & Brodie, 1985). Two endmember flow processes can be postulated:

- Buoyant upflow of material driven by density contrasts.
- Upflow of material driven by forced flow.

The first process requires that the high pressure rocks and their matrix have a relatively low bulk density compared to the surrounding rocks. It was proposed by England & Holland (1979) to exhume eclogitic blocks in a carbonate rich matrix and by Takasu (1989) to exhume blocks of HPM rocks in a serpentinite matrix. This mechanism cannot be used to exhume continuous large sections of HPM rocks.

The second process is based on the corner flow concept of Cowan & Silling (1978), who used a dynamic scaled model to study the development of an accretionary prism. They found the expected underthrusting at the toe of the prism (e.g., Karig, 1974), but also that appreciable amounts of sediments were carried below the wedge and were accreted there, and that material began to flow upward from the deepest part of the accretionary prism (Fig. 32). If the rocks in an accretionary prism behave as a viscous fluid, this forced flow could bring material from the deepest part of the accretionary prism to shallower levels in the wedge. This can be considered as an initial stage in the development of an accretionary wedge that, with ongoing subduction and accretion, will develop in a critical tapered wedge (e.g., Platt, 1986; 1987).

The subduction channel concept is a modification of the corner flow model for a narrowing channel and was proposed by Cloos (1982) to explain observations in the Franciscan subduction complex. It was further developed (Shreve & Cloos, 1986; Cloos & Shreve, 1988 a; 1988b) to describe the processes of prism accretion, sediment subduction and melange formation.

The concept assumes that subducting sediments deform approximately as a viscous fluid, when they are dragged by the descending plate beneath the overriding plate and the accretionary prism. This layer of deforming sediments forms a shear zone, called the subduction channel. The subduction

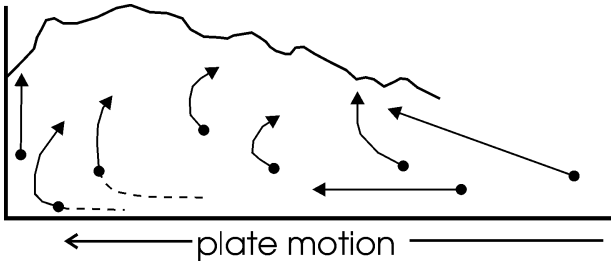

Figure 32

Simplified cross section illustrating successive positions and trajectories of identifiable points in the dynamic scaled wedge model of Cowan & Silling (1978).

channel has a certain width, that depends on the velocity and angle of subduction, as well as on surface slope and material in the hanging wall. The width of the subduction channel determines its capacity, the amount of sediment that can be transported downwards along the subduction channel. If enough sediment is available at the inlet of the subduction channel, it will be filled to capacity. Where the dip of the descending plate changes or where the rear of an accretionary wedge abuts basement rock the subduction channel changes its width (control point). At the control point the capacity of the subduction channel decreases. If the subduction channel was filled to capacity, not all incoming material can pass the control point. Material will accumulate at the control point and the channel thickens. When this happens, the upward directed force due the adverse pressure gradient and the buoyancy of the sediment, becomes larger as the downward directed force due to shearing and a zone of reverse flow or upflow will develop. The material that flows up consists of low viscous metasedimentary rocks that are intensely deformed. In this low viscous matrix, small blocks of high viscous material that have retained their HPM imprint, that is almost completely wiped out in the low viscous material, can be included and brought to shallow crustal levels (concept of Cloos, 1982). The flowing material exerts a viscous drag (shear stress) on the walls of the channel (Shreve & Cloos, 1986). Without reverse flow this viscous drag is downward directed for the hanging wall and can result in incorporation of hanging wall material in the subduction channel (subduction erosion). In a zone of reverse flow the viscous drag on the hanging wall is upward directed and could move larger sheets of previously accreted (HPM) rocks to the surface (Cloos & Shreve, 1988a).

The weak point of the subduction channel concept is the nature and the deformation mechanism of the low viscous material in the channel. In the quantitative subduction channel models of Shreve & Cloos (1986), water saturated sediment is taken as the low viscosity material. This may be valid for the upper few kilometres of the subduction channel, but at depths of 90 km or more, necessary to exhume UHPM rocks with this concept, a different yet unspecified material and deformation mechanism operating in this material are required.

Forced flow concepts were proposed to explain the exhumation of (U)HPM rocks in the Western Alps by Fry & Barnicoat (1987) for the Zermatt Saas zone and by Michard et al. (1993) for the Dora Maira Massif. The interpretation of Michard et al. (1993) postulates, the oldest HP metamorphism for ca. 100 Ma old and a period of ca. 60 m.y. of subduction, but can be readily adapted to younger HP metamorphism and a shorter subduction time span.

These concepts (Fig. 33) assume onset of subduction of oceanic crust (rocks of the Zermatt Saas zone) with offscraping of parts of the southern continent (Sesia zone). To accrete parts of the subducting oceanic crust to the overlying plate, Fry & Barnicoat (1987) suggest geometric irregularities along the subducting slab or rheological irregularities in the slab, to cause detachment from the subducting slab. With the onset of continental collision, fragments of the thinned continental margin (Monte Rosa, Dora Maira) are also subducted. The density contrast between the deeply subducted continental rocks (3.09 gr/cm^3) and the surrounding mantle rocks (3.3 gr/cm^3) adds buoyant uprise to the forces that can cause detachment from the subducting slab and accretion to the overlying

plate (Michard et al., 1993). Exhumation occurs by forced return flow in a narrowing subduction channel driven by continuing continental collision. During exhumation UHPM rocks become mixed with rocks that experienced HP metamorphism at lower pressures (Michard et al., 1993). After forced flow exhumation to mid crustal levels, further exhumation was achieved by other mechanisms.

7.2 Evaluation of published exhumation scenarios for exhumation from depths of approx. 90 km to 30 km

Only the upflow (e.g., Fry & Barnicoat, 1987; Michard et al., 1993) and the critical wedge (Platt, 1986; 1987) concepts, stay within the limits posed by the PTD-path of this study and geochronological data (e.g., Amato et al., 1999; Barnicoat et al., 1995). Essential for a scenario that uses extensional tectonics to explain the exhumation of HPM rocks, is the identification of extensional structures that were active during the exhumation of the HPM rocks. In the area around Valtournanche the only described extensional structure is the ”Combin fault”, that is considered part of the Mischabel backfold/backthrust system (e.g., Wheeler & Butler, 1993; Barnicoat et al., 1995). On this fault system extensional activity under lower greenschist facies PT-conditions took place at ca. 40 Ma (Barnicoat et al., 1995), post-dating the greenschist facies overprint of the HPM rocks in the Zermatt area (Barnicoat et al., 1995). Therefore, this structure was active as the HPM rocks of the Zermatt Saas zone were already at a midcrustal level. In its present configuration this fault cannot be responsible for the exhumation of the HPM rocks. As long as from the Northern part of the Western Alps no extensional structures are described, that predate the greenschist facies overprint of the HPM rocks, the critical wedge model of Platt (1986; 1987) is not applicable to the exhumation of the UHPM rocks of Lago di Cignana.

The forced flow concept requires that during exhumation, the UHPM rocks are embedded in a matrix of low viscous material that precludes the buildup of higher differential stresses at depth in the subduction channel (Shreve & Cloos, 1986). Low differential stresses at depth in subduction zones are inferred from geological evidence (e.g., Stöckhert et al., 1997; 1999) and from geophysical reasoning (e.g., Pacheco et al., 1993; Wang et al., 1995). The nature of the material in the subduction channel and the deformation processes operating in this material are unknown (e.g., Platt, 1993). At Lago di Cignana the serpentinites, that occur in large volumes in the Zermatt Saas zone and the locally preserved HP metasedimentary rocks of the Zermatt Saas zone, could have been these low viscosity rocks. The metasedimentary rocks of the Zermatt Saas zone consist mainly of quartz-phengite-garnet schists, that locally have preserved their HPM imprint as inclusions in rigid minerals (e.g., Reinecke, 1995). During the later exhumation, however, microstructures in the rock were completely modified and inferences about deformation processes during UHPM conditions can no longer be made. The same holds for the serpentinites that have preserved deformation structures (e.g., Vogler, 1987), but because of the PT insensitive mineral paragenesis, these cannot be unequivocally attributed to specific segments of the PT-path.

A subduction channel is characterised by high strain rates at relatively low temperatures and the deformation process operating should preclude high differential stresses. Most geologic materials

require for deformation by dislocation creep at these conditions (e.g., Carter & Tsenn, 1986), differential stresses that are much too high for the postulated viscosities (10^{-17}-10^{-18} Pa s, Shreve & Cloos, 1986). Altough most minerals in crustal rocks deforming by dislocation creep are weaker then expected (Stöckhert & Renner, 1998), they are still not weak enough. Diffusional flow deformation mechanisms can achieve deformation at low differential stress, but at the relatively low temperature conditions only diffusion precipitation creep in the presence of a fluid phase is a feasible mechanism. Stöckhert et al. (1999) estimated for the HPM phyllite quarzite unit of Crete, which deformed mainly by dissolution precipitation creep (Schwarz & Stöckhert, 1996), a bulk viscosity of ca. 10^{-19} Pa s, still a factor 10 higher as the viscosity in normal subduction channel models (e.g., Shreve & Cloos, 1986), although Mancktelow (1995) used viscosities between 10^{-17}-10^{-19} Pa s to model tectonic overpressures in a subduction channel setting. A deformation process, similar to liquid phase sintering is considered feasible to explain the inferred low strenghth of UHPM rocks by Stöckhert & Renner (1998), but microstructural evidence in geologic materials for this process has not yet been presented.

Although the nature of the material and the deformation mechanism operating in this material in the subduction channel are not unequivocally identified, a forced flow subduction channel concept can be applied to explain the exhumation from 90 km to 25 km depth of the UHPM rocks of Lago di Cignana. A forced flow subduction channel scenario for the UHPM rocks of Lago di Cignana will be presented and discussed in the next section.

7.3 Scenario for exhumation from ca. 90 km to ca. 25 km depth

In a forced flow subduction channel scenario for the UHPM rocks of Lago di Cignana, several points must be discussed. A short description of the scenario is given and the numbered points will be discussed.

The oceanic crust at Lago di Cignana was subducted down to depths of ca. 90 km. Deformation during subduction was concentrated in the weak subduction channel above the oceanic crust (Fig. 33). At this depth, a part of the oceanic crust was detached from the downgoing slab (1) and incorporated in the subduction channel. Assumming a control point in ca. 90 km depth (2) and a subduction channel filled over the capacity of the control point (3), the oceanic slab was transported upward along the subduction channel (4) through a forced return flow in a low viscous material. Where the drag force of the hanging wall became larger than the driving force of the return flow, the material was either accreted to the hanging wall (5) or the material flowed down again.

Point (1), detachment of the downgoing plate, requires localised deformation of the downgoing slab at or close to maximum PT-conditions. At first, this seems to contradict the subduction channel model, because deformation is assummed to be concentrated in the weak material of the subduction channel. The record of the eclogites at Lago di Cignana, however, shows at maximum PT-conditions deformation of the rock by dislocation creep of omphacite. At these conditions jadeite may flow at differential stresses of a few MPa (Stöckhert & Renner, 1998) and omphacite probably flows at somewhat higher stresses. This is a similar magnitude as the differential stress that in subduction

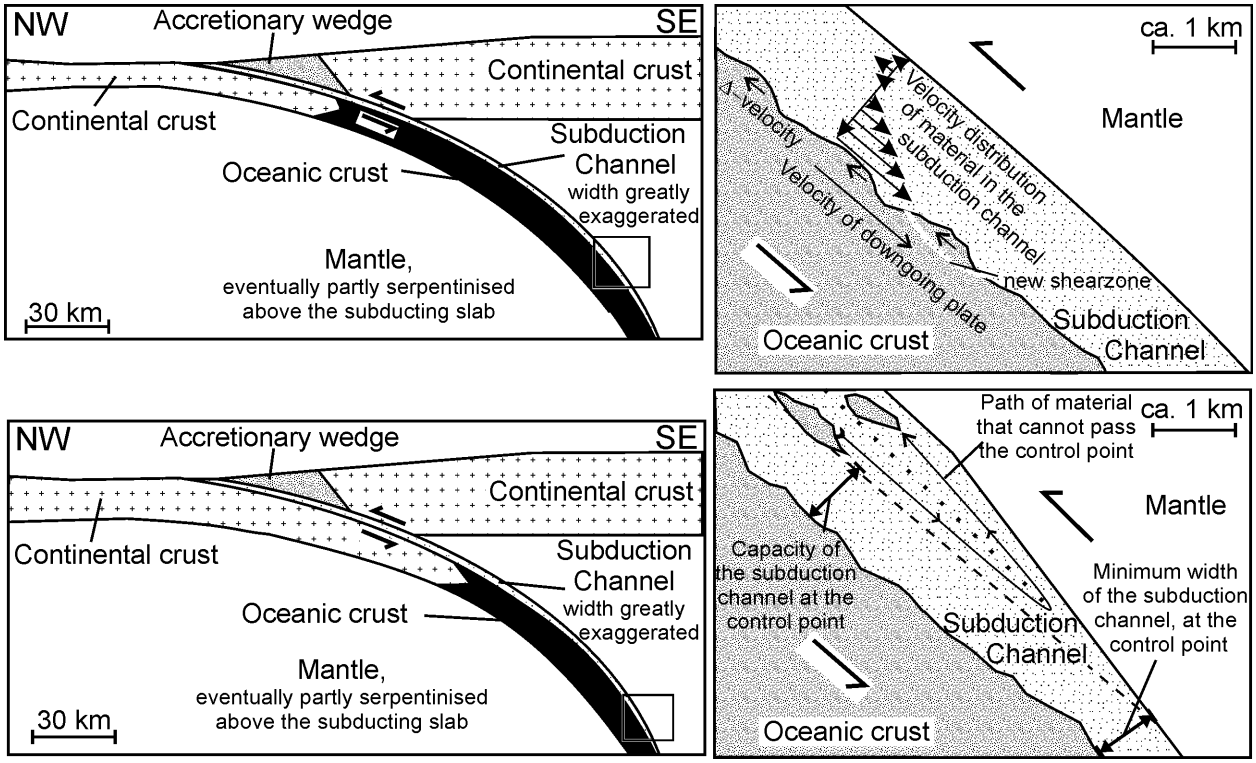

Figure 33

A tentative schematic sketch illustrating some important points of the proposed exhumation scenario for the UHPM rocks of Lago di Cignana.

The upper sketches show the configuration at UHPM conditions before exhumation. In the right sketch the situation in the subduction channel is shown. The velocity distribution in the subduction channel is qualitatively only and adapted from England & Holland (1979). Δ-velocity is the difference between the velocity of the downgoing plate and the material in the subduction channel close to the plate-channel interface and a measure for the magnitude of the viscous drag, that is assummed to have caused deformation by dislocation creep in omphacite. Localisation of deformation results in the development of a shearzone in the downgoing plate and in detachment of UHP metamorphic rocks from this plate.

The lower sketches show the configuration at the onset of exhumation. The right sketch shows the situation in the subduction channel at the control point. The width of the subduction channel at the control point, determines the amount of material that can pass. In the sketch, all material below the dashed line can pass the control point and is subducted. Material between the dashed and dotted lines is downflowing material in the subduction channel, that cannot pass the control point and will follow a path given by the arrow. Between dotted line and the mantle wedge of the overlying plate a zone of reverse flow occurs, that allows for exhumation of material.

channel models (e.g., Shreve & Cloos, 1986) is produced by viscous drag of the flowing material on the walls of the channel. The magnitude of the viscous drag in these models depends on the vicosity of the material in the subduction channel, the channel width, the velocity of the downgoing plate, and on the change in hydraulic potential and channel width in direction of subduction (Shreve & Cloos, 1986). Most of these parameters are only approximately known, but varying the parameters within reasonable limits (factor 10 higher or lower viscosities, plate velocities between 1 and 10 cm/year, subduction channel thickness between 300-5000 m) gives similar magnitudes for the differential stress (e.g., Shreve & Cloos, 1986; Mancktelow, 1995). This suggests that at maximum PT-conditions the eclogites at Lago di Cignana were deformed, because of the viscous drag of the

material flowing in the subduction channel on the downgoing plate. Detachment of the rocks from the downgoing plate requires localisation of the deformation in a shear zone below these rocks. The heterogeneous deformation at UHPM conditions at Lago di Cignana (this study) is also observed at other UHPM localities (e.g., Michard et al., 1993; 1995), therefore, localisation of deformation has to be expected. Because the shear zone rocks could not be identified, nothing can be said about deformation mechanisms in the shear zone. Possible mechanisms are dissolution precipitation creep as inferred from microstructures by Stöckhert et al., (1997) for rocks from the Tauern Window deformed under HPM conditions or grain size sensitive flow that, however, would require an extreme grainsize reduction in the shear zone (e.g., Walker et al., 1990).

Point (2) concerns the control point in ca. 90 km depth. At the control point, the width of the subduction channel changes. Cloos & Shreve (1988a; 1988b) propose a change of material in the overlying plate (e.g. accretionary wedge to crystalline basement) or a change of dip in the downgoing plate as possible causes for the development of a control point. The only possible material change in the overlying plate in this depth range is the crust mantle transition. Present day crustal thickness in mountain belts, however, rarely exceeds 70 km (e.g., Tanimoto, 1995) and a crustal thickness of 90 km implies extreme thickening of the overlying plate and this seems improbable, because large scale continental collision is considered to occur later (e.g., Steck & Hunziker, 1994). The alternative is, that the downgoing plate changes its dip at ca. 90 km depth. According to Jarrard (1986), the greatest change in dip in the downgoing plates in present day subduction zones occurs between depths of 60 and 100 km. From his data, it is not clear which parameter influence the depth of the dip change, therefore, it cannot be ascertained whether or not the plate tectonic configuration of the Western Alps at ca. 44 Ma could produce a change of dip in the downgoing plate at approx. 90 km depth. It is, however, the most probable explanation for the existence of a control point at approx. 90 km depth.

Point (3) is concerned with the amount of material in the subduction channel above the control point. If this amount is smaller than the capacity at the control point, return flow and exhumation cannot occurr. The amount of material in the subduction channel cannot be estimated. The schistes lustres or Bundnerschiefer (calcschists and greenschists of the Combin zone), however, are interpreted to have formed in an accretionary wedge (e.g., Deville et al., 1992). The formation of an accretionary wedge requires a certain amount of sediment on the downgoing plate (e.g., Pavlis & Bruhn, 1983). This does not prove that parts of this sediments were subducted to great depths, but it shows at least that at shallower depths enough material was available to fill the subduction channel to capacity (e.g., Cloos & Shreve, 1988b).

Point (4), the upward transport along the subduction channel in a matrix of low viscous rocks, explains the almost isothermal decompression with slight cooling and no notable deformation, as recorded in the UHPM rocks of Lago di Cignana, because thermal models for subduction zones (e.g., Peacock, 1987; 1996), show that isotherms are subparallel to the subduction channel. These models, however, cannot be quantitatively applied, because they do not account for the return flow of material. Qualitatively the return flow of hotter material from below, will result in higher

temperatures at given depth as expected from thermal modelling without return flow. The magnitude of this temperature rise will depend on the velocity and the amount of material flowing back. The presence of cold material below the zone of return flow, will qualitatively result in cooling of this material during exhumation, as for example recorded by the rocks of Lago di Cignana.

Point (5) is the accretion of the upward transported slice of UHPM material to the hanging wall. The material in the hanging wall has a non-negligible strength and can transmit higher stresses. This results in deformation of the accreted rock during further exhumation as described for example by Stöckhert et al. (1997) for HPM rocks of the Tauern window. The change in decompression rate in the UHPM rocks of Lago di Cignana that coincides with a change in orientation of the stress field and an increase in maximum differential stress, suggests that the rocks became accreted to the overlying plate at temperatures of ca. 500 °C and a depth of ca. 25 km.

7.4 The scenario for the later exhumation from depths of ca. 25 km to the surface

This part of the exhumation path is also divided in two parts, exhumation from depths of ca. 25 km to depths of ca. 10 km and from there towards the surface. For this last part, this study offers no constraints and it will not be discussed.

A comparison with published data for the Northwestern Alps (e.g., Mazurek, 1986; Ellis et al., 1989; Wust & Silverberg, 1989; Sartori, 1990; Wheeler & Butler, 1993; Barnicoat et al., 1995) allows the integration of the data of Lago di Cignana in the regional framework and the development of an exhumation scenario for this part of the exhumation path. Formation of the greenschists (D_{3e}) in the metabasic and D_{2s} in the metasedimentary rocks are tentatively correlated with top to the NW movement of several regional faults under greenschist facies conditions (e.g., Ellis et al., 1989; Barnicoat et al., 1995). This deformation is related to the onset of nappe stacking due to SE directed underthrusting of the European continental crust below the Adriatic or Apulian continental crust (e.g., Butler, 1986; Steck & Hunziker, 1994). In this thrusting event that occurred between 43 Ma (age of static greenschist facies overprint, Barnicoat et al., 1995) and 40 Ma (age of SE directed fault zone, Barnicoat et al., 1995), the rocks of the Zermatt Saas zone were juxtaposed between the rocks of the Monte Rosa unit and the rocks of the Combin zone (Fig. 34A). The thrusts bounding the Zermatt Saas zone then became inactive and new thrusts developed further north.

The localised D_{3s} and D_{4e} deformation at Lago di Cignana is tentatively correlated with top to the SE movement. This late top to the SE movement is traditionally interpreted as backthrusting or backfolding (e.g., Steck, 1990; Sartori, 1987), because it often stacks external units on top of internal units. Recently, some late structures with top to the SE and E displacement have been interpreted as hinterland dipping extensional shearzones (e.g., Phillipot, 1990; Wheeler & Butler, 1993). The contradictionary interpretations for these shearzones, result from possible reorientation of these structures through later deformation (Wheeler & Butler, 1993). If these shears are interpreted as backthrusts (e.g., Steck, 1994), the main exhumation mechanism must have been erosion, which would require relative high erosion rates (Allen, 1997) of between 2 and 3 mm/year. Therefore, I

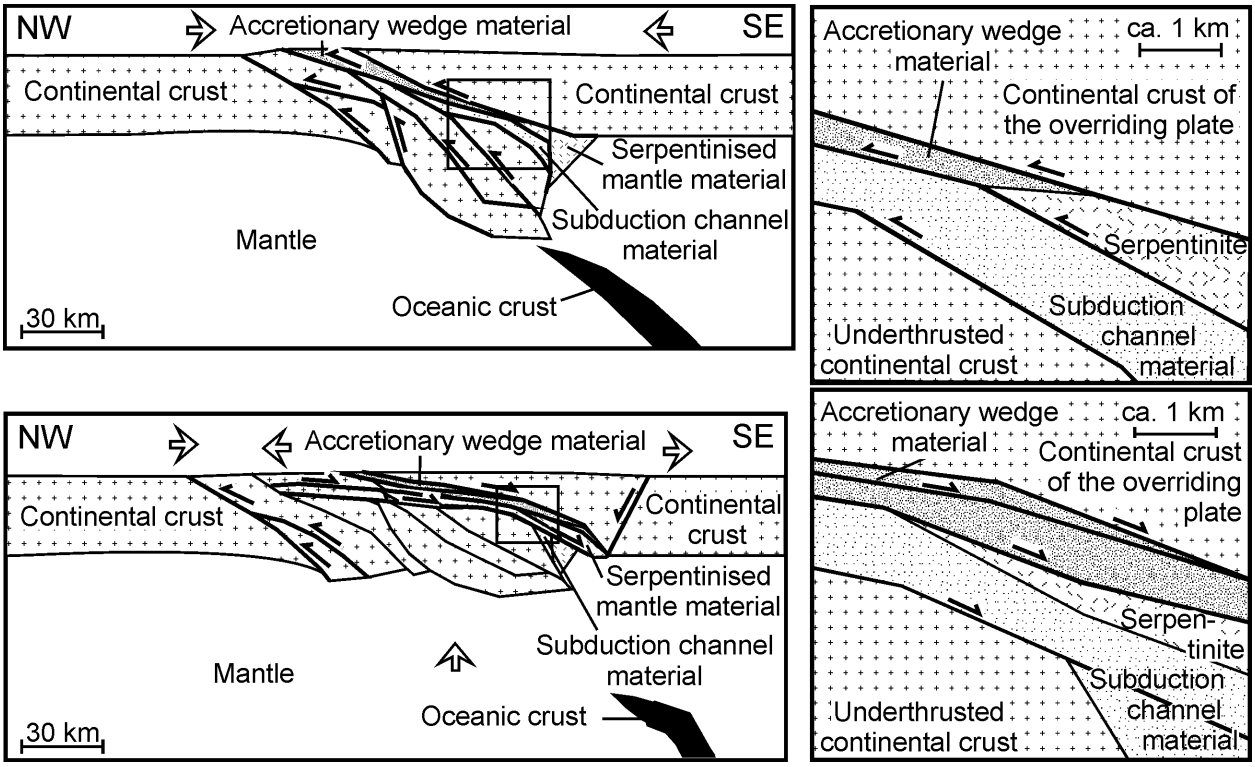

Figure 34

A tentative schematic sketch illustrating the proposed exhumation scenario for the UHPM rocks of Lago di Cignana from depths of 25 km to ca. 10 km.

The upper sketches show the configuration just after breakoff of the oceanic crustal slab (see text for discussion). The crust at the former subduction zone was already thickened by thrusting and is further thickened by buoyant uprise of deeply subducted slabs of continental material along former thrusts. The right sketch shows, that at this stage the already exhumed UHPM rocks in the subduction channel material, become juxtaposed between underthrusted continental crust (Monte Rosa unit) and serpentinites and material from the accretionary wedge (Combin zone).

The lower sketches shows the proposed exhumation scenario. See text for discussion. During extensional shearing, favourably orientated thrust were reactivated as low angle normal faults. Where thrusts were not favourably orientated they were cut off by low angle normal faults.

prefer to interpret most of theses shears as extensional shears. A tentative interpretation of these top to the SE shears as extensional shearzones in combination with top to the NW thrusting after the interpretation of Wheeler & Butler (1993) is shown in figure 34B.

The described features can be explained in a scenario that combines features from the critical wedge concept of Platt (1986; 1987) and the slab breakoff concept of von Blankenburg & Davies (1995). Prior to subduction of buoyant continental crust, slab pull of the downgoing slab is the force, that mainly determines the configuration of a subduction zone (e.g., Royden, 1993). With the onset of subduction of continental crust, buoyancy disturbs the force balance and will lead to a changed stress situation in the downgoing slab. Ultimately, the heavy oceanic slab will break off (Davies & von Blanckenburg, 1995). Because further subduction of buoyant continental crust is not possible, the ongoing convergence between the plates must be accommodated otherwise. The interface between continental crust (quartzo-feldspatic rocks) and mantle (olivine rocks) is, due to the compositional change, also a rheologic interface between relatively weak crustal rocks and strong

mantle rocks (e.g., Kusznir & Park, 1986). Therefore, crust and mantle can decouple along this interface (e.g., van den Beukel, 1992). With ongoing convergence the mantle part of the lithosphere will be subducted and convergence in the crust is taken up by thrusting (e.g., Laubscher, 1990). At the same time, however, already subducted continental crust, rises along the subduction zone, and this results in extreme thickening of the crust and in reorientation of the older thrust surfaces, which are no longer favourably orientated for thrusting. Further shortening of the crust is taken up in new thrust zones that developed further to the North. The thickening of the continental crust results in isostatic uplift of the surface. The vertical stress generated by this uplift is, however, no longer balanced by a horizontal stress and the result is horizontal extension with the development of low-angle normal faults (e.g., von Blanckenburg & Davies, 1994).

For the exhumation from a depth of ca. 10 km as the rocks had a temperature close to 300 °C to surface conditions, this study offers no constraints. Discontinuous uplift of discrete blocks with different erosion rates caused by dextral transpression is discussed as possibility in the literature (e.g., Laubscher, 1990; Hurford et al., 1991; Steck & Hunziker, 1994; Escher et al., 1997; Marchant & Stampfli, 1997).

8 Conclusions

The PTD- path for the exhumation of UHPM rocks of Lago di Cignana can be partly reconstructed by combining petrological and (micro)structural observations. This PTD-path combined with published radiometric ages, divides the exhumation history in two parts. The first part of the exhumation is very fast, almost isothermal decompression from depths of approx. 90 km to depths of approx. 25 km, with differential stresses too low to drive deformation in the metabasic rocks. At around 500 °C and 0.8 GPa, the slope of the PT-path as well as the orientation of the stress field changes. The second part of the exhumation is slower, with pronounced cooling during uplift from depths of approx. 25 km to depths of approx. 10 km and deformation at higher differential stresses.

The exhumation mechanism for this first part of the exhumation path that obeys most constraints imposed by the PTDt-path is a modified forced flow/subduction channel model, as proposed by Shreve & Cloos (1986) and Cloos & Shreve (1988 a; 1988b). For the second part of the exhumation path a modified slab break off model (e.g., Davies & von Blanckenburg, 1995) is feasible.

For the UHPM rocks of Lago di Cignana following scenario is considered. The oceanic rocks were subducted to depths of about 90 km and metamorphosed at pressures of 2.6-2.8 GPa and a temperature of ca. 600 °C. Under these conditions, the eclogites were heterogeneously deformed with differential stresses, high enough to drive deformation by dislocation creep in omphacite. This deformation is tentatively attributed to the viscous drag between the material flowing in the subduction channel and the foot wall. At these conditions the material must have been transferred from the downgoing plate to the subduction channel, possibly by further localisation of deformation in a shear zone that is no longer preserved. Subsequently, differential stress was too low to drive further deformation in the metabasic rocks. Exhumation of the slice of UHP material to depths of approx. 25 km is attributed to a forced return flow in a matrix of weak material. For the forced return flow to occur a control point at approx. 90 km depth has to be assummed.

Accretion of the slice of UHP material to the hanging wall occured at a depth of approx. 25 km and a temperature of ca. 500 °C. Accretion was closely followed by wholesale continent-continent collision. At this stage the subduction channel became inactive and the Zermatt Saas zone probably became a coherent unit, composed of several subunits that had followed slightly different PT-paths before (e.g., Ellis et al., 1989; Barnicoat & Fry, 1986; Meyer, 1983; Reinecke, 1991; 1995; this study). After accretion, higher stresses were possible, resulting in development of the greenschists in the metabasic rocks and intensive deformation D_{2s} in the metasedimentary rocks. This deformation is correlated with NW directed overthrusting under greenschistfacies conditions between 43 and 40 Ma (Barnicoat et al., 1995).

Exhumation of the UHPM rocks from Lago di Cignana from depths of ca. 25 km to depths of ca. 10 km between 40 and 33 Ma under lower greenschist facies conditions is attributed to hinterland-directed shears (e.g., Steck & Hunziker, 1994; Wheeler & Butler, 1993), that are tentatively correlated with the late localised deformation in the rocks of Lago di Cignana.

An important objekt for further study are the deformation mechanisms in the weak material in the subduction channel. Stöckhert & Renner (1998) propose a mechanism similar to liquid phase sintering in the presence of a highly saline fluid phase or a melt, as possible deformation mechanism, but also state that microstructures indicative for this process have not been observed and that experimental evidence on geologic materials for this mechanism is also not available.

Another subject is the regional study of structures, active under greenschist facies conditions and with top to the SE movement. These structures are traditionally interpreted as backthrusts (e.g., Steck & Hunziker, 1994), but must be reeinterpreted as rotated extensional shear zones (e.g., Wheeler & Butler, 1993) to validate the postulated model for exhumation from 25 to 10 km depth.

9 References

AI Y. (1994): A revision of the garnet-clinopyroxene Fe^{2+} - Mg exchange geothermometer. - Contrib. Mineral. Petrol. 115: 467-473.

ALLEN P.A. (1997) Earth Surface Processes. - Blackwell Science, Oxford; 404 pp.

AMATO J.M., JOHNSON C.M., BAUMGARTNER L.P. & BEARD B.L. (1999): Rapid exhumation of the Zermatt-Saas ophiolite deduced from high-precision Sm-Nd and Rb-Sr geochronology. - Earth and Planetary Science Letters 171: 425-438.

AMES L., ZHOU G. & XIONG B. (1996): Geochronology and isotopic character of ultrahigh-pressure metamorphism with implications for collision of the Sino-Korean and Yangtze cratons. - Tectonics 15, 472-489.

ANDERSEN T.B., JAMTVEIT B., DEWEY J.F. & SWENSSON E. (1991): Subduction ans eduction of continental crust: Major mechanisms during continent-continent collision and orogenic extensional collapse, a model based on the South Norwegian Caledonides. - Terra Nova 3: 303-310.

ANOVITZ L.M. & ESSENE E.J. (1987): Phase equilibria in the system CaCO3-MgCO3-FeCO3. - J. Petrol. 28: 389-414.

ARANOVICH L.Y. & PATTISON D.R.M. (1995): Reassessment of the garnet-clinopyroxene Fe-Mg exchange thermometer: I. Evaluation of the Pattison and Newton (1989) experiments. - Contrib. Mineral. Petrol. 119: 16-29.

ATKINSON B.K. (1980): Stress corrosion and rate dependent tensile failure of a fine-grained quartz rock. - Tectonophysics 65: 281-290.

AYRTON S., BUGNON C., HAARPAINTER T., WEIDMANN M. & FRANK E. (1982): Geologie du front de la nappe de la Dent blanche dans le region des Monts Dolins, Valais. - Eclogae Geol. Helv. 75: 269-286.

BAKKER R. J. (1994): On modifications of fluid inclusions in quartz: re-equilibration experiments and thermodynamical calculations on fluids in natural quartz. (Ph. D. Thesis) - Geologica Ultraiectina 94, 189 pp.

BAKKER R. J. & JANSEN J.B.H. (1990): Preferential water leakage from fluid inclusions by means of mobile dislocations. - Nature 345: 58-60.

BALLÈVRE M. & MERLE O. (1993): The Combin Fault: Compressional reactivation of a Late Cretaceous-Early Tertiary detachment fault in the Western Alps. - Schweiz. Mineral. Petrogr. Mitt. 73: 205-227.

BANNO S.(1970): Classification of eclogites in terms of their physical conditions of origin. - Phys. Earth Planet. Inter. 3: 405-421.

BARNICOAT A.C. (1988a): Zoned high-pressure assemblages in pillow lavas of the Zermatt-Saas ophiolite zone, Switzerland. - Lithos 21: 227-236.

BARNICOAT A.C. (1988b): The mechanism of veining and retrograde alteration of Alpine eclogites. - J. Metamorphic Geol. 6: 545-558.

BARNICOAT A.C. & FRY N. (1986): High-pressure metamorphism of the Zermatt-Saas ophiolite zone, Switzerland. - J. Geol. Soc. London 143: 607-618.

BARNICOAT A.C. & FRY N. (1989): Eoalpine high-pressure metamorphism in the Piemonte zone of the Alps: south-west Switzerland and north-west Italy. - In: DALY J.S., CLIFF R.A. & YARDLEY B.W.D. (eds.) Evolution of metamorphic belts, Geol. Soc. London, Spec. Publ. 43: 539-544.

BARNICOAT A.C., REX D.C., GUISE P.G. & CLIFF R.A. (1995): The timing of and nature of greenschist facies deformation and metamorphism in the upper Pennine Alps. - Tectonics 14: 279-293.

BEARTH P. (1952): Geologie und Petrographie des Monte Rosa. - Beitrage zur Geologischer Karte Schweiz, N.F. 96.

BEARTH P. (1959): Über Eklogite, Glaukophanschiefer und metamorphe Pillowlaven. - Schweiz. Mineral. Petrogr. Mitt. 39: 267-286.

BECCALUVA L., DAL PIAZ G.V. & MACCIOTTA G. (1984): Transitional to normal morb affinities in ophiolitic metabasites from the Zermatt-Saas, Combin and Antrona Units, western Alps: implications for the paleogeographic evolution of the western Tethyan basin. - Geol. Mijnbouw 7716-7746: 165-177.

BEHRMANN J.H. & RATSCHBACHER L. (1989): Archimedes revisited: a structural test of eclogite emplacement models in the Austrian Alps. - Terra Research 1: 242-252.

BERMAN R.G. (1988): Internally-consistent thermodynamic data for minerals in the system Na2O-K2O-CaO-MgO-FeO-Fe2O3-Al2O3-SiO2-TiO2-H2O-CO2. - J. Petrol. 29: 445-522.

BERMAN R.G., ARANOVICH L.Y. & PATTISON D.R.M. (1995): Reassessment of the garnet-clinopyroxene Fe-Mg exchange thermometer: II. Thermodynamic analysis. - Contrib. Mineral. Petrol. 119: 30-42.

BERNHARDT H.J., MASSONNE H.-J., REINECKE T., REINHARDT J. & WILLNER A. (1995): Digital element distribution maps, an aid for petrological investigations. - Ber. Deutsch. Mineral. Ges. Beih. Eur. J. Mineral. 7: 28.

VAN DEN BEUKEL J. (1992): Some thermomechanical aspects of the subduction of continental lithosphere. - Tectonics 11: 316-329.

BIRD J.E., MUKHERJEE A.K. & DORN J.F. (1969): Correlations between hightemperature creep behavior and structure. - In: BRANDON D.G. & ROSEN R. (eds.): Quantative relations between properties and microstructure 255-342.

BLACIC J:D: (1972): Effect of water on the experimental deformation of olivine. - In: HEARD H.C., BORCH I.Y., Carter N.L. & RAYLEIGH C.B. (eds.): Flow and Fracture of Rocks, The Griggs Volume, Geophys. Monogr. Ser., 16; 109-115.

BLAKE M.C. jr. & JAYKO A.S. (1990): Uplift of very high pressure rocks in the western Alps: evidence for structural attenuation along low-angle faults. - In: ROURE F., HEITZMANN P. & POLINO R. (eds.) Deep structure of the Alps, Mem. Soc. geol. Fr. 156: 237-246.

VON BLANCKENBURG F. & DAVIES J.H. (1994): Slab breakoff: A model for syncollisional magmatism and tectonics in the Alps. - Tectonics 14: 120-131.

BLUNDY J.D. & HOLLAND T.J.B. (1990): Calcic amphibole equilibria and a new amphibole-plagioclase geothermometer. - Contrib. Mineral. Petrol. 104: 208-224.

BOHLEN S.R. & BOETTCHER A.L. (1982): The quartz-coesite transformation: a precise determination and the effects of other components. - J. Geophys. Res. 87: 7073-7078.

BOUILLIER, A.-M., MICHOT, G., PECHER, A & BARRES, O. (1989): Diffussion and/or plastic deformation around fluid inclusions in synthetic quartz: new investigations. - In: BRIDGEWATER, D. (ed.) Fluid movements - Element Transport and Composition of the Deep Crust; NATO ASI Series, C281: 345-360.

BOLAND J.N. & TULLIS T.E. (1986): Deformation behavior of wet and dry clinopyroxenite in the brittle to ductile transition region. - Geophys. Monograph AGU 36: 35-49.

BOWTELL S.A., CLIFF R.A. & BARNICOAT A.C. (1994): Sm-Nd isotopic evidence on the age of eclogitization in the Zermatt-Saas ophiolite. - J. Metamorphic Geol. 12: 187-196.

BROWN T.H., BERMAN R.G. & PERKINS E.H. (1988): GeO-Calc: Software package for calculation and display of pressure-temperature-composition phase diagrams using an IBM or compatible Personal Computer. - Computer & Geoscience 14: 279-289.

BROWN P.E. & LAMB W.M. (1989): P-V-T properties of fluids in the system H2O+/- CO2+/-NaCl: new graphical presentations and implications for fluid inclusion studies. - Geochim. Cosmochim. Acta 53: 1209-1221.

BUATIER M., VAN ROERMUND H.L.M., DRURY M.R. & LARDEAUX J.M. (1991): Deformation and recrystallization mechanisms in naturally deformed omphacites from the Sesia-Lanzo zone; geophysical consequences. - Tectonophysics 195: 11-27.

BUCHER K. & FREY M. (1994): Petrogenesis of Metamorphic Rocks. - Springer: Berlin, Heidelberg, New York, 318 pp.

BUTLER R.W.H. (1986): Thrust tectonics, deep structure and crustal subduction in the Alps and Himalayas. - J. Geol. Soc. London 143: 857-873.

CARPENTER M.A., DOMENEGHETTI M.C. & TAZOLLI V. (1990): Application of Landau theory to cation ordering in omphacite. I. Equilibrium behaviour. - Eur. J. Mineral. 2: 7-18.

CARTER N.L. & TSENN M.C. (1987): Flow properties of continental lithosphere. - Tectonophysics 136: 27-63.

CHAKRABORTY & GANGULY J. (1990): Compositional zoning and cation diffusion in garnets. - In: GANGULY J.(ed.). - Diffusion, Atomic ordering and Mass Transport. - Advances in Phys. Geochem. 8: 121-175.

CHAPPLE W.M. (1978): Mechanics of thin Skinned Fold-and Thrust Belts. - Geol. Soc. Am. Bull. 89: 1189-1198.

CHEMENDA A.I., MATTAUER M., MALAVIEILLE J. & BOKUN A.N. (1995): A mechanism for syn-collisional rock exhumation and associated normal faulting: Results from physical modelling. - Earth Planet. Sci. Lett. 132: 225-232.

CHOPIN C. (1984): Coesite and pure pyrope in high grade blueschists of the Western Alps: a first record and some consequences. - Contrib. Mineral. Petrol. 86: 107-118.

CHOPIN C. & MONIE P. (1984): A unique magnesio-chloritoid bearing high pressure assemblage from the Monte Rosa, Western Alps: petrologic and 40Ar-39Ar radiometric study. - Contrib. Mineral. Petrol. 87: 388-398.

CLOOS M. (1982): Flow Melanges: Numerical Modeling and Geologic Constraints on Their Origin in the Francisian Subduction Complex. - Geol. Soc. Am. Bull. 93: 330-345.

CLOOS M. & SHREVE R.L. (1988a): Subduction-Channel Model of Prism Accretion, Melange Formation, Sediment Subduction, and Subduction Erosion at Convergence Plate Margins: 1. Background and Description. - PAGEOPH 128: 455-500.

CLOOS M. & SHREVE R.L. (1988b): Subduction-Channel Model of Prism Accretion, Melange Formation, Sediment Subductin, Subduction Erosion at Convergence Plate Margins: 2. Implications and Discussion. - PAGEOPH 128: 501-545.

COLEMAN R.G. & WANG X. (eds.). (1995): Ultrahigh Pressure Metamorphism; Cambridg University Press, New York, 528 pp.

COWAN D.S. & SILLING R.M. (1978): A dynamic, scaled model of accretion at trenches and its implications for the tectonic evolution of subduction complexes. - J. Geophys. Res. 83: 5389-5396.

COWARD M. & DIETRICH D. (1989): Alpine tectonics - an overview. - In: COWARD M.P., DIETRICH D. & PARK R.G. (eds.), Alpine tectonics. Geol. Soc. London, Spec. Publ. 45: 1-29.

DAHLEN F.A., SUPPE J. & DAVIS D. (1984): Mechanics of fold-and-thrust belts and accretionary wedges: Cohesive Coulomb theory. - J. Geophys. Res. 89: 10087-10102.

DAL PIAZ G.V. (1988): Revised setting of the Piedmont zone in the northern Aosta valley, western Alps. - Ofioliti 13(2/3): 157-162.

DAL PIAZ G.V., HUNZIKER J.C. & MARTINOTTI G. (1971): La zona Sesia-Lanzo e l'evoluzione tettonico-metamorfica delle Alpi Nordoccidentale interne. - Mem. Soc. Geol. It. 11: 433-460.

DAL PIAZ G.V. & ERNST W.G. (1978): Areal geology and petrology of eclogites and associated metabasites of the Piemonte ophiolite nappe, Breuil - St.Jaques area, Italian Western Alps. - Tectonophysics 51: 99-126.

DAL PIAZ G.V., VENTURELLI G., SPADEA P. & DI BATTISTINI G. (1981): Geochemical features of metabasalts and metagabbros from the Piemonte ophiolite nappe, italien western Alps. - N. Jb. Mineral. Abh. 142: 248-269.

DAVIES J.H. & VON BLANCKENBURG F. (1995): Slab breakoff: A model of lithosphere detachment and its test in the magmatism and deformation of collisional orogens. - Earth Planet. Sci. Lett. 129: 85-102.

DAVIS D.M., SUPPE J. & DAHLEN F.A. (1983): Mechanics of fold-and-thrust belts and accretionary wedges. - J. Geophys. Res. 88: 1153-1172.

DEBELMAS J. & LEMOINE M. (1970): The western Alps: palaeogeography and structure. - Earth Science Reviews 6: 221 -256.

DERBY B. (1991): The dependance of grain size on stress during dynamic recrystallisation. - Acta metall. mater. 39: 955-962

DERBY B. & ASHBY M.F. (1987): On dynamic recrystallisation. - Scripta met. 21: 879-884.

DESMONS J. (1992): The Briancon basement (Pennine western Alps): mineral composition and polymetamorphic evolution. - Schweiz. Mineral. Petrogr. Mitt. 72: 37-55.

DEVILLE E., FUDRAL S., LAGABRIELLE Y., MARTHALER M. & SARTORI M. (1992): From oceanic closure to continental collision: a synthesis of the „Schistes lustres“ metamorphic complex of the western Alps. - Geol. Soc. Am. Bull. 104: 127-139.

DEWEY J.F. (1988): Extensional Collapse of Orogens. - Tectonics 7: 1123 - 1139.

DEWEY J.F., HELMAN M.L., TURCO E., HUTTON D.H.W. & KNOTT S.D. (1989): Kinematics of the western Mediterranean. - In: COWARD M.P., DIETRICH D. & PARK R.G. (eds.), Alpine tectonics. Geol. Soc. London, Spec. Publ. 45: 265-283.

ELLIS D.J. & GREEN D.H. (1979): An experimental study of the effect of Ca upon garnet-clinopyroxene Fe-Mg exchange equilibria. - Contrib. Mineral. Petrol. 71: 13-22.

ELLIS A.C., BARNICOAT A.C. & FRY N. (1989): Structural and metamorphic constraints on the tectonic evolution of the upper Pennine Alps. - In: COWARD M.P., DIETRICH D. & PARK R.G. (eds.) Alpine tectonics, Geol. Soc. London, Spec. Publ. 45: 173-188.

EMERMAN S.H. & TURCOTTE D.L. (1983): A fluid model for the shape of accretionary wedges. - Earth Planet. Sci. Lett. 63: 379-384.

ENGLAND P.C. & HOLLAND T.J.B. (1979): Archimedes and the Tauern Eclogites: the role of buoyancy in the preservation of exotic eclogite blocks. - Earth Planet. Sci. Lett. 44: 287-294.

ENGLAND P. & HOUSEMAN G. (1986): Finite strain calculations of continental deformation: 2. Comparison with the India-Asia collision zone. - J. Geophys. Res. 91: 3664-3676.

ENGLAND P. & HOUSEMAN G. (1989): Extension during continental convergence, with application to the Tibetan plateau. - J. Geophys. Res. 94: 17561-17579.

ENGLAND P. & MOLNAR P. (1990): Surface uplift, uplift of rocks, and exhumation of rocks. - Geology 18: 1173-1177.

ERNST W.G. & DAL PIAZ G.V. (1978): Mineral parageneses of eclogitic rocks and related mafic schists of the Piemonte ophiolite nappe, Breuil-St. Jacques area, Italian Western Alps. - Am. Miner. 63: 621-640.

ESCHER A., HUNZIKER J.C., MARTHALER M., MASSON H., SARTORI M. & STECK A. (1997): Geologic framework and structural evolution of the Western Swiss-Italian Alps. - In: PFIFFNER O.A., LEHNER P., HEITZMANN P., MUELLER S. & STECK A. (eds.) Deep structure of the Swiss Alps: results of NRP 20: 205-222.

ESSENE E.J. (1989): The current status of thermobarometry in metamorphic rocks. - In: DALY J.S., CLIFF R.A. & YARDLEY B.W.D. (eds.), Evolution of metamorphic belts. Geol. Soc. London, Spec. Publ. 43: 1-44.

ETHERIDGE M.A. (1983): Differential stress magnitudes during regional deformation and metamorphism: Upper bound imposed by tensile fracturing. - Geology 11: 231-234.

EVANS B.W. (1990): Phase relations of epidote-blueschists. - Lithos 24: 3-23.

FREEMAN S.R., INGER S., BUTLER W.H. & CLIFF R.A. (1997): Dating deformation using Rb-Sr in white mica: Greenschist facies deformation ages from the Entrelor shear zone, Italian Alps. - Tectonics 16: 57-76.

FREY M., HUNZIKER J.C., O´NEILL J.R. & SCHWANDER H.W. (1976): Equilibrium-disequilibrium relations in the Monte Rosa granite, Western Alps: petrological, Rb-Sr and stable isotope data. - Contrib. Mineral. Petrol. 55: 147-179.

FRY N. & BARNICOAT A.C. (1987): The tectonic implications of high-pressure metamorphism in the western Alps. - J. Geol. Soc. London 144: 653-659.

GEBAUER D., SCHERTL H.-P., BRIX M. & SCHREYER W. (1997): 35 Ma old ultrahigh-pressure metamorphism and evidence for very rapid exhumation in the Dora Maira Massif, Western Alps. - In: SCHREYER W. & STÖCKHERT B. (eds.) High pressure metamorphism in nature and experiment. Lithos 41: 5-24.

GILLET P., DAVY P.H., BALLEVRE M. & CHOUKROUNE P. (1985): Thermomechanical evolution of a collision zone: the example of the Western Alps. - Terra cognita 5: 399-404.

GILLET P., CHOUKROUNE P., BALLEVRE M. & DAVY P. (1986): Thickening history of the Western Alps. - Earth Planet. Sci. Lett. 78: 44-52.

GLEASON G.C., TULLIS J. & HEIDELBACH F. (1993): The role of dynamic recrystallization in the development of lattice preferred orientations in experimentally deformed quartz aggregates. - J. Struct. Geol. 15: 1145-1168.

GLOVER G. & SELLARS C.M. (1973): Recovery and recrystallisation during high temperature deformation of α-iron. - Metallurgical Trans. 4: 765-775.

GODARD G. & VAN ROERMUND H.L.M. (1995): Deformation-induced clinopyroxene fabrics from eclogites. - J. Struct. Geol. 17: 1425-1443.

GOLDSMITH J.R. & NEWTON R.C. (1969):P-T-X relations in the system $CaCO_3$-$MgCO_3$ at high temperatures and pressures. - Am. J. Sci. 267A: 160-190.

GREEN T.H. & ADAM J. (1991): Assessment of the garnet-clinopyroxene Fe-Mg exchange thermometer using new experimental data. - J. Metamorphic Geol. 9: 341-347

GREEN II H.W. & BORCH R.S. (1989): A new molten salt cell for precision stress measurement at high pressure. - Eur. J. Mineral. 1: 213-219.

GREEN II H.W. & BORCH R.S. (1990): High pressure temperature deformation experiments in a liquid confining medium. - Geophys. Monograph AGU 56: 195-200.

GRIGGS D.T. (1967): Hydrolytic weakening of quartz and other silicates. - Geophys. J. Roy. Astron. Soc. 14, 19-31.

HAAS J.L. Jr. (1976): Physical properties of the coexisting phases and the thermochemical properties of the H2O component in boiling NaCl solutions. - U.S. Geol. Surv. Bull. 1421-A: 73pp.

HABERMANN D. (1992): Strukturelle Entwicklung und Metamorphose der Gesteine östlich des Lago di Cignana. - Unpubl. diploma thesis, Inst. für Geologie, Ruhr-Universität Bochum, pp.80.

HACKER B.R. & WANG Q. (1995): Ar/Ar geochronology of ultrahigh-pressure metamorphism in central China. - Tectonics 14: 994-1006.

HARBOTT W., KÜSTER M. & STÖCKHERT B. (1990): A new vacuum chamber microthermometry apparatus for analysis of fluid inclusions. - Terra abstr. 2: 54;

HARLEY S.L. & CARSWELL D.A. (1995): Ultradeep crustal metamorphism: A prospective view. - J. Geophys. Res. 100: 8367-8380.

HARMS T.A., JAYKO A.S. & BLAKE M.C. jr. (1992): Kinematic evidence for extensional unroofing of the Franciscan complex along the Coast Range fault, northern Diabolo Range, California. - Tectonics 11: 228-241.

HAUGERUD R.A. & ZEN E.-A. (1991): An essay on metamorphic path studies or Cassandra in P-T-t space. In: PERCHUK L.L. (ed.) Progress in metamorphic and magmatic petrology, 323-348; Cambridge University Press, Cambridge.

HEIM A. (1922): Geologie der Schweiz. Tauchnitz; Leipzig

HENRY C., MICHARD A. & CHOPIN C. (1993): Geometry and structural evolution of ultra-high-pressure and high-pressure rocks from the Dora-Maira massif, Western Alps, Italy. - J. Struct. Geol. 15: 965-981.

HOBBS B.E. (1985): Quartzites. In: WENK H.-R. (ed.) Prefferred orientation in deformed metals and rocks. An introduction to modern texture analysis, 361-384.

HODGES K.V. (1991): Pressure-temperature-time paths. - Ann. Rev. Earth Planet. Sci. 19: 207-236.

HODGES K.V. & MCKENNA L.W. (1987): Realistic propagation of uncertainties in geologic thermobarometry. - American Mineralogist 72: 671-680.

HOLLAND T.J.B. (1979): Experimental determination of the reaction paragonite = jadeite + kyanite + H2O, and internally consistent thermodynamic data for part of the system Na2O - Al2O3 - SiO2 - H2O, with applications to eclogites and blueschists. - Contrib. Mineral. Petrol. 68: 293-301.

HOLLAND T.J.B. (1980): The reaction albite = jadeite + quartz determined experimentally in the range 600-1200°C. - Am. Mineralogist 65: 129-134.

HOLLAND T.J.B. (1990): Activities of components in omphacitic solid solutions. - Contrib. Mineral. Petrol. 105: 446-453.

HOLLAND T.J.B. & POWELL R. (1992): Plagioclase feldspars: activity-composition relations based on Darken´s Quadratic Formalism and Landau theory. - Am. Mineral. 77: 53-61.

HOLLAND T. & BLUNDY J. (1994): Non-ideal interactions in calcic amphiboles and their bearing on amphibole-plagioclase thermometry. - Contrib. Mineral. Petrol. 116: 433-447.

HOLLISTER L.S., BURRUS R.C., HENRY D.L. & HENDEL E.M. (1979): Physical conditions during uplift of metamorphic terranes, as recorded by fluid inclusions. - Bull. Mineral. 102: 555-566.

HOLLISTER L.S. & CRAWFORD M.L. (1981): Short course in fluid inclusions: Application to petrology. - Mineralogical Association of Canada short course handbook 6: 304 pp.

HSÜ K.J. (1991): Exhumation of high-pressure metamorphic rocks. - Geology 19: 107-110.

HUNZIKER J.C. (1974): Rb-Sr and K-Ar age determination and the Alpine tectonic history of the Western Alps.- Mem. Ist. Geol. Min. Univ. Padova 31: 54 pp.

HUNZIKER J.C. (1986): The Alps: a case of multiple collision. - In: COWARD M.P. & RIES A.C. (eds.), 1986, Collision Tectonics, Geol. Soc. Spec. Publ. No.19: 221-227.

HUNZIKER J.C., DESMONS J. & MARTINOTTI G. (1989): Alpine thermal evolution in the central and the western Alps. - In: COWARD M.P., DIETRICH D. & PARK R.G. (eds.), Alpine tectonics. Geol. Soc. London, Spec. Publ. 45: 353-367.

HURFORD A.J., HUNZIKER J.C. & STÖCKHERT B. (1991): Constraints on the late thermotectonic evolution of the western Alps: evidence for episodic rapid uplift. - Tectonics 10: 758-769.

INGER S., RAMSBOTHAM W., CLIFF R.A. & REX D.C. (1996): Metamorphic evolution of the Sesia-Lanzo Zone, Western Alps: time constarints from multi-system geochronology. - Contrib. Mineral. Petrol. 126: 152-168.

JAEGER J.C. & COOK N.G.W. (1979): Fundamentals of rock mechanics. - N.Y. (Chapman & Hall): 513 pp.

JARRARD R.D. (1986): Relations among subduction parameters. - Rev. Geophys. 24: 217-284.

JOHANNES W. & PUHAN D. (1971): The calcite - aragonite transition, reinvestigated. - Contrib. Mineral. Petrol. 31: 28-38.

JOLIVET L., GOFFÉ B., MONIÉ P., TRUFFERT-LUXEY C., PATRIAT M. & BONNEAU M. (1996): Miocene detachment in Crete and exhumation P-T-t paths of high pressure metamorphic rocks. - Tectonics 15: 1129-1153.

KARIG D.E. (1974): Evolution of arc systems in the western Pacific. - Ann. Rev. Earth Planet. Sci. 2: 51-75.

VAN DER KLAUW S.N.G.C., REINECKE T. & STÖCKHERT B. (1997): Exhumation of ultahigh-pressure metamorphic oceanic crust from Lago di Cignana, Piemontese zone, western Alps: the structural record in metabasites. - In: SCHREYER W. & STÖCKHERT B. (eds.) High pressure metamorphism in nature and experiment. Lithos 41: 79-102.

KOCH P.S. (1983): Rheology and microstructures of experimentally deformed quartz aggregates. Ph D. Thesis Univ. of California, 464 pp.

KOCH P.S., CHRISTIE J.M., ORD A. & GEORGE R.P. jr. (1989): Effect of water on the rheology of experimentally deformed quartzite. - J. Geophys. Res. 94: 13975-13996.

KOHN M.J. & SPEAR F.S. (1991a): Error propagation for barometers: 1. Accuracy and precision of experimentally located end-member reactions. - American Mineralogist 76: 128-137.

KOHN M.J. & SPEAR F.S. (1991b): Error propagation for barometers: 2. Application to rocks. - American Mineralogist 76: 138-147.

KOONS P.O. (1984): Implications to garnet-clinopyroxene geothermometry of non-ideal solid solution in jadeitic pyroxenes. - Contrib. Mineral. Petrol. 88: 340-347.

KOONS P.O. (1990): Two-sided orogen: Collision and erosion from the sandbox to the Southern Alps, New Zealand. - Geology 18: 679-682.

KREULEN R. (1980): CO2-rich fluids during regional metamorphism on Naxos (Greece): carbon isotopes and fluid inclusions. - Am. J. Sci. 280: 745-771.

KROGH E.J. (1988): The garnet-clinopyroxene Fe-Mg geothermometer - a reinterpretation of existing experimental data. - Contrib. Mineral. Petrol. 99: 44-48.

KÜSTER M. (1994): Fluid-Einschlüsse in niedrigtemperierten Hockdruckmetamorphiten und Geothermobarometrie am Beispiel der Phyllit-Quarzit-Einheit auf Kreta (Ägäis). - Diss. Ruhr-Universität Bochum, 101pp.;

KÜSTER M. & STÖCKHERT B. (1997): Density changes of fluid inclusions in high-pressure low-temperature metamorphic rocks from Crete: A thermobarometric approach based on the creep strength of the host minerals. - In: SCHREYER W. & STÖCKHERT B. (eds.) High pressure metamorphism in nature and experiment. Lithos 41: 151-167.

KÜSTER M. & STÖCKHERT B. (1999): High differential stress and sublithostatic pore fluid pressure in the ductile regime - microstructural evidence for short term postseismic creep in the Sesia Zone. Western Alps. - In: SCHMID S.M, STÜNITZ H., HEILBRONNER R.P. & PANOZZO R. (eds.) Deformation mechanisms. Tectonophysics 303: 263-271.

KUSZNIR N.J. & PARK R.G. (1986): Continental litoshere strength: The critical role of lower crustal deformation. - In: DAWSON J.B., CARSWELL D.A., HALL J. & WEDEPOHL K.H. (eds.) The nature of te lower continental crust, 79-94; Oxford (Blackwell).

LAUBSCHER H.P. (1990): Deep seismic data from the central Alps: Mass distributions and their kinematics. - Mem. Soc. Geol. France 156: 335-343.

LEAKE B.E. (1978): Nomenclature of amphiboles. - Can. Mineral. 16: 501-520.

LEMMLEIN G.G. & KLIYA M.O. (1952): Distictive features of the healing of a crack in a crystal under conditions of declining temperatures. - Int. Geol. Rev. 2: 125-128.

LISTER G.S. (1977): Discussion: Crossed-girdle c-axis fabrics in quartzites plastically deformed by plane strain and progressiv simple shear. - Tectonophysics 39: 51-53.

LISTER G.S. & DAVIS G.A. (1989): The origin of metamorphic core complexes and detachment faults dormed during Tertiary continental extension in the northern Colorado River region, U.S.A. - J. Struct. Geol. 11: 65-94.

LOOMIS T.P. (1983): Zoned Minerals. - In: SAXENA S.K. (ed.) Selected topics in Geochemistry; Kinetics and Equilibrium in Mineral Reactions, 1-37.

LUTON M.J. & SELLARS C.M. (1969): Dynamic recrystallisation in nickel and nickel-iron alloys during high temperature deformation. - Acta Metallurgica 17: 1033-1043.

MANCKTELOW N.S. (1995): Nonlithostatic pressure during sediment subduction and the development and exhumation of high pressure metamorphic rocks. - J. Geophys. Res. 100: 571-583.

MARCHANT R.H. & STAMPFLI G.M. (1997): Crustal and lithospheric structures of the Western Alps: geodynamic significance. - In: PFIFFNER O.A., LEHNER P., HEITZMANN P., MUELLER S. & STECK A. (eds.) Deep structure of the Swiss Alps: results of NRP 20: 326-338.

MARSHALL D.J. (1988): Cathodoluminesence of geological materials. - Unwin Hyman Ltd. London 146 pp.

MARTHALER M. & STAMPFLI G.M. (1989): Les schists lustres a ophiolites de la nappe du Tsate: un ancien prisme d‘accretion issu de la marge active apulienne? - Schweiz. Mineral. Petrogr. Mitt. 69: 211-216.

MAZUREK M. (1986): Structural evolution and metamorphism of the Dent Blanche nappe and the Combin Zone west of Zermatt (Switzerland). - Eclogae Geol. Helv. 79: 41-56.

MERCIER J.-C.C., ANDERSON D.A. & CARTER N.L. (1977): Stress in the lithosphere: inferences from steady-state flow of rocks. - J. Pure Appl. Geophys. 115: 199-226.

MICHARD A., CHOPIN C. & HENRY C. (1993): Compression versus extension in the exhumation of the Dora-Maira coesite-bearing unit, western Alps, Italy. - Tectonophysics 221: 173-193.

MICHARD A., HENRY C. & CHOPIN C. (1995): Structures in UHPM Rocks: A Case study from the Alps - In: COLEMAN R.G. & WANG X. (eds.). - Ultrahigh Pressure Metamorphism, 132-158; Cambridg University Press, New York.

MIRWALD P.W. & MASSONNE H.-J. (1980): Quartz = coesite transition and the comparative friction measurements in piston-cylinder apparatus using talc-AalSimag-glass (TAG) and NaCl high pressure cells: A discussion. - N. Jb. Mineral. Mh. 1980: 469-477.

MEYER J. (1983): Mineralogie und Petrologie des Allalingabbros. - Diss. Univ. Basel, 329pp.

MONIÉ P. (1990): Preservation of Hercynian $^{40}Ar/^{39}Ar$ ages through high-pressure low-temperature Alpine metamorphism in the Western Alps. - Eur. J. Mineral. 2: 343-361.

NEUSER R.D. (1995): A new high-intensity cathodoluminescence microscope and its application to weakly luminescing minerals. - In: SCHREYER W., RUMMEL F. & STÖCKHERT B. (eds.), Abstr. Vol.: Intern. Coll. “High-Pressure Metamorphism in Nature and Experiment”. Bochumer Geol. u. Geotech. Arb. 44: 116-118.

OBERHÄNSLI R. (1980): P-T Bestimmungen anhand von Mineralanalysen in Eklogiten und Glaukophaniten der Ophiolithe von Zermatt. - Schweiz. Mineral. Petrogr. Mitt. 60: 215-235.

OBERHÄNSLI R. (1982): The p-t-history of some pillow lavas from Zermatt. - Ofioliti 213: 431-436.

OKAY A.I. (1995): Paragonite eclogites from Dabie Shan, China: Re-equilibration during exhumation? - J. Metamorphic Geol. 13: 449-460.

ORD A. & CHRISTIE J.M. (1984): Flow stresses from microstructures in mylonitic quartzites of the Moine Thrust zone, Assynt area, Scotland. - J. Struct. Geol. 6: 639-654.

PATERSON M.S. & LUAN F.C. (1990): Quartzite rheology under geological conditions. In: KNIPE R.J. & RUTTER E.H. (eds.) Deformation mechanisms, rheology and tectonics. - Geological Society Special Publication 54: 299-307.

PACHECO J.F., SYKES L.R. & SCHOLZ C.H. (1993): Nature of seismic coupling along simple plate boundaries of the subduction type. - J. Geophys. Res. 98: 14,133-14,159.

PATTISON D.R.M. & NEWTON R.C. (1989): Reversed experimental calibration of the garnet-clinopyroxene Fe-Mg exchange thermometer. - Contrib. Mineral. Petrol. 101: 87-103.

PAVLIS T.L. & BRUHN R.B. (1983): Deep-seated flow as a mechanism for the uplift of broad forearc ridges and its role in the exposure of high P/T metamorphic terranes. - Tectonics 2: 473-497.

PEACOCK S.M. (1987): Thermal effects of metamorphic fluids in subduction zones. - Geology 15: 1057-1060.

PEACOCK S.M. (1996): Thermal and petrologic structure of subduction zones. - In: BEBOUT G.E., SCHOLL D.W., KIRBY S.H. & PLATT J.P. (eds.), Subduction , Top to Bottom. Geophys. Monogr. 96: 119-133.

PECHER A. (1981): Experimental decrepitation and re-equilibration of fluid inclusions in synthetic quartz. - Tectonophysics 78: 567-583.

PECHER A. & BOULLIER A.-M. (1984): Evolution a pression et temperature elevees d'inclusions fluides dans un quartz synthetique. - Bull. Mineral. 107: 139-153.

PFEIFER H.-R., COLOMBI A. & GANGUIN J. (1989): Zermatt-Saas and Antrona Zone: a petrographic and geochemical comparison of polyphase metamorphic ophiolites of the western-central Alps. - Schweiz. Mineral. Petrogr. Mitt. 69: 217-236.

PHILIPPOT P. (1990): Opposite vergence of nappes and crustal extension in the French-Italian Western Alps. - Tectonics 9: 1143-1164.

PLATT J.P. (1986): Dynamics of orogenic wedges and the uplift of high-pressure metamorphic rocks. - Geol. Soc. Am. Bull. 97: 1037-1053.

PLATT J.P. (1987): The uplift of high-pressure-low-temperature metamorphic rocks. - Philos. Trans. R. Soc. London 321: 87-103.

PLATT J.P. (1993): Exhumation of high-pressure rocks: A review of concepts and processes. - Terra nova 5: 119-133.

PLATT J.P. & BEHRMANN J.H. (1986): Structures and fabrics in a crustal-scale shear zone, Betic Cordillera, SE Spain. - J. Struct. Geol. 8: 15-33.

POLINO R., DAL PIAZ G.V. & GOSSO G. (1990): Tectonic erosion at the Adria margin and accretionary processes for the Cretaceous orogeny in the alps. - In: ROURE F., HEITZMANN P. & POLINO R. (eds.), Deep structure of the Alps, Mem. Soc. geol. Fr. 156: 345-367.

POTTER R.W. II & BROWN D.L. (1977): The volumetric properties of aqueous sodium chloride solutions from 0 to 500 °C and pressure up to 2000 bars based on a regression of available data in the literature. - Bull. U.S. Geol. Surv. 1421-C.

POUCHOU J.L. & PICHOIR F. (1984): A new model for quantitative X-ray microanalysis. Part I: Application to the analysis of homogeneous samples. - Rech. Aerosp. 3: 13-38.

POWELL R. (1985): Regression diagnostics and robust regression in geothermometer/geobarometer calibration: the garnet-clinopyroxene geothermometer revisited. - J. Metamorphic Geol. 3: 231-243.

POWELL R., CONDLIFFE D.M. & CONDLIFFE E. (1984): Calcite-dolomite geothermometry in the system CaCO3-MgCO3-FeCO3: an experimental study. - J. Metamorphic Geol. 2: 33-41.

PRICE G.P. (1985): Preferred orientations in quartzites. - In: WENK H.-R. (ed.) Preferred Orientation in Deformed Metals and Rocks: An Introduction to Modern Texture Analysis, 385-405; Academic Press, London.

PUTNIS A. (1992): Introduction to mineral sciences. - Cambridge University Press, Cambridge: 452 pp.

RAHEIM A. & GREEN D.H. (1974): Experimental determination of the temperature and pressure dependance of the Fe-Mg partition coefficients for coexisting garnet and clinopyroxene. - Contrib. Mineral. Petrol. 48: 179-203.

RATSCHBACHER L., FRISCH W., NEUBAUER F., SCHMID S.M. & NEUGEBAUER J. (1989): Extension in compressional orogenic belts: the eastern Alps. - Geology 17: 404-407.

REED S.J.B. (1996): Electron microprobe analysis and scanning electron microscopy in geology. - Cambridge University Press, Cambridge: 201 pp.

REINECKE T. (1991): Very-high-pressure metamorphism and uplift of coesite-bearing metasediments from the Zermatt-Saas zone, Western Alps. - Eur. J. Mineral. 3: 7-17.

REINECKE T. (1995): Ultrahigh and high-pressure metamorphic rocks of the Zermatt-Saas zone, Western Alps - records of burial and exhumation paths. - In: SCHREYER W., RUMMEL F. & STÖCKHERT B. (eds.), Abstr. Vol.: Intern. Coll. “High-Pressure Metamorphism in Nature and Experiment”. Bochumer Geol. u. Geotech. Arb. 44: 152-157.

REINECKE T. (1998): Prograde high- to ultrahigh-pressure metamorphism and exhumation of oceanic sediments at Lago di Cignana, Zermatt-Saas Zone, western Alps. - Lithos 42: 147-189.

REINECKE T., VAN DER KLAUW S.N. & STÖCKHERT B. (1994): UHP metamorphic oceanic crust of the Zermatt-Saas Zone (Piemontese Zone) at Lago di Cignana, Valtournanche, Italy. - In: COMPAGNONI R. & MESSIGA B. (eds.) High pressure metamorphism in the Western Alps; 16th IMA Meeting; Guide book to field excursion B1: 117-126; Pisa.

REINSCH D. (1977): High pressure rocks from Val Chuisella (Sesia-Lanzo Zone, Italian Alps). - N. Jb. Mineral. Abh. 130: 89-102.

RIDLEY J. (1984): Evidence of a Temperature-dependent Blueschist to Eclogite Transformation in High-pressure Metamorphism of Metabasic Rocks. - J. Petrol. 25: 852-870.

ROEDDER E. (1962): Studies of fluid inclusions I. Low temperature application of a dual-purpose freezing and heating stage. - Econ. Geol. 57: 1045-1061.

ROEDDER E. (1967): Metastable superheated ice in liquid-water inclusions under high negative pressure. - Science 155: 1413-1417.

ROEDDER E. (1972): The composition of fluid inclusions, in data of geochemistry. - U.S. Geological Survey Professional Paper 440 pp.

ROEDDER E. (1984): Fluid inclusions - Rev. Min. 12: Mineralogical Soc. Am. 1984; 644 pp.

ROYDEN L.H. (1993): The tectonic expression of slab pull at continental convergent boundaries. - Tectonics 12: 303-325.

RUBATTO D., GEBAUER D. & FANNING M. (1998): Jurassic formation and Eocene subduction of the Zermatt-Saas-Fee ophiolites: implications for the geodynamic evolution of the Central and Western Alps. - Contrib. Mineral. Petrol. 132: 269-287.

RUTTER E.H. (1976): The kinetics of rock deformation by pressure solution. - Roy. Soc. London Phil. Trans. Ser. A 283: 203-219.

RUTTER E.H. (1983): Pressure solution in nature, theory and experiment. - J. Geol. Soc. London 140: 725-740.

RUTTER E.H. & BRODIE K.H. (1985): The permeation of water into hydrating shear zones. In: THOMPSON A.B. & RUBIE D.C. (eds.) Metamorphic reactions: kinetics, textures and deformation: 242-249.

SARTORI M. (1987): Structure de la Zone du Combin entre les Diablons et Zermatt (Valais). -Eclogae Geol. Helv. 80: 789-814.

SARTORI M. (1990): L' unité du Barrhorn (Zone pennique, Valais, Suisse) Mém. Géol. Laussanne 6, 156pp.

SCHERTL H.-P., SCHREYER W. & CHOPIN C. (1991): The pyrope-coesite rocks and their country rocks at Parigi, Dora Maira massif, western Alps: detailed petrography, mineral chemistry and PT-path. - Contrib. Mineral. Petrol. 108: 1-21.

SCHMID S.M. & CASEY M. (1986): Complete fabric analysis as some commonly observed quartz c-axis patterns. - Geophys. Monograph AGU 36: 263-286

SCHREYER W. (1995): Ultradeep metamorphic rocks: The retrospective viewpoint. - J. Geophys. Res. 100: 8353-8366.

SCHULZE D.J. & HELMSTAEDT H. (1988): Coesite-sanidine eclogites from kimberlite: products of mantle fractionation or subduction? - J. Geol. 96: 435-443.

SCHWARZ S. & STÖCKHERT B. (1996): Pressure solution in siliciclastic HP-LT metamorphic rocks - constraints on the state of stress in deep levels of accretionary complexes. - Tectonophysics 225: 203-209.

SELVERSTONE J. (1985): Petrologic constraints on imbrication, metamorphism, and uplift in the SW Tauern Window, Eastern Alps. - Tectonics 4: 687-704.

SHATSKY V.S., JAGOUTZ E. KOZMENKO O.A., PARKHOMENKO V.S., TROESCH M. & SOBOLEV N.V. (1999): Geochemistry and age of ultra-high pressure rocks from the Kokchetav Massif (northern Kazachstan). - Contrib. Mineral. Petrol. 137: 185-205.

SHEPERD T.J. (1981): Temperature programmable heating-freezing stage for microthermometric analysis of fluid inclusions. - Econ. Geol. 76: 1244-1247.

SHEPHERD T.J., RANKIN A.H. & ALDERTON D.H.M. (1985): A practical guide to fluid inclusion studies. - XI, Glasgow (Blackie): 239 pp.

SHREVE R.L. & CLOOS M. (1986): Dynamics of sediment subduction, melange formation, and prism accretion. - J. Geophys. Res. 91: 10229-10245.

SIBSON R.H. (1985): A note on fault reactivation. - J. Struct. Geol. 7: 751-754.

SKROTZKI W. (1992): The geological significance of microstructural analyses by transmission electron microscopy. - Geotekt. Forsch. 78: 1-53.

SMITH D.G.W. (1976) (ed.): Short course in Microbeam Techniques. - Mineralogical association of Canada, Edmonton: 186 pp.

SONDER L.J., ENGLAND P.C., WERNICKE B.P. & CHRISTIANSEN R.L. (1987): A physical model for Cenozoic extension of western North America. - Geol. Soc. Spec. Paper 28: 187-201.

SPEAR F.S. (1988): The Gibbs method and Duhem's theorem: the quantitative relationships among P, T, chemical potential, phase composition and reaction progress in igneous and metamorphic systems. - Contrib. Mineral. Petrol. 99: 249-256.

SPEAR F.S. (1993): Metamorphic phase equilibria and pressure-temperature-time paths. MSA Monograph, Washington D.C. 797 pp.

SPEAR F.S. & MENARD T. (1989): Programm GIBBS: A generalized Gibbs method algorithm. - American Mineralogist 74: 942-943.

SPRUNT E.S. & NUR A. (1979): Microcracking and healing in granites: New evidence from cathodoluminesence. - Science 205: 495-497.

STECK A. (1990): A map of ductile shear zones of the Central Alps. - Eclogae Geol. Helv. 83: 603-628.

STECK A. & HUNZIKER J. (1994): The Tertiary structural and thermal evolution of the Central Alps - Compressional and extensional structures in an orogenic belt. - Tectonophysics 238: 229-254.

STERNER S.M. & BODNAR R.J. (1989): Synthetic fluid inclusions - VII. Re-equilibration of fluid inclusions in quartz during laboratory-simulated metamorphic burial and uplift. - J. Metamorphic Geol. 7: 243-260.

STÖCKHERT B. & RENNER J. (1998): Rheology of Crustal Rocks at Ultrahigh Pressure. - In: HACKER B.R. & LIOU J.G. (eds.) When Continents Collide: Geodynamics and Geochemistry of Ultrahigh-Pressure Rocks, 57-95.

STÖCKHERT B., MASSONNE H.-J. & NOWLAN E.U. (1997): Low differential stress during high-presssure metamorphism: The microstructural record of a metapelite from the Eclogite Zone, Tauern Window, Eastern Alps - In: SCHREYER W. & STÖCKHERT B. (eds.) High pressure metamorphism in nature and experiment. Lithos 41: 103-118.

STÖCKHERT B., WACHMANN M., KÜSTER M. & BIMMERMANN S. (1999): Low effective viscosity during high pressure metamorphism due to dissolution precipitation creep: The record of HP-LT metamorphic carbonates and siliciclastic rocks from Crete. - In: SCHMID S:M, STÜNITZ H., HEILBRONNER R.P. & PANOZZO R. (eds.) Deformation mechanisms. Tectonophysics 303: 299-319.

SWANENBERG H.E.C. (1981): Fluid inclusions in high.grade metamorphic rocks from S.W. Norway. - (Ph.D.Thesis) Geologica Ultraiectina, 25, 147 pp.

TAGAMI T. & DIMITRU T.A. (1996): Provenance and thermal history of the Fransiscan accretionary complex: Constraints from zircon fission track thermochronology. - J. Geophys. Res. 101: 11353-11364.

TAKASU A. (1989): P-T histories of peridotite and amphibolite tectonic blocks in the Sanbagawa metamorphic belt, Japan. - Spec. Publ. Geol. Soc. London, 43: 533-536.

TANIMOTO T. (1995): Crustal Structure of the Earth. - In: AHRENS T.J. (ed.) Global earth physics : a handbook of physical references: 214-224.

THOMSON S.N., STÖCKHERT B. & BRIX M. (1998): Thermochronology of the high-pressure metamorphic rocks of Crete, Greece: Implications for the speed of tectonic processes. - Geology 26: 193-288.

TILTON G.R., SCHREYER W. & SCHERTL H.-P. (1991): Pb-Sr-Nd isotopic behavior of deeply subducted crustal rocks from the Dora Maira massif, western Alps, Italy II: what is the age of the ultrahigh-pressure metamorphism? - Contrib. Mineral. Petrol. 108: 22-33.

TURNER J. & WEISS L.E. (1963): Structural analysis of metamorphic tectonites. - 545pp.; McGraw - Hill Book Comp. Inc.

TWISS R.J. (1977): Theory and applicability of a recrystallized grain size paleopiezometry. - Pure Appl. Geophys. 115: 227-244;

TWISS R.J. (1986): Variable sensitivity piezometric equations for dislocation density and subgrain diameter and their relevance to olivine and quartz. - Geophys. Monograph AGU 36: 247-261.

VANNAY J.C. & ALLEMANN R. (1990): La zone piémontaise dans le Haut-Valtournanche (Val d‘Aoste, Italie). - Eclogae Geol. Helv. 83: 21-39.

VOGLER W.S. (1987): Fabric development in a fragment of Tethyan oceanic lithosphere from the Piemonte ophiolite nappe of the western Alps, Valtournanche, Italy. - J. Struct. Geol. 9: 935-954.

WAGNER G.A., COYLE D.A., DUYSTER J., HENJES-KUNST F., PETEREK A., SCHRÖDER B., STÖCKHERT B. WEMMER K. & ZULAUF G. (1997): Post Variscan thermal and tectonic evolution of the KTB site and its surroundings. - J. Geophys. Res.102: 18221-18232.

WAGNER-ZWEIGEL P. (1993): Areal geology, fabrics and petrology of rocks SW of Lago di Cignana (Valtournanche, N-Italy). - Unpubl. diploma thesis, Inst. für Geologie, Ruhr-Universität Bochum, pp. 103.

WALKER A.N., RUTTER E.H. & BRODIE K.H. (1990): Experimental study of grain-size sensitive flow of synthetic, hot-pressed calcite rocks. In: KNIPE R.J. & RUTTER E.H. (eds.) Deformation mechanisms, rheology and tectonics. - Geological Society Special Publication 54: 259-284.

WANG K., MULDER T., ROGERS G.C. & HYNDMAN R.D. (1995): Case for very low coupling stress on the Cascadia subduction fault. - J. Geophys. Res. 100: 12,907-12,918.

WHEELER J. (1991): Structural evolution of a subducted continental sliver: the northern Dora Maira massif, Italian Alps. - J. Geol. Soc. London 148: 1101-1113.

WHEELER J. & BUTLER R.W.H. (1993): Evidence for extension in the western Alpine orogen: The contact between the oceanic Piemonte and overlying continental Sesia units. - Earth Planet. Sci. Lett. 117: 457-474.

WHEELER J. & BUTLER R.W.H. (1994): Criteria for identifying structures related to true crustal extension in orogens. - J. Struct. Geol. 16: 1023.1027.

WILKINS R.W.T. & BARKAS J.P. (1978): Fluid inclusions, deformation and recrystallization in granite tectonites. - Contrib. Mineral. Petrol. 65: 293-299.

WILLIAMS P.F. & COMPAGNONI R. (1983): Deformation and metamorphism in the Bard area of the Sesia Lanzo Zone, Western Alps, during subduction and uplift. - J. Metamorphic Geol. 1: 117-140.

WUST G.H. & BAEHNI L.A. (1986): The distinctive tectonometamorphic evolution of two basement complexes belonging to the Grand-Saint-Bernard nappe (Val de Bagnes, Valais). - Schweiz. Mineral. Petrogr. Mitt. 66: 53-71.

WUST G.H. & SILVERBERG D.S. (1989): Northern Combin zone complex - Dent Blanche nappe contact: extension within the convergent Alpine belt.- Schweiz. Mineral. Petrogr. Mitt. 69: 251-259.

ZHANG Y.-G. & FRANTZ J.D. (1987): Determination of the homogenization temperatures and densities of supercritical fluids in the system NaCl-KCl-CaCl2-H2O using synthetic fluid inclusions. - Chem. Geol. 64: 335-350.

Lebenslauf

Name:	Sebastiaan Nicolaas Gerardus Cornelis van der Klauw
Geburtsdatum:	28. September 1966
Geburtsort:	Gouda
Staatsangehörigkeit:	Niederländisch
Familienstand:	Ledig

Akademischer Werdegang

08.78 - 05.84	St. Willibrord Gymnasium in Deurne
05.84	Abitur
09.84 - 11.90	Geologiestudium an der Rijksuniversiteit Utrecht
30.11.90	Examen zum Diplom-Geologen
04.91 - 03.94	Wissenschaftlicher Mitarbeiter am Institut für Geologie der Ruhr-Universität Bochum (Promotionsstelle)
04.94 - 09.94	Wissenschaftlicher Hilfskraft am Institut für Geologie der Ruhr-Universität Bochum
04.96 -	Wissenschaftlicher Mitarbeiter am Institut für Geowissenschaften des Friedrich-Schiller-Universität Jena

APPENDIX A Methods

A1 Sampling

Mapping in the area around Lago di Cignana (unpublished Diplomkartierung, Habermann, 1992, Wagner-Zweigel, 1993) showed that the UHPM rocks are extremely well exposed on the southern shore of the lake. All of the about 120 samples (Table C1) for this study were taken from this well exposed area (Fig. A1). Due to these good exposures the lower PT-overprint could be correlated with m- to dm- scale structures in the metabasic rocks and several series of samples were taken to investigate the relation between structures and lower PT-overprint. Due to the very heterogeneous bulk rock composition of the metasedimentary rocks, such a correlation was not possible for that material and sampling was concentrated on small scale folds and veins.

A2 Preparation

From all samples thin sections were made to study with a polarising microscope; usually one thin section was made approximately parallel to the stretching lineation and normal to the foliation, and another thin section normal to the stretching lineation and the foliation. In samples with no apparent stretching lineation a thin section normal to the foliation was cut. From vein samples, thin sections with both vein and host rock were made.

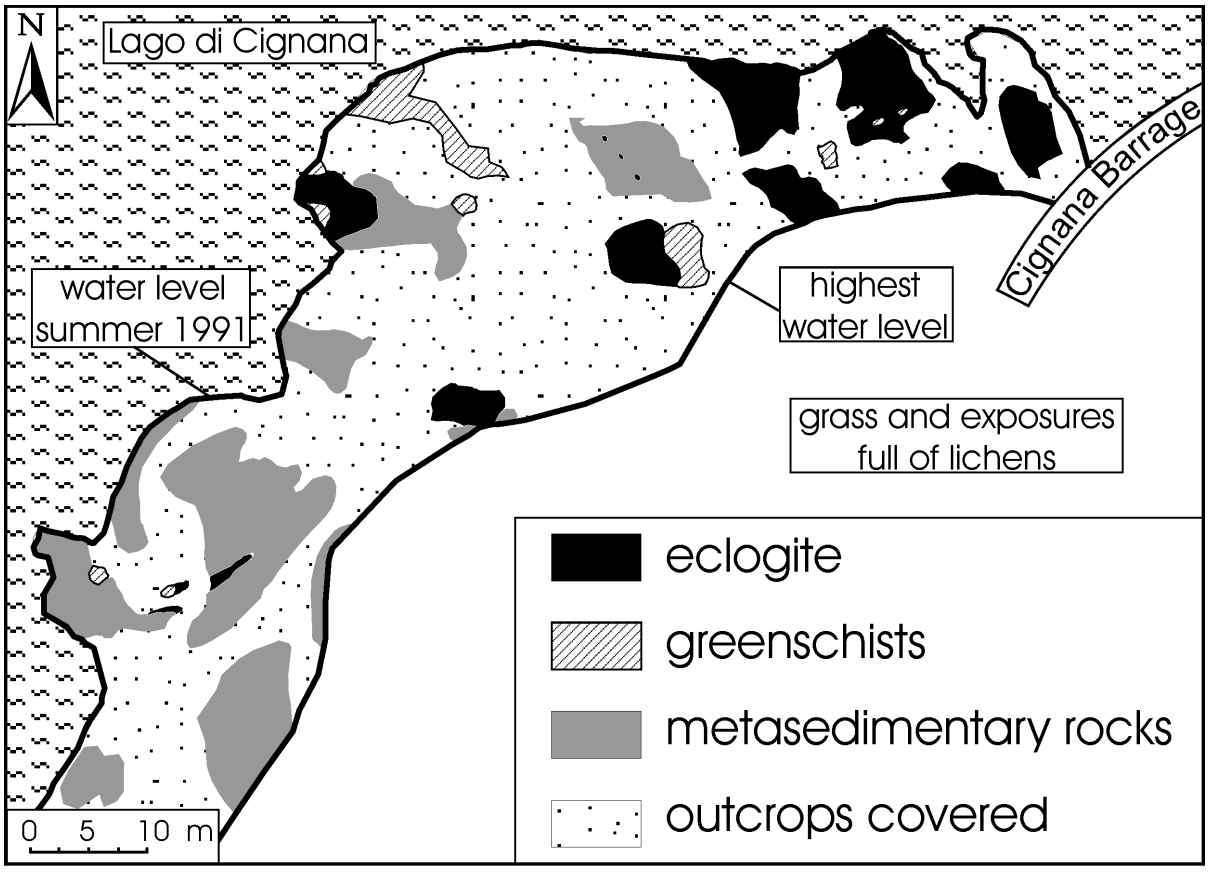

Figure A1

Distribution of the different lithologies at the southern shore of Lago di Cignana.

A small part of most samples was finely grounded for investigation with X-ray diffractometry to distinguish between paragonitic and phengitic white mica. From selected samples thin sections polished on both sides and without cover slip were made for investigation with the electron microprobe (EMP, Table C3 -C22), Scanning electron microscope (SEM) and cathodoluminesence microscope (CL). From several vein samples, 200 µm thick sections were made for the investigation of fluid inclusions by microthermometry. After study of the thin sections a series of seven samples from fresh (group 1) to completely overprinted (group 4) eclogite was selected for X-ray fluorescence (XRF) whole rock chemistry (Table C2).

A3 Analytical methods

In order to determine the phases and their compositions in the metabasic and the metasedimentary rocks as well as to determine the relative volumes and shape preferred orientations of some of these phases, and for fluid inclusion studies, the following analytical methods were used:

- polarising microscopy
- powder X-ray diffractometry
- electron microprobe analysis
- X-ray fluorescence spectroscopy,
- scanning electron microscopy,
- cathodoluminesence microscopy
- image analysis
- microthermometry

A3.1 Polarising microscopy

A polarising microscope allows determination of phases present in a thin section and also to establish the spatial relations between these phases. Furthermore, it allows observation of deformation microstructures for the different phases.

Polarising microscopes of Zeiss, Leitz and Olympus were used in this study. Important observations were photographed with an Olympus OM 10 camera mounted on an Olympus polarising microscope. A Leitz microscope with long working distance objectives was used for Universal stage measurements.

A3.2 powder X- ray diffraction

For powder X-ray diffraction a representative part of the sample is finely grounded (1- 10 µm), to obtain a large amount of grains of the different minerals, so that it is likely that all grain orientations for all minerals are present. The powdered specimen is brought into a beam of monochromatic parallel X-rays and slowly rotated. The incident X-rays will be scattered by the atomic planes in the specimen. These diffracted X-rays will usually interfere destructively with each other and no signal will be produced. For specific incedent angles however, the spacing of the atomic planes is such,

that the diffracted X-rays interfere positively with each other and a signal can be recorded. This is Braggs law, in formula

$$n \lambda = 2 d \sin\theta$$

with λ wavelength of the X-rays, d distance between the atomic planes, θ incident angle of the X-ray beam and n an integer (usually taken as 1). When the wavelength of the X-rays is known and the different incident angles at which a signal occurred are recorded, the d values for the unknown specimen may be calculated. These d-values together with the intensities of the signals are material specific. By comparing the recorded values with reference values in the A.S.T.M. powder data file, the unknown material(s) may be identified. More information on X-ray diffraction may be found in Zussmann (1977) and Putnis (1992).

Philips X-ray diffractometers at the "Institut für Mineralogie" and the " Institut für Geologie" at the Ruhr-University Bochum were used in this study. All scans were made with Cu K_α X-rays over a range of θ angles from 5° to 50° with steps of 0.1° and 2 seconds counting time.

A3.3 Electron microprobe and X-ray fluorescence spectroscopy

Electron microprobe and X-ray fluorescence use the same principles, but different excitating media to produce X-rays. When an electron with sufficient energy strikes matter, X-rays are produced. X-rays may also be produced, when these primary X-rays strike matter. These secondary X-rays are called fluorescence. The X-ray spectrum produced by incedent electrons may be divided in a continuous spectrum (background) and a characteristic spectrum. Excitation by primary X-rays differs from excitation by electrons in that no continuous spectrum is formed. The characteristic spectrum is produced when the incident electrons remove an electron from the inner shells of an atom. The X-ray photons that are produced when outer electrons fall back have an energy that is characteristic for a particular element. The energies (or wavelengths) and intensities of the excited X-rays are measured in a spectrometer. From the measured wavelengths the different elements that are present in the material can be inferred. By comparing the intensities of the X-rays with intensities obtained from materials with known composition, the absolute amounts of the different elements may be obtained. More about these techniques may be found in Zussman (1977), Smith (1976), and Reed (1996).

A3.3.1 The electron microprobe (EMP)

The EMP uses a beam of electrons to produce characteristic X-rays. This beam is focused using magnetic lenses, without loss of intensity. Therefore, the electron microprobe can be used to obtain spot analyses (1 μm diameter) from a material. However due to the superposition of continuous and characteristic X-ray spectra the accuracy of the EMP is not as high as the accuracy of the XRF. To prevent the build up of heat and electrical charge on the specimen, samples must be coated with a conductive thin carbon or gold film. In this study the electron microprobe was used to measure the composition of minerals in thin section in specific microstructural settings.

A Camebax microprobe in WDS mode at the "Bereich Zentrale Elektronen-Mikrosonde" of the Ruhr-University Bochum was used. Operating conditions were 15 kV accelerating voltage and a

14 nA beam current for most minerals. For albite and mica the beam was slightly defocused and a 12 nA beam current was used to yield better results for the alkali elements. A 12 nA beam current was also used for carbonates. Natural and synthetic minerals were used as standards and the PAP (Pouchou & Pichoir, 1984) correction procedure was used.

A3.3.2 X-ray fluorescence spectroscopy (XRF)

X-ray fluorescence spectroscopy uses X-rays to produce characteristic X-rays. X-rays cannot be focused without loss of intensity. Therefore, XRF gives information about the composition of a larger area. To ensure that this area is homogeneous and representative of the sample, part of the sample is dissolved in lithium borate glass and the glass is analysed or the sample is finely grounded and a pressed powder tablet is analysed. These analyses give information about the bulk composition of a sample. A more detailed description of the XRF technique can be found in Zussmann (1977).

A Philips PW 1400 X-ray fluoresence spectrometer at the “Institut für Mineralogie” at the Ruhr university Bochum was used for XRF-analyses.

A3.4 Scanning electron microscopy (SEM)

When electrons with sufficient energy strike matter, not only X-rays are produced but also other signals. In the SEM, the signals provided by the backscattered electrons and the secondary electrons are used. Secondary electrons are the electrons that are removed from the electron shells around an atom by the incident electrons. Their energy ranges from 0 to about 50 eV, partly depending on the material. Backscattered electrons are electrons of the incident beam that are rebounded in the specimen. They have generally higher energies than the secondary electrons, ranging between zero and the energy of the incident electrons. Their intensity is related to the mean atomic number of the material under the beam. Both signals can be detected when they leave the surface of the specimen and give information about the surface topography of the sample and some qualitative information about the material under the beam. When the sample has a smooth surface the SEM can be used much the same way as a normal light optical microscope, with the advantages that the range of possible magnification is larger and that SEM has a better depth of focus. More information about this technique can be found in Reed (1996).

In this study SEM was used to provide images of the symplectitic intergrowths in the metabasic rocks. SEM images were made with a Cambridge Stereoscan 250 Mk III at the “Bereich Zentrales Rasterelektronenmikroskop” of the Ruhr University Bochum. Accelerating voltage for the electronbeam varied between 15 and 20 kV. SEM images were made with assistance of Dr. Neuser.

A3.5 Cathodoluminescence (CL)

Another signal that may be emitted when a material is struck by electrons is light in the visible wavelength area. This may be an intrinsic property of the material under the beam, for example in scheelite or benthonite, but may also be due to the presence of trace impurities in the mineral e.g., Mn and REE in calcite or defects in crystal structure e.g., quartz (Marshall, 1988).

In this study CL was used to image the zoning of calcite around dolomite, that could not be seen

in polarisation microscope. A cathodoluminescence microscope HC1-LM at the “Institut für Geowissenschaften Ruhr Universität Bochum”, developed by Dr. Neuser (Neuser, 1995) was used in this study. A standard camera mounted on the microscope was used to obtain photographs of the CL-images. Dr. Neuser and Dipl.-Geol Habermann assisted with the CL investigations.

A3.6 Image analysis

Image analysis was used to obtain qualitative information on shape, area, and shape preferred orientation of minerals in thin sections or on back scattered electron images. The image is digitised and a computer program approximates area, perimeter, longest dimension, direction of longest dimension, and other parameters from this image.

The VIDS IV image analysis system (AI-Tektron) combined with a videocamera (JVC BY-110) mounted on a Zeiss microscope and a digitising tablet were used in this study.

A3.7 Microthermometry

With the microthermometry it is possible to obtain information about density and composition of fluid inclusions without destroying the inclusions. A heating-freezing stage installed on a microscope allows to observe phase transitions in the fluid inclusionsas a function of temperature.

Two heating-freezing stages were used, a Linkam THM 600, described in Sheperd (1981) and Roedder (1984) and a stage specially for low temperature measurements, constructed by W. Harbott at the “Institut für Geologie der Ruhr Universität Bochum”. This last stage is described by Harbott et al. (1990) and Küster (1994).

Both stages were calibrated with natural standards (e.g. Calanda Quartz provided by J. Mullis) in the low temperature region and with the melting point of several pure chemicals (Fa. Merck) in the high temperature region.

Appendix B Geothermobarometry

In this study several different methods were used to estimate pressures and temperatures during UHP metamorphism and exhumation. A short description of these methods is presented below.

B1 Thermometer

B1.1 Garnet clinopyroxene thermometry

This thermometer is based on Fe, Mg exchange between garnet and clinopyroxene as defined in the following reaction

$$1/3\text{Pyrope} + \text{Hedenbergite} = 1/3\text{Almandine} + \text{Diopside}$$

$$Mg_3Al_2Si_3O_{12} \quad CaFeSi_2O_6 \quad Fe_3Al_2Si_3O_{12} \quad CaMgSi_2O_6$$

with equilibrium constant K (Banno, 1970) defined as

$$K = \frac{(a^{grt}_{Fe})^{1/3}}{(a^{grt}_{Mg})^{1/3}} * \frac{(a^{cpx}_{Mg})}{(a^{cpx}_{Fe})}$$

with a^{grt}_{Fe} the activity of Fe in garnet, a^{cpx}_{Mg} the activity of Mg in clinopyroxene etc. At equilibrium, taking a standard state of pure solids at the temperature and pressure of interest $\Delta G°(P,T) = 0$,

$$\Delta H° - T\Delta S° + (P-1)\Delta V° = -RT\ln K$$

assuming ideal solid solution for the minerals (a = x) gives

$$K = \frac{(X^{Gt}_{Fe})}{(X^{Gt}_{Mg})} * \frac{(X^{Cpx}_{Mg})}{(X^{Cpx}_{Fe})} = Kd$$

This last assumption is not completely valid and a correct treatment requires knowledge of the mixing properties of garnet and pyroxene.

First experiments to calibrate this thermometer were made by Raheim & Green, (1974). Ellis and Green (1979) experimentally evaluated the effect of the grossular component in garnet and assuming that the non-ideal mixing behaviour of garnet and clinopyroxene was concentrated in X_{Ca} of garnet proposed following empirical calibration:

$$T(K) = \frac{3104\ X^{Gt}_{Ca} + 3030 + 10.86\ P(kb)}{\ln Kd + 1.9034}.$$

The same data set was used by Powell (1985) using robust regression and regression diagnostics to give the calibration a better statistical fundament. He derived following relation:

$$T(K) = \frac{3140\ X^{Gt}_{Ca} + 2790 + 10\ P(kb)}{\ln Kd + 1.735}.$$

Another calibration using this data set is Krogh's (1988). Here the dependence of Kd on X_{Ca} was assumed to be curvilinear instead of linear as in the previous calibrations. He derived following relation:

$$T(K) = \frac{-6173(X^{Gt}_{Ca})^2 + 6731X^{Gt}_{Ca} + 1879 + 10\ P(kb)}{\ln Kd + 1.393}\ .$$

All these three calibrations assume an independence of Kd from the Mg number of garnet, which was postulated by Ellis & Green (1979). A new experimental calibration of this thermometer by Pattison & Newton, (1989), not only shows a dependence of Kd on X_{Ca} but also on the Mg number of garnet. Their calibration has the general form

$$T(K) = \frac{a'X^3 + b'X^2 + c'X + d'}{\ln Kd + a_0X^3 + b_0X^2 + c_0X4 + d_0} + 5.5\ (P(kb)-15),$$

where the constants a´, a_0, etc. depend on X_{Ca} in garnet (Table B1). X is the Mg number in garnet ($Mg/(Mg+Fe^{2+})$).

The experimental data from these studies together with data from other studies were used by Ai (1994) to propose a different calibration with a curvilinear dependence of Kd on Ca and a linear dependence of Kd on the Mg-number of garnet. His calibration has the form:

$$T(K) = \frac{-1629(X^{Gt}_{Ca})^2 + 3648.55X^{Gt}_{Ca} - 6.59\ X^{Gt}_{Mg} + 1987.98 + 17.66\ P(kb)}{\ln Kd + 1.076}\ .$$

The experimental data of Pattison & Newton (1989) were evaluated and thermodynamically analysed by Aranovich & Pattison (1995) and Berman, Aranovich & Pattison (1995). These authors tried to take the mixing properties of garnet and pyroxene into account and proposed a different calibration of the garnet-clinopyroxene thermometer, that gives similar results to the Ai (1994) calibration.

None of the calibrations takes the jadeite content of clinopyroxene into account. It was, however, shown by Koons (1984), that jadeite contents up to X^{cpx}_{jd} <0.6 do not affect temperatures calculated with the Ellis & Green (1979) calibration.

Results calculated for all calibrations are presented in table B2. The Pattison and Newton (1989) calibration gives consistently the lowest temperatures for the eclogites of Lago Cignana. Since the authors suggest application of their calibration only in high grade amphibolite and eclogite facies rock as well as in granulite facies rocks this calibration is discarded. The Ellis and Green (1979) calibration gives always the highest temperatures and is discarded, because other studies (e.g. Green & Adam, 1991) have shown that this calibration gives temperatures that are often 50 to 150 ° too high. From the remaining three calibrations the Powell (1985) calibration is preferred, because it gives an adequate description of the experimental data with a minimum number of variables.

Table B1

Parameters for the Pattison & Newton (1989) calibration of the garnet clinopyroxene thermometer.

$X^{grt} = 0.2$	$a_0 = 3.606$	$b_0 = -5.172$	$c_0 = 2.317$	$d_0 = 0.1742$
	$a' = 26370$	$b' = -32460$	$c' = 11050$	$d' = 1012$
$X^{grt} = 0.3$	$a_0 = 15.87$	$b_0 = -20.30$	$c_0 = 7.468$	$d_0 = -0.1479$
	$a' = 43210$	$b' = -53230$	$c' = -18120$	$d' = 776$

B1.2 Amphibole-plagioclase thermometer (Holland & Blundy, 1994)

This thermometer or better these two thermometers are based on the reactions:

A) 1 edenite + 4 quartz = tremolite + albite

$NaCa_2Mg_5Si_4(AlSi_3)O_{22}(OH)_2$ SiO_2 $Ca_2Mg_5Si_8O_{22}(OH)_2$ $NaAlSi_3O_8$

B) 2 edenite + albite = richterite + anorthite

$NaCa_2Mg_5(AlSi_3)Si_4O_{22}(OH)_2$ $NaAlSi_3O_8$ $Na(CaNa)Mg_5Si_8O_{22}(OH)_2$ $CaAl_2Si_2O_8$

Only the thermometer based on the first reaction is discussed here, because the second reaction requires plagioclase compositions with $X_{an} > 0.1$, that are not found in the metabasic rocks of Lago di Cignana.

The thermometer was calibrated using an experimental data set (Blundy & Holland, 1990), combined with data from natural samples to expand the compositional relatively small range of the experimental data set.

To use the first reaction as a thermometer, activity models for plagioclase and amphibole are needed. For plagioclase a simplified version of the DQF (Darkens Quadratic Formalism) model given by Holland & Powell (1992) is used. For amphibole the situation is more complicated, because different non ideal interactions are important. Using a symmetrical form of non ideal interaction to model the multi-site-solid-solution in amphibole and using a relative simple system involving distribution of [ ]-K-Na-Ca-Mg-Fe^{2+}-Fe^{3+}-AlSi over the A, M4, M1, M2, M3 and T1 crystallographic sites in amphibole, the number of non ideal interaction terms is reduced to 8. These 8 terms do not have thermodynamic meaning but are a simplification useful for developing the thermometric expression (Holland & Blundy, 1994).

The equilibrium condition for the first reaction is given by:

$$\Delta\mu_A = 0 = \Delta H°_A - T\Delta S°_A + P\Delta V°_A + RT\ln K(^{Ed\text{-}Tr}{}_{id}) + RT\ln\gamma_{ab} + RT\ln\gamma_{trem} - RT\ln\gamma_{ged}$$

with $K^{Ed\text{-}Tr}{}_{id} = 27/256 * ((X^A{}_{[\,]} * X^{T1}{}_{Si})/(X^A{}_{Na} * X^{T1}{}_{Al})) * X^{plag}{}_{An}$

and $RT\ln\gamma_{ab} = Y_{ab} = 0$ for $X_{ab} > 0.5$

and $W_{plag}(1-X_{ab})^2 + I_{ab}$ for $X_{ab} < 0{,}5$

$W_{plag} = 12$ Kj, $I_{ab} = -3{,}0$ Kj

and $Y_{(ed\text{-}tr)} = RT\ln\gamma_{ed} - RT\ln\gamma_{trem} = X^A{}_{Na} * A_1 + X^A{}_K * A_2 + X^{M4}{}_{Na} * A_3 + X^{M13}{}_{Fe} * A_4 + X^{M2}{}_{Al} * A_5 +$

$X^{M2}{}_{Fe} * A_6 + X^{M2}{}_{Fe3+} * A_7 + X^{T1}{}_{Al} * A_8 * A_9$

The result is a thermometric expression for the Edenite-Tremolite thermometer:

$$T(K) = \frac{\Delta H°_A + P\Delta V°_A + Y_{ab} + Y_{(ed\text{-}tr)}}{\Delta S°_A - R\ln K^{Ed\text{-}Tr}{}_{id}}$$

values for $\Delta H°_A$, $\Delta V°_A$, $\Delta S°_A$ and for A_1 to A_9 were determined by regression of the experimental and the natural amphibole plagioclase pairs. A_9 was incorporated in $\Delta H°_A$. A_3, A_4, A_6, A_7 and A_8 had regression values within 1 σ from zero and were removed from the regression. Following values were determined:

ΔH^*(kJ) = -76.95, $\Delta S°$(kJ K^{-1}) = -0.065, $\Delta V°$(kJ $kbar^{-1}$) = 0.79, A_1(kJ) = 39.4, A_2(kJ) = 22.4, A_5(kJ) = 41.5 - P(kbar) * 2.89. This thermometer can be used in a temperature range between 400 and 900 °C, with amphiboles that have $Na^A > 0.02$ pfu, $Al^{vi} < 1.8$ pfu and Si between 6.0 and 7.7 pfu, plagioclase must have $X_{an} < 0.9$. Typical temperature uncertainty due to the calibration lies around 40 °C. Results for this thermometer are presented in Table B3.

Calcite - Dolomite solvus thermometry

For this thermometer the calibration of Anovitz & Essene (1987) was used. These authors used all available reversed experimental data on binary solvi in the system $CaCO_3$-$MgCO_3$-$FeCO_3$ and analyses of natural carbonates to model ternary activity/composition relationships for calcite and dolomite structure carbonates. These data were used to model the mole fraction of $MgCO_3$ in calcite as a function of temperature along the calcite dolomite solvus. The least squares fit for the solvus between 200 °C and 900 °C has the form:

$$T_{Mg}(K) = A(X_{MgCO3}) + B/(X_{MgCO3}) + C(X_{MgCO3})^2 + D(X_{MgCO3})^{0.5} + E$$

with X_{MgCO3} the $MgCO_3$ concentration in Calcite. The values of the regression parameters are given in Table B4. This thermometer and further data were used to develop a thermometer in the ternary system $CaCO_3$ - $MgCO_3$ - $FeCO_3$. This thermometer has the form:

$$T_{FeMg}(K) = T_{Mg} + a(X_{FeCO3}) + b(X_{FeCO3})^2 + c(X_{FeCO3} / X_{MgCO3}) + d(X_{FeCO3} * X_{MgCO3}) + e(X_{FeCO3} / X_{MgCO3})^2 + f(X_{FeCO3} * X_{MgCO3})^2 .$$

with X_{FeCO3} and X_{MgCO3} respectively the $FeCO_3$ and $MgCO_3$ concentrations in Calcite. The values of the regression parameters can also be found in Table B4.

Comparison of the results of this calibration (Table B5) with results of the calibration of Powell et al. (1984) shows no significant temperature differences.

B2 Barometer

In this study three reactions were used to estimate pressures. Two polymorphic transition reactions that divide the P-T field in two parts were either one or the other polymorph is the stable phase. One net transfer reaction gives a pressure estimate that depends on the composition of the reacting phases.

The polymorphic transition reaction Coesite - Quartz gives a minimum pressure for the UHP metamorphism. This equilibrium has been well located as a function of P and T (e.g., Mirwald & Massonne, 1980; Bohlen & Boettcher, 1982).

Table B4

Regression parameters for the Anovitz & Essenne (1987) calibration of the calcite dolomite solvus thermometer in the system $CaCO_3$ - $MgCO_3$ and the system $CaCO_3$ - $MgCO_3$-$FeCO_3$.

$T_{(Mg)}$	a = -2360	b = -0.01345	c = 2620	d = 2608	e = 334	
$T_{(Fe,Mg)}$	a = 1718	b = -10610	c = 22.49	d = -26260	e = 1.333	$f = 0.32837*10^{-7}$

The polymorphic reaction Calcite-Aragonite gives a maximum pressure for the onset of lower PT-transformation of the eclogitic mineral assemblage. This equilibrium has been well located as a function of P and T (e.g., Johannes & Puhan, 1971; Goldsmith & Newton, 1969).

The net transfer reaction used for geobarometry is the reaction (Holland, 1980):

$$NaAlSi_2O_6 + SiO_2 = NaAlSi_3O_8$$
$$\text{Jadeite} + \text{Quartz} = \text{Albite}$$

The equilibrium condition for this reaction is given by

$$\Delta\mu = 0 = \Delta H° - T\Delta S° + P\Delta V° + RT\ln K$$

with

$$K = \frac{a_{Qz} * a_{Jd}}{a_{Ab}}$$

The position of this reaction in the PT-field was calculated using the PTX-programm of Brown et al. (1988) with the Bermann (1988) data base. Albite and quartz activities were taken as 1. The jadeite activity in omphacite was calculated, with the method of Holland (1990) using Landau theory to mixture according to the formula:

$$RT \ln a_{jd} = RT \ln (X_{NaM1} * X_{AlM2}) + RT \ln \gamma_{NaAl}$$

with

$$RT \ln \gamma_{NaAl} = X_{CaM2} * (X_{MgM1} W_A + X_{Fe2+M1} W_B + X_{Fe3+M1} W_C),$$

W_A = 26 kJ, W_B = 25 kJ and W_C = 0 and with Na and Ca on the M2 site and Al, Mg, Fe^{2+} and Fe^{3+} on the M1 site. A main uncertainty factor is the ordering state of omphacite. The calculated activity is for disordered omphacite. At the temperatures in the studied rocks between 400 and 600 °C, omphacite should be ordered (Carpenter et al., 1990). The activity for ordered omphacites should be lower as for disordered omphacites (Holland et al., 1990) and the pressures calculated with this barometer (Table B6) are therefore maximum pressures only.

Group	A1	A2	A3	B2	B3	B4	B5	B6	B7	B8
Position	r	r	i	r	i	i	i	i	i	i
Sample	Bk 7	Bk 7	Bk 7	Bk 7	Bk 7	Bk 7	Bk 7	Bk 7	Bk 7	Bk 7
X^{grt}_{Mg}	0,323	0,354	0,258	0,293	0,256	0,276	0,229	0,288	0,269	0,269
X^{grt}_{Ca}	0,171	0,148	0,199	0,177	0,244	0,250	0,208	0,166	0,222	0,213
X^{grt}_{Mg}	0,833	0,846	0,837	0,828	0,782	0,827	0,816	0,849	0,833	0,803
Temperaturen (°C) at 2.7 GPa										
E&G	633	625	584	616	688	652	588	574	616	652
Powell	607	599	559	591	665	629	563	547	592	627
Krogh	560	540	521	545	643	606	527	497	562	596
P&N	522	513	470	514	560	507	472	474	488	535
Ai	614	604	556	594	680	636	560	543	594	636

Group	C1	D1	D2	A1	A1	B1	B2	B3	B4all	C1
Position	r	r	i	r	r	r	i	i	i	r
Sample	Bk 7	Bk 7	Bk 7	Bk 8	Bk 39	Bk 39	Bk 39	Bk 39	Bk 39	Bk 39
X^{grt}_{Mg}	0,216	0,322	0,279	0,370	0,205	0,263	0,186	0,198	0,233	0,249
X^{grt}_{Ca}	0,262	0,177	0,238	0,141	0,268	0,239	0,251	0,217	0,208	0,247
X^{grt}_{Mg}	0,834	0,801	0,787	0,850	0,821	0,862	0,816	0,750	0,780	0,810
Temperaturen (°C) at 2.7 GPa										
E&G	587	685	704	628	595	580	570	635	637	644
Powell	564	661	681	602	572	556	547	611	613	621
Krogh	539	618	659	540	548	528	519	580	579	597
P&N	436	582	576	511	440	439	418	516	529	507
Ai	558	678	700	607	567	551	539	616	619	626

Group	C4	C5	C6	D1	D2	A1	B1	B2	B3	B4
Position	r	r	r	i	r	r	i	i	i	i
Sample	Bk 39	Bk 39	Bk 39	Bk 39	Bk 39	Cig 91-1	Cig 90\40\2	Cig 90\40\2	Cig 90\40\2	Cig 90\40\2
X^{grt}_{Mg}	0,259	0,266	0,271	0,224	0,258	0,346	0,150	0,206	0,151	0,154
X^{grt}_{Ca}	0,251	0,258	0,232	0,236	0,241	0,135	0,231	0,241	0,227	0,223
X^{grt}_{Mg}	0,872	0,844	0,842	0,797	0,817	0,815	0,695	0,766	0,750	0,697
Temperaturen (°C) at 2.7 GPa										
E&G	568	622	613	626	641	658	632	645	579	631
Powell	544	599	589	602	617	632	608	621	554	607
Krogh	517	575	560	575	592	567	581	596	523	577
P&N	420	472	477	496	506	571	477	512	422	484
Ai	536	599	589	605	622	644	613	627	550	611

Group	B5
Position	i
Sample	Cig 90\40\2
X^{grt}_{Mg}	0,177
X^{grt}_{Ca}	0,232
X^{grt}_{Mg}	0,712
Temperaturen (°C) at 2.7 GPa	
E&G	657
Powell	633
Krogh	607
P&N	523
Ai	643

Sample	Bk 10 B	Bk 10 B	Bk 10 B	Bk 10 B	Bk 10 B	Bk 10 B	Bk 10 B	Bk 10 B	Bk 10 B	Bk 10 B	Bk 10 B
Analysis	9	16	17	20	21	33	34	39	42	47	49
Date	18.10.93	18.10.93	18.10.93	18.10.93	18.10.93	18.10.93	18.10.93	18.10.93	18.10.93	18.10.93	18.10.93
SiO2	52,29	51,72	53,18	49,60	50,50	52,09	53,01	53,50	51,84	50,45	49,79
TiO2	0,08	0,02	0,02	0,05	0,10	0,07	0,11	0,11	0,09	0,07	0,10
Al2O3	5,18	6,18	5,12	8,46	8,08	5,49	5,00	4,69	6,04	8,47	6,99
Cr2O3	0,03	0,02	0,00	0,00	0,00	0,00	0,01	0,22	0,06	0,00	0,00
Fe2O3	2,95	3,37	4,99	4,79	4,94	3,33	0,92	2,41	3,50	4,01	3,31
FeO	9,17	8,16	7,26	9,35	8,33	6,70	8,82	8,23	7,07	8,12	8,72
MnO	0,16	0,12	1,15	0,17	0,09	0,00	0,00	0,14	0,09	0,05	0,00
MgO	14,75	15,30	15,22	12,74	13,18	16,12	15,97	16,02	15,75	13,77	14,53
CaO	10,75	10,93	11,01	9,93	9,58	10,82	11,18	11,21	10,86	9,73	11,06
ZnO	0,18	0,20	0,26	0,37	0,16	0,70	0,07	0,20	0,10	0,02	0,00
Na2O	1,62	1,93	1,53	2,41	2,18	1,93	1,53	1,46	1,68	2,39	1,66
K2O	0,15	0,17	0,15	0,26	0,22	0,17	0,14	0,16	0,19	0,25	0,30
Total	97,31	98,12	99,89	98,13	97,37	97,41	96,76	98,35	97,27	97,33	96,46
H2O	2,09	2,11	2,14	2,09	2,09	2,10	2,10	2,12	2,10	2,10	2,06
norm 23 oxygen, Fe3 over Si+Ti+Al+Cr+Fe+Mg+Mn+Zn = 16											
Si	7,503	7,353	7,442	7,131	7,246	7,421	7,582	7,551	7,387	7,218	7,230
Alt	0,497	0,647	0,558	0,869	0,754	0,579	0,418	0,449	0,613	0,782	0,770
	8,000	8,000	8,000	8,000	8,000	8,000	8,000	8,000	8,000	8,000	8,000
Alo	0,379	0,388	0,286	0,564	0,612	0,343	0,424	0,332	0,402	0,646	0,426
Fe3	0,318	0,360	0,526	0,518	0,534	0,357	0,099	0,256	0,375	0,432	0,362
Cr	0,003	0,002	0,000	0,000	0,000	0,000	0,001	0,025	0,007	0,000	0,000
Ti	0,006	0,002	0,002	0,004	0,008	0,005	0,008	0,008	0,007	0,005	0,008
Mg	3,155	3,242	3,174	2,730	2,819	3,423	3,404	3,370	3,345	2,937	3,145
Fe2	1,100	0,970	0,849	1,124	1,000	0,798	1,055	0,971	0,843	0,972	1,059
Mn	0,019	0,014	0,136	0,021	0,011	0,000	0,000	0,017	0,011	0,006	0,000
Zn	0,019	0,021	0,027	0,039	0,017	0,074	0,007	0,021	0,011	0,002	0,000
	5,000	5,000	5,000	5,000	5,000	5,000	5,000	5,000	5,000	5,000	5,000
Ca	1,653	1,665	1,651	1,530	1,473	1,652	1,713	1,695	1,658	1,492	1,721
Na	0,347	0,335	0,349	0,470	0,527	0,348	0,287	0,305	0,342	0,508	0,279
	2,000	2,000	2,000	2,000	2,000	2,000	2,000	2,000	2,000	2,000	2,000
Na	0,103	0,197	0,066	0,201	0,079	0,185	0,137	0,095	0,122	0,155	0,188
K	0,028	0,031	0,027	0,049	0,041	0,032	0,026	0,029	0,035	0,047	0,057
	0,131	0,228	0,093	0,250	0,120	0,216	0,164	0,124	0,158	0,201	0,245
sum	15,131	15,228	15,093	15,250	15,120	15,216	15,164	15,124	15,158	15,201	15,245
OH	2,000	2,000	2,000	2,000	2,000	2,000	2,000	2,000	2,000	2,000	2,000
T in °C	497	540	491	565	513	529	489	486	521	542	554

Sample	Bk 10 B	Bk 10 B	Bk 10 B	Bk 10 B	Bk 10 B	Bk 10 B	Bk 10 B	Bk 10 B	Bk 10 B	Bk 10 B	Bk 10 B
Analysis	50	51	52	53	54	55	57	58	2	3	4
Date	18.10.93	18.10.93	18.10.93	18.10.93	18.10.93	18.10.93	18.10.93	18.10.93	19.10.93	19.10.93	19.10.93
SiO2	52,18	50,95	50,37	46,30	50,52	50,26	51,24	49,81	47,24	50,20	50,94
TiO2	0,10	0,06	0,08	0,13	0,03	0,05	0,16	0,13	0,02	0,05	0,06
Al2O3	5,46	8,45	6,49	11,18	6,70	7,06	8,23	8,33	9,24	5,58	5,32
Cr2O3	0,00	0,00	0,00	0,00	0,04	0,09	0,00	0,00	0,00	0,00	0,02
Fe2O3	4,39	5,20	4,62	3,51	4,81	2,72	4,81	6,07	6,94	4,17	5,70
FeO	7,08	7,21	8,97	10,23	7,46	9,23	7,57	6,77	7,11	8,02	6,79
MnO	0,11	0,09	0,10	0,15	0,13	0,08	0,00	0,04	0,00	0,15	0,24
MgO	15,72	14,04	14,18	11,97	14,65	14,55	13,32	13,79	13,57	15,06	15,43
CaO	10,97	9,78	11,08	10,46	10,82	11,18	8,63	9,74	10,78	11,26	11,31
ZnO	0,25	0,09	0,25	0,20	0,50	0,35	0,19	0,17	0,00	0,25	0,30
Na2O	1,51	2,25	1,58	2,67	1,71	1,97	2,68	2,13	1,83	1,50	1,24
K2O	0,22	0,24	0,30	0,43	0,25	0,29	0,22	0,23	0,37	0,27	0,23
Total	97,99	98,36	98,02	97,23	97,62	97,83	97,04	97,21	97,09	96,52	97,58
H2O	2,11	2,12	2,09	2,05	2,09	2,09	2,10	2,09	2,06	2,06	2,09
norm 23 oxygen, Fe3 over Si+Ti+Al+Cr+Fe+Mg+Mn+Zn = 16											
Si	7,405	7,203	7,240	6,774	7,246	7,223	7,323	7,144	6,859	7,299	7,305
Alt	0,595	0,797	0,760	1,226	0,754	0,777	0,677	0,856	1,141	0,701	0,695
	8,000	8,000	8,000	8,000	8,000	8,000	8,000	8,000	8,000	8,000	8,000
Alo	0,319	0,611	0,339	0,701	0,378	0,419	0,709	0,552	0,440	0,255	0,204
Fe3	0,469	0,553	0,500	0,386	0,519	0,294	0,517	0,655	0,758	0,457	0,616
Cr	0,000	0,000	0,000	0,000	0,005	0,010	0,000	0,000	0,000	0,000	0,002
Ti	0,008	0,005	0,006	0,010	0,002	0,004	0,012	0,010	0,002	0,004	0,005
Mg	3,325	2,959	3,038	2,610	3,132	3,117	2,837	2,948	2,937	3,264	3,298
Fe2	0,841	0,853	1,078	1,252	0,895	1,109	0,904	0,812	0,863	0,976	0,814
Mn	0,013	0,011	0,012	0,019	0,016	0,010	0,000	0,005	0,000	0,018	0,029
Zn	0,026	0,009	0,027	0,022	0,053	0,037	0,020	0,018	0,000	0,027	0,032
	5,000	5,000	5,000	5,000	5,000	5,000	5,000	5,000	5,000	5,000	5,000
Ca	1,668	1,481	1,706	1,640	1,663	1,721	1,321	1,497	1,677	1,754	1,738
Na	0,332	0,519	0,294	0,360	0,337	0,279	0,679	0,503	0,323	0,246	0,262
	2,000	2,000	2,000	2,000	2,000	2,000	2,000	2,000	2,000	2,000	2,000
Na	0,084	0,098	0,147	0,397	0,138	0,270	0,064	0,089	0,192	0,177	0,083
K	0,041	0,044	0,056	0,082	0,047	0,054	0,041	0,043	0,070	0,051	0,043
	0,124	0,142	0,203	0,479	0,185	0,325	0,105	0,132	0,262	0,228	0,126
sum	15,124	15,142	15,203	15,479	15,185	15,325	15,105	15,132	15,262	15,228	15,126
OH	2,000	2,000	2,000	2,000	2,000	2,000	2,000	2,000	2,000	2,000	2,000
T in °C	505	529	550	594	547	556	487	535	605	551	524

Sample	Bk 10 B	Bk 10 B	Bk 10 B	Bk 17	Bk 17	Bk 17	Bk 17	Bk 17	Bk 17	Bk 17	Bk 17
Analysis	16	12	13	27	28	29	30	51	52	53	54
Date	19.10.93	26.11.93	26.11.93	25.7.94	25.7.94	25.7.94	25.7.94	3.7.94	3.7.94	3.7.94	3.7.94
SiO2	51,55	51,71	49,99	51,72	52,21	52,44	52,81	46,91	47,42	47,18	48,70
TiO2	0,08	0,13	0,14	0,11	0,09	0,07	0,08	0,09	0,21	0,20	0,16
Al2O3	6,84	5,87	6,83	4,23	3,78	3,89	2,86	7,81	10,63	10,35	7,68
Cr2O3	0,05	0,04	0,02	0,04	0,02	0,01	0,00	0,07	0,01	0,01	0,03
Fe2O3	1,75	3,83	4,48	3,14	3,60	4,04	2,44	3,81	4,37	4,36	5,94
FeO	8,69	8,25	8,56	10,41	10,37	10,35	11,29	12,34	9,75	9,61	9,77
MnO	0,04	0,10	0,20	0,18	0,20	0,27	0,27	0,36	0,13	0,14	0,30
MgO	14,71	14,74	13,93	14,28	14,30	14,08	14,73	11,87	11,55	11,96	12,31
CaO	10,61	10,63	10,65	10,89	10,95	10,63	11,67	11,53	9,03	9,25	9,72
ZnO	0,15	0,18	0,16	0,01	0,00	0,02	0,05	0,02	0,06	0,00	0,00
Na2O	1,77	1,62	1,73	1,50	1,29	1,50	1,01	1,73	3,14	3,21	2,47
K2O	0,17	0,17	0,21	0,16	0,13	0,13	0,11	0,29	0,30	0,32	0,26
Total	96,41	97,26	96,90	96,68	96,94	97,42	97,31	96,83	96,60	96,59	97,35
H2O	2,08	2,09	2,07	2,06	2,07	2,08	2,07	2,02	2,05	2,05	2,06
norm 23 oxygen, Fe3 over Si+Ti+Al+Cr+Fe+Mg+Mn+Zn = 16											
Si	7,418	7,412	7,244	7,526	7,574	7,574	7,651	6,974	6,932	6,907	7,102
Alt	0,582	0,588	0,756	0,474	0,426	0,426	0,349	1,026	1,068	1,093	0,898
	8,000	8,000	8,000	8,000	8,000	8,000	8,000	8,000	8,000	8,000	8,000
Alo	0,578	0,404	0,411	0,252	0,220	0,236	0,139	0,343	0,764	0,693	0,422
Fe3	0,189	0,413	0,488	0,344	0,393	0,439	0,266	0,426	0,480	0,480	0,652
Cr	0,006	0,005	0,002	0,005	0,002	0,001	0,000	0,008	0,001	0,001	0,003
Ti	0,006	0,010	0,011	0,012	0,010	0,008	0,009	0,010	0,023	0,022	0,018
Mg	3,155	3,149	3,009	3,097	3,092	3,031	3,181	2,630	2,517	2,610	2,676
Fe2	1,045	0,989	1,037	1,267	1,258	1,250	1,367	1,535	1,192	1,176	1,192
Mn	0,005	0,012	0,025	0,022	0,025	0,033	0,033	0,045	0,016	0,017	0,037
Zn	0,016	0,019	0,017	0,001	0,000	0,002	0,005	0,002	0,006	0,000	0,000
	5,000	5,000	5,000	5,000	5,000	5,000	5,000	5,000	5,000	5,000	5,000
Ca	1,636	1,633	1,654	1,698	1,702	1,645	1,811	1,837	1,414	1,451	1,519
Na	0,364	0,367	0,346	0,302	0,298	0,355	0,189	0,163	0,586	0,549	0,481
	2,000	2,000	2,000	2,000	2,000	2,000	2,000	2,000	2,000	2,000	2,000
Na	0,130	0,083	0,140	0,121	0,065	0,065	0,095	0,335	0,304	0,362	0,217
K	0,032	0,032	0,040	0,030	0,025	0,024	0,021	0,056	0,057	0,061	0,049
	0,161	0,115	0,179	0,151	0,089	0,090	0,116	0,392	0,362	0,423	0,267
sum	15,161	15,115	15,179	15,151	15,089	15,090	15,116	15,392	15,362	15,423	15,267
OH	2,000	2,000	2,000	2,000	2,000	2,000	2,000	2,000	2,000	2,000	2,000
T in °C	511	501	548	507	483	482	480	577	563	559	569

Sample	Bk 17	Bk 17	Bk 17	Bk 17	Bk 17	Bk 17	Bk 17	Bk 17	Bk 17	Bk 17	Bk 17
Analysis	55	1	6	8	9	10	12	41	42	43	48
Date	3.7.94	9.7.94	9.7.94	9.7.94	9.7.94	9.7.94	9.7.94	9.7.94	9.7.94	9.7.94	9.7.94
SiO2	46,87	52,39	51,88	51,77	49,39	50,82	50,79	43,53	46,45	45,16	49,01
TiO2	0,25	0,05	0,12	0,12	0,21	0,15	0,11	0,12	0,25	0,21	0,18
Al2O3	9,16	1,95	5,41	4,02	4,80	6,73	3,34	11,09	10,09	11,60	7,68
Cr2O3	0,04	0,00	0,03	0,05	0,02	0,15	0,00	0,05	0,05	0,04	0,02
Fe2O3	6,07	3,78	5,08	5,27	3,40	5,29	2,18	4,38	6,18	6,70	4,29
FeO	10,13	10,37	8,89	11,10	14,19	9,05	15,28	13,54	11,22	12,03	11,21
MnO	0,32	0,35	0,29	0,21	0,40	0,21	0,50	0,32	0,15	0,11	0,34
MgO	11,01	15,08	13,62	12,95	11,86	12,96	11,93	10,29	10,42	9,08	11,91
CaO	9,17	12,08	9,56	10,00	11,61	9,15	11,83	11,70	9,30	8,76	9,91
ZnO	0,12	0,00	0,12	0,08	0,04	0,00	0,07	0,00	0,03	0,11	0,00
Na2O	2,75	0,50	2,08	1,79	1,26	2,47	0,88	2,27	2,85	3,29	2,34
K2O	0,33	0,07	0,14	0,17	0,20	0,16	0,17	0,51	0,39	0,46	0,26
Total	96,23	96,62	97,22	97,54	97,38	97,14	97,09	97,80	97,38	97,55	97,15
H2O	2,02	2,05	2,08	2,06	2,02	2,08	2,02	2,01	2,04	2,03	2,05
norm 23 oxygen, Fe3 over Si+Ti+Al+Cr+Fe+Mg+Mn+Zn = 16											
Si	6,948	7,651	7,472	7,525	7,322	7,338	7,547	6,508	6,840	6,684	7,170
Alt	1,052	0,349	0,528	0,475	0,678	0,662	0,453	1,492	1,160	1,316	0,830
	8,000	8,000	8,000	8,000	8,000	8,000	8,000	8,000	8,000	8,000	8,000
Alo	0,548	0,000	0,390	0,214	0,160	0,484	0,132	0,462	0,591	0,708	0,495
Fe3	0,677	0,416	0,551	0,577	0,380	0,575	0,244	0,492	0,685	0,746	0,473
Cr	0,005	0,000	0,003	0,006	0,002	0,017	0,000	0,006	0,006	0,005	0,002
Ti	0,028	0,005	0,013	0,013	0,023	0,016	0,012	0,013	0,028	0,023	0,020
Mg	2,433	3,283	2,924	2,806	2,621	2,789	2,642	2,293	2,287	2,003	2,597
Fe2	1,256	1,266	1,071	1,350	1,759	1,093	1,899	1,693	1,382	1,490	1,371
Mn	0,040	0,043	0,035	0,026	0,050	0,026	0,063	0,041	0,019	0,014	0,042
Zn	0,013	0,000	0,013	0,009	0,004	0,000	0,008	0,000	0,003	0,012	0,000
	5,000	5,013	5,000	5,000	5,000	5,000	5,000	5,000	5,000	5,000	5,000
Ca	1,456	1,890	1,475	1,557	1,844	1,416	1,883	1,874	1,467	1,389	1,553
Na	0,544	0,110	0,525	0,443	0,156	0,584	0,117	0,126	0,533	0,611	0,447
	2,000	2,000	2,000	2,000	2,000	2,000	2,000	2,000	2,000	2,000	2,000
Na	0,247	0,032	0,056	0,062	0,206	0,107	0,137	0,532	0,281	0,333	0,217
K	0,064	0,013	0,026	0,032	0,039	0,030	0,033	0,099	0,075	0,089	0,050
	0,310	0,045	0,082	0,094	0,245	0,137	0,170	0,631	0,356	0,422	0,267
sum	15,310	15,058	15,082	15,094	15,245	15,137	15,170	15,631	15,356	15,422	15,267
OH	2,000	2,000	2,000	2,000	2,000	2,000	2,000	2,000	2,000	2,000	2,000
T in °C	577	447	491	493	551	527	509	575	581	580	555

Sample	Bk 17	Bk 17	Bk 17	Bk 18	Bk 18	Bk 18	Bk 18	Bk 18	Bk 18	Bk 18	Bk 18
Analysis	49	50	51	36	38	50	51	52	53	55	56
Date	9.7.94	9.7.94	9.7.94	25.7.94	25.7.94	25.7.94	25.7.94	25.7.94	25.7.94	25.7.94	25.7.94
SiO2	47,24	50,60	50,27	52,08	51,85	52,36	50,25	49,57	51,68	52,85	51,72
TiO2	0,15	0,14	0,16	0,15	0,16	0,03	0,07	0,04	0,06	0,05	0,07
Al2O3	9,61	6,68	7,38	4,40	3,02	4,47	5,45	8,16	5,44	4,97	6,72
Cr2O3	0,01	0,03	0,02	0,00	0,05	0,07	0,02	0,06	0,07	0,04	0,04
Fe2O3	4,74	4,31	4,87	2,15	2,61	1,31	3,86	4,40	4,00	4,05	5,35
FeO	10,92	10,42	9,39	12,42	11,30	8,85	8,39	8,68	7,98	7,93	7,71
MnO	0,31	0,44	0,32	0,25	0,24	0,16	0,23	0,24	0,20	0,23	0,29
MgO	11,14	12,53	12,89	13,14	14,17	16,10	14,87	13,15	14,83	14,74	13,38
CaO	9,36	9,39	9,46	10,45	11,27	11,82	11,33	9,69	10,39	9,92	8,71
ZnO	0,00	0,00	0,03	0,00	0,00	0,22	0,30	0,32	0,21	0,24	0,26
Na2O	2,90	2,55	2,56	1,75	1,07	1,29	1,48	2,58	1,82	1,83	2,56
K2O	0,37	0,19	0,20	0,17	0,10	0,12	0,15	0,25	0,16	0,13	0,15
Total	96,74	97,28	97,55	96,96	95,84	96,80	96,40	97,14	96,84	96,98	96,96
H2O	2,04	2,07	2,08	2,06	2,04	2,08	2,06	2,07	2,08	2,09	2,09
norm 23 oxygen, Fe3 over Si+Ti+Al+Cr+Fe+Mg+Mn+Zn = 16											
Si	6,959	7,341	7,251	7,592	7,633	7,531	7,320	7,170	7,440	7,567	7,423
Alt	1,041	0,659	0,749	0,408	0,367	0,469	0,680	0,830	0,560	0,433	0,577
	8,000	8,000	8,000	8,000	8,000	8,000	8,000	8,000	8,000	8,000	8,000
Alo	0,627	0,483	0,506	0,348	0,157	0,288	0,256	0,561	0,363	0,406	0,560
Fe3	0,525	0,470	0,529	0,236	0,289	0,142	0,423	0,479	0,434	0,436	0,578
Cr	0,001	0,003	0,002	0,000	0,006	0,008	0,002	0,007	0,008	0,005	0,005
Ti	0,017	0,015	0,017	0,016	0,018	0,003	0,008	0,004	0,006	0,005	0,008
Mg	2,446	2,709	2,771	2,855	3,109	3,451	3,229	2,835	3,182	3,146	2,862
Fe2	1,345	1,265	1,132	1,514	1,391	1,065	1,022	1,050	0,960	0,949	0,925
Mn	0,039	0,054	0,039	0,031	0,030	0,019	0,028	0,029	0,024	0,028	0,035
Zn	0,000	0,000	0,003	0,000	0,000	0,023	0,032	0,034	0,022	0,025	0,028
	5,000	5,000	5,000	5,000	5,000	5,000	5,000	5,000	5,000	5,000	5,000
Ca	1,477	1,460	1,462	1,632	1,778	1,821	1,768	1,502	1,603	1,522	1,339
Na	0,523	0,540	0,538	0,368	0,222	0,179	0,232	0,498	0,397	0,478	0,661
	2,000	2,000	2,000	2,000	2,000	2,000	2,000	2,000	2,000	2,000	2,000
Na	0,306	0,177	0,178	0,127	0,083	0,181	0,186	0,225	0,111	0,030	0,052
K	0,071	0,036	0,038	0,032	0,019	0,022	0,028	0,047	0,030	0,024	0,028
	0,377	0,213	0,216	0,159	0,102	0,204	0,215	0,272	0,141	0,054	0,080
sum	15,377	15,213	15,216	15,159	15,102	15,204	15,215	15,272	15,141	15,054	15,080
OH	2,000	2,000	2,000	2,000	2,000	2,000	2,000	2,000	2,000	2,000	2,000
T in °C	559	533	547	489	480	510	550	552	516	454	490

Sample	Bk 18	Bk 18	Bk 39	Bk 39	Bk 39	Bk 39	Bk 39	Bk 39.1	Bk 7	Bk 7	Bk 7
Analysis	57	58	52	53	25	27	28	43	72	73	1
Date	25.7.94	25.7.94	24.6.92	24.6.92	13.3.93	13.3.93	13.3.93	27.8.92	6.7.92	6.7.92	7.7.92
SiO2	52,96	48,73	49,03	49,01	50,53	51,45	48,34	48,82	47,98	47,21	49,75
TiO2	0,05	0,06	0,11	0,10	0,17	0,08	0,10	0,05	0,08	0,03	0,05
Al2O3	5,66	7,14	6,99	7,84	6,63	6,46	10,46	8,82	10,23	11,72	7,78
Cr2O3	0,03	0,06	0,03	0,00	0,02	0,02	0,02	0,02	0,06	0,07	0,00
Fe2O3	2,41	3,91	2,85	2,88	1,08	3,28	3,03	4,04	3,80	3,47	3,40
FeO	6,72	8,97	8,68	9,06	8,17	7,47	10,05	9,71	9,50	11,23	9,41
MnO	0,11	0,22	0,09	0,08	0,08	0,11	0,16	0,18	0,16	0,19	0,16
MgO	15,83	13,75	14,76	13,86	15,83	15,57	11,90	12,73	11,44	10,24	12,87
CaO	9,87	10,88	10,56	9,63	10,78	10,25	8,26	8,65	7,74	7,66	8,55
ZnO	0,13	0,28	0,00	0,00	0,11	0,21	0,11	0,00	0,00	0,00	0,00
Na2O	2,09	1,94	2,68	3,18	2,55	2,67	4,15	4,05	3,99	4,41	3,43
K2O	0,12	0,18	0,19	0,19	0,22	0,18	0,26	0,18	0,18	0,22	0,15
Total	95,98	96,12	95,97	95,84	96,17	97,76	96,83	97,25	95,16	96,45	95,55
H2O	2,10	2,04	2,05	2,05	2,07	2,11	2,06	2,07	2,03	2,04	2,05
norm 23 oxygen, Fe3 over Si+Ti+Al+Cr+Fe+Mg+Mn+Zn = 16											
Si	7,573	7,152	7,176	7,176	7,312	7,326	7,032	7,087	7,078	6,933	7,292
Alt	0,427	0,848	0,824	0,824	0,688	0,674	0,968	0,913	0,922	1,067	0,708
	8,000	8,000	8,000	8,000	8,000	8,000	8,000	8,000	8,000	8,000	8,000
Alo	0,527	0,387	0,381	0,529	0,443	0,410	0,825	0,596	0,857	0,962	0,636
Fe3	0,259	0,431	0,314	0,318	0,117	0,352	0,331	0,441	0,422	0,384	0,375
Cr	0,003	0,007	0,003	0,000	0,002	0,002	0,002	0,002	0,007	0,008	0,000
Ti	0,005	0,007	0,009	0,008	0,013	0,006	0,008	0,004	0,006	0,002	0,004
Mg	3,374	3,008	3,220	3,025	3,414	3,304	2,580	2,755	2,516	2,242	2,812
Fe2	0,804	1,102	1,062	1,110	0,989	0,890	1,222	1,179	1,172	1,379	1,153
Mn	0,013	0,027	0,011	0,010	0,010	0,013	0,020	0,022	0,020	0,024	0,020
Zn	0,014	0,030	0,000	0,000	0,012	0,022	0,012	0,000	0,000	0,000	0,000
	5,000	5,000	5,000	5,000	5,000	5,000	5,000	5,000	5,000	5,000	5,000
Ca	1,512	1,711	1,656	1,511	1,671	1,564	1,287	1,345	1,223	1,205	1,343
Na	0,488	0,289	0,344	0,489	0,329	0,436	0,713	0,655	0,777	0,795	0,657
	2,000	2,000	2,000	2,000	2,000	2,000	2,000	2,000	2,000	2,000	2,000
Na	0,092	0,263	0,416	0,414	0,387	0,301	0,458	0,485	0,365	0,461	0,317
K	0,022	0,034	0,036	0,036	0,041	0,033	0,049	0,034	0,035	0,042	0,029
	0,114	0,297	0,453	0,450	0,428	0,334	0,507	0,519	0,399	0,503	0,346
sum	15,114	15,297	15,453	15,450	15,428	15,334	15,507	15,519	15,399	15,503	15,346
OH	2,000	2,000	2,000	2,000	2,000	2,000	2,000	2,000	2,000	2,000	2,000
T in °C	480	566	552	543	528	540	540	541	550	548	533

Sample	Bk 7	Bk 7	Bk 7	Bk 7	Bk 7	Bk 7	Bk 8	Bk 8	Bk 8	Bk 8	Bk 9
Analysis	7	55	43	47	48	49	15	17	18	19	6
Date	7.7.92	7.7.92	7.8.92	7.8.92	7.8.92	7.8.92	14.3.93	14.3.93	14.3.93	14.3.93	23.2.94
SiO2	40,82	46,90	46,57	47,26	52,24	51,52	49,98	51,23	48,24	52,13	52,04
TiO2	0,07	0,15	0,06	0,04	0,01	0,07	0,15	0,03	0,05	0,05	0,12
Al2O3	15,52	10,55	9,65	9,51	4,93	7,56	8,95	6,46	10,67	4,87	4,99
Cr2O3	0,00	0,04	0,03	0,00	0,06	0,01	0,08	0,00	0,00	0,00	0,04
Fe2O3	3,20	1,72	3,05	3,37	1,49	4,84	3,04	0,62	2,86	1,71	0,87
FeO	15,40	10,49	10,18	9,64	6,94	6,64	8,07	8,83	8,18	6,67	9,15
MnO	0,24	0,18	0,19	0,21	0,15	0,22	0,12	0,11	0,10	0,11	0,05
MgO	6,81	12,07	12,44	12,86	17,03	14,02	13,80	15,53	13,26	17,17	15,62
CaO	8,72	9,28	10,01	10,10	11,31	8,27	9,20	10,70	9,37	11,57	11,43
ZnO	0,00	0,00	0,20	0,15	0,23	0,24	0,16	0,19	0,23	0,17	0,19
Na2O	4,45	3,58	3,22	3,10	1,93	3,26	3,19	2,52	3,38	1,55	1,39
K2O	0,55	0,24	0,21	0,20	0,08	0,14	0,24	0,16	0,26	0,16	0,13
Total	95,78	95,20	95,82	96,44	96,40	96,80	96,98	96,37	96,60	96,16	96,02
H2O	1,96	2,02	2,02	2,04	2,09	2,10	2,09	2,08	2,07	2,09	2,07
norm 23 oxygen, Fe3 over Si+Ti+Al+Cr+Fe+Mg+Mn+Zn = 16											
Si	6,258	6,955	6,906	6,939	7,487	7,365	7,179	7,393	6,980	7,482	7,535
Alt	1,742	1,045	1,094	1,061	0,513	0,635	0,821	0,607	1,020	0,518	0,465
	8,000	8,000	8,000	8,000	8,000	8,000	8,000	8,000	8,000	8,000	8,000
Alo	1,063	0,799	0,593	0,584	0,320	0,639	0,695	0,492	0,799	0,306	0,386
Fe3	0,369	0,192	0,341	0,372	0,161	0,521	0,329	0,067	0,311	0,184	0,095
Cr	0,000	0,005	0,004	0,000	0,007	0,001	0,009	0,000	0,000	0,000	0,005
Ti	0,006	0,012	0,005	0,003	0,001	0,005	0,012	0,002	0,004	0,004	0,009
Mg	1,556	2,668	2,750	2,814	3,638	2,987	2,955	3,340	2,860	3,673	3,371
Fe2	1,974	1,302	1,263	1,184	0,832	0,794	0,970	1,065	0,989	0,801	1,108
Mn	0,031	0,023	0,024	0,026	0,018	0,027	0,015	0,013	0,012	0,013	0,006
Zn	0,000	0,000	0,022	0,016	0,024	0,025	0,017	0,020	0,025	0,018	0,020
	5,000	5,000	5,000	5,000	5,000	5,000	5,000	5,000	5,000	5,000	5,000
Ca	1,432	1,475	1,590	1,589	1,737	1,267	1,416	1,654	1,453	1,779	1,773
Na	0,568	0,525	0,410	0,411	0,263	0,733	0,584	0,346	0,547	0,221	0,227
	2,000	2,000	2,000	2,000	2,000	2,000	2,000	2,000	2,000	2,000	2,000
Na	0,755	0,504	0,516	0,471	0,273	0,170	0,304	0,359	0,401	0,211	0,163
K	0,110	0,046	0,041	0,038	0,015	0,026	0,045	0,030	0,049	0,030	0,025
	0,865	0,550	0,557	0,510	0,288	0,196	0,349	0,390	0,450	0,241	0,188
sum	15,865	15,550	15,557	15,510	15,288	15,196	15,349	15,390	15,450	15,241	15,188
OH	2,000	2,000	2,000	2,000	2,000	2,000	2,000	2,000	2,000	2,000	2,000
T in °C	665	545	565	569	519	525	548	516	560	521	505

Sample	Bk 9	Bk 9	Bk 9	Bk 9	Bk 9	Bk 9	Bk 9	Bk 9	Bk 9	Bk 9	Bk 9
Analysis	8	12	13	20	14	15	16	25	26	27	29
Date	23.2.94	23.2.94	23.2.94	23.2.94	24.2.94	24.2.94	24.2.94	24.2.94	24.2.94	24.2.94	24.2.94
SiO2	51,45	53,63	50,36	45,27	47,26	48,16	48,38	45,99	46,74	49,40	49,44
TiO2	0,08	0,05	0,12	0,15	0,30	0,28	0,40	0,22	0,04	0,00	0,14
Al2O3	6,81	4,35	8,09	11,04	10,26	9,90	8,34	10,27	9,89	8,10	8,46
Cr2O3	0,00	0,04	0,03	0,05	0,01	0,04	0,10	0,00	0,02	0,06	0,00
Fe2O3	1,97	0,08	1,78	4,45	3,26	3,26	3,30	3,44	3,30	2,73	1,71
FeO	8,11	9,28	8,80	10,60	10,01	9,96	9,70	11,09	10,47	7,98	9,58
MnO	0,11	0,08	0,12	0,17	0,09	0,14	0,12	0,14	0,11	0,05	0,07
MgO	14,74	16,25	13,95	11,04	12,03	11,79	12,90	11,46	12,04	14,56	13,45
CaO	10,05	11,49	10,03	10,02	9,72	9,04	10,25	10,16	10,18	10,57	9,99
ZnO	0,14	0,11	0,23	0,12	0,07	0,17	0,18	0,16	0,10	0,11	0,12
Na2O	2,15	1,42	2,37	2,77	2,81	3,03	2,27	2,78	2,68	2,31	2,54
K2O	0,14	0,08	0,18	0,28	0,26	0,23	0,23	0,29	0,28	0,14	0,21
Total	95,75	96,86	96,06	95,96	96,09	95,99	96,17	95,99	95,85	96,00	95,71
H2O	2,07	2,10	2,07	2,01	2,04	2,04	2,04	2,02	2,02	2,07	2,05
norm 23 oxygen, Fe3 over Si+Ti+Al+Cr+Fe+Mg+Mn+Zn = 16											
Si	7,436	7,661	7,295	6,741	6,949	7,066	7,102	6,841	6,922	7,172	7,223
Alt	0,564	0,339	0,705	1,259	1,051	0,934	0,898	1,159	1,078	0,828	0,777
	8,000	8,000	8,000	8,000	8,000	8,000	8,000	8,000	8,000	8,000	8,000
Alo	0,596	0,393	0,676	0,679	0,727	0,777	0,545	0,642	0,648	0,558	0,680
Fe3	0,214	0,008	0,194	0,498	0,361	0,360	0,365	0,385	0,368	0,298	0,188
Cr	0,000	0,005	0,003	0,006	0,001	0,005	0,012	0,000	0,002	0,007	0,000
Ti	0,006	0,004	0,009	0,012	0,024	0,022	0,032	0,018	0,003	0,000	0,011
Mg	3,175	3,460	3,012	2,450	2,636	2,578	2,822	2,541	2,657	3,151	2,929
Fe2	0,980	1,109	1,066	1,320	1,231	1,222	1,191	1,379	1,297	0,969	1,171
Mn	0,013	0,010	0,015	0,021	0,011	0,017	0,015	0,018	0,014	0,006	0,009
Zn	0,015	0,012	0,025	0,013	0,008	0,018	0,020	0,018	0,011	0,012	0,013
	5,000	5,000	5,000	5,000	5,000	5,000	5,000	5,000	5,000	5,000	5,000
Ca	1,556	1,759	1,557	1,599	1,531	1,421	1,612	1,619	1,615	1,644	1,564
Na	0,444	0,241	0,443	0,401	0,469	0,579	0,388	0,381	0,385	0,356	0,436
	2,000	2,000	2,000	2,000	2,000	2,000	2,000	2,000	2,000	2,000	2,000
Na	0,159	0,152	0,222	0,398	0,332	0,283	0,258	0,421	0,385	0,294	0,283
K	0,026	0,015	0,034	0,054	0,050	0,044	0,044	0,056	0,054	0,026	0,040
	0,185	0,167	0,256	0,453	0,382	0,327	0,302	0,477	0,439	0,321	0,323
sum	15,185	15,167	15,256	15,453	15,382	15,327	15,302	15,477	15,439	15,321	15,323
OH	2,000	2,000	2,000	2,000	2,000	2,000	2,000	2,000	2,000	2,000	2,000
T in °C	513	476	536	604	579	564	572	587	580	561	544

Sample	Bk 9	Bk 9	Cig 91-1	Cig 91-1
Analysis	22	23	73	74
Date	4.3.94	4.3.94	17.6.93	17.6.93
SiO2	48,77	48,77	47,67	45,18
TiO2	0,14	0,17	0,28	0,26
Al2O3	9,26	8,58	8,82	12,61
Cr2O3	0,05	0,00	0,00	0,02
Fe2O3	3,70	2,85	0,98	1,63
FeO	10,28	10,57	9,38	10,11
MnO	0,15	0,15	0,09	0,12
MgO	12,30	12,67	15,05	12,40
CaO	9,96	10,27	11,68	10,24
ZnO	0,20	0,16	0,00	0,00
Na2O	2,60	2,45	2,66	3,55
K2O	0,25	0,25	0,33	0,40
Total	97,66	96,90	96,94	96,51
H2O	2,07	2,05	2,06	2,04
norm 23 oxygen, Fe3 over Si+Ti+Al+Cr+Fe+Mg+Mn+Zn = 16				
Si	7,061	7,116	6,939	6,640
Alt	0,939	0,884	1,061	1,360
	8,000	8,000	8,000	8,000
Alo	0,641	0,592	0,453	0,824
Fe3	0,403	0,313	0,108	0,180
Cr	0,006	0,000	0,000	0,002
Ti	0,011	0,013	0,022	0,021
Mg	2,654	2,756	3,265	2,716
Fe2	1,245	1,290	1,141	1,242
Mn	0,018	0,019	0,011	0,015
Zn	0,021	0,017	0,000	0,000
	5,000	5,000	5,000	5,000
Ca	1,545	1,606	1,822	1,612
Na	0,455	0,394	0,178	0,388
	2,000	2,000	2,000	2,000
Na	0,275	0,299	0,572	0,624
K	0,047	0,048	0,063	0,077
	0,322	0,346	0,635	0,701
sum	15,322	15,346	15,635	15,701
OH	2,000	2,000	2,000	2,000
T in °C	572	564	556	574

sample	Bk 7	Bk 7	Bk 7	Bk 7	Bk 7	Bk 7	Bk 7	Bk 7	Bk 7	Bk 7	Bk 7Th
analysis	7	8	21	22	63	64	2	4	10	33	3
date	26.4.93	26.4.93	26.4.93	26.4.93	26.4.93	26.4.93	6.7.92	6.7.92	6.7.92	6.7.92	11.6.94
CL colour	yellow	brown	yellow	yellow	yellow	yellow	yellow	yellow	orange	yellow	yellow
CaO	52,39	50,90	51,10	50,55	53,28	51,92	63,61	62,28	59,98	62,60	54,90
MgO	1,97	2,55	2,39	2,43	1,31	1,30	1,24	1,68	2,18	1,01	1,85
FeO	2,13	2,41	2,19	2,45	1,47	1,57	1,40	2,11	2,72	1,87	1,20
MnO	0,65	0,65	0,56	0,53	0,63	0,57	0,86	1,06	1,29	1,07	0,64
Sum	57,14	56,51	56,24	55,96	56,69	55,36	67,11	67,13	66,17	66,55	58,59
CO2	44,97	44,61	44,40	44,15	44,53	43,48	52,66	52,66	51,92	52,04	46,24
total	102,11	101,12	100,64	100,11	101,22	98,84	119,77	119,79	118,09	118,59	104,83
Ca	0,914	0,895	0,903	0,898	0,939	0,937	0,948	0,928	0,907	0,944	0,932
Mg	0,048	0,062	0,059	0,060	0,032	0,033	0,026	0,035	0,046	0,021	0,044
Fe	0,029	0,033	0,030	0,034	0,020	0,022	0,016	0,025	0,032	0,022	0,016
Mn	0,009	0,009	0,008	0,007	0,009	0,008	0,010	0,012	0,015	0,013	0,009
CO3	1,000	1,000	1,000	1,000	1,000	1,000	1,000	1,000	1,000	1,000	1,000
T(Mg)°C	518	572	560	564	442	445	400	457	510	362	501
T(Fe,Mg)°C	538	577	568	571	470	475	429	488	533	407	516

---

sample	Bk 7Th	Bk 7Th	Bk 7Th	Bk 7Th	Bk 7Th	Bk 7Th	Bk 7Th	Bk 7Th	Bk 7Th	Bk 7Th	Bk 7Th
analysis	4	7	16	17	18	19	20	21	22	23	24
date	11.6.94	11.6.94	11.6.94	11.6.94	11.6.94	11.6.94	11.6.94	11.6.94	11.6.94	11.6.94	11.6.94
CL colour	yellow	orange	yellow	orange	orange	yellow	yellow	orange	orange	orange	yellow
CaO	54,28	53,65	51,42	51,38	52,79	51,54	52,91	49,87	50,59	50,05	50,21
MgO	1,77	1,97	1,75	1,83	1,96	1,30	1,26	1,66	1,62	1,70	1,41
FeO	1,54	1,85	1,43	2,12	2,52	1,77	1,73	1,96	1,90	1,80	1,79
MnO	0,68	0,73	0,50	0,96	0,82	0,72	0,71	0,74	0,68	0,69	0,54
Sum	58,27	58,20	55,10	56,29	58,09	55,33	56,61	54,23	54,79	54,24	53,95
CO2	45,90	45,84	43,45	44,21	45,62	43,40	44,40	42,61	43,06	42,66	42,37
total	104,17	104,04	98,55	100,50	103,71	98,73	101,01	96,84	97,85	96,90	96,32
Ca	0,928	0,918	0,929	0,912	0,908	0,932	0,935	0,919	0,922	0,921	0,930
Mg	0,042	0,047	0,044	0,045	0,047	0,033	0,031	0,043	0,041	0,044	0,036
Fe	0,021	0,025	0,020	0,029	0,034	0,025	0,024	0,028	0,027	0,026	0,026
Mn	0,009	0,010	0,007	0,013	0,011	0,010	0,010	0,011	0,010	0,010	0,008
CO3	1,000	1,000	1,000	1,000	1,000	1,000	1,000	1,000	1,000	1,000	1,000
T(Mg)°C	494	515	502	507	515	446	435	496	489	500	465
T(Fe,Mg)°C	513	533	520	530	537	479	469	520	514	522	495

---

sample	Bk 7Th	Bk 7Th	Bk 7Th	Bk 7Th	Bk 7Th	Bk 7Th	Bk 7Th	Bk 7Th	Bk 7Th	Bk 7Th	Bk 7Th
analysis	25	26	28	29	30	31	33	34	33	34	36
date	11.6.94	11.6.94	11.6.94	11.6.94	11.6.94	11.6.94	11.6.94	11.6.94	11.6.94	11.6.94	11.6.94
CL colour	orange	yellow	orange	orange	yellow	orange	yellow	yellow	yellow	yellow	brown
CaO	49,40	51,13	49,92	50,64	50,64	50,92	50,63	52,62	50,63	52,62	50,98
MgO	1,69	1,34	1,76	1,71	1,75	1,38	1,50	1,05	1,50	1,05	1,60
FeO	1,98	1,57	2,27	1,94	2,13	1,97	2,02	1,60	2,02	1,60	1,94
MnO	0,74	0,59	0,62	0,70	0,67	0,60	0,46	0,55	0,46	0,55	0,70
Sum	53,81	54,63	54,57	54,99	55,19	54,87	54,61	55,82	54,61	55,82	55,22
CO2	42,29	42,92	42,87	43,23	43,37	43,05	42,89	43,76	42,89	43,76	43,38
total	96,10	97,55	97,44	98,22	98,56	97,92	97,50	99,58	97,50	99,58	98,60
Ca	0,917	0,935	0,914	0,919	0,916	0,928	0,926	0,944	0,926	0,944	0,922
Mg	0,044	0,034	0,045	0,043	0,044	0,035	0,038	0,026	0,038	0,026	0,040
Fe	0,029	0,022	0,032	0,027	0,030	0,028	0,029	0,022	0,029	0,022	0,027
Mn	0,011	0,009	0,009	0,010	0,010	0,009	0,007	0,008	0,007	0,008	0,010
CO3	1,000	1,000	1,000	1,000	1,000	1,000	1,000	1,000	1,000	1,000	1,000
T(Mg)°C	501	453	506	499	502	458	475	403	475	403	485
T(Fe,Mg)°C	524	482	530	522	526	492	505	441	505	441	512

sample	Bk 7Th	Bk 7Th	Bk 7Th	Bk 7Th	Bk 7Th	Bk 7Th	Bk 7Th	Bk 7Th	Bk 7Th	Bk 7Th	Bk 7Th
analysis	37	38	40	41	42	43	44	45	46	47	48
date	11.6.94	11.6.94	11.6.94	11.6.94	11.6.94	11.6.94	11.6.94	11.6.94	11.6.94	11.6.94	11.6.94
CL colour	brown	brown	brown	yellow	yellow	yellow	yellow	yellow	yellow	yellow	yellow
CaO	50,37	50,52	51,27	53,03	52,14	53,13	51,72	52,47	52,24	53,38	51,47
MgO	1,64	1,60	1,51	0,72	0,98	0,71	1,33	1,22	1,00	0,72	1,60
FeO	1,79	1,93	1,69	0,75	0,97	0,73	0,93	0,98	0,87	0,92	1,45
MnO	0,66	0,60	0,68	0,69	0,65	0,62	0,55	0,75	0,58	0,56	0,70
Sum	54,46	54,65	55,15	55,19	54,74	55,19	54,53	55,42	54,69	55,58	55,22
CO2	42,83	42,95	43,34	43,29	42,99	43,30	42,95	43,58	42,98	43,59	43,46
total	97,29	97,60	98,49	98,48	97,73	98,49	97,48	99,00	97,67	99,17	98,68
Ca	0,923	0,923	0,928	0,961	0,952	0,963	0,945	0,945	0,954	0,961	0,929
Mg	0,042	0,041	0,038	0,018	0,025	0,018	0,034	0,031	0,025	0,018	0,040
Fe	0,026	0,028	0,024	0,011	0,014	0,010	0,013	0,014	0,012	0,013	0,020
Mn	0,010	0,009	0,010	0,010	0,009	0,009	0,008	0,011	0,008	0,008	0,010
CO3	1,000	1,000	1,000	1,000	1,000	1,000	1,000	1,000	1,000	1,000	1,000
T(Mg)°C	492	487	474	329	393	326	452	433	397	328	485
T(Fe,Mg)°C	516	513	500	355	419	352	470	454	420	359	506

---

sample	Bk 7Th	Bk 7Th	Bk 7Th	Bk 7Th
analysis	49	50	51	52
date	11.6.94	11.6.94	11.6.94	11.6.94
CL colour	orange	orange	orange	orange
CaO	51,19	52,24	51,58	52,05
MgO	1,52	1,43	1,41	1,40
FeO	1,29	1,46	1,19	1,16
MnO	0,71	0,64	0,52	0,64
Sum	54,71	55,77	54,70	55,25
CO2	43,06	43,85	43,07	43,48
total	97,77	99,62	97,77	98,73
Ca	0,933	0,935	0,940	0,939
Mg	0,039	0,036	0,036	0,035
Fe	0,018	0,020	0,017	0,016
Mn	0,010	0,009	0,007	0,009
CO3	1,000	1,000	1,000	1,000
T(Mg)°C	477	462	462	459
T(Fe,Mg)°C	497	487	484	480

Appendix B Table B6 jadeite-quartz-albite barometer

sample	Bk 39	Bk 39	Bk 39	Bk 39	Bk 39	Bk 39	Bk 39	Bk 39	BK 39	BK 39	Bk 39
analysis	1,3	9,2	10,2	12,2	13,2	14,2	8	9	10	2,3	1,1
date	4.5.92	4.5.92	4.5.92	4.5.92	4.5.92	4.5.92	23.3.92	23.3.92	23.3.92	4.5.92	5.5.92
Si	1,995	1,998	2,002	1,999	1,988	1,993	1,973	1,936	1,945	1,997	1,989
Alt	0,005	0,002	-0,002	0,001	0,012	0,007	0,027	0,064	0,055	0,003	0,011
	2,000	2,000	2,000	2,000	2,000	2,000	2,000	2,000	2,000	2,000	2,000
Alo	0,474	0,445	0,452	0,432	0,464	0,429	0,435	0,447	0,426	0,481	0,467
Fe3	0,033	0,029	0,024	0,041	0,066	0,065	0,156	0,056	0,055	0,039	0,077
Ti	0,001	0,001	0,001	0,001	0,001	0,001	0,000	0,001	0,001	0,000	0,001
	0,509	0,475	0,477	0,473	0,530	0,496	0,591	0,504	0,482	0,521	0,545
Mg	0,431	0,456	0,451	0,451	0,420	0,442	0,385	0,431	0,440	0,413	0,368
Fe2	0,083	0,080	0,088	0,091	0,057	0,069	0,016	0,269	0,177	0,076	0,110
Mn	0,000	0,001	0,000	0,000	0,001	0,001	0,000	0,003	0,002	0,001	0,001
Ca	0,474	0,513	0,503	0,512	0,473	0,502	0,443	0,352	0,472	0,471	0,440
Na	0,503	0,474	0,480	0,472	0,519	0,489	0,564	0,439	0,426	0,518	0,534
K	0,001	0,000	0,000	0,001	0,000	0,000	0,000	0,003	0,001	0,000	0,001
	1,491	1,525	1,523	1,527	1,470	1,504	1,409	1,496	1,518	1,479	1,455
sum	2,000	2,000	2,000	2,000	2,000	2,000	2,000	2,000	2,000	2,000	2,000
at T (K)	823	823	823	823	823	823	823	823	823	823	823
P (Gpa)	1,30	1,30	1,30	1,28	1,27	1,27	1,21	1,26	1,27	1,29	1,27

sample	Bk 39	Bk 39	Bk 39	Bk 39	Bk 39	Bk 39	Bk 39	Bk 39	Bk 39	Bk 39	Bk 39
analysis	2,1	3,2	4,2	5,1	6,1	8,1	10,1	11,1	1	3	4
date	5.5.92	5.5.92	5.5.92	5.5.92	5.5.92	5.5.92	5.5.92	5.5.92	24.6.92	24.6.92	24.6.92
Si	1,993	1,998	2,001	1,997	1,995	2,002	1,987	1,992	1,990	2,012	1,985
Alt	0,007	0,002	-0,001	0,003	0,005	-0,002	0,013	0,008	0,010	-0,012	0,015
	2,000	2,000	2,000	2,000	2,000	2,000	2,000	2,000	2,000	2,000	2,000
Alo	0,450	0,460	0,463	0,468	0,479	0,531	0,469	0,464	0,493	0,490	0,470
Fe3	0,057	0,074	0,057	0,068	0,066	0,078	0,070	0,094	0,102	0,021	0,073
Ti	0,001	0,001	0,001	0,001	0,001	0,001	0,001	0,001	0,000	0,001	0,001
	0,508	0,536	0,523	0,538	0,546	0,611	0,539	0,559	0,596	0,513	0,545
Mg	0,425	0,390	0,387	0,393	0,385	0,306	0,406	0,377	0,342	0,395	0,389
Fe2	0,074	0,084	0,093	0,072	0,078	0,093	0,097	0,069	0,076	0,134	0,083
Mn	0,002	0,000	0,000	0,000	0,000	0,000	0,000	0,001	0,002	0,002	0,000
Ca	0,490	0,455	0,472	0,461	0,450	0,375	0,430	0,443	0,398	0,430	0,452
Na	0,502	0,535	0,525	0,535	0,541	0,613	0,526	0,551	0,586	0,526	0,530
K	0,000	0,000	0,000	0,000	0,000	0,001	0,001	0,000	0,000	0,000	0,000
	1,492	1,464	1,477	1,462	1,454	1,389	1,461	1,441	1,404	1,487	1,455
sum	2,000	2,000	2,000	2,000	2,000	2,000	2,000	2,000	2,000	2,000	2,000
at T (K)	823	823	823	823	823	823	823	823	823	823	823
P (Gpa)	1,28	1,27	1,28	1,27	1,28	1,28	1,27	1,26	1,26	1,30	1,27

sample	Bk 39	Bk 39	Bk 39	Bk 39	Bk 39	Bk 39	Bk 39	Bk 39	Bk 39	Bk 39	Bk 39
analysis	38	61	4	5	10	11	13	14	29	30	31
date	24.6.92	24.6.92	28.8.92	28.8.92	28.8.92	28.8.92	28.8.92	28.8.92	28.8.92	28.8.92	28.8.92
Si	1,997	2,000	1,988	1,977	1,991	1,976	1,995	1,989	1,985	1,988	1,985
Alt	0,003	0,000	0,012	0,023	0,009	0,024	0,005	0,011	0,015	0,012	0,015
	2,000	2,000	2,000	2,000	2,000	2,000	2,000	2,000	2,000	2,000	2,000
Alo	0,412	0,479	0,471	0,451	0,452	0,428	0,465	0,461	0,465	0,442	0,447
Fe3	0,062	0,029	0,086	0,123	0,102	0,173	0,081	0,067	0,058	0,048	0,058
Ti	0,001	0,001	0,001	0,001	0,001	0,001	0,003	0,001	0,001	0,000	0,001
	0,476	0,511	0,557	0,576	0,555	0,603	0,549	0,530	0,525	0,490	0,507
Mg	0,425	0,414	0,381	0,383	0,385	0,326	0,378	0,387	0,411	0,456	0,452
Fe2	0,110	0,093	0,076	0,040	0,061	0,074	0,091	0,091	0,080	0,061	0,046
Mn	0,000	0,000	0,001	0,000	0,000	0,000	0,001	0,000	0,001	0,001	0,000
Ca	0,515	0,472	0,439	0,445	0,449	0,416	0,433	0,472	0,472	0,514	0,501
Na	0,474	0,511	0,545	0,553	0,546	0,580	0,547	0,519	0,510	0,478	0,491
K	0,000	0,000	0,000	0,001	0,000	0,000	0,000	0,000	0,000	0,000	0,001
	1,524	1,489	1,443	1,424	1,445	1,397	1,451	1,470	1,475	1,510	1,493
sum	2,000	2,000	2,000	2,000	2,000	2,000	2,000	2,000	2,000	2,000	2,000
at T (K)	823	823	823	823	823	823	823	823	823	823	823
P (Gpa)	1,27	1,30	1,26	1,24	1,25	1,20	1,26	1,27	1,28	1,28	1,28

sample	Bk 39	Bk 39	Bk 39	Bk 39	Bk 39	Bk 39	Bk 39	Bk 39	Bk 39	Bk 39	Bk 39
analysis	32	33	34	35	36	37	39	40	41	42	53
date	28.8.92	28.8.92	28.8.92	28.8.92	28.8.92	28.8.92	28.8.92	28.8.92	28.8.92	28.8.92	28.8.92
Si	1,982	1,977	1,981	1,984	1,985	1,982	1,990	1,990	1,988	1,988	1,979
Alt	0,018	0,023	0,019	0,016	0,015	0,018	0,010	0,010	0,012	0,012	0,021
	2,000	2,000	2,000	2,000	2,000	2,000	2,000	2,000	2,000	2,000	2,000
Alo	0,444	0,388	0,444	0,445	0,429	0,395	0,395	0,457	0,470	0,459	0,385
Fe3	0,063	0,072	0,069	0,051	0,062	0,098	0,073	0,043	0,041	0,042	0,126
Ti	0,001	0,001	0,002	0,001	0,001	0,000	0,001	0,000	0,001	0,001	0,001
	0,507	0,461	0,515	0,496	0,493	0,495	0,469	0,500	0,513	0,503	0,512
Mg	0,447	0,502	0,448	0,458	0,460	0,446	0,451	0,442	0,437	0,443	0,406
Fe2	0,056	0,043	0,038	0,052	0,048	0,065	0,087	0,063	0,064	0,067	0,087
Mn	0,000	0,001	0,000	0,000	0,001	0,002	0,000	0,002	0,002	0,001	0,002
Ca	0,501	0,553	0,501	0,512	0,519	0,511	0,533	0,501	0,483	0,493	0,498
Na	0,489	0,438	0,496	0,481	0,479	0,477	0,459	0,490	0,502	0,490	0,489
K	0,001	0,000	0,001	0,001	0,000	0,001	0,001	0,001	0,000	0,001	0,002
	1,493	1,539	1,485	1,504	1,507	1,505	1,531	1,500	1,487	1,497	1,488
sum	2,000	2,000	2,000	2,000	2,000	2,000	2,000	2,000	2,000	2,000	2,000
at T (K)	823	823	823	823	823	823	823	823	823	823	823
P (Gpa)	1,27	1,25	1,27	1,28	1,27	1,24	1,25	1,29	1,29	1,29	1,21

sample	Bk 39	Bk 39	Bk 39	Bk 39	Bk 39	Bk 7	Bk 7	Bk 7	Bk 7	Bk 7	Bk 7
analysis	54	55	55	57	60	38	12	23	55	68	74
date	28.8.92	28.8.92	28.1.93	28.1.93	28.1.93	25.6.92	6.7.92	6.7.92	6.7.92	6.7.92	6.7.92
Si	1,977	1,969	1,973	1,995	1,982	1,986	1,995	1,994	1,986	1,978	1,999
Alt	0,023	0,031	0,027	0,005	0,018	0,014	0,005	0,006	0,014	0,022	0,001
	2,000	2,000	2,000	2,000	2,000	2,000	2,000	2,000	2,000	2,000	2,000
Alo	0,391	0,393	0,421	0,461	0,436	0,414	0,462	0,494	0,417	0,420	0,451
Fe3	0,118	0,112	0,139	0,065	0,083	0,070	0,076	0,062	0,108	0,101	0,051
Ti	0,001	0,001	0,001	0,001	0,001	0,001	0,001	0,001	0,001	0,001	0,000
	0,510	0,506	0,563	0,527	0,521	0,486	0,540	0,556	0,528	0,523	0,503
Mg	0,398	0,416	0,388	0,395	0,430	0,426	0,377	0,380	0,387	0,398	0,408
Fe2	0,088	0,088	0,050	0,086	0,057	0,085	0,087	0,069	0,095	0,083	0,097
Mn	0,003	0,002	0,011	0,001	0,001	0,002	0,001	0,001	0,004	0,000	0,001
Ca	0,513	0,510	0,448	0,465	0,479	0,528	0,458	0,444	0,470	0,494	0,487
Na	0,486	0,474	0,535	0,522	0,498	0,473	0,537	0,549	0,515	0,502	0,503
K	0,001	0,002	0,001	0,000	0,005	0,000	0,000	0,001	0,000	0,000	0,000
	1,490	1,494	1,437	1,473	1,479	1,514	1,460	1,444	1,472	1,477	1,497
sum	2,000	2,000	2,000	2,000	2,000	2,000	2,000	2,000	2,000	2,000	2,000
at T (K)	823	823	823	823	823	823	823	823	823	823	823
P (Gpa)	1,22	1,22	1,22	1,27	1,26	1,26	1,27	1,28	1,24	1,24	1,28

sample	Bk 7	Bk 7	Bk 7	Bk 7	Bk 7	Bk 7	Bk 7	Bk 7	Bk 7	Bk 7	Bk 7
analysis	3	4	6	42	45	46	50	57	15	17	18
date	7.7.92	7.7.92	7.7.92	7.7.92	7.7.92	7.7.92	7.7.92	7.7.92	27.8.92	27.8.92	27.8.92
Si	1,994	1,987	1,981	1,995	1,981	1,978	1,977	2,006	1,977	1,977	1,993
Alt	0,006	0,013	0,019	0,005	0,019	0,022	0,023	-0,006	0,023	0,023	0,007
	2,000	2,000	2,000	2,000	2,000	2,000	2,000	2,000	2,000	2,000	2,000
Alo	0,453	0,434	0,431	0,518	0,433	0,461	0,433	0,452	0,425	0,429	0,441
Fe3	0,048	0,062	0,080	0,056	0,092	0,066	0,091	0,039	0,090	0,083	0,034
Ti	0,001	0,000	0,000	0,001	0,001	0,001	0,001	0,001	0,001	0,001	0,001
	0,503	0,496	0,512	0,576	0,526	0,530	0,525	0,494	0,518	0,515	0,476
Mg	0,398	0,412	0,411	0,357	0,397	0,391	0,401	0,407	0,413	0,409	0,406
Fe2	0,102	0,084	0,072	0,074	0,065	0,113	0,059	0,120	0,060	0,066	0,119
Mn	0,000	0,002	0,002	0,001	0,000	0,003	0,003	0,003	0,002	0,001	0,002
Ca	0,498	0,522	0,509	0,421	0,506	0,454	0,509	0,476	0,508	0,509	0,517
Na	0,498	0,483	0,494	0,571	0,507	0,508	0,502	0,500	0,494	0,493	0,469
K	0,000	0,001	0,000	0,000	0,000	0,001	0,000	0,000	0,001	0,000	0,000
	1,497	1,504	1,488	1,424	1,474	1,470	1,475	1,506	1,482	1,485	1,524
sum	2,000	2,000	2,000	2,000	2,000	2,000	2,000	2,000	2,000	2,000	2,000
at T (K)	823	823	823	823	823	823	823	823	823	823	823
P (Gpa)	1,28	1,27	1,26	1,29	1,25	1,27	1,25	1,29	1,25	1,25	1,29

sample	Bk 7	Bk 7	Bk 7	Bk 7	Bk 7	Bk 7	Bk 7	Bk 7	Bk 8	Bk 8	Bk 8
analysis	28	30	35	37	41	42	51	53	14	36	37
date	27.8.92	27.8.92	27.8.92	27.8.92	27.8.92	27.8.92	27.8.92	27.8.92	14.3.93	14.3.93	14.3.93
Si	1,989	1,975	1,980	1,975	1,965	1,981	1,980	1,984	1,985	1,984	1,983
Alt	0,011	0,025	0,020	0,025	0,035	0,019	0,020	0,016	0,015	0,016	0,017
	2,000	2,000	2,000	2,000	2,000	2,000	2,000	2,000	2,000	2,000	2,000
Alo	0,449	0,380	0,445	0,383	0,366	0,404	0,449	0,428	0,538	0,457	0,468
Fe3	0,027	0,072	0,055	0,077	0,107	0,051	0,075	0,063	0,065	0,061	0,060
Ti	0,000	0,000	0,001	0,000	0,000	0,001	0,000	0,001	0,001	0,001	0,001
	0,478	0,455	0,503	0,462	0,473	0,456	0,524	0,491	0,605	0,519	0,529
Mg	0,434	0,477	0,427	0,458	0,486	0,462	0,405	0,411	0,358	0,401	0,399
Fe2	0,094	0,056	0,072	0,065	0,025	0,078	0,066	0,092	0,043	0,071	0,073
Mn	0,002	0,002	0,001	0,001	0,002	0,002	0,002	0,001	0,001	0,002	0,000
Ca	0,522	0,571	0,510	0,571	0,569	0,560	0,493	0,523	0,396	0,500	0,481
Na	0,467	0,431	0,482	0,436	0,437	0,435	0,503	0,476	0,564	0,503	0,511
K	0,000	0,000	0,001	0,001	0,001	0,001	0,001	0,000	0,026	0,001	0,001
	1,522	1,545	1,497	1,538	1,527	1,544	1,476	1,509	1,395	1,481	1,471
sum	2,000	2,000	2,000	2,000	2,000	2,000	2,000	2,000	2,000	2,000	2,000
at T (K)	823	823	823	823	823	823	823	823	823	823	823
P (Gpa)	1,30	1,25	1,28	1,25	1,22	1,27	1,26	1,27	1,28	1,27	1,28

sample	Bk 8	Bk 8	Bk 8	Bk 8	Bk 8	Bk 8	Bk 8	Bk 8	Bk 8	Bk 8	Bk 8
analysis	38	39	42	43	3	4	5	14	20	21	23
date	14.3.93	14.3.93	14.3.93	14.3.93	29.1.93a	29.1.93a	29.1.93a	29.1.93a	29.1.93a	29.1.93a	29.1.93a
Si	1,992	1,995	1,992	1,995	1,991	2,000	1,997	1,980	1,986	1,992	1,983
Alt	0,008	0,005	0,008	0,005	0,009	0,000	0,003	0,020	0,014	0,008	0,017
	2,000	2,000	2,000	2,000	2,000	2,000	2,000	2,000	2,000	2,000	2,000
Alo	0,439	0,457	0,438	0,453	0,513	0,512	0,487	0,452	0,556	0,475	0,470
Fe3	0,027	0,024	0,066	0,049	0,016	0,004	0,014	0,063	0,060	0,079	0,053
Ti	0,002	0,000	0,000	0,001	0,008	0,006	0,004	0,001	0,001	0,000	0,000
	0,468	0,481	0,504	0,504	0,538	0,523	0,505	0,516	0,618	0,555	0,523
Mg	0,435	0,423	0,405	0,381	0,403	0,397	0,385	0,413	0,341	0,381	0,405
Fe2	0,107	0,102	0,089	0,110	0,082	0,110	0,125	0,073	0,054	0,081	0,079
Mn	0,002	0,002	0,002	0,002	0,000	0,002	0,007	0,002	0,001	0,001	0,001
Ca	0,522	0,509	0,500	0,496	0,429	0,436	0,468	0,495	0,376	0,433	0,480
Na	0,462	0,476	0,496	0,499	0,529	0,528	0,506	0,496	0,604	0,547	0,505
K	0,000	0,001	0,001	0,001	0,007	0,001	0,000	0,001	0,001	0,001	0,002
	1,532	1,519	1,496	1,496	1,462	1,477	1,495	1,484	1,382	1,445	1,477
sum	2,000	2,000	2,000	2,000	2,000	2,000	2,000	2,000	2,000	2,000	2,000
at T (K)	823	823	823	823	823	823	823	823	823	823	823
P (Gpa)	1,30	1,30	1,27	1,28	1,31	1,32	1,31	1,27	1,29	1,27	1,28

sample	Bk 8	Cig90/40/2	Cig90\40\1	Cig90\40\1	Cig90\40\1	Cig90\40\1	Cig90\40\1	Cig90\40\1
analysis	12	45	33	48	65	66	67	68
date	29.1.93b	6.1.91	?	?	?	?	?	?
Si	1,995	2,003	1,998	2,003	1,993	1,981	1,995	2,000
Alt	0,005	0,000	0,002	0,000	0,007	0,019	0,005	0,000
	2,000	2,003	2,000	2,003	2,000	2,000	2,000	2,000
Alo	0,565	0,502	0,507	0,511	0,429	0,471	0,479	0,465
Fe3	0,018	0,048	0,060	0,043	0,083	0,111	0,076	0,075
Ti	0,002	0,001	0,001	0,001	0,001	0,001	0,001	0,000
	0,586	0,550	0,568	0,555	0,513	0,583	0,556	0,540
Mg	0,343	0,368	0,362	0,369	0,362	0,376	0,376	0,383
Fe2	0,087	0,103	0,086	0,092	0,136	0,040	0,081	0,088
Mn	0,001	0,001	0,000	0,000	0,000	0,000	0,000	0,000
Ca	0,392	0,418	0,417	0,419	0,482	0,434	0,436	0,449
Na	0,581	0,557	0,567	0,563	0,507	0,565	0,552	0,540
K	0,001	0,000	0,000	0,000	0,000	0,000	0,000	0,000
	1,414	1,447	1,432	1,441	1,487	1,417	1,444	1,460
sum	2,000	1,997	2,000	1,997	2,000	2,000	2,000	2,000
at T (K)	823	823	823	823	823	823	823	823
P (Gpa)	1,32	1,29	1,28	1,30	1,25	1,25	1,27	1,27

Table C1

List of samples, XRD is powder X-ray diffraction, EMP is electron microprobe, CL is cathodoluminescence, SEM is scanning electron microscopy, XRF is X-ray fluorescence spectroscopy, UST is universal stage, IA is image analysis, FIS is microthermometry

sample number	short description	thin sections	XRD	other methods
Bk 1	group 1 eclogite	3	par	
Bk 2	type 4 ab vein in group 4 eclogite	1	par	
Bk 3	type 3 qtz vein in group 3 eclogite	1	par	
Bk 4	type 2 qtz vein in group 2 eclogite	3	par	vein EMS, XRF, UST, IA
Bk 5	type 1 qtz vein in group 1 eclogite	3	par	UST, IA
Bk 6	type 1 qtz vein in group 2 eclogite	1	par	UST, IA
Bk 7	gln rich group 1 eclogite	3	par/phe	EMS, XRF, CL
Bk 8	type 1 qtz vein in group 2 eclogite	2	par	rock EMS, UST, IA
Bk 9	group 2/3 eclogite	2	par	EMS, XRF, IA
Bk 10	group 3 eclogite	2	par/phe	EMS, XRF, IA
Bk 11	white mica rich group 2 eclogite	1	phe	
Bk 12	group 1 eclogite with type 1 zoi vein	1	par	
Bk 13	group 4 eclogite with shearbands	1	par	XRF
Bk 14	type 4 albite vein in group 4 eclogite	1	par	
Bk 15	type 4 albite vein in group 4 eclogite	1	par	
Bk 16	type 4 albite vein in group 4 eclogite	1	par	
Bk 17	type 4 albite vein in group 4 eclogite	1	par	rock EMS, CL
Bk 18	type 1/2 qtz-zoi vein in group 3 eclogite	1	par	rock EMS, CL
Bk 19	type 3 qtz vein in group 4 eclogite	1	par	
Bk 20	type 2 qtz vein in group 3 eclogite	2	phe	UST, IA, FIS
Bk 21	type 1 qtz vein in group 3 eclogite	1	par	
Bk 22	group 4 eclogite	1	par	
Bk 23	greenschist	2	-	
Bk 24	group 4 eclogite	1	par	XRF, IA
Bk 25	group 4 eclogite	2	par	
Bk 26	greenschist	1	par	
Bk 27	red-brown grt in metasedimentary rock	1	phe	
Bk 28	compositionally layered metasedimentary rock	1	phe	
Bk 29	grt rich metasedimentary rock	1	phe	
Bk 30a	small scale fold of foliation in metasedimentary rock	1	phe	
Bk 30b	small scale fold of foliation in metasedimentary rock	1	phe	
Bk 31	small scale fold of foliation in metasedimentary rock	2	phe	
Bk 32	second foliation in metasedimentary rock	1	phe	
Bk 33	second foliation in metasedimentary rock	1	phe	EMS
Bk 34	small scale fold of foliation in metasedimentary rock	2	phe	
Bk 35	small scale fold of foliation in metasedimentary rock	1	phe	
Bk 36	type 4 albite vein in metasedimentary rock	3	phe	

Table C1 continued

List of samples, XRD is powder X-ray diffraction, EMP is electron microprobe, CL is cathodoluminescence, SEM is scanning electron microscopy, XRF is X-ray fluorescence spectroscopy, UST is universal stage, IA is image analysis, FIS is microthermometry

sample number	short description	thin sections	XRD	other methods
Bk 37	pink grt in metasedimentary rock	1	phe	
Bk 38	type 1 qtz-grt vein in metasedimentary rock	1	phe	
Bk 39	group 1 eclogite with shearband	1	par	EMS, XRF, SEM, IA
Bk 40	isoclinally folded type 1 qtz-grt vein in metasedimentary rock	3	phe	UST ,IA
Bk 41	type 1 qtz-grt vein in metasedimentary rock	1	phe	
Bk 42	small scale fold of foliation in metasedimentary rock	1	phe	
Bk 43	small scale fold of foliation in metasedimentary rock	2	phe	
Bk 44	type 3 qtz-amp-zoi vein in metasedimentary rock	1	phe	
Bk 45	metasedimentary rock in contact with group 4 eclogite	1	phe	
Bk 46	type 2 qtz vein in metasdimentary rock	1	phe	UST, IA
Bk 47	group 4 eclogite with shearbands	1	par	
Bk 48	group 4 eclogite with shearbands	1	par	
Bk 49	group 4 eclogite with shearbands	2	par	
Bk 50	group 4 eclogite with ab blasts	2	par	
Bk 51	greenschist	1	-	
Bk 52	group 4 eclogite	1	par	
Bk 53	chl lens in greenschist	1	-	
Bk 54	fold of foliated amp layer in greenschist	1	-	
Bk 55	type 1 qtz-zoi vein in group 1 eclogite	3	par	
Bk 56	group 4 eclogite with ab blasts	2	-	
Bk 57	type 4 ab vein in group 4 eclogite	2	-	
Bk 58	strongly weathered metasedimentary rock	2	phe	
Bk 59	type 2/3 qtz vein in metasedimentary rock	1	phe	
Bk 60	folded greenschist in metasedimentary rock	1	par	
Bk 61	strongly weathered metasedimentary rock	2	phe	
Bk 62	chl lens in greenschist	1	-	
Bk 63a	folded greenschist in metasedimentary rock	1	-	
Bk 63b	folded greenschist in metasedimentary rock	1	-	
Bk 64	small scale folds of foliation in metasedimentary rock	2	phe	
Bk 65	group 4 eclogite with ab blasts	1	phe	
Bk 66	tourmaline bearing metasedimentary rock	2	phe	
Bk 67	folds of foliation in greenschist	1	phe	
Bk 68	greenschist	1	par	
Bk 69	small scale folds of foliation in metasedimentary rock	1	phe	
Bk 70	small scale folds of foliation in metasedimentary rock	2	phe	
Bk 71	small scale folds of foliation in metasedimentary rock	1	phe	
Bk 72	small scale folds of foliation in metasedimentary rock	1	phe	

Table C1 continued

List of samples, XRD is powder X-ray diffraction, EMP is electron microprobe, CL is cathodoluminescence, SEM is scanning electron microscopy, XRF is X-ray fluorescence spectroscopy, UST is universal stage, IA is image analysis, FIS is microthermometry

sample number	short description	thin sections	XRD	other methods
Bk 73	core of a m-scale fold in metasedimentary rock	1	phe	
Bk 74	m-scale fold in metasedimentary rock	1	phe	
Bk 75	group 4 eclogite in contact with metasedimentary rock	1	par	
Bk 76	metasedimentary rock in contact with group 4 eclogite	1	phe	
Bk 77	fold of foliation and type 1 qtz vein in metasedimentary rock	2	phe	UST ,IA
Bk 78	folded fold of foliation in metasedimentary rock	5	phe	
Bk 79	small scale folds in amp rich metasedimentary rock	2	phe	
Bk 80	small scale folds of foliation in metasedimentary rock	2	phe	
Bk 81	small scale folds of foliation in metasedimentary rock	2	phe	
Bk 82	group 3/4 eclogite	1	par	
Bk 83	group 4 eclogite with shearbands	2	par	
Bk 84	group 4 eclogite with small scale folds	1	par	
Bk 85	type 4 ab vein in group 4 eclogite with ab blasts	1	par	
Bk 86	compositional layering in metasedimentary rock	1	phe	
Bk 87	dense metasedimentary rock	2	phe	
Bk 88a	folded type 2 qtz vein in metasedimentary rock	1	phe	UST, IA
Bk 88b	folded type 2 qtz vein in metasedimentary rock	1	phe	
Bk 89	type 3 qtz-czo vein in metasedimentary rock	1	-	
Bk 95	group 1 eclogite as m-scale lens in metasedimentary rock	1	-	
Bk 96a	group 1 eclogite as m-scale lens in metasedimentary rock	1	-	
Bk 96b	group 1 eclogite as m-scale lens in metasedimentary rock	1	-	
Bk 97	extensional shearbands in group 3 eclogite	3	-	EMS, CL
Bk 98	type 1 qtz vein in group 3 eclogite	1	-	
Bk 99	type 2 qtz vein in metasedimentary rock	2	-	UST, IA
Bk 100	type 1 qtz vein in a group 1 eclogite	1	-	FIS
Bk 101	type 2 qtz vein in a group 3 eclogite	1	-	FIS
Bk 102	type 3 qtz vein in a group 4 eclogite	1	-	
Bk 103	qtz segregation in boudin neck in metasedimentary rock	1	-	
Bk 104	qtz segragation in boudin neck in metasedimentary rock	1	-	
Bk 105	type 4 ab vein in metasedimentary rock	1	-	
Bk 106	group 1 qtz vein in metasedimentary rock	2	-	UST, IA
Bk 110	type 1/2 qtz vein in group 4 eclogite	1	-	
Bk 111	type 3 qtz vein in group 4 eclogite	1	-	
Bk 112	type 3 qtz vein in group 3 eclogite	1	-	
Bk 113	type 2 qtz vein in group 3 eclogite	1	-	

Table C1 continued

List of samples, XRD is powder X-ray diffraction, EMP is electron microprobe, CL is cathodoluminescence, SEM is scanning electron microscopy, XRF is X-ray fluorescence spectroscopy, UST is universal stage, IA is image analysis, FIS is microthermometry

sample number	short description	thin sections	XRD	other methods
Bk 114	type 4 ab vein in group 4 eclogite	1	-	
Bk 115	type 1/2 qtz vein in group 2 eclogite	1	-	
Bk 116	type 3 qtz vein in group 3 eclogite	1	-	
Bk 117	type 3 qtz vein in group 3 eclogite	1	-	
Bk 118	type 3 qtz vein in group 3 eclogite	1	-	UST, IA
Bk 119	type 3 qtz vein in group 3 eclogite in a late shearzone	1	-	UST, IA
Bk 120	type 2 qtz vein in group 3 eclogite	2	-	
Bk 121	type 3 qtz vein in group 3 eclogite in a late shearzone	1	-	
Bk 122	type 1 qtz vein in group 1 eclogite	2	-	UST, IA
Bk 123	type 2 qtz vein in goup 3 eclogite	2	-	
Bk 124	type 1 qtz vein in group 2 eclogite	2	-	
Bk 125	piemontite quartzite in metasedimentary rock	1	-	
Bk 126	mica rich group 1 eclogite	1	phe	
Bk 127	type 3 qtz- zoi vein in group 3 eclogite	2	-	
Bk 128	type 4 ab vein in group 4 eclogite	1	-	
Bk 129	type 3 qtz-czo vein in group 4 eclogite	1	-	
Bk 130	type 3 qtz vein in group 4 eclogite close to late shearzone	1	-	UST, IA
Bk 131a	15 cm thick qtz-ab vein as late shearzone	1	-	UST, IA
Bk 131b	15 cm thick qtz-ab vein as late shearzone	1	-	UST, IA
Bk 132	type 4 ab vein in group 4 eclogite	1	-	
Bk 133	type 2 qtz vein in group 4 eclogite	1	-	
Cig 90/40	mica rich group 1 eclogite	2	par	EMS
Cig 91-1	group 1 eclogite	4	phe	EMS, CL

Table C2

Whole rock analyses fpr major and trace elementsfrom samples of group 1 to 4 eclogites

	Group 1		Group 2		Group 3	Group 4	
in wt.%	Bk 39	Bk 7	Bk 4	Bk 9	Bk 10	Bk 24	Bk 13
SiO_2	48.67	49.90	49.50	48.50	49.90	49.55	48.60
TiO_2	2.31	1.99	2.09	1.65	1.68	1.86	2.31
Al_2O_3	15.28	1585	15.80	16.20	16.40	15.47	15.50
Fe_2O_3	3.92	3.35	3.06	2.53	2.96	3.87	3.55
FeO_x	6.04	5.78	6.31	6.17	5.27	5.42	6.51
MnO_x	0.18	0.16	0.17	0.17	0.14	0.19	0.17
MgO_x	5.62	6.11	5.87	6.23	6.54	6.99	7.71
CaO_x	11.86	10.13	10.10	10.90	10.50	9.40	5.19
Na_2O	4.87	4.73	4.38	3.51	3.73	3.98	4.94
K_2O	0.04	0.07	0.16	0.12	0.23	0.10	0.11
P_2O_5	0.28	0.33	0.34	0.23	0.24	0.34	0.33
H_2O^+	0.81	1.12	1.36	1.86	2.13	2.42	3.55
H_2O^-		0.05	0.12	0.10	0.09	0.14	0.51
CO_2	0.05	0.80	0.16	1.46	0.48	0.04	0.77
Sum	99,93	100,40	99.83	99.63	100.29	99.72	99.75
in ppm	in ppm	in ppm	in ppm	in ppm	in ppm	in ppm	in ppm
S	197	908	670	40	30	244	60
Sc	41	39	38	28	34	37	30
V	258	230	256	221	231	222	268
Cr	150	189	144	207	214	145	136
Co	52	87	110	54	55	43	47
Ni	99	74	63	77	84	77	70
Cu	30	72	60	42	56	45	44
Zn	84	80	90	72	72	91	98
Ga	18	17	18	16	16	17	17
As	1	-	1	2	1	-	2
Rb	19	13	13	-	18	10	11
Sr	168	178	195	281	222	226	131
Y	44	39	46	39	31	42	43
Zr	211	209	222	145	146	205	225
Nb	15	10	13	12	8	11	12
Sb	3	4	2	2	1	2	2
Cs	-	-	-	-	-	-	-
Ba	11	4	7	-	6	8	-
Hf	9	4	7	4	1	6	5
Ta	4	4	9	3	-	2	2
Pb	3	5	4	4	4	7	6
Bi	-	2	3	5	2	2	4
Th	14	18	10	3	11	6	21
U	5	-	3	2	-	3	-
La	56	50	61	54	52	62	54
Ce	46	33	23	9	19	25	21
Nd	38	27	24	26	13	29	21

sample	Bk 39	Bk 39	Bk 39	Bk 39	Bk 39	Bk 39	Bk 39	Bk 39	Bk 39	Bk 39	Bk 39
analysis	8,2	9,2	6	7	8	12	13	17	19	20	1
date	13.3.93	13.3.93	23.3.92	23.3.92	23.3.92	23.3.92	23.3.92	23.3.92	23.3.92	23.3.92	24.6.92
position	i (gnt)	i (gnt)	i (gnt)	i (gnt)	i (gnt)	core	core	i (gnt)	core	core	gnt
SiO2	55,79	55,85	55,55	55,88	54,93	55,12	55,56	55,20	55,19	55,35	55,21
TiO2	0,04	0,06	0,03	0,03	0,00	0,04	0,02	0,03	0,02	0,05	0,02
Al2O3	10,80	10,75	12,36	12,67	10,90	10,46	10,67	11,97	10,84	10,34	11,85
Cr2O3	0,03	0,13	0,05	0,00	0,00	0,04	0,00	0,04	0,03	0,02	0,00
Fe2O3	6,55	5,37	3,72	2,24	5,78	5,03	2,84	3,87	4,53	2,40	3,78
FeO	2,31	2,64	2,32	3,24	0,54	1,12	1,19	2,58	1,58	1,59	2,52
MnO	0,02	0,07	0,03	0,04	0,01	0,02	0,03	0,00	0,00	0,02	0,06
MgO	5,97	6,30	5,90	5,90	7,19	7,28	8,40	6,10	7,15	8,57	6,36
CaO	10,63	11,05	9,98	9,82	11,50	11,58	13,13	10,33	11,58	13,40	10,31
ZnO	0,15	0,17	n.a	n.a	n.a	n.a	n.a	n.a	n.a	n.a	n.a
Na2O	8,61	8,32	8,79	8,72	8,10	7,97	7,21	8,47	7,94	6,93	8,39
K2O	0,03	0,00	0,01	0,01	0,01	0,01	0,00	0,02	0,01	0,01	0,00
total	100,93	100,71	98,74	98,54	98,96	98,66	99,05	98,61	98,87	98,68	98,50
normed to 4 cations, Fe3 over charge balance (12+)											
Si	1,982	1,987	1,993	2,005	1,973	1,987	1,987	1,989	1,985	1,989	1,990
Alt	0,018	0,013	0,007	0,000	0,027	0,013	0,013	0,011	0,015	0,011	0,010
	2,000	2,000	2,000	2,005	2,000	2,000	2,000	2,000	2,000	2,000	2,000
Alo	0,435	0,437	0,516	0,541	0,435	0,431	0,436	0,497	0,445	0,427	0,493
Fe3	0,175	0,144	0,100	0,060	0,156	0,136	0,076	0,105	0,123	0,065	0,102
Cr	0,001	0,004	0,001	0,000	0,000	0,001	0,000	0,001	0,001	0,001	0,000
Ti	0,001	0,001	0,001	0,001	0,000	0,001	0,000	0,001	0,000	0,001	0,000
	0,611	0,586	0,618	0,602	0,591	0,570	0,513	0,603	0,569	0,493	0,596
Mg	0,316	0,334	0,316	0,316	0,385	0,391	0,448	0,328	0,383	0,459	0,342
Fe2	0,069	0,078	0,070	0,097	0,016	0,034	0,036	0,078	0,048	0,048	0,076
Mn	0,001	0,002	0,001	0,001	0,000	0,001	0,001	0,000	0,000	0,001	0,002
Ca	0,405	0,421	0,384	0,377	0,443	0,447	0,503	0,399	0,446	0,516	0,398
Zn	0,004	0,004	-	-	-	-	-	-	-	-	-
Na	0,593	0,574	0,611	0,607	0,564	0,557	0,500	0,592	0,554	0,483	0,586
K	0,001	0,000	0,000	0,000	0,000	0,000	0,000	0,001	0,000	0,000	0,000
	1,389	1,414	1,382	1,398	1,409	1,430	1,487	1,397	1,431	1,507	1,404
sum	4,000	4,000	4,000	4,000	4,000	4,000	4,000	4,000	4,000	4,000	4,000

---

sample	Bk 39	Bk 39	Bk 39	Bk 39	Bk 39	Bk 39	Bk 39	Bk 39	Bk 39	Bk 39	Bk 39
analysis	4	15	16	38	61	11	13	14	15	16	17
date	24.6.92	24.6.92	24.6.92	24.6.92	24.6.92	28.1.93	28.1.93	28.1.93	28.1.93	28.1.93	28.1.93
position	i (gnt)	i (gnt)	i (gnt)	cpx	gnt	i (gnt)	i (gnt)	i (gnt)	i (gnt)	i (gnt)	i (gnt)
SiO2	55,23	54,86	54,57	54,85	55,70	55,29	55,18	55,15	55,07	54,60	54,21
TiO2	0,05	0,05	0,00	0,04	0,05	0,01	0,07	0,06	0,07	0,03	0,05
Al2O3	11,46	10,56	10,67	9,67	11,33	10,58	11,30	11,50	11,24	9,82	9,33
Cr2O3	0,03	0,06	0,03	0,04	0,05	0,05	0,05	0,08	0,05	0,06	0,02
Fe2O3	2,68	3,50	3,73	2,26	1,07	4,00	2,23	3,98	6,01	7,07	6,47
FeO	2,77	3,49	3,53	3,61	3,09	3,26	5,04	2,91	3,31	3,16	4,64
MnO	0,01	0,08	0,10	0,01	0,00	0,06	0,02	0,02	0,04	0,03	0,06
MgO	7,26	6,51	6,51	7,83	7,73	6,84	6,03	6,29	5,24	5,65	5,39
CaO	11,74	11,55	11,64	13,21	12,26	11,87	10,35	10,87	9,56	10,58	10,60
ZnO	n.a	n.a	n.a	n.a	n.a	0,20	0,00	0,13	0,21	0,32	0,13
Na2O	7,61	7,69	7,57	6,71	7,34	7,59	7,97	8,14	8,78	8,22	7,94
K2O	0,01	0,00	0,00	0,00	0,01	0,01	0,00	0,02	0,02	0,03	0,01
total	98,85	98,35	98,35	98,23	98,63	99,76	98,24	99,15	99,60	99,57	98,86
normed to 4 cations, Fe3 over charge balance (12+)											
Si	1,985	1,995	1,987	1,997	2,000	1,986	2,006	1,984	1,985	1,982	1,990
Alt	0,015	0,005	0,013	0,003	0,000	0,014	0,000	0,016	0,015	0,018	0,010
	2,000	2,000	2,000	2,000	2,000	2,000	2,006	2,000	2,000	2,000	2,000
Alo	0,470	0,448	0,445	0,412	0,479	0,433	0,490	0,472	0,462	0,402	0,394
Fe3	0,073	0,096	0,102	0,062	0,029	0,108	0,061	0,108	0,163	0,193	0,179
Cr	0,001	0,002	0,001	0,001	0,001	0,001	0,001	0,002	0,001	0,002	0,001
Ti	0,001	0,001	0,000	0,001	0,001	0,000	0,001	0,001	0,001	0,001	0,001
	0,545	0,546	0,548	0,476	0,511	0,543	0,554	0,583	0,628	0,597	0,574
Mg	0,389	0,353	0,353	0,425	0,414	0,366	0,327	0,337	0,282	0,306	0,295
Fe2	0,083	0,106	0,108	0,110	0,093	0,098	0,153	0,087	0,100	0,096	0,143
Mn	0,000	0,002	0,003	0,000	0,000	0,002	0,001	0,001	0,001	0,001	0,002
Ca	0,452	0,450	0,454	0,515	0,472	0,457	0,403	0,419	0,369	0,411	0,417
Zn	-	-	-	-	-	0,005	0,000	0,003	0,006	0,009	0,004
Na	0,530	0,542	0,534	0,474	0,511	0,528	0,562	0,568	0,614	0,579	0,565
K	0,000	0,000	0,000	0,000	0,000	0,000	0,000	0,001	0,001	0,001	0,000
	1,455	1,454	1,452	1,524	1,489	1,457	1,446	1,417	1,372	1,403	1,426
sum	4,000	4,000	4,000	4,000	4,000	4,000	4,000	4,000	4,000	4,000	4,000

position means analysis of: i(x), inclusion of cpx in mineral x, core is core position in a cpx grain, mineral x, rim position in cpx grain in contact with mineral x, mineral x(i), cpx at an inclusion of mineral x in cpx

sample	Bk 39	Bk 39	Bk 39	Bk 39	Bk 39	Bk 39	Bk 39	Bk 39	Bk 39	Bk 39	Bk 39
analysis	22	24	25	29	31	34	55	57	60	72	3
date	28.1.93	28.1.93	28.1.93	28.1.93	28.1.93	28.1.93	28.1.93	28.1.93	28.1.93	28.1.93	28.8.92
position	i (gnt)	i (gnt)	i (gnt)	i (gnt)	i (gnt)	i (gnt)	gnt	gnt	gnt	i (gnt)	coes (i)
SiO2	55,27	55,19	54,99	54,56	55,46	55,41	54,66	56,55	55,59	54,86	55,56
TiO2	0,01	0,01	0,22	0,47	0,07	0,11	0,05	0,03	0,06	0,00	0,03
Al2O3	11,39	10,95	10,99	9,22	11,00	10,99	10,54	11,21	10,82	10,02	11,19
Cr2O3	0,05	0,12	0,04	0,12	0,02	0,06	0,07	0,00	0,02	0,00	0,05
Fe2O3	3,78	4,48	3,90	6,84	5,63	6,01	5,11	2,44	3,09	5,64	0,86
FeO	3,16	2,64	2,95	4,05	2,49	2,40	1,66	2,93	1,91	3,58	2,77
MnO	0,07	0,03	0,03	0,02	0,05	0,56	0,35	0,03	0,02	0,05	0,04
MgO	6,11	6,70	6,59	6,04	6,03	5,83	7,22	7,52	8,09	5,78	8,21
CaO	10,53	11,38	11,28	11,02	9,73	10,10	11,59	12,30	12,54	10,58	12,79
ZnO	0,26	0,20	0,20	0,18	0,08	0,16	0,14	0,12	0,36	0,29	0,00
Na2O	8,23	7,88	7,84	7,85	8,73	8,59	7,65	7,63	7,21	8,15	7,03
K2O	0,03	0,03	0,06	0,01	0,02	0,02	0,02	0,01	0,11	0,02	0,01
total	98,89	99,61	99,09	100,37	99,30	100,23	99,06	100,77	99,82	98,98	98,54
normed to 4 cations, Fe3 over charge balance (12+)											
Si	1,994	1,981	1,984	1,975	1,994	1,983	1,973	1,995	1,982	1,996	1,995
Alt	0,006	0,019	0,016	0,025	0,006	0,017	0,027	0,005	0,018	0,004	0,005
	2,000	2,000	2,000	2,000	2,000	2,000	2,000	2,000	2,000	2,000	2,000
Alo	0,479	0,444	0,452	0,368	0,460	0,446	0,421	0,461	0,436	0,426	0,469
Fe3	0,103	0,121	0,106	0,186	0,152	0,162	0,139	0,065	0,083	0,154	0,023
Cr	0,001	0,003	0,001	0,003	0,001	0,002	0,002	0,000	0,001	0,000	0,001
Ti	0,000	0,000	0,004	0,009	0,001	0,002	0,001	0,001	0,001	0,000	0,001
	0,583	0,569	0,563	0,567	0,614	0,612	0,563	0,527	0,521	0,580	0,494
Mg	0,329	0,358	0,354	0,326	0,323	0,311	0,388	0,395	0,430	0,313	0,439
Fe2	0,095	0,079	0,089	0,123	0,075	0,072	0,050	0,086	0,057	0,109	0,083
Mn	0,002	0,001	0,001	0,001	0,002	0,017	0,011	0,001	0,001	0,002	0,001
Ca	0,407	0,438	0,436	0,427	0,375	0,387	0,448	0,465	0,479	0,412	0,492
Zn	0,007	0,005	0,005	0,005	0,002	0,004	0,004	0,003	0,009	0,008	0,000
Na	0,576	0,548	0,548	0,551	0,609	0,596	0,535	0,522	0,498	0,575	0,489
K	0,001	0,001	0,003	0,000	0,001	0,001	0,001	0,000	0,005	0,001	0,000
	1,417	1,431	1,437	1,433	1,386	1,388	1,437	1,473	1,479	1,420	1,506
sum	4,000	4,000	4,000	4,000	4,000	4,000	4,000	4,000	4,000	4,000	4,000

---

sample	Bk 39	Bk 39	Bk 39	Bk 39	Bk 39	Bk 39	Bk 39	Bk 39	Bk 39	Bk 39	Bk 39
analysis	4	5	6	8	9	10	11	13	14	29	30
date	28.8.92	28.8.92	28.8.92	28.8.92	28.8.92	28.8.92	28.8.92	28.8.92	28.8.92	28.8.92	28.8.92
position	cpx	cpx	coes (i)	coes (i)	core	cpx	cpx	cpx	cpx	sympl	cpx
SiO2	55,37	54,85	55,43	55,47	55,90	55,78	54,97	55,55	55,24	55,51	55,85
TiO2	0,03	0,06	0,03	0,04	0,04	0,03	0,05	0,17	0,07	0,06	0,02
Al2O3	11,42	11,16	10,97	12,13	11,78	10,94	10,67	11,08	11,13	11,39	10,83
Cr2O3	0,00	0,03	0,03	0,00	0,02	0,02	0,03	0,02	0,00	0,02	0,00
Fe2O3	3,19	4,52	1,96	3,07	2,24	3,79	6,39	2,99	2,47	2,16	1,79
FeO	2,53	1,33	1,76	3,37	2,88	2,06	2,47	3,02	3,01	2,68	2,04
MnO	0,02	0,01	0,04	0,00	0,01	0,00	0,00	0,03	0,00	0,02	0,04
MgO	7,13	7,13	8,44	6,06	6,93	7,24	6,09	7,06	7,22	7,72	8,59
CaO	11,42	11,53	13,16	10,79	11,48	11,75	10,80	11,25	12,24	12,33	13,48
ZnO	0,00	0,04	0,07	0,03	0,08	0,10	0,03	0,01	0,01	0,00	0,00
Na2O	7,83	7,91	7,01	8,26	7,94	7,89	8,32	7,86	7,44	7,36	6,93
K2O	0,01	0,03	0,01	0,01	0,01	0,01	0,00	0,01	0,01	0,01	0,00
total	98,95	98,60	98,91	99,23	99,31	99,61	99,82	99,05	98,84	99,26	99,57
normed to 4 cations, Fe3 over charge balance (12+)											
Si	1,988	1,977	1,985	1,989	1,996	1,991	1,976	1,995	1,989	1,985	1,988
Alt	0,012	0,023	0,015	0,011	0,004	0,009	0,024	0,005	0,011	0,015	0,012
	2,000	2,000	2,000	2,000	2,000	2,000	2,000	2,000	2,000	2,000	2,000
Alo	0,471	0,451	0,448	0,502	0,492	0,452	0,428	0,465	0,461	0,465	0,442
Fe3	0,086	0,123	0,053	0,083	0,060	0,102	0,173	0,081	0,067	0,058	0,048
Cr	0,000	0,001	0,001	0,000	0,001	0,001	0,001	0,001	0,000	0,001	0,000
Ti	0,001	0,001	0,001	0,001	0,001	0,001	0,001	0,003	0,001	0,001	0,000
	0,557	0,576	0,502	0,585	0,553	0,555	0,603	0,549	0,530	0,525	0,490
Mg	0,381	0,383	0,450	0,324	0,369	0,385	0,326	0,378	0,387	0,411	0,456
Fe2	0,076	0,040	0,053	0,101	0,086	0,061	0,074	0,091	0,091	0,080	0,061
Mn	0,001	0,000	0,001	0,000	0,000	0,000	0,000	0,001	0,000	0,001	0,001
Ca	0,439	0,445	0,505	0,415	0,439	0,449	0,416	0,433	0,472	0,472	0,514
Zn	0,000	0,001	0,002	0,001	0,002	0,003	0,001	0,000	0,000	0,000	0,000
Na	0,545	0,553	0,487	0,574	0,550	0,546	0,580	0,547	0,519	0,510	0,478
K	0,000	0,001	0,000	0,000	0,000	0,000	0,000	0,000	0,000	0,000	0,000
	1,443	1,424	1,498	1,415	1,447	1,445	1,397	1,451	1,470	1,475	1,510
sum	4,000	4,000	4,000	4,000	4,000	4,000	4,000	4,000	4,000	4,000	4,000

position means analysis of: i(x), inclusion of cpx in mineral x, core is core position in a cpx grain, mineral x, rim position in cpx grain in contact with mineral x, mineral x(i), cpx at an inclusion of mineral x in cpx

sample	Bk 39	Bk 39	Bk 39	Bk 39	Bk 39	Bk 39	Bk 39	Bk 39	Bk 39	Bk 39	Bk 39
analysis	31	32	33	34	35	36	37	38	39	40	41
date	28.8.92	28.8.92	28.8.92	28.8.92	28.8.92	28.8.92	28.8.92	28.8.92	28.8.92	28.8.92	28.8.92
position	cpx	cpx	cpx	cpx	cpx	cpx	cpx	core	cpx	cpx	cpx
SiO2	55,55	55,56	55,42	55,66	55,69	55,80	55,13	55,47	55,33	55,68	55,72
TiO2	0,03	0,04	0,04	0,09	0,06	0,06	0,01	0,05	0,04	0,01	0,06
Al2O3	10,99	10,98	9,79	11,06	10,97	10,58	9,75	11,26	9,54	11,07	11,45
Cr2O3	0,05	0,00	0,01	0,00	0,00	0,03	0,05	0,00	0,00	0,02	0,02
Fe2O3	2,15	2,34	2,68	2,57	1,89	2,32	3,63	2,54	2,71	1,60	1,54
FeO	1,55	1,86	1,43	1,26	1,75	1,61	2,15	2,73	2,89	2,12	2,14
MnO	0,01	0,00	0,04	0,01	0,00	0,02	0,05	0,02	0,00	0,05	0,06
MgO	8,48	8,40	9,45	8,45	8,62	8,67	8,32	7,24	8,42	8,30	8,21
CaO	13,09	13,10	14,46	13,15	13,41	13,62	13,27	11,99	13,82	13,09	12,63
ZnO	0,07	0,00	0,03	0,00	0,00	0,00	0,13	0,05	0,01	0,01	0,00
Na2O	7,09	7,07	6,34	7,19	6,96	6,95	6,84	7,60	6,58	7,07	7,25
K2O	0,02	0,02	0,01	0,03	0,02	0,00	0,02	0,02	0,02	0,02	0,01
total	99,07	99,37	99,70	99,48	99,37	99,66	99,35	98,96	99,36	99,04	99,09
normed to 4 cations, Fe3 over charge balance (12+)											
Si	1,985	1,982	1,977	1,981	1,984	1,985	1,982	1,992	1,990	1,990	1,988
Alt	0,015	0,018	0,023	0,019	0,016	0,015	0,018	0,008	0,010	0,010	0,012
	2,000	2,000	2,000	2,000	2,000	2,000	2,000	2,000	2,000	2,000	2,000
Alo	0,447	0,444	0,388	0,444	0,445	0,429	0,395	0,468	0,395	0,457	0,470
Fe3	0,058	0,063	0,072	0,069	0,051	0,062	0,098	0,068	0,073	0,043	0,041
Cr	0,001	0,000	0,000	0,000	0,000	0,001	0,001	0,000	0,000	0,001	0,001
Ti	0,001	0,001	0,001	0,002	0,001	0,001	0,000	0,001	0,001	0,000	0,001
	0,507	0,507	0,461	0,515	0,496	0,493	0,495	0,537	0,469	0,500	0,513
Mg	0,452	0,447	0,502	0,448	0,458	0,460	0,446	0,387	0,451	0,442	0,437
Fe2	0,046	0,056	0,043	0,038	0,052	0,048	0,065	0,082	0,087	0,063	0,064
Mn	0,000	0,000	0,001	0,000	0,000	0,001	0,002	0,001	0,000	0,002	0,002
Ca	0,501	0,501	0,553	0,501	0,512	0,519	0,511	0,461	0,533	0,501	0,483
Zn	0,002	0,000	0,001	0,000	0,000	0,000	0,003	0,001	0,000	0,000	0,000
Na	0,491	0,489	0,438	0,496	0,481	0,479	0,477	0,529	0,459	0,490	0,502
K	0,001	0,001	0,000	0,001	0,001	0,000	0,001	0,001	0,001	0,001	0,000
	1,493	1,493	1,539	1,485	1,504	1,507	1,505	1,463	1,531	1,500	1,487
sum	4,000	4,000	4,000	4,000	4,000	4,000	4,000	4,000	4,000	4,000	4,000

---

sample	Bk 39	Bk 39	Bk 39	Bk 39	Bk 39	Bk 39	Bk 39	Bk 39	Bk 39	Bk 39	Bk 39
analysis	42	53	54	1,3	2,2	2,3	6,2	7,2	8,2	9,2	10,2
date	28.8.92	28.8.92	28.8.92	4.5.92	4.5.92	4.5.92	4.5.92	4.5.92	4.5.92	4.5.92	4.5.92
position	cpx	gnt	gnt	gnt	i (gnt)	gnt	i (gnt)	i (gnt)	i (gnt)	gnt	gnt
SiO2	55,81	55,12	54,36	56,00	55,42	56,09	55,09	55,17	55,20	55,83	55,64
TiO2	0,05	0,04	0,03	0,05	0,04	0,01	0,02	0,02	0,04	0,06	0,04
Al2O3	11,23	9,59	9,67	11,42	11,45	11,54	10,48	11,03	12,01	10,61	10,63
Cr2O3	0,03	0,01	0,00	0,02	0,02	0,04	0,09	0,05	0,00	0,01	0,01
Fe2O3	1,56	4,66	4,32	1,23	3,35	1,46	3,80	3,85	3,40	1,07	0,88
FeO	2,25	2,89	2,91	2,78	2,94	2,55	3,08	3,29	2,24	2,68	2,92
MnO	0,03	0,06	0,10	0,00	0,01	0,02	0,04	0,05	0,05	0,04	0,01
MgO	8,34	7,58	7,35	8,11	6,59	7,78	6,79	6,48	6,43	8,55	8,41
CaO	12,92	12,95	13,17	12,41	11,02	12,36	11,86	11,24	10,78	13,38	13,06
ZnO	0,10	0,15	0,00	n.a.	n.a.	n.a.	n.a.	n.a.	n.a.	n.a.	n.a.
Na2O	7,10	7,03	6,89	7,29	8,07	7,50	7,65	7,90	8,29	6,83	6,88
K2O	0,02	0,05	0,03	0,02	0,02	0,01	0,00	0,02	0,01	0,01	0,00
total	99,44	100,13	98,82	99,32	98,93	99,36	98,90	99,10	98,45	99,07	98,49
normed to 4 cations, Fe3 over charge balance (12+)											
Si	1,988	1,979	1,977	1,995	1,993	1,997	1,991	1,989	1,988	1,998	2,002
Alt	0,012	0,021	0,023	0,005	0,007	0,003	0,009	0,011	0,012	0,002	0,000
	2,000	2,000	2,000	2,000	2,000	2,000	2,000	2,000	2,000	2,000	2,002
Alo	0,459	0,385	0,391	0,474	0,478	0,481	0,438	0,458	0,498	0,445	0,452
Fe3	0,042	0,126	0,118	0,033	0,091	0,039	0,103	0,104	0,092	0,029	0,024
Cr	0,001	0,000	0,000	0,001	0,001	0,001	0,003	0,001	0,000	0,000	0,000
Ti	0,001	0,001	0,001	0,001	0,001	0,000	0,000	0,000	0,001	0,001	0,001
	0,503	0,512	0,510	0,509	0,570	0,521	0,544	0,564	0,591	0,475	0,477
Mg	0,443	0,406	0,398	0,431	0,353	0,413	0,366	0,348	0,345	0,456	0,451
Fe2	0,067	0,087	0,088	0,083	0,088	0,076	0,093	0,099	0,067	0,080	0,088
Mn	0,001	0,002	0,003	0,000	0,000	0,001	0,001	0,002	0,002	0,001	0,000
Ca	0,493	0,498	0,513	0,474	0,425	0,471	0,459	0,434	0,416	0,513	0,503
Zn	0,003	0,004	0,000	-	-	-	-	-	-	-	-
Na	0,490	0,489	0,486	0,503	0,563	0,518	0,536	0,552	0,579	0,474	0,480
K	0,001	0,002	0,001	0,001	0,001	0,000	0,000	0,001	0,000	0,000	0,000
	1,497	1,488	1,490	1,491	1,430	1,479	1,456	1,436	1,409	1,525	1,523
sum	4,000	4,000	4,000	4,000	4,000	4,000	4,000	4,000	4,000	4,000	4,000

position means analysis of: i(x), inclusion of cpx in mineral x, core is core position in a cpx grain, mineral x, rim position in cpx grain in contact with mineral x, mineral x(i), cpx at an inclusion of mineral x in cpx

sample	Bk 39	Bk 39	Bk 39	Bk 39	Bk 39	Bk 39	Bk 39	Bk 39	Bk 39	Bk 39	39
analysis	13,2	14,2	2,1	3,1	3,2	4,1	4,2	5,1	6,1	7,1	8,1
date	4.5.92	4.5.92	5.5.92	5.5.92	5.5.92	5.5.92	5.5.92	5.5.92	5.5.92	5.5.92	5.5.92
position	gnt	gnt	par	core	clz	core	clz	cpx	cpx	core	cpx
SiO2	55,75	55,47	55,32	55,49	55,45	55,72	55,52	55,34	55,50	55,54	55,57
TiO2	0,03	0,03	0,05	0,07	0,05	0,04	0,07	0,04	0,03	0,06	0,07
Al2O3	11,31	10,29	10,74	12,60	10,90	12,56	10,87	11,09	11,43	12,23	12,46
Cr2O3	0,01	0,05	0,00	0,00	0,05	0,01	0,04	0,04	0,00	0,00	0,04
Fe2O3	2,45	2,42	2,10	2,80	2,72	2,56	2,10	2,52	2,45	2,14	2,87
FeO	1,92	2,29	2,45	3,51	2,78	3,67	3,09	2,39	2,60	2,85	3,09
MnO	0,03	0,03	0,05	0,04	0,01	0,01	0,00	0,01	0,00	0,00	0,00
MgO	7,90	8,26	7,92	5,50	7,26	5,63	7,20	7,31	7,18	6,33	5,70
CaO	12,37	13,05	12,68	9,76	11,78	9,69	12,22	11,92	11,69	10,63	9,71
ZnO	n.a.	n.a.	n.a.	n.a.	n.a.	n.a.	n.a.	n.a.	n.a.	n.a.	n.a.
Na2O	7,50	7,02	7,18	8,73	7,66	8,72	7,51	7,65	7,76	8,34	8,78
K2O	0,01	0,01	0,01	0,02	0,00	0,03	0,01	0,01	0,01	0,01	0,03
total	99,28	98,92	98,50	98,52	98,65	98,64	98,63	98,31	98,65	98,12	98,32
normed to 4 cations, Fe3 over charge balance (12+)											
Si	1,988	1,993	1,993	1,999	1,998	2,003	2,001	1,997	1,995	2,002	2,002
Alt	0,012	0,007	0,007	0,001	0,002	0,000	0,000	0,003	0,005	0,000	0,000
	2,000	2,000	2,000	2,000	2,000	2,003	2,001	2,000	2,000	2,002	2,002
Alo	0,464	0,429	0,450	0,533	0,460	0,535	0,463	0,468	0,479	0,521	0,531
Fe3	0,066	0,065	0,057	0,076	0,074	0,069	0,057	0,068	0,066	0,058	0,078
Cr	0,000	0,001	0,000	0,000	0,001	0,000	0,001	0,001	0,000	0,000	0,001
Ti	0,001	0,001	0,001	0,001	0,001	0,001	0,001	0,001	0,001	0,001	0,001
	0,530	0,496	0,508	0,611	0,536	0,605	0,523	0,538	0,546	0,580	0,611
Mg	0,420	0,442	0,425	0,295	0,390	0,302	0,387	0,393	0,385	0,340	0,306
Fe2	0,057	0,069	0,074	0,106	0,084	0,110	0,093	0,072	0,078	0,086	0,093
Mn	0,001	0,001	0,002	0,001	0,000	0,000	0,000	0,000	0,000	0,000	0,000
Ca	0,473	0,502	0,490	0,377	0,455	0,373	0,472	0,461	0,450	0,410	0,375
Zn	-	-	-	-	-	-	-	-	-	-	-
Na	0,519	0,489	0,502	0,610	0,535	0,608	0,525	0,535	0,541	0,583	0,613
K	0,000	0,000	0,000	0,001	0,000	0,001	0,000	0,000	0,000	0,000	0,001
	1,470	1,504	1,492	1,389	1,464	1,395	1,477	1,462	1,454	1,420	1,389
sum	4,000	4,000	4,000	4,000	4,000	4,000	4,000	4,000	4,000	4,000Bk	4,000

---

sample	Bk 39	Bk 39	Bk 39	Bk 7	Bk 7	Bk 7	Bk 7	Bk 7	Bk 7	Bk 7	Bk 7
analysis	9,1	10,1	11,1	38	2	3	38	40	41	42	15
date	5.5.92	5.5.92	5.5.92	25.6.92	26.4.93	26.4.93	26.4.93	26.4.93	26.4.93	26.4.93	27.8.92
position	core	par	par	gnt	gnt	gnt	i (gnt)	i (gnt)	i (gnt)	i (gnt)	par
SiO2	55,51	54,97	55,33	54,91	56,24	56,07	55,97	56,31	55,34	55,10	54,97
TiO2	0,06	0,04	0,03	0,03	0,03	0,15	0,11	0,04	0,04	0,07	0,04
Al2O3	11,14	11,30	11,13	10,04	11,67	12,23	10,27	12,12	10,91	10,89	10,57
Cr2O3	0,03	0,01	0,03	0,04	0,03	0,13	0,00	0,10	0,03	0,03	0,07
Fe2O3	1,30	2,56	3,46	2,56	1,83	0,73	1,40	2,42	2,00	2,22	3,33
FeO	2,41	3,21	2,30	2,82	2,72	3,72	3,86	2,42	3,87	4,01	2,01
MnO	0,02	0,01	0,04	0,08	0,08	0,07	0,06	0,02	0,09	0,09	0,07
MgO	8,05	7,54	7,02	7,90	7,47	7,09	7,71	6,99	7,46	7,12	7,70
CaO	12,73	11,09	11,48	13,62	11,56	11,26	12,39	10,72	11,53	11,96	13,19
ZnO	n.a.	n.a.	n.a.	n.a.	0,29	0,22	0,09	0,15	0,12	0,21	0,13
Na2O	7,18	7,51	7,89	6,74	7,77	7,77	7,20	8,31	7,32	7,24	7,09
K2O	0,01	0,02	0,01	0,00	0,02	0,02	0,00	0,02	0,04	0,02	0,02
total	98,44	98,27	98,73	98,74	99,70	99,46	99,06	99,62	98,75	98,96	99,19
normed to 4 cations, Fe3 over charge balance (12+)											
Si	1,995	1,987	1,992	1,986	1,998	1,998	2,012	1,998	1,997	1,990	1,977
Alt	0,005	0,013	0,008	0,014	0,002	0,002	0,000	0,002	0,003	0,010	0,023
	2,000	2,000	2,000	2,000	2,000	2,000	2,012	2,000	2,000	2,000	2,000
Alo	0,467	0,469	0,464	0,414	0,487	0,511	0,435	0,505	0,461	0,454	0,425
Fe3	0,035	0,070	0,094	0,070	0,049	0,020	0,038	0,065	0,054	0,060	0,090
Cr	0,001	0,000	0,001	0,001	0,001	0,004	0,000	0,003	0,001	0,001	0,002
Ti	0,001	0,001	0,001	0,001	0,001	0,003	0,002	0,001	0,001	0,001	0,001
	0,504	0,539	0,559	0,486	0,537	0,537	0,475	0,574	0,517	0,516	0,518
Mg	0,431	0,406	0,377	0,426	0,396	0,376	0,413	0,370	0,401	0,383	0,413
Fe2	0,073	0,097	0,069	0,085	0,081	0,111	0,116	0,072	0,117	0,121	0,060
Mn	0,001	0,000	0,001	0,002	0,002	0,002	0,002	0,001	0,003	0,003	0,002
Ca	0,490	0,430	0,443	0,528	0,440	0,430	0,477	0,408	0,446	0,463	0,508
Zn	-	-	-	-	0,008	0,006	0,002	0,004	0,003	0,006	0,003
Na	0,500	0,526	0,551	0,473	0,535	0,537	0,502	0,572	0,512	0,507	0,494
K	0,000	0,001	0,000	0,000	0,001	0,001	0,000	0,001	0,002	0,001	0,001
	1,496	1,461	1,441	1,514	1,463	1,463	1,512	1,426	1,483	1,484	1,482
sum	4,000	4,000	4,000	4,000	4,000	4,000	4,000	4,000	4,000	4,000	4,000

position means analysis of: i(x), inclusion of cpx in mineral x, core is core position in a cpx grain, mineral x, rim position in cpx grain in contact with mineral x, mineral x(i), cpx at an inclusion of mineral x in cpx

sample	Bk 7	Bk 7	Bk 7	Bk 7	Bk 7	Bk 7	Bk 7	Bk 7	Bk 7	Bk 7	Bk 7
analysis	16	17	18	28	30	35	37	38	39	40	41
date	27.8.92	27.8.92	27.8.92	27.8.92	27.8.92	27.8.92	27.8.92	27.8.92	27.8.92	27.8.92	27.8.92
position	core	par	par	gl	cpx	par	par	core	core	core	par
SiO2	55,87	55,18	55,03	55,52	54,74	54,93	54,61	55,35	54,80	54,33	54,67
TiO2	0,06	0,05	0,04	0,02	0,02	0,05	0,01	0,05	0,05	0,01	0,02
Al2O3	13,12	10,69	10,51	10,90	9,52	10,96	9,57	11,11	10,99	9,76	9,47
Cr2O3	0,08	0,06	0,00	0,03	0,09	0,05	0,03	0,03	0,03	0,01	0,01
Fe2O3	1,48	3,09	1,25	1,00	2,65	2,04	2,83	1,16	2,31	2,52	3,96
FeO	2,84	2,21	3,92	3,13	1,84	2,40	2,15	3,04	1,88	2,01	0,84
MnO	0,00	0,03	0,06	0,06	0,06	0,03	0,02	0,05	0,05	0,05	0,06
MgO	6,77	7,66	7,53	8,12	8,86	7,95	8,50	8,03	8,05	8,73	9,08
CaO	10,41	13,26	13,33	13,61	14,76	13,22	14,72	13,29	13,59	14,71	14,77
ZnO	0,27	0,26	0,39	0,13	0,34	0,10	0,25	0,27	0,30	0,15	0,24
Na2O	8,26	7,09	6,68	6,72	6,16	6,90	6,22	6,79	6,81	6,10	6,27
K2O	0,02	0,01	0,01	0,01	0,00	0,03	0,02	0,02	0,01	0,03	0,03
total	99,18	99,59	98,74	99,25	99,05	98,66	98,93	99,20	98,87	98,40	99,42
normed to 4 cations, Fe3 over charge balance (12+)											
Si	1,988	1,977	1,993	1,989	1,975	1,980	1,975	1,985	1,972	1,972	1,965
Alt	0,012	0,023	0,007	0,011	0,025	0,020	0,025	0,015	0,028	0,028	0,035
	2,000	2,000	2,000	2,000	2,000	2,000	2,000	2,000	2,000	2,000	2,000
Alo	0,539	0,429	0,441	0,449	0,380	0,445	0,383	0,454	0,438	0,389	0,366
Fe3	0,040	0,083	0,034	0,027	0,072	0,055	0,077	0,031	0,063	0,069	0,107
Cr	0,002	0,002	0,000	0,001	0,003	0,001	0,001	0,001	0,001	0,000	0,000
Ti	0,001	0,001	0,001	0,000	0,000	0,001	0,000	0,001	0,001	0,000	0,000
	0,581	0,515	0,476	0,478	0,455	0,503	0,462	0,487	0,503	0,459	0,473
Mg	0,359	0,409	0,406	0,434	0,477	0,427	0,458	0,429	0,432	0,472	0,486
Fe2	0,085	0,066	0,119	0,094	0,056	0,072	0,065	0,091	0,057	0,061	0,025
Mn	0,000	0,001	0,002	0,002	0,002	0,001	0,001	0,002	0,002	0,002	0,002
Ca	0,397	0,509	0,517	0,522	0,571	0,510	0,571	0,511	0,524	0,572	0,569
Zn	0,007	0,007	0,010	0,003	0,009	0,003	0,007	0,007	0,008	0,004	0,006
Na	0,570	0,493	0,469	0,467	0,431	0,482	0,436	0,472	0,475	0,429	0,437
K	0,001	0,000	0,000	0,000	0,000	0,001	0,001	0,001	0,000	0,001	0,001
	1,419	1,485	1,524	1,522	1,545	1,497	1,538	1,513	1,497	1,541	1,527
sum	4,000	4,000	4,000	4,000	4,000	4,000	4,000	4,000	4,000	4,000	4,000

---

sample	Bk 7	Bk 7	Bk 7	Bk 7	Bk 7	Bk 7	Bk 7	Bk 7	Bk 7	Bk 7	Bk 7
analysis	42	51	53	7	8	12	13	14	18	23	44
date	27.8.92	27.8.92	27.8.92	6.7.92	6.7.92	6.7.92	6.7.92	6.7.92	6.7.92	6.7.92	6.7.92
position	cpx	gl	clz	core	core	gnt	i (gnt)	i (gnt)	amph	gnt	i (gnt)
SiO2	54,51	55,32	54,91	55,38	55,08	55,65	55,81	55,23	54,04	55,60	55,34
TiO2	0,03	0,01	0,05	0,05	0,03	0,06	0,06	0,05	0,01	0,03	0,04
Al2O3	9,90	11,13	10,43	11,70	10,73	11,06	12,85	12,35	8,18	11,83	9,82
Cr2O3	0,00	0,00	0,00	0,02	0,03	0,02	0,02	0,03	0,00	0,00	0,06
Fe2O3	1,85	2,79	2,30	2,20	1,45	2,83	1,56	3,02	3,67	2,29	2,69
FeO	2,58	2,19	3,03	2,16	3,74	2,92	2,33	1,86	3,35	2,30	3,80
MnO	0,06	0,05	0,04	0,00	0,05	0,02	0,02	0,00	0,08	0,04	0,06
MgO	8,54	7,59	7,64	7,31	7,36	7,05	6,74	6,73	8,18	7,11	7,62
CaO	14,39	12,86	13,50	11,95	13,08	11,93	10,77	10,94	14,97	11,55	12,99
ZnO	0,17	0,26	0,22	n.a.	n.a.	n.a.	n.a.	n.a.	n.a.	n.a.	n.a.
Na2O	6,18	7,25	6,79	7,71	6,94	7,72	8,32	8,24	5,91	7,90	6,92
K2O	0,03	0,02	0,01	0,00	0,01	0,00	0,01	0,00	0,01	0,02	0,01
total	98,25	99,47	98,92	98,48	98,51	99,25	98,50	98,44	98,40	98,67	99,35
normed to 4 cations, Fe3 over charge balance (12+)											
Si	1,981	1,980	1,984	1,990	1,994	1,995	1,995	1,983	1,983	1,994	1,995
Alt	0,019	0,020	0,016	0,010	0,006	0,005	0,005	0,017	0,017	0,006	0,005
	2,000	2,000	2,000	2,000	2,000	2,000	2,000	2,000	2,000	2,000	2,000
Alo	0,404	0,449	0,428	0,485	0,452	0,462	0,537	0,506	0,337	0,494	0,413
Fe3	0,051	0,075	0,063	0,059	0,040	0,076	0,042	0,082	0,101	0,062	0,073
Cr	0,000	0,000	0,000	0,001	0,001	0,001	0,001	0,001	0,000	0,000	0,002
Ti	0,001	0,000	0,001	0,001	0,001	0,001	0,001	0,001	0,000	0,001	0,001
	0,456	0,524	0,491	0,546	0,493	0,540	0,581	0,589	0,438	0,556	0,488
Mg	0,462	0,405	0,411	0,392	0,397	0,377	0,359	0,360	0,447	0,380	0,410
Fe2	0,078	0,066	0,092	0,065	0,113	0,087	0,070	0,056	0,103	0,069	0,114
Mn	0,002	0,002	0,001	0,000	0,002	0,001	0,001	0,000	0,002	0,001	0,002
Ca	0,560	0,493	0,523	0,460	0,507	0,458	0,413	0,421	0,588	0,444	0,502
Zn	0,005	0,007	0,006	-	-	-	-	-	-	-	-
Na	0,435	0,503	0,476	0,537	0,487	0,537	0,577	0,574	0,420	0,549	0,484
K	0,001	0,001	0,000	0,000	0,000	0,000	0,000	0,000	0,000	0,001	0,000
	1,544	1,476	1,509	1,454	1,507	1,460	1,419	1,411	1,562	1,444	1,512
sum	4,000	4,000	4,000	4,000	4,000	4,000	4,000	4,000	4,000	4,000	4,000

position means analysis of: i(x), inclusion of cpx in mineral x, core is core position in a cpx grain, mineral x, rim position in cpx grain in contact with mineral x, mineral x(i), cpx at an inclusion of mineral x in cpx

sample	Bk 7	Bk 7	Bk 7	Bk 7	Bk 7	Bk 7	Bk 7	Bk 7	Bk 7	Bk 7	Bk 7
analysis	45	47	55	64	68	74	3	4	6	21	24
date	6.7.92	6.7.92	6.7.92	6.7.92	6.7.92	6.7.92	7.7.92	7.7.92	7.7.92	7.7.92	7.7.92
position	i (gnt)	i (gnt)	gnt	i (gnt)	gnt	sympl	amph	calcit	amph	i (gnt)	i (gnt)
SiO2	54,99	55,51	54,75	55,10	55,03	55,14	55,39	54,82	54,85	55,19	55,31
TiO2	0,02	0,02	0,03	0,04	0,03	0,02	0,06	0,01	0,02	0,06	0,02
Al2O3	9,99	11,86	10,08	10,38	10,43	10,58	10,82	10,45	10,57	11,30	12,03
Cr2O3	0,10	0,02	0,08	0,08	0,04	0,03	0,01	0,00	0,01	0,07	0,00
Fe2O3	2,87	2,65	3,97	2,99	3,75	1,88	1,76	2,28	2,96	3,48	2,26
FeO	3,29	2,18	3,14	2,91	2,76	3,21	3,40	2,78	2,38	1,78	2,76
MnO	0,13	0,04	0,12	0,02	0,00	0,03	0,00	0,07	0,05	0,08	0,00
MgO	7,68	6,97	7,16	7,25	7,43	7,56	7,42	7,62	7,64	7,33	6,97
CaO	13,22	11,30	12,09	12,16	12,83	12,55	12,92	13,43	13,14	12,07	11,24
ZnO	n.a.	n.a.	n.a.	n.a.	n.a.	n.a.	n.a.	n.a.	n.a.	n.a.	n.a.
Na2O	6,84	8,03	7,32	7,43	7,20	7,15	7,13	6,87	7,05	7,68	7,88
K2O	0,00	0,01	0,01	0,01	0,00	0,00	0,01	0,02	0,01	0,01	0,01
total	99,14	98,60	98,75	98,37	99,50	98,15	98,93	98,35	98,68	99,05	98,48
normed to 4 cations, Fe3 over charge balance (12+)											
Si	1,986	1,992	1,986	1,997	1,978	1,999	1,994	1,987	1,981	1,979	1,989
Alt	0,014	0,008	0,014	0,003	0,022	0,001	0,006	0,013	0,019	0,021	0,011
	2,000	2,000	2,000	2,000	2,000	2,000	2,000	2,000	2,000	2,000	2,000
Alo	0,411	0,494	0,417	0,440	0,420	0,451	0,453	0,434	0,431	0,457	0,499
Fe3	0,078	0,072	0,108	0,082	0,101	0,051	0,048	0,062	0,080	0,094	0,061
Cr	0,003	0,001	0,002	0,002	0,001	0,001	0,000	0,000	0,000	0,002	0,000
Ti	0,000	0,000	0,001	0,001	0,001	0,000	0,001	0,000	0,000	0,001	0,000
	0,493	0,567	0,528	0,525	0,523	0,503	0,503	0,496	0,512	0,554	0,560
Mg	0,413	0,373	0,387	0,392	0,398	0,408	0,398	0,412	0,411	0,392	0,374
Fe2	0,100	0,066	0,095	0,088	0,083	0,097	0,102	0,084	0,072	0,053	0,083
Mn	0,004	0,001	0,004	0,001	0,000	0,001	0,000	0,002	0,002	0,002	0,000
Ca	0,512	0,435	0,470	0,472	0,494	0,487	0,498	0,522	0,509	0,464	0,433
Zn	-	-	-	-	-	-	-	-	-	-	-
Na	0,479	0,559	0,515	0,522	0,502	0,503	0,498	0,483	0,494	0,534	0,549
K	0,000	0,000	0,000	0,000	0,000	0,000	0,000	0,001	0,000	0,000	0,000
	1,507	1,433	1,472	1,475	1,477	1,497	1,497	1,504	1,488	1,446	1,440
sum	4,000	4,000	4,000	4,000	4,000	4,000	4,000	4,000	4,000	4,000	4,000

---

sample	Bk 7	Bk 7	Bk 7	Bk 7	Bk 7	Bk 7	Bk 7	Bk 8	Bk 8	Bk 8	Bk 8
analysis	28	29	32	42	45	46	50	14	36	37	38
date	7.7.92	7.7.92	7.7.92	7.7.92	7.7.92	7.7.92	7.7.92	14.3.93	14.3.93	14.3.93	14.3.93
position	i (gnt)	i (gnt)	i (gnt)	par	gnt	gnt	gnt	cpx	gnt	gnt	gnt
SiO2	55,14	54,71	54,45	55,81	55,10	54,95	54,72	56,34	55,36	55,56	55,25
TiO2	0,07	0,04	0,08	0,05	0,04	0,07	0,04	0,03	0,06	0,03	0,10
Al2O3	11,39	10,34	10,05	12,41	10,67	11,38	10,70	13,31	11,21	11,52	10,51
Cr2O3	0,07	0,06	0,01	0,02	0,00	0,05	0,00	0,05	0,00	0,00	0,00
Fe2O3	3,73	4,11	3,77	2,09	3,40	2,45	3,35	2,46	2,27	2,25	1,01
FeO	1,46	2,94	3,12	2,49	2,16	3,75	1,96	1,47	2,36	2,43	3,54
MnO	0,01	0,06	0,08	0,02	0,00	0,09	0,09	0,03	0,05	0,01	0,05
MgO	7,18	6,78	7,15	6,70	7,40	7,29	7,45	6,82	7,50	7,50	8,09
CaO	11,88	12,39	12,50	10,99	13,13	11,76	13,15	10,50	13,03	12,58	13,52
ZnO	n.a.	n.a.	n.a.	n.a.	n.a.	n.a.	n.a.	0,21	0,15	0,23	0,13
Na2O	7,87	7,43	7,16	8,24	7,27	7,28	7,17	8,26	7,24	7,39	6,61
K2O	0,00	0,01	0,00	0,01	0,01	0,03	0,01	0,57	0,02	0,02	0,01
total	98,80	98,87	98,37	98,83	99,18	99,11	98,65	100,09	99,25	99,51	98,82
normed to 4 cations, Fe3 over charge balance (12+)											
Si	1,980	1,983	1,984	1,995	1,981	1,978	1,977	1,985	1,984	1,983	1,992
Alt	0,020	0,017	0,016	0,005	0,019	0,022	0,023	0,015	0,016	0,017	0,008
	2,000	2,000	2,000	2,000	2,000	2,000	2,000	2,000	2,000	2,000	2,000
Alo	0,462	0,424	0,415	0,518	0,433	0,461	0,433	0,538	0,457	0,468	0,439
Fe3	0,101	0,112	0,103	0,056	0,092	0,066	0,091	0,065	0,061	0,060	0,027
Cr	0,002	0,002	0,000	0,001	0,000	0,001	0,000	0,001	0,000	0,000	0,000
Ti	0,001	0,001	0,002	0,001	0,001	0,001	0,001	0,001	0,001	0,001	0,002
	0,566	0,539	0,520	0,576	0,526	0,530	0,525	0,605	0,519	0,529	0,468
Mg	0,384	0,366	0,388	0,357	0,397	0,391	0,401	0,358	0,401	0,399	0,435
Fe2	0,044	0,089	0,095	0,074	0,065	0,113	0,059	0,043	0,071	0,073	0,107
Mn	0,000	0,002	0,002	0,001	0,000	0,003	0,003	0,001	0,002	0,000	0,002
Ca	0,457	0,481	0,488	0,421	0,506	0,454	0,509	0,396	0,500	0,481	0,522
Zn	-	-	-	-	-	-	-	0,005	0,004	0,006	0,003
Na	0,548	0,522	0,506	0,571	0,507	0,508	0,502	0,564	0,503	0,511	0,462
K	0,000	0,000	0,000	0,000	0,000	0,001	0,000	0,026	0,001	0,001	0,000
	1,434	1,461	1,480	1,424	1,474	1,470	1,475	1,395	1,481	1,471	1,532
sum	4,000	4,000	4,000	4,000	4,000	4,000	4,000	4,000	4,000	4,000	4,000

position means analysis of: i(x), inclusion of cpx in mineral x, core is core position in a cpx grain, mineral x, rim position in cpx grain in contact with mineral x, mineral x(i), cpx at an inclusion of mineral x in cpx

sample	Bk 8	Bk 8	Bk 8	Bk 8	Bk 8	Bk 8	Bk 8	Bk 8	Bk 8	Bk 8	Bk 8
analysis	39	40	41	42	43	44	3	4	5	6	14
date	14.3.93	14.3.93	14.3.93	14.3.93	14.3.93	14.3.93	29.1.93a	29.1.93a	29.1.93a	29.1.93a	29.1.93a
position	gnt	core	core	cpx	cpx	core	rut	rut	ap	core	gnt
SiO2	55,83	56,07	55,97	55,56	55,70	56,31	55,96	55,55	55,12	55,66	55,37
TiO2	0,01	0,04	0,05	0,01	0,05	0,02	0,41	0,30	0,19	0,11	0,04
Al2O3	10,96	12,37	10,99	10,55	10,86	12,19	12,46	12,07	11,47	12,40	11,19
Cr2O3	0,00	0,03	0,00	0,04	0,01	0,02	0,03	0,03	0,02	0,09	0,02
Fe2O3	0,90	2,66	1,83	2,43	1,82	1,16	0,61	0,16	0,50	0,93	2,35
FeO	3,41	2,36	3,03	2,95	3,68	2,57	2,77	3,64	4,14	3,20	2,43
MnO	0,07	0,00	0,01	0,05	0,07	0,07	0,00	0,05	0,23	0,35	0,07
MgO	7,94	6,57	7,68	7,57	7,14	7,46	7,60	7,39	7,12	6,98	7,74
CaO	13,29	10,69	13,07	13,01	12,93	11,31	11,26	11,29	12,06	11,34	12,91
ZnO	0,21	0,21	0,15	0,16	0,26	0,32	0,42	0,14	0,12	0,17	0,17
Na2O	6,87	8,41	7,14	7,13	7,18	7,88	7,67	7,57	7,20	7,74	7,15
K2O	0,02	0,04	0,08	0,02	0,02	0,03	0,16	0,02	0,01	0,02	0,03
total	99,51	99,45	99,99	99,51	99,74	99,35	99,35	98,22	98,18	98,99	99,48
normed to 4 cations, Fe3 over charge balance (12+)											
Si	1,995	1,995	1,992	1,992	1,995	2,001	1,991	2,000	1,997	1,992	1,980
Alt	0,005	0,005	0,008	0,008	0,005	0,000	0,009	0,000	0,003	0,008	0,020
	2,000	2,000	2,000	2,000	2,000	2,001	2,000	2,000	2,000	2,000	2,000
Alo	0,457	0,514	0,453	0,438	0,453	0,510	0,513	0,512	0,487	0,514	0,452
Fe3	0,024	0,071	0,049	0,066	0,049	0,031	0,016	0,004	0,014	0,025	0,063
Cr	0,000	0,001	0,000	0,001	0,000	0,001	0,001	0,001	0,001	0,003	0,001
Ti	0,000	0,001	0,001	0,000	0,001	0,000	0,008	0,006	0,004	0,002	0,001
	0,481	0,586	0,503	0,504	0,504	0,542	0,538	0,523	0,505	0,544	0,516
Mg	0,423	0,348	0,407	0,405	0,381	0,395	0,403	0,397	0,385	0,372	0,413
Fe2	0,102	0,070	0,090	0,089	0,110	0,077	0,082	0,110	0,125	0,096	0,073
Mn	0,002	0,000	0,000	0,002	0,002	0,002	0,000	0,002	0,007	0,011	0,002
Ca	0,509	0,408	0,498	0,500	0,496	0,431	0,429	0,436	0,468	0,435	0,495
Zn	0,006	0,006	0,004	0,004	0,007	0,008	0,011	0,004	0,003	0,004	0,004
Na	0,476	0,580	0,493	0,496	0,499	0,543	0,529	0,528	0,506	0,537	0,496
K	0,001	0,002	0,004	0,001	0,001	0,001	0,007	0,001	0,000	0,001	0,001
	1,519	1,414	1,497	1,496	1,496	1,457	1,462	1,477	1,495	1,456	1,484
sum	4,000	4,000	4,000	4,000	4,000	4,000	4,000	4,000	4,000	4,000	4,000

---

sample	Bk 8	Bk 8	Bk 8	Bk 8	Bk 8	Bk 8	Bk 8	Bk 8	Bk 8	Bk 8	Bk 8
analysis	20	21	23	26	1	11	12	36	37	38	39
date	29.1.93a	29.1.93a	29.1.93a	29.1.93a	29.1.93b	29.1.93b	29.1.93b	29.1.93b	29.1.93b	29.1.93b	29.1.93b
position	gnt	gnt	gnt	i (rut)	i (rut)	core	sympl	core	core	core	core
SiO2	55,98	55,32	55,48	55,66	56,24	56,27	56,23	55,98	55,84	56,02	56,21
TiO2	0,05	0,02	0,02	0,27	0,26	0,16	0,08	0,00	0,04	0,03	0,03
Al2O3	13,64	11,38	11,56	13,24	13,88	12,54	13,65	12,20	12,14	12,22	12,25
Cr2O3	0,04	0,03	0,00	0,00	0,00	0,01	0,06	0,00	0,04	0,03	0,05
Fe2O3	2,23	2,91	1,96	0,14	2,19	2,21	0,67	0,94	0,33	2,95	0,00
FeO	1,83	2,67	2,64	3,32	1,35	1,66	2,95	2,87	3,39	1,09	4,15
MnO	0,02	0,04	0,03	0,03	0,05	0,01	0,03	0,02	0,04	0,01	0,03
MgO	6,45	7,10	7,60	6,83	6,60	7,28	6,49	7,35	7,48	7,54	7,16
CaO	9,90	11,21	12,53	10,12	9,91	10,99	10,32	10,87	11,37	11,27	10,95
ZnO	0,19	0,07	0,18	0,19	0,20	0,11	0,28	0,20	0,00	0,54	0,21
Na2O	8,78	7,83	7,29	8,19	8,91	8,31	8,45	7,94	7,65	7,97	7,76
K2O	0,02	0,02	0,04	0,03	0,02	0,01	0,03	0,01	0,00	0,19	0,03
total	99,13	98,60	99,33	98,02	99,61	99,56	99,24	98,37	98,31	99,87	98,35
normed to 4 cations, Fe3 over charge balance (12+)											
Si	1,986	1,992	1,983	1,999	1,983	1,991	1,995	2,006	2,004	1,983	2,017
Alt	0,014	0,008	0,017	0,001	0,017	0,009	0,005	0,000	0,000	0,017	0,000
	2,000	2,000	2,000	2,000	2,000	2,000	2,000	2,006	2,004	2,000	2,017
Alo	0,556	0,475	0,470	0,559	0,559	0,514	0,565	0,521	0,517	0,492	0,535
Fe3	0,060	0,079	0,053	0,004	0,058	0,059	0,018	0,025	0,009	0,079	0,000
Cr	0,001	0,001	0,000	0,000	0,000	0,000	0,002	0,000	0,001	0,001	0,001
Ti	0,001	0,000	0,000	0,005	0,005	0,003	0,002	0,000	0,001	0,001	0,001
	0,618	0,555	0,523	0,568	0,622	0,576	0,586	0,546	0,528	0,572	0,524
Mg	0,341	0,381	0,405	0,366	0,347	0,384	0,343	0,393	0,400	0,398	0,383
Fe2	0,054	0,081	0,079	0,100	0,040	0,049	0,087	0,086	0,102	0,032	0,125
Mn	0,001	0,001	0,001	0,001	0,001	0,000	0,001	0,001	0,001	0,000	0,001
Ca	0,376	0,433	0,480	0,389	0,374	0,417	0,392	0,417	0,437	0,427	0,421
Zn	0,005	0,002	0,005	0,005	0,005	0,003	0,007	0,005	0,000	0,014	0,006
Na	0,604	0,547	0,505	0,570	0,609	0,570	0,581	0,552	0,532	0,547	0,540
K	0,001	0,001	0,002	0,001	0,001	0,000	0,001	0,000	0,000	0,009	0,001
	1,382	1,445	1,477	1,432	1,378	1,424	1,414	1,454	1,472	1,428	1,476
sum	4,000	4,000	4,000	4,000	4,000	4,000	4,000	4,000	4,000	4,000	4,000

position means analysis of: i(x), inclusion of cpx in mineral x, core is core position in a cpx grain, mineral x, rim position in cpx grain in contact with mineral x, mineral x(i), cpx at an inclusion of mineral x in cpx

sample	Cig 90/40	Cig 90/40	Cig 90/40	Cig 90/40	Cig 90/40	Cig 90/40	Cig 90/40	Cig 90/40	Cig 90/40	Cig 90/40	Cig 90/40
analysis	45	53	55	3	4	2	3	6	7	43	44
date	6.1.91	6.1.91	6.1.91	6.1.91a	6.1.91a	6.1.91b	6.1.91b	6.1.91b	6.1.91b	6.1.91b	6.1.91b
position	cpx	i (gnt)	i (gnt)	i (gnt)	i (gnt)	i (gnt)	i (gnt)	i (gnt)	i (gnt)	coes (i)	coes (i)
SiO2	55,68	53,18	55,38	55,29	54,69	54,87	54,37	54,82	54,77	55,14	55,74
TiO2	0,04	0,03	0,06	0,04	0,05	0,03	0,04	0,05	0,05	0,05	0,03
Al2O3	11,83	10,68	11,22	11,39	9,43	9,28	8,93	9,75	8,45	10,64	11,49
Cr2O3	0,00	0,02	0,00	0,03	0,03	0,04	0,05	0,05	0,07	0,01	0,00
Fe2O3	1,78	4,32	2,32	2,47	2,43	1,89	4,58	2,62	3,01	1,90	2,40
FeO	3,41	5,36	3,89	3,10	5,07	6,00	4,34	4,94	5,46	3,95	2,96
MnO	0,04	0,08	0,10	0,04	0,01	0,02	0,06	0,00	0,02	0,00	0,04
MgO	6,86	6,84	7,24	6,89	7,05	6,86	6,59	6,98	7,51	7,37	7,13
CaO	10,84	12,16	12,28	11,31	12,79	12,86	12,26	12,80	13,74	11,73	11,33
ZnO	n.a.	n.a.	n.a.	n.a.	n.a.	n.a.	n.a.	n.a.	n.a.	n.a.	n.a.
Na2O	7,98	6,55	7,24	7,80	6,76	6,66	7,15	6,86	6,26	7,30	7,86
K2O	0,01	0,01	0,02	0,00	0,00	0,01	0,01	0,00	0,00	0,00	0,00
total	98,49	99,22	99,75	98,50	98,41	98,52	98,38	98,86	99,40	98,09	98,98
normed to 4 cations, Fe3 over charge balance (12+)											
Si	2,003	1,942	1,983	1,996	2,002	2,009	1,997	1,995	1,996	2,002	1,997
Alt	0,000	0,058	0,017	0,004	0,000	0,000	0,003	0,005	0,004	0,000	0,003
	2,003	2,000	2,000	2,000	2,002	2,009	2,000	2,000	2,000	2,002	2,000
Alo	0,502	0,402	0,456	0,480	0,407	0,400	0,383	0,414	0,359	0,455	0,483
Fe3	0,048	0,119	0,063	0,067	0,067	0,052	0,127	0,072	0,083	0,052	0,065
Cr	0,000	0,001	0,000	0,001	0,001	0,001	0,001	0,001	0,002	0,000	0,000
Ti	0,001	0,001	0,001	0,001	0,001	0,001	0,001	0,001	0,001	0,001	0,001
	0,550	0,522	0,520	0,549	0,476	0,454	0,512	0,488	0,445	0,508	0,548
Mg	0,368	0,372	0,386	0,371	0,385	0,374	0,361	0,379	0,408	0,399	0,381
Fe2	0,103	0,164	0,116	0,093	0,155	0,184	0,133	0,150	0,166	0,120	0,089
Mn	0,001	0,002	0,003	0,001	0,000	0,001	0,002	0,000	0,001	0,000	0,001
Ca	0,418	0,476	0,471	0,437	0,502	0,505	0,482	0,499	0,537	0,456	0,435
Zn	-	-	-	-	-	-	-	-	-	-	-
Na	0,557	0,464	0,503	0,546	0,480	0,473	0,509	0,484	0,442	0,514	0,546
K	0,000	0,000	0,001	0,000	0,000	0,000	0,000	0,000	0,000	0,000	0,000
	1,447	1,478	1,480	1,451	1,523	1,536	1,488	1,512	1,555	1,489	1,452
sum	4,000	4,000	4,000	4,000	4,000	4,000	4,000	4,000	4,000	4,000	4,000

---

sample	Cig 90/40	Cig 90/40	Cig 90/40	Cig 90/40	Cig 90/40	Cig 90/40	Cig 90/40	Cig 90/40	Cig 90/40	Cig 90/40	Cig 90/40
analysis	31	32	33	43	44	46	47	48	63	64	65
date	?	?	?	?	?	?	?	?	?	?	?
position	coes (i)	coes (i)	par	par (i)	par (i)	coes (i)	coes (i)	i (gnt)	i (gnt)	i (gnt)	cpx
SiO2	55,80	55,60	56,00	55,20	55,80	55,50	55,70	55,90	55,60	55,50	54,90
TiO2	0,04	0,05	0,04	0,05	0,04	0,05	0,05	0,05	0,04	0,05	0,05
Al2O3	11,00	11,30	12,10	10,30	10,70	11,70	11,50	12,10	11,90	12,00	10,20
Cr2O3	0,00	0,00	0,00	0,00	0,00	0,00	0,00	0,00	0,00	0,00	0,00
Fe2O3	2,62	3,26	2,24	1,93	1,67	3,53	3,13	1,61	3,39	3,36	3,04
FeO	3,04	2,37	2,88	3,26	3,50	1,63	2,28	3,05	2,35	1,68	4,47
MnO	0,00	0,00	0,00	0,00	0,00	0,00	0,00	0,00	0,07	0,00	0,00
MgO	7,30	7,10	6,80	7,90	7,60	7,10	7,10	6,90	6,60	7,00	6,70
CaO	11,70	11,60	10,90	13,40	13,10	11,00	11,40	10,90	10,80	11,10	12,40
ZnO	n.a.	n.a.	n.a.	n.a.	n.a.	n.a.	n.a.	n.a.	n.a.	n.a.	n.a.
Na2O	7,70	7,90	8,20	6,80	7,10	8,20	8,00	8,10	8,30	8,20	7,20
K2O	0,00	0,00	0,00	0,00	0,00	0,00	0,00	0,00	0,00	0,00	0,00
total	99,20	99,18	99,16	98,84	99,51	98,70	99,16	98,61	99,05	98,89	98,95
normed to 4 cations, Fe3 over charge balance (12+)											
Si	1,999	1,991	1,998	1,992	1,997	1,989	1,992	2,003	1,991	1,985	1,993
Alt	0,001	0,009	0,002	0,008	0,003	0,011	0,008	0,000	0,009	0,015	0,007
	2,000	2,000	2,000	2,000	2,000	2,000	2,000	2,003	2,000	2,000	2,000
Alo	0,464	0,468	0,507	0,430	0,449	0,484	0,477	0,511	0,493	0,491	0,429
Fe3	0,071	0,088	0,060	0,053	0,045	0,095	0,084	0,043	0,091	0,090	0,083
Cr	0,000	0,000	0,000	0,000	0,000	0,000	0,000	0,000	0,000	0,000	0,000
Ti	0,001	0,001	0,001	0,001	0,001	0,001	0,001	0,001	0,001	0,001	0,001
	0,535	0,557	0,568	0,483	0,495	0,580	0,562	0,555	0,585	0,583	0,513
Mg	0,390	0,379	0,362	0,425	0,405	0,379	0,378	0,369	0,352	0,373	0,362
Fe2	0,091	0,071	0,086	0,098	0,105	0,049	0,068	0,092	0,070	0,050	0,136
Mn	0,000	0,000	0,000	0,000	0,000	0,000	0,000	0,000	0,002	0,000	0,000
Ca	0,449	0,445	0,417	0,518	0,502	0,422	0,437	0,419	0,414	0,425	0,482
Zn	-	-	-	-	-	-	-	-	-	-	-
Na	0,535	0,548	0,567	0,476	0,493	0,570	0,555	0,563	0,576	0,569	0,507
K	0,000	0,000	0,000	0,000	0,000	0,000	0,000	0,000	0,000	0,000	0,000
	1,465	1,443	1,432	1,517	1,505	1,420	1,438	1,441	1,415	1,417	1,487
sum	4,000	4,000	4,000	4,000	4,000	4,000	4,000	4,000	4,000	4,000	4,000

position means analysis of: i(x), inclusion of cpx in mineral x, core is core position in a cpx grain, mineral x, rim position in cpx grain in contact with mineral x, mineral x(i), cpx at an inclusion of mineral x in cpx

sample	Cig 90/40	Cig 90/40	Cig 90/40	Cig 91-1	Cig 91-1	Cig 91-1	Cig 91-1	Cig 91-1	Cig 91-1	Cig 91-1	Cig 91-1
analysis	66	67	68	5	7	33	34	35	6	11	12
date	?	?	?	16.6.93	16.6.93	16.6.93	16.6.93	16.6.93	28.11.93	28.11.93	28.11.93
position	cpx	cpx	cpx	cpx	gnt	coes (i)	coes (i)	cpx	phe	phe	phe
SiO2	55,70	55,40	55,30	56,34	56,69	56,85	56,57	56,33	56,01	56,08	56,23
TiO2	0,06	0,05	0,00	0,03	0,04	0,04	0,03	0,00	0,04	0,05	0,10
Al2O3	11,70	11,40	10,90	10,68	11,71	11,52	11,57	10,63	11,02	10,68	10,68
Cr2O3	0,00	0,00	0,00	0,02	0,00	0,01	0,00	0,02	0,01	0,02	0,07
Fe2O3	4,16	2,79	2,77	1,42	1,98	1,74	1,26	1,65	2,15	2,31	1,57
FeO	1,36	2,69	2,91	3,44	3,04	2,86	4,02	3,77	2,90	3,62	4,34
MnO	0,00	0,00	0,00	0,04	0,00	0,01	0,04	0,05	0,07	0,07	0,06
MgO	7,10	7,00	7,10	8,07	7,16	7,67	7,11	7,58	7,18	7,38	7,25
CaO	11,40	11,30	11,60	12,94	11,33	12,20	11,88	12,77	11,75	12,70	12,79
ZnO	n.a.	n.a.	n.a.	0,15	0,07	0,04	0,01	0,04	0,01	0,09	0,06
Na2O	8,20	7,90	7,70	7,07	8,04	7,70	7,68	7,24	7,78	7,29	7,22
K2O	0,00	0,00	0,00	0,01	0,05	0,03	0,03	0,02	0,03	0,03	0,02
total	99,68	98,53	98,28	100,21	100,11	100,67	100,20	100,10	98,96	100,32	100,39
normed to 4 cations, Fe3 over charge balance (12+)											
Si	1,981	1,995	2,000	2,000	2,006	2,001	2,006	2,005	2,008	1,996	2,002
Alt	0,019	0,005	0,000	0,000	0,000	0,000	0,000	0,000	0,000	0,004	0,000
	2,000	2,000	2,000	2,000	2,006	2,001	2,006	2,005	2,008	2,000	2,002
Alo	0,471	0,479	0,465	0,447	0,488	0,478	0,483	0,446	0,466	0,444	0,448
Fe3	0,111	0,076	0,075	0,038	0,053	0,046	0,034	0,044	0,058	0,062	0,042
Cr	0,000	0,000	0,000	0,001	0,000	0,000	0,000	0,001	0,000	0,001	0,002
Ti	0,001	0,001	0,000	0,001	0,001	0,001	0,001	0,000	0,001	0,001	0,002
	0,583	0,556	0,540	0,486	0,542	0,525	0,518	0,491	0,525	0,507	0,494
Mg	0,376	0,376	0,383	0,427	0,378	0,402	0,376	0,402	0,384	0,392	0,385
Fe2	0,040	0,081	0,088	0,102	0,090	0,084	0,119	0,112	0,087	0,108	0,129
Mn	0,000	0,000	0,000	0,001	0,000	0,000	0,001	0,002	0,002	0,002	0,002
Ca	0,434	0,436	0,449	0,492	0,429	0,460	0,451	0,487	0,451	0,484	0,488
Zn	-	-	-	0,004	0,002	0,001	0,000	0,001	0,000	0,002	0,002
Na	0,565	0,552	0,540	0,487	0,552	0,525	0,528	0,500	0,541	0,503	0,498
K	0,000	0,000	0,000	0,000	0,002	0,001	0,001	0,001	0,001	0,001	0,001
	1,417	1,444	1,460	1,514	1,453	1,475	1,477	1,504	1,467	1,493	1,504
sum	4,000	4,000	4,000	4,000	4,000	4,000	4,000	4,000	4,000	4,000	4,000

---

sample	Cig 91-1	Cig 91-1	Cig 91-1
analysis	3	4	8
date	16.6.93	16.6.93	16.6.93
position	coes (i)	coes (i)	gnt
SiO2	56,82	56,93	56,96
TiO2	0,04	0,01	0,04
Al2O3	11,86	11,24	12,03
Cr2O3	0,00	0,01	0,01
Fe2O3	1,47	0,58	1,97
FeO	3,26	4,29	2,72
MnO	0,03	0,00	0,04
MgO	7,15	7,43	7,04
CaO	11,15	12,20	10,89
ZnO	0,00	0,02	0,00
Na2O	8,10	7,52	8,37
K2O	0,03	0,01	0,02
total	99,91	100,24	100,10
normed to 4 cations, Fe3 over charge balance (12+)			
Si	2,011	2,016	2,010
Alt	0,000	0,000	0,000
	2,011	2,016	2,010
Alo	0,495	0,469	0,500
Fe3	0,039	0,015	0,052
Cr	0,000	0,000	0,000
Ti	0,001	0,000	0,001
	0,535	0,485	0,554
Mg	0,377	0,392	0,370
Fe2	0,096	0,127	0,080
Mn	0,001	0,000	0,001
Ca	0,423	0,463	0,412
Zn	0,000	0,001	0,000
Na	0,556	0,516	0,573
K	0,001	0,000	0,001
	1,454	1,499	1,437
sum	4,000	4,000	4,000

position means analysis of: i(x), inclusion of cpx in mineral x, core is core position in a cpx grain, mineral x, rim position in cpx grain in contact with mineral x, mineral x(i), cpx at an inclusion of mineral x in cpx

sample	Bk 10B	Bk 10B	Bk 10B	Bk 10B	Bk 10B	Bk 10B	Bk 10B	Bk 10B	Bk 10B	Bk 10B	Bk 10B
analysis	33	34	35	36	1	2	3	4	1	30	31
date	19.10.93a	19.10.93a	19.10.93a	19.10.93a	19.10.93b	19.10.93b	19.10.93b	19.10.93b	27.11.93	27.11.93	27.11.93
position	chl	chl	chl	chl	core	core	core	chl	chl	chl	chl
SiO2	37,65	37,34	37,42	37,79	36,72	36,83	37,05	37,35	37,50	37,46	37,64
TiO2	0,06	0,06	0,12	0,11	0,02	0,12	0,11	0,14	0,08	0,06	0,07
Al2O3	21,10	20,86	20,71	21,09	20,52	20,57	20,45	20,71	21,13	20,99	20,87
Cr2O3	0,22	0,00	0,00	0,04	0,00	0,03	0,00	0,01	0,01	0,06	0,05
Fe2O3	0,63	1,56	1,35	1,21	2,12	1,92	1,55	1,51	0,99	1,10	1,27
FeO	28,29	27,97	27,37	28,14	26,35	24,96	26,41	25,99	27,28	27,88	28,04
MnO	0,80	0,33	0,80	0,94	3,26	3,88	1,92	0,80	0,64	0,98	0,89
MgO	3,82	4,22	2,97	3,13	2,08	2,00	2,52	3,49	4,21	3,22	2,95
CaO	7,30	7,23	8,94	8,45	8,76	9,54	9,11	9,32	7,64	8,21	8,59
total	99,87	99,58	99,69	100,90	99,83	99,85	99,11	99,32	99,48	99,96	100,38
normed to 24 oxygens, Fe3 over charge balance											
Si	5,951	5,897	5,930	5,923	5,851	5,861	5,919	5,912	5,923	5,924	5,932
Alt	0,049	0,103	0,070	0,077	0,149	0,139	0,081	0,088	0,077	0,076	0,068
Alo	3,881	3,779	3,798	3,819	3,705	3,719	3,770	3,775	3,857	3,836	3,809
Fe3	0,075	0,186	0,161	0,143	0,254	0,230	0,186	0,180	0,117	0,131	0,151
Cr	0,027	0,000	0,000	0,005	0,000	0,004	0,000	0,001	0,001	0,008	0,006
Ti	0,005	0,005	0,010	0,009	0,002	0,010	0,009	0,012	0,007	0,005	0,006
	3,995	3,985	3,982	3,987	3,981	3,981	3,980	3,982	3,991	3,990	3,985
Mg	0,900	0,993	0,702	0,731	0,494	0,474	0,600	0,823	0,991	0,759	0,693
Fe2	3,740	3,694	3,628	3,688	3,512	3,322	3,529	3,441	3,604	3,687	3,696
Mn	0,107	0,044	0,107	0,125	0,440	0,523	0,260	0,107	0,086	0,131	0,119
Ca	1,236	1,223	1,518	1,419	1,496	1,627	1,559	1,581	1,293	1,391	1,451
	5,983	5,955	5,954	5,963	5,941	5,946	5,948	5,952	5,973	5,969	5,959
sum	15,978	15,940	15,937	15,951	15,923	15,927	15,928	15,933	15,965	15,958	15,943

---

sample	Bk 10B	Bk 10B	Bk 10B	Bk 10B	Bk 10B	Bk 10B	BK 17	Bk 18	Bk 18	Bk 18	Bk 18
analysis	34	35	36	37	38	40	49	2	3	5	6
date	27.11.93	27.11.93	27.11.93	27.11.93	27.11.93	27.11.93	3.7.94	5.8.94	5.8.94	5.8.94	5.8.94
position	chl	chl	core	chl	chl	chl	chl	chl	chl	core	chl
SiO2	37,40	37,78	37,57	37,33	37,78	38,05	37,67	38,02	37,58	37,75	37,80
TiO2	0,08	0,08	0,16	0,06	0,05	0,02	0,05	0,07	0,15	0,14	0,05
Al2O3	20,91	20,91	20,77	20,99	21,16	21,43	21,02	21,41	21,31	21,17	21,23
Cr2O3	0,00	0,05	0,03	0,00	0,02	0,01	0,00	0,01	0,02	0,00	0,00
Fe2O3	1,00	1,03	1,30	1,49	1,14	0,71	0,27	0,89	0,99	0,79	0,78
FeO	27,92	27,85	25,83	28,20	27,78	24,71	29,12	27,16	27,11	21,42	26,19
MnO	0,78	0,85	2,31	0,86	0,68	1,60	0,33	1,05	1,42	5,07	3,15
MgO	3,30	3,53	2,68	3,69	4,04	3,53	3,35	3,97	3,02	2,42	3,83
CaO	8,08	7,99	9,48	7,44	7,67	10,23	7,40	8,18	9,01	11,31	7,18
total	99,47	100,07	100,13	100,06	100,31	100,29	99,21	100,76	100,61	100,07	100,21
normed to 24 oxygens, Fe3 over charge balance											
Si	5,939	5,955	5,933	5,889	5,926	5,951	6,005	5,934	5,906	5,947	5,950
Alt	0,061	0,045	0,067	0,111	0,074	0,049	0,000	0,066	0,094	0,053	0,050
Alo	3,853	3,840	3,799	3,791	3,837	3,900	3,949	3,873	3,853	3,877	3,888
Fe3	0,120	0,123	0,154	0,177	0,134	0,084	0,033	0,104	0,117	0,094	0,092
Cr	0,000	0,006	0,004	0,000	0,002	0,001	0,000	0,001	0,002	0,000	0,000
Ti	0,007	0,007	0,014	0,005	0,004	0,002	0,004	0,006	0,013	0,012	0,004
	3,989	3,985	3,982	3,988	3,989	3,993	3,991	3,992	3,993	3,989	3,991
Mg	0,781	0,829	0,631	0,868	0,944	0,823	0,796	0,924	0,707	0,568	0,899
Fe2	3,708	3,671	3,412	3,720	3,643	3,232	3,881	3,546	3,563	2,821	3,448
Mn	0,105	0,113	0,309	0,115	0,090	0,212	0,045	0,139	0,189	0,676	0,420
Ca	1,375	1,349	1,604	1,257	1,289	1,714	1,264	1,368	1,517	1,909	1,211
	5,969	5,963	5,956	5,960	5,967	5,981	5,986	5,976	5,977	5,975	5,977
sum	15,957	15,949	15,937	15,948	15,956	15,973	15,981	15,968	15,970	15,964	15,968

position means analysis of: core is core position in a grt grain, mineral x, rim position in grt grain in contact with mineral x, mineral x(i), grt at an inclusion of mineral x in grt

sample	Bk 18	Bk 18	Bk 39	Bk 39	Bk 39	Bk 39	Bk 39	Bk 39	Bk 39	Bk 39	Bk 39
analysis	8	9	7,2	11,2	12,2	13,2	1	2	3	4	5
date	5.8.94	6.8.94	13.3.93	13.3.93	13.3.93	13.3.93	23.3.92	23.3.92	23.3.92	23.3.92	23.3.92
position	chl	core	amph (i)	core	core	core	amph	amph	cpx (i)	cpx (i)	cpx (i)
SiO2	37,69	38,11	36,64	37,10	37,47	37,61	37,04	38,21	36,93	37,46	37,08
TiO2	0,09	0,09	2,75	0,10	0,10	0,05	0,03	0,01	0,03	0,04	0,01
Al2O3	21,32	20,98	20,78	20,75	21,13	21,01	21,05	21,61	20,92	21,26	20,99
Cr2O3	0,04	0,06	0,12	0,00	0,08	0,06	0,00	0,04	0,01	0,00	0,03
Fe2O3	0,73	0,00	0,05	1,58	1,17	1,28	1,24	0,54	1,67	1,09	1,51
FeO	27,23	23,95	28,40	25,98	26,77	26,33	26,35	26,97	27,08	26,71	25,45
MnO	1,52	2,62	0,76	1,66	1,58	1,00	0,52	0,49	0,72	0,58	0,48
MgO	2,94	2,59	3,32	2,76	2,96	3,87	3,71	3,74	3,68	3,65	3,94
CaO	8,92	10,80	7,68	9,58	9,12	8,65	8,93	9,22	8,24	9,01	9,42
total	100,48	99,20	100,51	99,51	100,38	99,87	98,87	100,83	99,28	99,80	98,90
normed to 24 oxygens, Fe3 over charge balance											
Si	5,933	6,055	5,832	5,890	5,901	5,916	5,887	5,954	5,859	5,902	5,874
Alt	0,067	0,000	0,168	0,110	0,099	0,084	0,113	0,046	0,141	0,098	0,126
Alo	3,889	3,929	3,731	3,772	3,824	3,811	3,830	3,923	3,770	3,851	3,792
Fe3	0,087	0,000	0,006	0,189	0,138	0,152	0,149	0,063	0,199	0,129	0,179
Cr	0,005	0,008	0,015	0,000	0,010	0,007	0,000	0,005	0,001	0,000	0,004
Ti	0,008	0,008	0,235	0,009	0,008	0,004	0,003	0,001	0,003	0,003	0,001
	3,995	3,969	3,988	3,984	3,991	3,987	3,993	3,996	3,989	3,993	3,989
Mg	0,690	0,613	0,788	0,653	0,695	0,907	0,879	0,869	0,870	0,857	0,930
Fe2	3,585	3,183	3,781	3,449	3,526	3,464	3,502	3,515	3,592	3,519	3,371
Mn	0,203	0,353	0,102	0,223	0,211	0,133	0,070	0,065	0,097	0,077	0,064
Ca	1,505	1,838	1,310	1,629	1,539	1,458	1,521	1,539	1,401	1,521	1,599
	5,982	5,987	5,981	5,955	5,971	5,963	5,972	5,988	5,960	5,975	5,964
sum	15,977	16,011	15,968	15,939	15,962	15,950	15,964	15,984	15,949	15,968	15,954

---

sample	Bk 39	Bk 39	Bk 39	Bk 39	Bk 39	Bk 39	Bk 39	Bk 39	Bk 39	Bk 39	Bk 39
analysis	14	15	18	2	5	7	8	12	13	14	56
date	23.3.92	23.3.92	23.3.92	24.6.92	24.6.92	24.6.92	24.6.92	24.6.92	24.6.92	24.6.92	24.6.92
position	cpx (i)	amph	cpx (i)	cpx (i)	amph	amph	cpx (i)	core	core	cpx (i)	cpx
SiO2	37,19	36,74	36,87	37,37	37,09	36,82	37,79	36,50	36,73	36,64	37,69
TiO2	0,05	0,05	0,03	0,04	0,01	0,04	0,05	0,06	0,03	0,05	0,06
Al2O3	21,35	21,18	21,26	21,23	21,04	21,16	21,56	20,73	21,19	21,19	21,34
Cr2O3	0,03	0,03	0,03	0,06	0,00	0,00	0,03	0,02	0,08	0,03	0,01
Fe2O3	1,29	1,26	1,61	1,17	1,30	1,43	0,87	1,30	1,18	1,54	0,91
FeO	27,84	26,81	26,60	25,24	27,18	29,50	26,00	29,53	29,27	29,28	25,24
MnO	0,93	0,56	0,55	0,32	0,70	0,69	0,35	1,04	0,62	0,75	0,46
MgO	4,69	3,60	3,86	4,81	3,70	3,28	4,96	2,36	3,70	3,52	4,93
CaO	6,42	8,66	8,71	8,74	8,18	6,97	8,26	7,44	6,55	6,75	8,60
total	99,79	98,90	99,52	98,98	99,20	99,89	99,87	98,98	99,36	99,74	99,24
normed to 24 oxygens, Fe3 over charge balance											
Si	5,859	5,851	5,825	5,890	5,888	5,847	5,907	5,879	5,854	5,822	5,920
Alt	0,141	0,149	0,175	0,110	0,112	0,153	0,093	0,121	0,146	0,178	0,080
Alo	3,823	3,827	3,783	3,833	3,824	3,808	3,879	3,814	3,834	3,791	3,871
Fe3	0,153	0,151	0,191	0,139	0,155	0,171	0,102	0,158	0,142	0,184	0,108
Cr	0,004	0,004	0,004	0,007	0,000	0,000	0,004	0,003	0,010	0,004	0,001
Ti	0,004	0,004	0,003	0,003	0,001	0,003	0,004	0,005	0,003	0,004	0,005
	3,997	3,998	3,996	3,993	3,992	3,997	3,997	3,994	4,001	3,999	3,993
Mg	1,101	0,855	0,909	1,130	0,875	0,776	1,156	0,567	0,879	0,834	1,154
Fe2	3,668	3,572	3,515	3,326	3,609	3,918	3,399	3,977	3,902	3,890	3,315
Mn	0,124	0,076	0,074	0,043	0,094	0,093	0,046	0,142	0,084	0,101	0,061
Ca	1,084	1,478	1,474	1,476	1,391	1,186	1,383	1,284	1,118	1,149	1,447
	5,977	5,979	5,971	5,975	5,970	5,973	5,984	5,970	5,983	5,974	5,978
sum	15,973	15,977	15,967	15,968	15,962	15,970	15,981	15,963	15,983	15,973	15,971

position means analysis of: core is core position in a grt grain, mineral x, rim position in grt grain in contact with mineral x, mineral x(i), grt at an inclusion of mineral x in grt

sample	Bk 39	Bk 39	Bk 39	Bk 39	Bk 39	Bk 39	Bk 39	Bk 39	Bk 39	Bk 39	Bk 39
analysis	57	58	4	5	7	8	12	18	19	20	23
date	24.6.92	24.6.92	28.1.93	28.1.93	28.1.93	28.1.93	28.1.93	28.1.93	28.1.93	28.1.93	28.1.93
position	cpx	cpx (i)	cpx (i)	cpx (i)	cpx (i)	cpx (i)	cpx (i)	cpx (i)	cpx (i)	cpx (i)	cpx (i)
SiO2	37,09	37,22	36,60	37,22	37,15	36,73	37,24	36,99	37,09	37,12	37,41
TiO2	0,03	0,04	0,05	0,10	0,03	0,08	0,00	0,19	0,21	0,25	0,05
Al2O3	20,99	21,11	20,88	20,83	21,10	20,99	20,99	21,19	21,40	21,17	21,35
Cr2O3	0,03	0,01	0,03	0,00	0,06	0,07	0,00	0,00	0,03	0,00	0,05
Fe2O3	1,35	0,87	0,78	1,87	1,40	1,86	1,52	1,27	1,60	1,15	1,70
FeO	26,19	24,97	28,00	26,73	27,73	27,51	27,37	27,00	26,56	27,50	27,04
MnO	0,53	0,36	1,29	1,42	1,03	0,96	0,94	0,72	0,62	0,74	0,68
MgO	3,56	4,44	2,00	2,78	3,65	3,93	3,85	4,59	5,25	3,51	5,04
CaO	9,29	9,14	8,93	9,37	7,71	7,42	7,75	7,17	7,02	8,30	7,01
total	99,06	98,16	98,56	100,33	99,86	99,56	99,65	99,12	99,78	99,74	100,33
normed to 24 oxygens, Fe3 over charge balance											
Si	5,885	5,920	5,912	5,866	5,872	5,818	5,885	5,860	5,815	5,875	5,839
Alt	0,115	0,080	0,088	0,134	0,128	0,182	0,115	0,140	0,185	0,125	0,161
Alo	3,811	3,878	3,887	3,735	3,803	3,736	3,794	3,816	3,770	3,825	3,766
Fe3	0,161	0,104	0,095	0,222	0,167	0,222	0,180	0,151	0,189	0,137	0,200
Cr	0,004	0,001	0,004	0,000	0,007	0,009	0,000	0,000	0,004	0,000	0,006
Ti	0,003	0,003	0,004	0,008	0,003	0,007	0,000	0,016	0,018	0,021	0,004
	3,991	3,994	3,998	3,983	3,993	3,992	3,989	3,995	3,995	3,994	3,992
Mg	0,842	1,053	0,482	0,653	0,860	0,928	0,907	1,084	1,227	0,828	1,173
Fe2	3,475	3,321	3,782	3,523	3,665	3,645	3,616	3,577	3,482	3,640	3,530
Mn	0,071	0,049	0,176	0,190	0,138	0,129	0,126	0,097	0,082	0,099	0,090
Ca	1,579	1,558	1,545	1,582	1,306	1,259	1,312	1,217	1,179	1,408	1,172
	5,968	5,980	5,985	5,948	5,969	5,961	5,961	5,974	5,971	5,974	5,964
sum	15,958	15,974	15,983	15,931	15,962	15,952	15,950	15,969	15,966	15,968	15,956

sample	Bk 39	Bk 39	Bk 39	Bk 39	Bk 39	Bk 39	Bk 39	Bk 39	Bk 39	Bk 39	Bk 39
analysis	32	53	54	58	59	62	65	68	1.49	1.50	1.51
date	28.1.93	28.1.93	28.1.93	28.1.93	28.1.93	28.1.93	28.1.93	28.1.93	28.8.92	28.8.92	28.8.92
position	cpx (i)	ab	ab	cpx	cpx	amph	core	core	cpx	cpx	cpx
SiO2	36,89	37,34	37,10	37,57	37,65	37,10	36,97	37,15	37,15	37,15	37,37
TiO2	0,17	0,06	0,00	0,08	0,26	0,13	0,04	0,01	0,02	0,06	0,04
Al2O3	20,76	21,19	20,95	21,32	21,24	21,01	20,83	20,84	21,44	21,25	21,44
Cr2O3	0,00	0,02	0,00	0,00	0,34	0,02	0,05	0,00	0,02	0,00	0,04
Fe2O3	2,14	1,84	1,75	2,04	1,54	1,14	1,55	1,65	1,42	1,63	0,81
FeO	26,15	26,24	25,74	25,96	25,06	24,69	27,30	27,17	26,36	25,82	26,14
MnO	1,84	0,50	0,55	0,45	0,39	0,37	1,50	1,24	0,51	0,49	0,48
MgO	2,45	3,63	3,47	5,37	5,05	4,77	2,67	3,02	4,19	3,76	3,75
CaO	9,84	9,62	9,83	7,73	8,96	8,87	8,79	8,71	8,68	9,64	9,41
total	100,23	100,44	99,40	100,52	100,49	98,10	99,69	99,80	99,78	99,80	99,48
normed to 24 oxygens, Fe3 over charge balance											
Si	5,829	5,841	5,862	5,827	5,846	5,896	5,877	5,883	5,840	5,841	5,899
Alt	0,171	0,159	0,138	0,173	0,154	0,104	0,123	0,117	0,160	0,159	0,101
Alo	3,694	3,747	3,763	3,724	3,733	3,831	3,779	3,772	3,813	3,779	3,887
Fe3	0,254	0,217	0,208	0,238	0,180	0,136	0,185	0,197	0,168	0,193	0,097
Cr	0,000	0,002	0,000	0,000	0,042	0,003	0,006	0,000	0,002	0,000	0,005
Ti	0,014	0,005	0,000	0,007	0,022	0,011	0,003	0,001	0,002	0,005	0,003
	3,983	3,988	3,987	3,986	3,990	3,991	3,989	3,986	3,997	3,992	3,999
Mg	0,577	0,846	0,817	1,241	1,169	1,130	0,633	0,713	0,982	0,881	0,882
Fe2	3,455	3,432	3,402	3,368	3,255	3,282	3,629	3,598	3,465	3,396	3,450
Mn	0,246	0,066	0,074	0,059	0,051	0,050	0,202	0,166	0,068	0,065	0,064
Ca	1,666	1,612	1,664	1,284	1,491	1,510	1,497	1,478	1,462	1,624	1,591
	5,944	5,957	5,957	5,952	5,965	5,972	5,961	5,955	5,977	5,966	5,988
sum	15,927	15,945	15,943	15,939	15,955	15,963	15,949	15,941	15,974	15,958	15,988

position means analysis of: core is core position in a grt grain, mineral x, rim position in grt grain in contact with mineral x, mineral x(i), grt at an inclusion of mineral x in grt

sample	Bk 39	Bk 39	Bk 39	Bk 39	Bk 39	Bk 39	Bk 39	Bk 39	Bk 39	Bk 39	Bk 39
analysis	1.52	1,1	1,2	2,1	4,1	5,1	6,1	7,1	8,1	9,1	10,1
date	28.8.92	4.5.92	4.5.92	4.5.92	4.5.92	4.5.92	4.5.92	4.5.92	4.5.92	4.5.92	4.5.92
position	cpx	cpx	cpx	cpx	cpx	cpx	cpx	cpx	cpx	cpx	cpx (i)
SiO2	37,13	37,19	37,11	37,46	37,61	37,72	37,79	37,48	37,64	37,48	36,98
TiO2	0,04	0,04	0,03	0,04	0,03	0,05	0,07	0,04	0,04	0,08	0,06
Al2O3	21,19	21,09	21,31	21,34	21,19	21,20	21,03	21,17	21,12	21,04	20,82
Cr2O3	0,00	0,01	0,06	0,04	0,01	0,02	0,02	0,07	0,02	0,01	0,09
Fe2O3	1,21	1,06	1,21	1,19	1,21	1,41	1,48	1,30	1,18	1,47	0,99
FeO	25,90	25,76	26,36	25,15	24,85	24,42	24,13	24,36	25,91	24,55	26,82
MnO	0,54	0,49	0,50	0,26	0,25	0,31	0,31	0,32	0,42	0,32	0,58
MgO	3,75	4,06	4,07	4,70	4,71	5,07	5,09	5,41	5,10	4,97	3,47
CaO	9,35	8,98	8,69	9,13	9,31	9,24	9,38	8,65	7,77	9,05	8,62
total	99,11	98,69	99,34	99,31	99,17	99,44	99,30	98,80	99,20	98,97	98,43
normed to 24 oxygens, Fe3 over charge balance											
Si	5,881	5,905	5,863	5,884	5,909	5,897	5,911	5,891	5,919	5,893	5,919
Alt	0,119	0,095	0,137	0,116	0,091	0,103	0,089	0,109	0,081	0,107	0,081
Alo	3,836	3,852	3,832	3,835	3,832	3,802	3,787	3,813	3,833	3,792	3,846
Fe3	0,144	0,127	0,144	0,140	0,143	0,166	0,174	0,154	0,140	0,174	0,120
Cr	0,000	0,001	0,007	0,005	0,001	0,002	0,002	0,009	0,002	0,001	0,011
Ti	0,003	0,003	0,003	0,003	0,003	0,004	0,006	0,003	0,003	0,007	0,005
	3,994	3,993	3,997	3,994	3,989	3,987	3,982	3,990	3,988	3,986	3,982
Mg	0,885	0,961	0,959	1,100	1,103	1,181	1,187	1,267	1,195	1,165	1,828
Fe2	3,431	3,421	3,483	3,304	3,265	3,193	3,156	3,202	3,407	3,228	3,589
Mn	0,072	0,066	0,067	0,035	0,033	0,041	0,041	0,043	0,056	0,043	0,079
Ca	1,587	1,528	1,471	1,537	1,567	1,548	1,572	1,457	1,309	1,525	1,478
	5,975	5,975	5,979	5,975	5,969	5,963	5,955	5,969	5,967	5,960	5,974
sum	15,969	15,968	15,977	15,969	15,958	15,949	15,938	15,959	15,956	15,946	15,966

---

sample	Bk 39	Bk 39	Bk 39	Bk 39	Bk 39	Bk 39	Bk 39	Bk 39	Bk 7	Bk 7	Bk 7
analysis	11,1	13,1	14,1	15,1	15,2	16,1	16,2	61	6	7	8
date	4.5.92	4.5.92	4.5.92	4.5.92	4.5.92	4.5.92	4.5.92	6.7.92	25.6.92	25.6.92	25.6.92
position	core	core	core	core	cpx	core	cpx	cpx	core	core	core
SiO2	36,36	36,61	36,77	36,37	37,48	36,79	37,85	37,38	36,99	37,15	37,52
TiO2	0,08	0,02	0,07	0,06	0,05	0,05	0,01	0,13	0,09	0,00	0,05
Al2O3	20,60	20,72	20,42	20,78	21,19	20,87	21,32	21,34	21,20	21,30	21,38
Cr2O3	0,00	0,03	0,00	0,00	0,01	0,00	0,00	0,04	0,00	0,04	0,04
Fe2O3	1,62	1,32	1,41	1,57	1,19	1,25	1,28	1,47	1,08	0,89	0,97
FeO	28,10	30,00	30,01	30,35	24,76	29,82	24,32	25,08	28,29	27,92	27,31
MnO	1,27	1,15	1,01	0,84	0,41	0,50	0,28	0,79	0,74	0,65	0,40
MgO	2,49	2,04	2,11	2,50	5,10	3,13	5,28	4,90	3,03	3,81	5,18
CaO	8,12	7,48	7,37	6,81	8,65	6,79	9,14	8,57	8,24	7,60	6,66
total	98,64	99,36	99,16	99,29	98,84	99,21	99,49	99,70	99,66	99,36	99,51
normed to 24 oxygens, Fe3 over charge balance											
Si	5,858	5,887	5,919	5,846	5,901	5,888	5,906	5,852	5,879	5,896	5,900
Alt	0,142	0,113	0,081	0,154	0,099	0,112	0,094	0,148	0,121	0,104	0,100
Alo	3,770	3,814	3,794	3,782	3,834	3,825	3,826	3,790	3,849	3,880	3,863
Fe3	0,196	0,159	0,170	0,190	0,141	0,151	0,151	0,173	0,129	0,106	0,115
Cr	0,000	0,004	0,000	0,000	0,001	0,000	0,000	0,005	0,000	0,005	0,005
Ti	0,007	0,002	0,006	0,005	0,004	0,004	0,001	0,011	0,008	0,000	0,004
	3,990	3,993	3,985	3,994	3,990	3,993	3,988	3,992	3,997	3,999	3,996
Mg	0,598	0,489	0,506	0,599	1,197	0,747	1,228	1,143	0,718	0,901	1,214
Fe2	3,787	4,034	4,040	4,080	3,260	3,991	3,174	3,283	3,759	3,705	3,591
Mn	0,173	0,157	0,138	0,114	0,055	0,068	0,037	0,105	0,100	0,087	0,053
Ca	1,402	1,289	1,271	1,173	1,459	1,164	1,528	1,438	1,403	1,292	1,122
	5,960	5,968	5,955	5,966	5,971	5,970	5,967	5,969	5,980	5,986	5,981
sum	15,950	15,961	15,940	15,960	15,961	15,964	15,955	15,961	15,977	15,986	15,977

position means analysis of: core is core position in a grt grain, mineral x, rim position in grt grain in contact with mineral x, mineral x(i), grt at an inclusion of mineral x in grt

sample	Bk 7	Bk 7	Bk 7	Bk 7	Bk 7	Bk 7	Bk 7	Bk 7	Bk 7	Bk 7	Bk 7
analysis	9	10	11	12	13	14	15	16	17	19	20
date	25.6.92	25.6.92	25.6.92	25.6.92	25.6.92	25.6.92	25.6.92	25.6.92	25.6.92	25.6.92	25.6.92
position	core	core	amph	cpx	cpx	cpx	cpx	cpx	ap (i)	ap (i)	cpx (i)
SiO2	37,24	37,65	37,62	37,83	38,33	38,35	37,90	37,87	37,77	37,14	37,57
TiO2	0,02	0,02	0,02	0,01	0,04	0,03	0,01	0,02	0,05	0,05	0,07
Al2O3	21,32	21,70	21,82	21,37	22,12	21,80	21,63	21,40	21,68	21,10	21,45
Cr2O3	0,40	0,03	0,01	0,00	0,13	0,02	0,01	0,00	0,02	0,01	0,00
Fe2O3	2,62	1,00	0,95	0,92	0,89	0,43	0,56	0,67	1,28	1,08	1,04
FeO	26,58	27,36	26,91	25,47	24,21	23,86	26,16	26,04	25,11	26,63	26,66
MnO	0,56	0,56	0,52	0,73	0,54	0,61	0,48	0,52	0,69	0,50	0,56
MgO	5,83	5,83	6,24	6,91	7,48	7,47	6,53	6,32	5,95	4,66	5,21
CaO	6,73	5,89	5,75	5,53	6,75	6,54	5,83	6,03	7,52	7,45	7,08
total	101,30	100,04	99,85	98,77	100,49	99,11	99,12	98,88	100,07	98,62	99,64
normed to 24 oxygens, Fe3 over charge balance											
Si	5,740	5,876	5,868	5,928	5,876	5,952	5,934	5,947	5,863	5,899	5,892
Alt	0,260	0,124	0,132	0,072	0,124	0,048	0,066	0,053	0,137	0,101	0,108
Alo	3,613	3,868	3,879	3,875	3,873	3,939	3,926	3,907	3,829	3,849	3,857
Fe3	0,304	0,118	0,112	0,109	0,103	0,051	0,067	0,080	0,149	0,129	0,123
Cr	0,049	0,004	0,001	0,000	0,016	0,002	0,001	0,000	0,002	0,001	0,000
Ti	0,002	0,002	0,002	0,001	0,003	0,003	0,001	0,002	0,004	0,004	0,006
	3,991	4,000	4,002	3,992	4,001	3,998	3,999	3,995	3,996	3,994	3,996
Mg	1,339	1,356	1,451	1,614	1,709	1,728	1,524	1,479	1,377	1,103	1,218
Fe2	3,427	3,571	3,510	3,338	3,104	3,097	3,426	3,420	3,259	3,537	3,497
Mn	0,073	0,074	0,069	0,097	0,070	0,080	0,064	0,069	0,091	0,067	0,074
Ca	1,111	0,985	0,961	0,928	1,109	1,087	0,978	1,015	1,251	1,268	1,190
	5,951	5,986	5,991	5,977	5,992	5,992	5,991	5,983	5,977	5,976	5,979
sum	15,942	15,986	15,993	15,969	15,993	15,991	15,990	15,978	15,973	15,969	15,975

sample	Bk 7	Bk 7	Bk 7	Bk 7	Bk 7	Bk 7	Bk 7	Bk 7	Bk 7	Bk 7	Bk 7
analysis	22	24	25	26	27	28	29	30	1	4	25
date	25.6.92	25.6.92	25.6.92	25.6.92	25.6.92	25.6.92	25.6.92	25.6.92	26.4.93	26.4.93	26.4.93
position	amph (i)	amph	amph (i)	amph	cpx	cpx	amph	core	cpx	cpx	phe (i)
SiO2	37,60	37,15	37,54	37,80	37,19	37,09	37,32	35,80	38,14	38,57	37,35
TiO2	0,05	0,03	0,08	0,03	0,05	0,06	0,06	0,06	0,05	0,00	0,05
Al2O3	21,37	21,25	21,46	21,45	21,13	21,08	21,15	21,02	21,99	21,99	21,33
Cr2O3	0,04	0,02	0,01	0,01	0,00	0,05	0,01	0,00	0,05	0,01	0,02
Fe2O3	1,17	0,77	1,12	1,03	1,16	0,89	1,04	1,98	0,67	0,55	0,92
FeO	27,52	28,28	26,96	28,72	29,48	28,88	28,05	26,37	26,11	24,78	25,91
MnO	0,57	0,33	0,57	0,43	0,38	0,57	0,59	0,74	0,77	0,57	0,55
MgO	4,52	4,86	5,05	4,59	3,62	3,50	3,46	3,87	6,50	7,07	4,26
CaO	7,38	6,03	7,09	6,55	6,84	7,17	8,06	8,12	6,14	6,69	8,76
total	100,22	98,73	99,88	100,60	99,85	99,29	99,73	97,96	100,42	100,22	99,15
normed to 24 oxygens, Fe3 over charge balance											
Si	5,890	5,910	5,882	5,908	5,893	5,910	5,908	5,754	5,900	5,939	5,901
Alt	0,110	0,090	0,118	0,092	0,107	0,090	0,092	0,246	0,100	0,061	0,099
Alo	3,836	3,894	3,845	3,860	3,840	3,869	3,854	3,736	3,909	3,930	3,872
Fe3	0,138	0,093	0,132	0,121	0,138	0,107	0,124	0,239	0,078	0,063	0,110
Cr	0,005	0,003	0,001	0,001	0,000	0,006	0,001	0,000	0,006	0,001	0,002
Ti	0,004	0,003	0,007	0,003	0,004	0,005	0,005	0,005	0,004	0,000	0,004
	3,994	3,999	3,996	3,994	3,994	3,996	3,994	3,999	4,002	3,999	3,997
Mg	1,055	1,152	1,179	1,069	0,855	0,831	0,816	0,927	1,499	1,623	1,003
Fe2	3,605	3,763	3,533	3,754	3,906	3,849	3,713	3,544	3,378	3,191	3,423
Mn	0,076	0,044	0,076	0,057	0,051	0,077	0,079	0,101	0,101	0,074	0,074
Ca	1,239	1,028	1,190	1,097	1,161	1,224	1,367	1,398	1,018	1,104	1,483
	5,975	5,987	5,978	5,977	5,974	5,981	5,975	5,970	5,995	5,991	5,983
sum	15,969	15,986	15,974	15,971	15,968	15,977	15,969	15,970	15,997	15,990	15,979

position means analysis of: core is core position in a grt grain, mineral x, rim position in grt grain in contact with mineral x, mineral x(i), grt at an inclusion of mineral x in grt

sample	Bk 7	Bk 7	Bk 7	Bk 7	Bk 7	Bk 7	Bk 7	Bk 7	Bk 7	Bk 7	Bk 7
analysis	27	28	39	43	44	65	2	3	4	5	12,1
date	26.4.93	26.4.93	26.4.93	26.4.93	26.4.93	26.4.93	27.8.91	27.8.91	27.8.91	27.8.91	4.5.92
position	phe (i)	amph (i)	cpx (i)	cpx (i)	cpx (i)	phe (i)	amph	amph	core	amph	core
SiO2	37,64	37,65	37,78	38,06	38,25	37,41	37,23	37,36	37,71	37,23	36,59
TiO2	0,06	0,11	0,21	0,14	0,04	0,04	0,06	0,00	0,04	0,10	0,09
Al2O3	21,25	21,41	21,40	21,39	21,66	21,32	21,71	21,84	21,96	21,11	20,47
Cr2O3	0,00	0,00	0,05	0,03	0,05	0,06	0,04	0,06	0,00	0,03	0,03
Fe2O3	1,19	0,89	1,02	0,79	0,48	1,31	1,04	0,52	1,32	1,75	1,77
FeO	24,88	24,83	24,56	24,64	24,82	25,93	26,20	26,10	25,58	24,88	28,68
MnO	1,13	1,08	0,70	0,67	0,76	0,71	0,56	0,85	0,72	0,92	1,10
MgO	4,62	4,60	4,85	4,99	6,26	4,47	5,65	6,10	6,10	4,06	2,14
CaO	8,78	8,92	9,24	9,03	7,23	8,50	6,87	6,07	7,10	9,62	8,38
total	99,55	99,49	99,80	99,74	99,55	99,75	99,35	98,90	100,53	99,70	99,25
normed to 24 oxygens, Fe3 over charge balance											
Si	5,905	5,911	5,901	5,941	5,954	5,872	5,845	5,883	5,830	5,847	5,871
Alt	0,095	0,089	0,099	0,059	0,046	0,128	0,155	0,117	0,170	0,153	0,129
Alo	3,834	3,873	3,840	3,877	3,928	3,816	3,862	3,935	3,832	3,754	3,742
Fe3	0,141	0,105	0,119	0,092	0,056	0,155	0,123	0,061	0,154	0,206	0,213
Cr	0,000	0,000	0,006	0,004	0,006	0,007	0,005	0,007	0,000	0,004	0,004
Ti	0,005	0,009	0,018	0,012	0,003	0,003	0,005	0,000	0,003	0,008	0,008
	3,990	3,994	3,992	3,991	3,997	3,994	4,004	4,009	4,000	3,988	3,985
Mg	1,080	1,076	1,129	1,161	1,452	1,046	1,322	1,432	1,406	0,950	0,512
Fe2	3,263	3,260	3,208	3,217	3,231	3,403	3,439	3,437	3,308	3,267	3,848
Mn	0,150	0,144	0,093	0,089	0,100	0,094	0,074	0,113	0,094	0,122	0,149
Ca	1,476	1,500	1,546	1,510	1,206	1,429	1,156	1,024	1,176	1,619	1,441
	5,970	5,981	5,976	5,977	5,990	5,973	5,992	6,006	5,984	5,959	5,950
sum	15,960	15,975	15,968	15,968	15,987	15,967	15,995	16,015	15,984	15,946	15,935

---

sample	Bk 7	Bk 7	k 7	Bk 7	Bk 7	Bk 7	Bk 7	Bk 7	Bk 7	Bk 7	Bk 7
analysis	21	22	24	26	27	28	29	31	36	38	46
date	6.7.92	6.7.92	6.7.92	6.7.92	6.7.92	6.7.92	6.7.92	6.7.92	6.7.92	6.7.92	6.7.92
position	core	cpx	amph	amph	core	core	ab	amph	amph	amph	cpx (i)
SiO2	37,33	38,21	37,98	37,28	36,90	36,67	37,93	36,51	37,10	37,16	36,75
TiO2	0,03	0,02	0,08	0,04	0,08	0,08	0,08	0,06	0,04	0,11	0,99
Al2O3	21,30	21,65	21,42	21,13	20,89	20,70	21,12	20,97	21,04	21,27	20,40
Cr2O3	0,04	0,01	0,03	0,00	0,02	0,02	0,00	0,03	0,03	0,02	0,00
Fe2O3	1,34	0,91	0,91	1,17	1,63	1,53	0,74	1,51	1,02	1,40	1,48
FeO	28,45	24,92	24,20	27,86	26,96	28,13	27,53	27,58	27,54	26,24	22,96
MnO	0,39	0,72	0,47	0,54	0,73	0,80	0,84	0,85	0,62	0,75	1,12
MgO	4,70	7,65	6,79	3,98	2,78	2,43	3,14	2,85	3,58	4,63	5,02
CaO	6,40	5,34	7,04	7,52	9,54	8,77	8,90	8,69	8,07	7,86	8,99
total	99,98	99,43	98,92	99,52	99,53	99,13	100,27	99,05	99,04	99,44	97,71
normed to 24 oxygens, Fe3 over charge balance											
Si	5,869	5,922	5,927	5,899	5,860	5,873	5,970	5,838	5,907	5,855	5,864
Alt	0,131	0,078	0,073	0,101	0,140	0,127	0,030	0,162	0,093	0,145	0,136
Alo	3,816	3,877	3,866	3,839	3,770	3,780	3,888	3,790	3,855	3,804	3,701
Fe3	0,158	0,106	0,107	0,139	0,195	0,185	0,087	0,182	0,123	0,165	0,178
Cr	0,005	0,001	0,004	0,000	0,003	0,003	0,000	0,004	0,004	0,002	0,000
Ti	0,003	0,002	0,007	0,003	0,007	0,007	0,007	0,005	0,003	0,009	0,085
	3,995	3,994	3,992	3,993	3,989	3,989	3,989	3,995	3,994	3,994	3,976
Mg	1,101	1,767	1,579	0,939	0,658	0,580	0,737	0,679	0,850	1,087	1,194
Fe2	3,741	3,231	3,158	3,686	3,581	3,767	3,624	3,688	3,667	3,458	3,063
Mn	0,052	0,095	0,062	0,072	0,098	0,109	0,112	0,115	0,084	0,100	0,151
Ca	1,078	0,887	1,177	1,275	1,623	1,505	1,501	1,489	1,377	1,327	1,537
	5,973	5,979	5,976	5,972	5,960	5,961	5,973	5,971	5,977	5,972	5,946
sum	15,967	15,973	15,968	15,965	15,949	15,950	15,962	15,966	15,971	15,966	15,922

position means analysis of: core is core position in a grt grain, mineral x, rim position in grt grain in contact with mineral x, mineral x(i), grt at an inclusion of mineral x in grt

sample	Bk 7	Bk 7	Bk 7	Bk 7	Bk 7	Bk 7	Bk 7	Bk 7	Bk 7	Bk 7	Bk 7
analysis	48	49	51	52	53	57	58	59	60	62	63
date	6.7.92	6.7.92	6.7.92	6.7.92	6.7.92	6.7.92	6.7.92	6.7.92	6.7.92	6.7.92	6.7.92
position	cpx (i)	cpx (i)	amph	gl (i)	amph (i)	cpx	core	core	core	core	qtz
SiO2	37,47	37,70	37,12	37,45	37,31	37,22	37,41	37,02	36,92	37,14	37,72
TiO2	0,10	0,07	0,03	0,04	0,05	0,02	0,09	0,09	0,10	0,12	0,03
Al2O3	21,21	21,36	21,34	21,40	21,29	21,32	21,11	21,10	21,12	21,17	21,52
Cr2O3	0,13	0,06	0,02	0,05	0,04	0,06	0,03	0,02	0,00	0,00	0,02
Fe2O3	1,08	1,00	0,96	0,88	1,13	0,86	1,26	1,64	1,42	1,44	0,88
FeO	24,30	24,94	27,70	25,74	25,19	28,13	25,71	26,12	26,11	25,71	24,59
MnO	1,04	0,95	0,43	0,80	0,79	0,45	1,35	1,69	1,20	0,79	0,58
MgO	5,08	4,82	4,81	4,53	4,87	4,58	3,82	3,08	3,66	4,23	6,32
CaO	8,58	8,67	6,59	8,42	8,31	6,58	8,89	9,25	8,72	8,72	7,21
total	99,00	99,57	99,00	99,31	98,98	99,22	99,68	100,00	99,25	99,32	98,87
normed to 24 oxygens, Fe3 over charge balance											
Si	5,897	5,909	5,884	5,902	5,884	5,898	5,896	5,845	5,855	5,861	5,908
Alt	0,103	0,091	0,116	0,098	0,116	0,102	0,104	0,155	0,145	0,139	0,092
Alo	3,831	3,854	3,871	3,876	3,842	3,880	3,817	3,771	3,802	3,798	3,881
Fe3	0,128	0,117	0,114	0,104	0,134	0,102	0,150	0,195	0,170	0,171	0,103
Cr	0,016	0,007	0,003	0,006	0,005	0,008	0,004	0,002	0,000	0,000	0,002
Ti	0,008	0,006	0,003	0,003	0,004	0,002	0,008	0,008	0,009	0,010	0,003
	3,993	3,993	3,999	3,997	3,995	3,999	3,990	3,991	3,993	3,992	3,996
Mg	1,192	1,126	1,136	1,064	1,145	1,082	0,897	0,725	0,865	0,995	1,475
Fe2	3,199	3,269	3,672	3,392	3,323	3,727	3,389	3,448	3,463	3,393	3,221
Mn	0,139	0,126	0,058	0,107	0,106	0,060	0,180	0,226	0,161	0,106	0,077
Ca	1,447	1,456	1,119	1,422	1,404	1,117	1,501	1,565	1,482	1,474	1,210
	5,976	5,977	5,986	5,985	5,978	5,987	5,968	5,964	5,971	5,968	5,984
sum	15,968	15,971	15,985	15,982	15,972	15,986	15,958	15,955	15,964	15,960	15,980

---

sample	Bk 7	Bk 7	Bk 7	Bk 7	Bk 7	Bk 7	Bk 7	Bk 7	Bk 7	Bk 7	Bk 7
analysis	65	66	67	8	9	19	22	23	25	26	30
date	6.7.92	6.7.92	6.7.92	7.7.92	7.7.92	7.7.92	7.7.92	7.7.92	7.7.92	7.7.92	7.7.92
position	cpx (i)	cpx	cpx	cpx	amph	amph	cpx (i)	cpx (i)	cpx (i)	cpx (i)	cpx (i)
SiO2	38,17	37,61	37,56	37,56	37,64	37,68	37,32	37,18	37,16	37,10	37,37
TiO2	0,00	0,02	0,01	0,03	0,03	0,02	0,02	0,04	0,05	0,01	0,01
Al2O3	21,16	21,34	21,40	21,60	21,61	21,68	21,55	21,56	21,22	21,50	21,39
Cr2O3	0,07	0,07	0,01	0,00	0,04	0,03	0,07	0,01	0,14	0,06	0,00
Fe2O3	0,89	1,10	0,75	1,04	0,91	0,66	0,95	1,26	1,05	1,42	0,95
FeO	27,35	26,24	25,76	24,79	24,45	25,26	26,51	26,70	25,31	25,30	25,76
MnO	0,69	0,80	0,53	0,58	0,56	0,59	0,63	0,52	0,55	0,72	0,58
MgO	4,56	5,83	6,26	6,00	6,41	6,03	6,32	5,75	5,26	5,19	5,24
CaO	7,40	6,34	6,20	7,52	7,26	7,11	5,54	6,29	7,76	7,98	7,53
total	100,29	99,35	98,48	99,12	98,91	99,07	98,90	99,31	98,51	99,28	98,84
normed to 24 oxygens, Fe3 over charge balance											
Si	5,967	5,899	5,922	5,879	5,890	5,907	5,873	5,842	5,882	5,829	5,897
Alt	0,033	0,101	0,078	0,121	0,110	0,093	0,127	0,158	0,118	0,171	0,103
Alo	3,866	3,844	3,899	3,864	3,876	3,912	3,870	3,835	3,840	3,811	3,875
Fe3	0,105	0,130	0,089	0,122	0,107	0,078	0,112	0,149	0,125	0,168	0,113
Cr	0,009	0,009	0,001	0,000	0,005	0,004	0,009	0,001	0,018	0,007	0,000
Ti	0,000	0,002	0,001	0,003	0,003	0,002	0,002	0,003	0,004	0,001	0,001
	3,987	3,994	3,997	3,998	3,998	4,001	4,001	4,000	3,997	3,999	3,997
Mg	1,063	1,363	1,471	1,400	1,495	1,409	1,482	1,347	1,241	1,215	1,232
Fe2	3,576	3,441	3,396	3,246	3,200	3,312	3,489	3,508	3,351	3,325	3,400
Mn	0,091	0,106	0,071	0,077	0,074	0,078	0,084	0,069	0,074	0,096	0,078
Ca	1,239	1,065	1,047	1,261	1,217	1,194	0,934	1,059	1,316	1,343	1,273
	5,969	5,976	5,986	5,984	5,987	5,994	5,989	5,983	5,981	5,980	5,983
sum	15,956	15,970	15,983	15,981	15,985	15,995	15,990	15,983	15,978	15,978	15,980

position means analysis of: core is core position in a grt grain, mineral x, rim position in grt grain in contact with mineral x, mineral x(i), grt at an inclusion of mineral x in grt

sample	Bk 7	Bk 7	Bk 7	Bk 7	Bk 7	Bk 7	Bk 7	Bk 7	Bk 7	Bk 7	Bk 7
analysis	31	33	34	35	36	37	47	48	51	61	73
date	7.7.92	7.7.92	7.7.92	7.7.92	7.7.92	7.7.92	7.7.92	7.7.92	7.7.92	7.7.92	7.7.92
position	cpx (i)	amph	ab	core	core	amph	cpx (i)	cpx (i)	cpx (i)	core	amph
SiO2	37,20	36,90	36,98	37,49	37,50	37,59	37,56	37,42	37,38	37,01	37,33
TiO2	0,00	0,06	0,15	0,05	0,07	0,04	0,06	0,10	0,03	0,14	0,03
Al2O3	21,43	21,26	21,23	21,54	21,29	21,44	21,29	21,21	21,23	21,15	21,18
Cr2O3	0,03	0,08	0,00	0,04	0,05	0,03	0,05	0,00	0,03	0,00	0,02
Fe2O3	1,31	1,22	1,63	1,13	1,61	0,87	0,27	1,38	1,18	1,42	0,95
FeO	25,54	25,85	24,78	23,41	24,07	26,75	24,17	24,34	26,84	24,52	26,67
MnO	0,63	0,70	0,92	0,80	0,87	0,52	1,85	0,99	1,36	0,99	0,63
MgO	5,35	4,44	4,16	4,91	5,25	5,99	2,87	4,00	4,75	3,60	4,20
CaO	7,59	8,29	9,48	9,92	8,86	5,91	10,90	10,10	6,74	10,29	8,07
total	99,08	98,80	99,32	99,29	99,57	99,15	99,03	99,54	99,54	99,12	99,07
normed to 24 oxygens, Fe3 over charge balance											
Si	5,853	5,852	5,829	5,870	5,856	5,907	5,966	5,879	5,892	5,855	5,913
Alt	0,147	0,148	0,171	0,130	0,144	0,093	0,034	0,121	0,108	0,145	0,087
Alo	3,827	3,826	3,773	3,845	3,775	3,879	3,952	3,807	3,836	3,799	3,868
Fe3	0,155	0,146	0,193	0,134	0,189	0,103	0,033	0,163	0,140	0,169	0,113
Cr	0,004	0,010	0,000	0,005	0,006	0,004	0,006	0,000	0,004	0,000	0,003
Ti	0,000	0,005	0,013	0,004	0,006	0,003	0,005	0,008	0,003	0,012	0,003
	3,997	3,998	3,992	3,997	3,989	3,997	3,999	3,990	3,993	3,992	3,994
Mg	1,255	1,050	0,977	1,146	1,222	1,403	0,680	0,937	1,116	0,849	0,992
Fe2	3,360	3,429	3,266	3,065	3,144	3,516	3,211	3,198	3,538	3,244	3,533
Mn	0,084	0,094	0,123	0,106	0,115	0,069	0,249	0,132	0,182	0,133	0,085
Ca	1,279	1,409	1,601	1,664	1,482	0,995	1,855	1,700	1,138	1,744	1,370
	5,979	5,981	5,967	5,981	5,964	5,984	5,995	5,967	5,974	5,970	5,979
sum	15,976	15,979	15,960	15,978	15,953	15,980	15,994	15,957	15,967	15,962	15,973

---

sample	Bk 8	Bk 8	Bk 8	Bk 8	Bk 8	Bk 8	Bk 8	Bk 8	Bk 8	Bk 8	Bk 8
analysis	30	31	32	33	34	35	51	52	53	54	55
date	14.3.93	14.3.93	14.3.93	14.3.93	14.3.93	14.3.93	14.3.93	14.3.93	14.3.93	14.3.93	14.3.93
position	amph	amph	cpx	cpx	cpx	cpx	amph	core	core	core	core
SiO2	38,18	37,84	37,84	37,77	37,91	38,11	38,38	37,90	37,24	37,36	37,11
TiO2	0,00	0,07	0,35	0,09	0,01	0,00	0,02	0,07	0,01	0,03	0,10
Al2O3	21,70	21,72	21,65	21,67	21,44	21,74	21,71	21,64	21,49	20,95	20,55
Cr2O3	0,00	0,00	0,00	0,00	0,03	0,00	0,00	0,02	0,03	0,01	0,01
Fe2O3	1,50	1,05	0,85	1,01	1,05	0,99	1,18	1,19	1,36	1,17	1,86
FeO	25,26	27,20	26,00	25,34	24,61	25,07	25,49	27,37	29,79	28,88	28,66
MnO	0,51	0,78	0,64	0,50	0,51	0,57	0,49	0,33	0,28	0,67	1,11
MgO	7,69	6,53	6,19	6,56	6,54	6,47	7,22	6,28	3,90	2,95	2,24
CaO	5,40	4,99	6,47	6,54	7,04	7,02	5,90	5,59	6,65	7,96	8,60
total	100,24	100,19	100,00	99,48	99,13	99,97	100,39	100,40	100,75	99,99	100,24
normed to 24 oxygens, Fe3 over charge balance											
Si	5,871	5,881	5,889	5,884	5,914	5,903	5,905	5,880	5,845	5,921	5,887
Alt	0,129	0,119	0,111	0,116	0,086	0,097	0,095	0,120	0,155	0,079	0,113
Alo	3,804	3,859	3,860	3,863	3,856	3,872	3,843	3,836	3,821	3,834	3,730
Fe3	0,174	0,123	0,100	0,118	0,123	0,115	0,137	0,140	0,160	0,140	0,222
Cr	0,000	0,000	0,000	0,000	0,004	0,000	0,000	0,002	0,004	0,001	0,001
Ti	0,000	0,006	0,029	0,008	0,001	0,000	0,002	0,006	0,001	0,003	0,009
	3,991	3,998	3,996	3,997	3,992	3,995	3,991	3,995	3,999	3,989	3,981
Mg	1,763	1,513	1,436	1,523	1,521	1,494	1,656	1,452	0,912	0,697	0,530
Fe2	3,248	3,536	3,384	3,302	3,210	3,247	3,279	3,552	3,910	3,828	3,802
Mn	0,066	0,103	0,084	0,066	0,067	0,075	0,064	0,043	0,037	0,090	0,149
Ca	0,890	0,831	1,079	1,092	1,177	1,165	0,973	0,929	1,118	1,352	1,462
	5,967	5,982	5,983	5,983	5,975	5,981	5,972	5,976	5,978	5,967	5,943
sum	15,957	15,980	15,979	15,980	15,967	15,976	15,963	15,971	15,978	15,956	15,923

position means analysis of: core is core position in a grt grain, mineral x, rim position in grt grain in contact with mineral x, mineral x(i), grt at an inclusion of mineral x in grt

sample	Bk 8	Bk 8	Bk 8	Bk 8	Bk 8	Bk 8	Bk 8	Bk 8	Bk 9	Bk 9	Bk 9
analysis	10	11	15	17	18	19	24	25	16	17	18
date	29.1.93	29.1.93	29.1.93	29.1.93	29.1.93	29.1.93	29.1.93	29.1.93	2.7.94	2.7.94	2.7.94
position	ap	cpx	core	core	core	cpx (i)	cpx (i)	core	amph	chl	core
SiO2	38,13	37,89	37,24	36,86	36,68	37,23	37,31	37,51	37,58	37,58	37,75
TiO2	0,01	0,00	0,07	0,19	0,28	0,00	0,13	0,12	0,05	0,10	0,10
Al2O3	22,02	22,03	21,13	20,78	20,97	21,27	21,18	21,24	21,31	20,89	20,77
Cr2O3	0,00	0,00	0,04	0,03	0,19	0,00	0,00	0,00	0,05	0,02	0,08
Fe2O3	1,17	1,29	1,62	1,19	1,71	1,61	1,38	1,48	0,98	1,25	1,03
FeO	25,01	24,70	25,70	26,85	27,31	25,04	25,38	24,54	27,81	24,33	20,46
MnO	0,40	0,55	1,46	0,70	1,15	1,52	1,53	1,19	0,68	2,74	6,01
MgO	8,24	8,12	3,82	3,05	2,91	3,71	3,42	4,58	4,04	1,69	2,54
CaO	5,02	5,23	8,86	9,06	8,87	9,54	9,60	9,09	7,62	11,75	10,95
total	100,00	99,81	99,94	98,71	100,07	99,91	99,93	99,75	100,12	100,35	99,69
normed to 24 oxygens, Fe3 over charge balance											
Si	5,863	5,839	5,856	5,897	5,810	5,849	5,874	5,872	5,909	5,929	5,965
Alt	0,137	0,161	0,144	0,103	0,190	0,151	0,126	0,128	0,091	0,071	0,035
Alo	3,853	3,840	3,772	3,816	3,725	3,788	3,804	3,792	3,859	3,814	3,833
Fe3	0,135	0,149	0,192	0,143	0,204	0,190	0,163	0,174	0,116	0,148	0,122
Cr	0,000	0,000	0,005	0,004	0,024	0,000	0,000	0,000	0,006	0,002	0,010
Ti	0,001	0,000	0,006	0,016	0,024	0,000	0,011	0,010	0,004	0,008	0,008
	3,998	4,000	3,989	3,990	3,993	3,992	3,990	3,988	3,995	3,984	3,981
Mg	1,888	1,865	0,895	0,727	0,687	0,869	0,803	1,069	0,947	0,397	0,598
Fe2	3,216	3,184	3,380	3,593	3,618	3,290	3,342	3,213	3,657	3,210	2,704
Mn	0,052	0,072	0,194	0,095	0,154	0,202	0,204	0,158	0,091	0,366	0,804
Ca	0,827	0,864	1,493	1,553	1,505	1,606	1,619	1,525	1,284	1,986	1,854
	5,983	5,984	5,963	5,968	5,965	5,967	5,968	5,964	5,978	5,960	5,961
sum	15,982	15,984	15,952	15,958	15,958	15,958	15,958	15,952	15,973	15,944	15,942

---

sample	Bk 9	Bk 9	Cig 90/40	Cig 90/40	Cig 90/40	Cig 90/40	Cig 90/40	Cig 90/40	Cig 90/40	Cig 90/40	Cig 90/40
analysis	19	20	46	47	48	49	50	56	57	1	2
date	2.7.94	2.7.94	1.6.91	1.6.91	1.6.91	1.6.91	1.6.91	1.6.91	1.6.91	1.6.91a	1.6.91a
position	core	chl	core	core	cpx	core	core	core	core	core	core
SiO2	37,83	38,33	37,08	37,09	37,37	36,82	36,94	37,74	37,21	37,00	37,24
TiO2	0,24	0,03	0,09	0,12	0,05	0,07	0,11	0,03	0,08	0,11	0,08
Al2O3	20,94	21,65	20,94	20,98	21,33	20,91	20,97	21,45	21,04	20,85	20,88
Cr2O3	0,07	0,02	0,01	0,00	0,02	0,00	0,02	0,03	0,00	0,05	0,04
Fe2O3	1,01	0,48	1,59	1,79	1,42	1,64	1,16	1,20	1,64	1,24	1,61
FeO	20,56	27,06	28,46	29,51	27,45	29,34	28,43	27,41	26,06	28,91	29,19
MnO	4,15	0,50	0,53	0,51	0,91	0,57	0,62	0,92	0,78	0,51	0,52
MgO	3,18	5,85	3,01	3,01	5,35	2,70	3,02	4,94	2,85	2,88	2,93
CaO	11,65	6,28	8,32	7,63	5,93	7,89	8,08	6,73	10,37	7,97	7,93
total	99,63	100,20	100,03	100,64	99,83	99,93	99,35	100,45	100,03	99,52	100,42
normed to 24 oxygens, Fe3 over charge balance											
Si	5,947	5,962	5,869	5,848	5,863	5,854	5,890	5,890	5,864	5,897	5,881
Alt	0,053	0,038	0,131	0,152	0,137	0,146	0,110	0,110	0,136	0,103	0,119
Alo	3,827	3,930	3,776	3,747	3,806	3,772	3,831	3,836	3,772	3,813	3,767
Fe3	0,119	0,057	0,189	0,213	0,167	0,196	0,139	0,141	0,195	0,149	0,192
Cr	0,009	0,002	0,001	0,000	0,002	0,000	0,003	0,004	0,000	0,006	0,005
Ti	0,020	0,003	0,008	0,010	0,004	0,006	0,009	0,003	0,007	0,009	0,007
	3,983	3,996	3,989	3,989	3,994	3,991	3,993	3,994	3,988	3,991	3,987
Mg	0,745	1,356	0,710	0,707	1,251	0,640	0,718	1,149	0,669	0,684	0,690
Fe2	2,703	3,519	3,768	3,891	3,602	3,901	3,791	3,578	3,435	3,853	3,855
Mn	0,553	0,066	0,071	0,068	0,121	0,077	0,084	0,122	0,104	0,069	0,070
Ca	1,962	1,047	1,411	1,289	0,997	1,344	1,380	1,125	1,751	1,361	1,342
	5,963	5,988	5,960	5,956	5,971	5,962	5,973	5,974	5,959	5,967	5,956
sum	15,946	15,984	15,949	15,944	15,964	15,953	15,966	15,968	15,947	15,958	15,943

position means analysis of: core is core position in a grt grain, mineral x, rim position in grt grain in contact with mineral x, mineral x(i), grt at an inclusion of mineral x in grt

sample	Cig 90/40	Cig 90/40	Cig 90/40	Cig 90/40	Cig 91-1	Cig 91-1	Cig 91-1	Cig 91-1	Cig 91-1	Cig 91-1	Cig 91-1
analysis	5	1	4	8	10	11	14	17	18	19	20
date	1.6.91a	1.6.91b	1.6.91b	1.6.91b	16.6.93	16.6.93	16.6.93	16.6.93	16.6.93	16.6.93	16.6.93
position	core	core	core	cpx	cpx	cpx	cz	gl	gl	biot	biot
SiO2	37,04	37,35	37,01	37,49	38,54	38,58	38,07	38,57	38,20	38,34	38,20
TiO2	0,10	0,09	0,09	0,03	0,01	0,02	0,05	0,04	0,05	0,06	0,01
Al2O3	20,84	21,02	20,92	21,18	21,92	21,93	21,60	21,71	21,53	21,63	21,73
Cr2O3	0,00	0,02	0,00	0,02	0,02	0,02	0,02	0,02	0,00	0,03	0,01
Fe2O3	1,50	1,01	1,46	1,16	0,82	0,90	1,12	1,21	1,49	0,78	1,34
FeO	29,04	29,14	27,89	27,25	26,25	26,02	25,04	26,63	26,83	27,86	27,97
MnO	0,52	0,53	0,59	0,74	0,35	0,29	1,26	0,36	0,32	0,44	0,49
MgO	3,01	2,92	3,37	5,42	7,70	7,83	5,69	7,12	6,83	5,94	6,02
CaO	7,75	7,93	8,12	5,98	4,87	4,97	7,52	5,37	5,41	5,68	5,61
total	99,80	100,01	99,46	99,28	100,48	100,56	100,37	101,03	100,66	100,76	101,37
normed to 24 oxygens, Fe3 over charge balance											
Si	5,884	5,922	5,877	5,906	5,922	5,917	5,901	5,912	5,887	5,938	5,881
Alt	0,116	0,078	0,123	0,094	0,078	0,083	0,099	0,088	0,113	0,062	0,119
Alo	3,785	3,850	3,793	3,838	3,891	3,880	3,846	3,834	3,798	3,887	3,824
Fe3	0,179	0,121	0,175	0,138	0,095	0,103	0,130	0,140	0,173	0,091	0,155
Cr	0,000	0,003	0,000	0,002	0,002	0,002	0,002	0,002	0,000	0,004	0,001
Ti	0,009	0,008	0,008	0,003	0,001	0,002	0,004	0,003	0,004	0,005	0,001
	3,988	3,992	3,990	3,992	3,996	3,995	3,993	3,990	3,988	3,994	3,993
Mg	0,713	0,690	0,798	1,273	1,763	1,790	1,315	1,627	1,569	1,371	1,381
Fe2	3,858	3,864	3,705	3,591	3,373	3,338	3,246	3,414	3,458	3,608	3,601
Mn	0,070	0,071	0,079	0,099	0,046	0,038	0,165	0,047	0,042	0,058	0,064
Ca	1,319	1,347	1,382	1,009	0,802	0,817	1,249	0,882	0,893	0,943	0,925
	5,960	5,972	5,963	5,971	5,984	5,982	5,975	5,969	5,962	5,980	5,971
sum	15,948	15,964	15,953	15,963	15,980	15,977	15,967	15,958	15,951	15,974	15,965

sample	Cig 91-1	Cig 91-1	Cig 91-1	Cig 91-1	Cig 91-1	Cig 91-1	Cig 91-1	Cig 91-1	Cig 91-1	Cig 91-1	Cig 91-1
analysis	21	22	24	25	26	27	28	29	38	39	40
date	16.6.93	16.6.93	16.6.93	16.6.93	16.6.93	16.6.93	16.6.93	16.6.93	16.6.93	16.6.93	16.6.93
position	biot	biot	qtz (i)	qtz (i)	gl	gl	gl	gl	biot	cpx (i)	biot
SiO2	38,22	38,33	38,24	38,12	38,77	38,90	38,84	38,97	39,42	39,10	39,31
TiO2	0,03	0,00	0,03	0,02	0,02	0,05	0,05	0,01	0,00	0,04	0,00
Al2O3	21,67	21,76	21,64	21,50	21,95	22,09	21,91	22,10	22,37	22,51	22,05
Cr2O3	0,02	0,00	0,00	0,00	0,00	0,02	0,00	0,05	0,03	0,00	0,05
Fe2O3	0,93	1,14	1,14	0,73	1,23	0,98	0,59	1,01	0,57	0,56	0,76
FeO	28,07	28,26	26,64	28,54	25,26	24,93	26,59	25,57	24,27	24,14	25,96
MnO	0,46	0,42	0,77	0,59	0,28	0,25	0,50	0,34	0,24	0,17	0,25
MgO	5,89	5,87	6,10	5,46	8,28	8,68	7,59	8,28	9,48	9,59	8,43
CaO	5,57	5,66	6,20	5,44	5,16	4,99	4,71	5,03	4,73	4,67	4,64
total	100,86	101,44	100,76	100,40	100,95	100,89	100,78	101,36	101,11	100,78	101,46
normed to 24 oxygens, Fe3 over charge balance											
Si	5,918	5,902	5,907	5,947	5,901	5,912	5,957	5,912	5,947	5,916	5,956
Alt	0,082	0,098	0,093	0,053	0,099	0,088	0,043	0,088	0,053	0,084	0,044
Alo	3,873	3,851	3,846	3,900	3,838	3,868	3,917	3,864	3,925	3,931	3,893
Fe3	0,108	0,133	0,133	0,086	0,141	0,112	0,068	0,115	0,064	0,064	0,087
Cr	0,002	0,000	0,000	0,000	0,000	0,002	0,000	0,006	0,004	0,000	0,006
Ti	0,002	0,000	0,002	0,002	0,002	0,004	0,004	0,001	0,000	0,003	0,000
	3,995	3,994	3,992	3,994	3,991	3,994	3,994	3,994	3,997	4,002	3,992
Mg	1,359	1,347	1,404	1,270	1,878	1,966	1,735	1,872	2,132	2,163	1,904
Fe2	3,635	3,639	3,442	3,724	3,216	3,168	3,410	3,245	3,062	3,054	3,290
Mn	0,060	0,055	0,101	0,078	0,036	0,032	0,065	0,044	0,031	0,022	0,032
Ca	0,924	0,934	1,026	0,909	0,841	0,812	0,774	0,818	0,765	0,757	0,753
	5,979	5,975	5,973	5,981	5,971	5,979	5,984	5,979	5,989	5,996	5,979
sum	15,974	15,969	15,965	15,975	15,962	15,973	15,979	15,972	15,986	15,998	15,970

position means analysis of: core is core position in a grt grain, mineral x, rim position in grt grain in contact with mineral x, mineral x(i), grt at an inclusion of mineral x in grt

sample	Cig 91-1	Cig 91-1	Cig 91-1	Cig 91-1	Cig 91-1	Cig 91-1	Cig 91-1	Cig 91-1	Cig 91-1	Cig 91-1	Cig 91-1
analysis	41	42	43	44	45	46	47	48	49	48	49
date	16.6.93	16.6.93	16.6.93	16.6.93	16.6.93	16.6.93	16.6.93	16.6.93	16.6.93	17.6.93	17.6.93
position	biot	biot	biot	cpx (i)	core	cpx (i)	biot	biot	biot	biot	biot
SiO2	38,83	38,75	38,60	38,86	38,86	39,05	38,74	38,59	38,96	38,93	38,97
TiO2	0,04	0,04	0,02	0,02	0,07	0,25	0,01	0,02	0,01	0,01	0,03
Al2O3	21,96	22,20	21,99	22,23	21,89	22,13	21,88	21,93	21,94	22,18	22,14
Cr2O3	0,00	0,03	0,02	0,02	0,02	0,03	0,01	0,06	0,00	0,00	0,00
Fe2O3	1,02	0,90	0,99	1,04	1,07	0,70	1,39	1,26	0,51	0,74	1,00
FeO	25,57	25,43	26,57	25,17	27,05	24,83	26,15	26,28	25,91	24,42	24,73
MnO	0,24	0,39	0,63	0,32	0,25	0,22	0,21	0,22	0,28	0,24	0,23
MgO	8,41	8,33	7,07	8,88	7,30	8,89	7,86	7,74	7,87	8,91	8,90
CaO	4,74	4,96	5,42	4,57	5,12	4,87	5,09	5,10	5,07	5,06	4,92
total	100,81	101,03	101,31	101,10	101,64	100,97	101,34	101,20	100,55	100,49	100,92
normed to 24 oxygens, Fe3 over charge balance											
Si	5,919	5,898	5,905	5,893	5,920	5,927	5,894	5,886	5,969	5,926	5,911
Alt	0,081	0,102	0,095	0,107	0,080	0,073	0,106	0,114	0,031	0,074	0,089
Alo	3,864	3,881	3,869	3,866	3,850	3,885	3,817	3,829	3,931	3,905	3,869
Fe3	0,117	0,103	0,114	0,118	0,123	0,080	0,159	0,145	0,059	0,085	0,114
Cr	0,000	0,004	0,002	0,002	0,002	0,004	0,001	0,007	0,000	0,000	0,000
Ti	0,003	0,003	0,002	0,002	0,006	0,020	0,001	0,002	0,001	0,001	0,002
	3,992	3,998	3,996	3,996	3,991	3,994	3,990	3,993	3,994	3,997	3,994
Mg	1,911	1,890	1,612	2,007	1,658	2,011	1,782	1,760	1,797	2,022	2,012
Fe2	3,260	3,237	3,399	3,191	3,447	3,152	3,328	3,352	3,320	3,109	3,137
Mn	0,031	0,050	0,082	0,041	0,032	0,028	0,027	0,028	0,036	0,031	0,030
Ca	0,774	0,809	0,888	0,742	0,836	0,792	0,830	0,834	0,832	0,825	0,800
	5,976	5,986	5,981	5,982	5,972	5,983	5,967	5,974	5,985	5,986	5,979
sum	15,968	15,984	15,976	15,978	15,963	15,978	15,956	15,967	15,980	15,983	15,972

sample	Cig 91-1	Cig 91-1	Cig 91-1	Cig 91-1	Cig 91-1	Cig 91-1	Cig 91-1	Cig 91-1	Cig 91-1	Cig 91-1	Cig 91-1
analysis	50	51	52	53	54	59	60	61	62	63	67
date	17.6.93	17.6.93	17.6.93	17.6.93	17.6.93	17.6.93	17.6.93	17.6.93	17.6.93	17.6.93	17.6.93
position	biot	biot	biot	core	core	core	core	core	core	core	phe(i)
SiO2	39,18	38,82	38,62	38,24	38,83	37,94	38,13	38,25	38,33	38,50	38,29
TiO2	0,13	0,00	0,11	0,03	0,00	0,12	0,04	0,07	0,08	0,07	0,01
Al2O3	22,33	21,87	21,90	21,45	21,59	21,08	21,14	21,19	21,37	21,22	21,48
Cr2O3	0,28	0,00	0,00	0,00	0,02	0,05	0,02	0,04	0,00	0,03	0,00
Fe2O3	0,45	0,92	0,49	1,24	1,13	1,20	1,38	1,16	1,60	1,34	1,48
FeO	25,22	25,45	26,99	27,24	26,14	26,03	25,79	25,11	25,54	25,06	27,09
MnO	0,26	0,34	0,60	0,44	0,30	1,41	1,14	1,20	0,95	0,88	0,83
MgO	8,80	8,25	6,81	6,27	7,64	4,48	5,04	5,28	5,99	5,78	5,27
CaO	4,89	4,86	5,27	5,65	5,08	7,92	7,71	7,90	7,08	7,70	6,97
total	101,53	100,51	100,79	100,55	100,73	100,23	100,39	100,21	100,94	100,58	101,42
normed to 24 oxygens, Fe3 over charge balance											
Si	5,924	5,937	5,950	5,918	5,947	5,932	5,929	5,945	5,900	5,943	5,900
Alt	0,076	0,063	0,050	0,082	0,053	0,068	0,071	0,055	0,100	0,057	0,100
Alo	3,903	3,878	3,926	3,830	3,843	3,817	3,803	3,827	3,777	3,804	3,801
Fe3	0,051	0,106	0,057	0,144	0,130	0,141	0,162	0,136	0,185	0,156	0,171
Cr	0,033	0,000	0,000	0,000	0,002	0,006	0,002	0,005	0,000	0,004	0,000
Ti	0,011	0,000	0,009	0,002	0,000	0,010	0,003	0,006	0,007	0,006	0,001
	4,002	3,992	3,997	3,988	3,986	3,985	3,983	3,984	3,983	3,981	3,987
Mg	1,983	1,881	1,564	1,446	1,744	1,044	1,168	1,223	1,374	1,330	1,210
Fe2	3,189	3,255	3,477	3,525	3,348	3,404	3,353	3,264	3,288	3,236	3,491
Mn	0,033	0,044	0,078	0,058	0,039	0,187	0,150	0,158	0,124	0,115	0,108
Ca	0,792	0,796	0,870	0,937	0,834	1,327	1,285	1,316	1,168	1,274	1,151
	5,997	5,976	5,989	5,966	5,964	5,961	5,956	5,961	5,954	5,954	5,960
sum	15,999	15,968	15,986	15,954	15,950	15,946	15,939	15,945	15,937	15,935	15,947

position means analysis of: core is core position in a grt grain, mineral x, rim position in grt grain in contact with mineral x, mineral x(i), grt at an inclusion of mineral x in grt

sample	Cig 91-1	Cig 91-1	Cig 91-1	Cig 91-1	Cig 91-1	Cig 91-1
analysis	83	84	85	86	87	5
date	17.6.93	17.6.93	17.6.93	17.6.93	17.6.93	28.11.93
position	biot	biot	core	core	core	core
SiO2	38,84	38,68	38,41	38,29	38,22	38,82
TiO2	0,01	0,04	0,03	0,04	0,14	0,33
Al2O3	22,01	21,86	21,84	21,20	21,50	21,91
Cr2O3	0,00	0,04	0,00	0,00	0,01	0,01
Fe2O3	0,98	1,16	1,12	1,54	0,71	0,47
FeO	25,79	25,79	28,57	26,14	28,07	26,01
MnO	0,18	0,27	0,34	1,13	1,27	0,33
MgO	8,20	7,98	6,15	5,25	4,96	7,91
CaO	4,93	5,06	5,19	7,32	6,05	4,88
total	100,94	100,88	101,65	100,91	100,93	100,67
normed to 24 oxygens, Fe3 over charge balance						
Si	5,919	5,907	5,899	5,921	5,947	5,950
Alt	0,081	0,093	0,101	0,079	0,053	0,050
Alo	3,873	3,841	3,852	3,785	3,890	3,908
Fe3	0,112	0,133	0,129	0,180	0,083	0,054
Cr	0,000	0,005	0,000	0,000	0,001	0,001
Ti	0,001	0,003	0,002	0,003	0,012	0,027
	3,993	3,991	3,994	3,981	3,993	3,994
Mg	1,863	1,816	1,408	1,210	1,150	1,807
Fe2	3,287	3,294	3,670	3,381	3,653	3,334
Mn	0,023	0,035	0,044	0,148	0,167	0,043
Ca	0,805	0,828	0,854	1,213	1,009	0,801
	5,978	5,973	5,976	5,952	5,979	5,985
sum	15,971	15,964	15,971	15,933	15,972	15,980

position means analysis of: core is core position in a grt grain, mineral x, rim position in grt grain in contact with mineral x, mineral x(i), grt at an inclusion of mineral x in grt

sample	Bk 39	Bk 39	Bk 39	Bk 39	Bk 39	Bk 39	Bk 39	Bk 39	Bk 39	Bk 7	Bk 7
analyse	27	28	39	41	44	44	45	1	2	43	44
date	24.6.92	24.6.92	24.6.92	24.6.92	27.8.92	3.7.94	3.7.94	5.5.92	5.5.92	2.7.94	2.7.94
position	core	core	core	core	rim	core	core	core	core	core	core
SiO2	56,29	55,93	56,10	56,72	58,17	57,58	56,91	55,49	56,68	57,61	57,37
TiO2	0,05	0,02	0,03	0,05	0,03	0,06	0,04	0,02	0,04	0,02	0,02
Al2O3	11,31	11,28	11,24	11,64	11,58	11,54	11,41	11,04	11,41	11,71	11,90
Cr2O3	0,04	0,04	0,02	0,07	0,00	0,00	0,00	0,00	0,02	0,07	0,02
Fe2O3	2,08	2,67	2,72	3,88	1,84	3,30	1,94	0,69	1,39	1,35	2,20
FeO	7,98	7,48	7,04	5,45	6,87	6,80	7,72	9,87	8,75	6,25	5,96
MnO	0,07	0,03	0,07	0,07	0,04	0,00	0,04	0,09	0,02	0,02	0,00
MgO	10,36	10,42	10,50	10,93	11,19	10,98	10,39	9,80	10,18	11,72	11,38
CaO	1,33	1,22	1,04	1,00	1,19	1,24	1,10	1,60	1,17	1,45	1,29
ZnO	n.a	n.a	n.a	n.a	0,12	0,10	0,10	n.a	n.a	0,17	0,29
Na2O	6,85	6,88	6,87	6,60	6,88	6,92	6,84	6,95	7,09	6,91	6,84
K2O	0,02	0,03	0,02	0,02	0,03	0,03	0,04	0,04	0,01	0,03	0,03
H2O	2,15	2,15	2,15	2,18	2,21	2,21	2,17	2,12	2,16	2,20	2,20
total	98,53	98,14	97,80	98,60	100,15	100,76	98,69	97,71	98,92	99,50	99,50
normed on 23 oxygen, Fe3 over Si+Ti+Al+Fe+Mn+Mg+Ca+Zn = 15											
Si	7,833	7,811	7,840	7,815	7,896	7,812	7,880	7,844	7,862	7,856	7,831
Alt	0,167	0,189	0,160	0,185	0,104	0,188	0,120	0,156	0,138	0,144	0,169
	8,000	8,000	8,000	8,000	8,000	8,000	8,000	8,000	8,000	8,000	8,000
Alo	1,688	1,668	1,691	1,706	1,749	1,657	1,742	1,683	1,728	1,739	1,745
Fe3	0,218	0,281	0,286	0,402	0,188	0,337	0,202	0,074	0,145	0,138	0,226
Cr	0,004	0,004	0,002	0,008	0,000	0,000	0,000	0,000	0,002	0,008	0,002
Ti	0,004	0,001	0,002	0,004	0,002	0,004	0,003	0,002	0,003	0,001	0,001
Mg	2,149	2,169	2,187	2,245	2,264	2,220	2,144	2,065	2,105	2,382	2,315
Fe2	0,928	0,873	0,823	0,628	0,780	0,772	0,894	1,166	1,015	0,712	0,681
Mn	0,008	0,004	0,008	0,008	0,005	0,000	0,005	0,011	0,002	0,002	0,000
Zn	-	-	-	-	0,012	0,010	0,010	-	-	0,017	0,029
	5,000	5,000	5,000	5,000	5,000	5,000	5,000	5,000	5,000	5,000	5,000
Ca	0,198	0,183	0,156	0,148	0,173	0,180	0,163	0,242	0,174	0,212	0,189
Na	1,802	1,817	1,844	1,763	1,811	1,820	1,836	1,758	1,826	1,788	1,810
	2,000	2,000	2,000	2,000	2,000	2,000	2,000	2,000	2,000	2,000	2,000
Na	0,047	0,045	0,017	0,000	0,000	0,000	0,000	0,147	0,081	0,039	0,000
K	0,004	0,005	0,004	0,004	0,005	0,005	0,007	0,007	0,002	0,005	0,005
	0,050	0,051	0,021	0,004	0,005	0,006	0,007	0,154	0,083	0,044	0,005
sum	15,050	15,051	15,021	15,004	15,005	15,006	15,007	15,154	15,083	15,044	15,005
OH	2	2	2	2	2	2	2	2	2	2	2

position means analysis of: core is core position in a gln grain, rim is rim position in a gln grain

sample	Bk 7	Bk 7	Bk 7	Bk 7	Bk 7	Bk 7	Bk 7	Bk 7	Bk 7	Bk 7	Bk 8
analyse	45	14	19	23	24	25	29	31	44	46	14
date	2.7.94	26.4.93	7.8.92	7.8.92	7.8.92	7.8.92	7.8.92	7.8.92	7.8.92	7.8.92	29.1.93b
position	core	rim	core	rim	core	rim	rim	rim	core	core	core
SiO2	56,68	57,15	57,13	56,06	56,84	55,95	55,26	56,57	55,83	56,90	57,50
TiO2	0,03	0,08	0,00	0,03	0,04	0,02	0,07	0,03	0,02	0,00	0,15
Al2O3	11,87	11,72	11,82	11,70	11,66	11,74	11,62	11,86	11,86	11,81	11,72
Cr2O3	0,07	0,12	0,01	0,00	0,00	0,00	0,00	0,01	0,03	0,04	0,00
Fe2O3	2,84	1,30	1,96	2,02	2,40	2,47	2,14	2,99	3,55	2,95	2,69
FeO	6,69	6,45	5,93	7,22	6,83	7,52	7,00	6,13	6,66	5,70	4,32
MnO	0,00	0,06	0,00	0,05	0,05	0,03	0,07	0,08	0,09	0,03	0,00
MgO	10,80	11,49	11,18	10,54	10,78	10,39	11,08	10,73	10,57	11,19	12,08
CaO	1,24	1,54	0,91	1,40	1,37	1,57	2,39	1,28	1,66	1,24	0,69
ZnO	0,26	0,19	0,23	0,24	0,23	0,28	0,17	0,23	0,21	0,20	0,19
Na2O	6,97	6,81	6,95	6,76	6,69	6,73	6,31	6,55	6,57	6,70	7,16
K2O	0,03	0,04	0,03	0,04	0,04	0,05	0,05	0,03	0,06	0,04	0,05
H2O	2,19	2,19	2,18	2,15	2,18	2,16	2,15	2,17	2,17	2,18	2,20
total	99,66	99,14	98,33	98,22	99,11	98,91	98,31	98,66	99,29	98,98	98,74
normed on 23 oxygen, Fe3 over Si+Ti+Al+Fe+Mn+Mg+Ca+Zn = 15											
Si	7,776	7,838	7,872	7,807	7,827	7,766	7,711	7,809	7,715	7,812	7,854
Alt	0,224	0,162	0,128	0,193	0,173	0,234	0,289	0,191	0,285	0,188	0,146
	8,000	8,000	8,000	8,000	8,000	8,000	8,000	8,000	8,000	8,000	8,000
Alo	1,695	1,732	1,792	1,727	1,720	1,686	1,622	1,738	1,647	1,723	1,741
Fe3	0,293	0,135	0,204	0,212	0,249	0,258	0,225	0,311	0,369	0,305	0,277
Cr	0,008	0,013	0,001	0,000	0,000	0,000	0,000	0,001	0,003	0,004	0,000
Ti	0,002	0,006	0,000	0,002	0,003	0,001	0,005	0,002	0,001	0,000	0,011
Mg	2,208	2,349	2,296	2,188	2,213	2,149	2,305	2,208	2,177	2,290	2,459
Fe2	0,767	0,739	0,684	0,841	0,786	0,873	0,817	0,707	0,770	0,654	0,493
Mn	0,000	0,007	0,000	0,006	0,006	0,004	0,008	0,009	0,011	0,003	0,000
Zn	0,026	0,019	0,023	0,025	0,023	0,029	0,018	0,023	0,021	0,020	0,019
	5,000	5,000	5,000	5,000	5,000	5,000	5,000	5,000	5,000	5,000	5,000
Ca	0,182	0,226	0,134	0,209	0,202	0,233	0,357	0,189	0,246	0,182	0,101
Na	1,818	1,774	1,857	1,791	1,786	1,767	1,643	1,753	1,754	1,784	1,896
	2,000	2,000	2,000	2,000	2,000	2,000	2,000	2,000	2,000	2,000	2,000
Na	0,036	0,037	0,000	0,034	0,000	0,045	0,065	0,000	0,006	0,000	0,000
K	0,005	0,007	0,005	0,007	0,007	0,009	0,009	0,005	0,011	0,007	0,009
	0,042	0,044	0,005	0,041	0,007	0,054	0,074	0,005	0,017	0,007	0,009
sum	15,042	15,044	15,005	15,041	15,007	15,054	15,074	15,005	15,017	15,007	15,009
OH	2	2	2	2	2	2	2	2	2	2	2

sample	Bk 8	Bk 8	Bk 8	Bk 8	Bk 9	Bk 9	Bk 9	Bk 9	Bk 9	Bk 9	Bk 9
analyse	15	17	18	20	6	7	10	11	4	1	2
date	29.1.93b	29.1.93b	29.1.93b	29.1.93b	2.7.94	2.7.94	2.7.94	2.7.94	23.2.94	23.2.94a	23.2.94a
position	rim	rim	core	rim	core	core	core	core	rim	rim	rim
SiO2	57,15	56,63	56,86	57,05	57,70	57,66	56,25	57,35	57,78	58,20	58,01
TiO2	0,03	0,03	0,02	0,03	0,04	0,05	0,05	0,01	0,02	0,02	0,07
Al2O3	11,81	11,59	11,92	11,63	11,46	11,66	10,82	11,73	11,80	12,01	11,56
Cr2O3	0,00	0,03	0,04	0,03	0,00	0,14	0,02	0,02	0,05	0,03	0,03
Fe2O3	2,40	2,61	1,58	2,80	2,38	2,12	2,31	3,60	2,36	2,32	2,48
FeO	5,75	7,02	6,60	6,72	5,77	6,00	6,71	4,64	5,23	5,18	5,22
MnO	0,04	0,08	0,01	0,01	0,05	0,06	0,05	0,00	0,02	0,05	0,01
MgO	11,51	10,35	10,91	10,56	11,57	11,40	11,88	11,85	11,48	11,55	11,59
CaO	1,36	1,07	0,87	0,89	1,40	1,30	3,04	1,14	1,06	1,04	1,09
ZnO	0,21	0,26	0,30	0,22	0,07	0,15	0,12	0,06	0,17	0,16	0,17
Na2O	6,80	6,74	7,17	6,89	6,52	6,70	5,83	6,78	6,57	6,62	6,54
K2O	0,05	0,06	0,06	0,04	0,04	0,02	0,07	0,05	0,04	0,03	0,03
H2O	2,19	2,16	2,17	2,18	2,20	2,20	2,17	2,20	2,19	2,21	2,20
total	99,30	98,63	98,52	99,05	99,19	99,46	99,33	99,43	98,77	99,42	99,00
normed on 23 oxygen, Fe3 over Si+Ti+Al+Fe+Mn+Mg+Ca+Zn = 15											
Si	7,817	7,845	7,850	7,854	7,880	7,864	7,759	7,807	7,895	7,894	7,909
Alt	0,183	0,155	0,150	0,146	0,120	0,136	0,241	0,193	0,105	0,106	0,091
	8,000	8,000	8,000	8,000	8,000	8,000	8,000	8,000	8,000	8,000	8,000
Alo	1,721	1,737	1,790	1,740	1,724	1,738	1,518	1,689	1,795	1,813	1,767
Fe3	0,247	0,272	0,165	0,290	0,244	0,217	0,240	0,368	0,243	0,237	0,254
Cr	0,000	0,003	0,004	0,003	0,000	0,015	0,002	0,002	0,005	0,003	0,003
Ti	0,002	0,002	0,001	0,002	0,004	0,005	0,005	0,001	0,002	0,002	0,007
Mg	2,347	2,137	2,245	2,167	2,355	2,317	2,443	2,404	2,338	2,335	2,355
Fe2	0,657	0,813	0,763	0,774	0,659	0,685	0,774	0,529	0,597	0,587	0,595
Mn	0,005	0,009	0,001	0,001	0,006	0,007	0,006	0,000	0,002	0,006	0,001
Zn	0,021	0,027	0,031	0,022	0,007	0,015	0,012	0,006	0,017	0,016	0,017
	5,000	5,000	5,000	5,000	5,000	5,000	5,000	5,000	5,000	5,000	5,000
Ca	0,199	0,159	0,129	0,131	0,205	0,190	0,449	0,166	0,155	0,151	0,159
Na	1,801	1,810	1,871	1,839	1,726	1,772	1,551	1,790	1,741	1,741	1,729
	2,000	2,000	2,000	2,000	1,931	1,962	2,000	1,956	1,896	1,892	1,888
Na	0,003	0,000	0,048	0,000	0,000	0,000	0,008	0,000	0,000	0,000	0,000
K	0,009	0,011	0,011	0,007	0,007	0,004	0,013	0,009	0,007	0,005	0,005
	0,012	0,011	0,059	0,007	0,007	0,004	0,021	0,009	0,007	0,005	0,005
sum	15,012	15,011	15,059	15,007	14,938	14,965	15,021	14,965	14,903	14,897	14,893
OH	2	2	2	2	2	2	2	2	2	2	2

sample	Bk 9	Bk 9	Cig 91-1	Cig 91-1	Cig 91-1	Cig 91-1	Cig 91-1	Cig 91-1
analyse	3	4	70	71	72	79	81	88
date	23.2.94a	23.2.94a	17.6.93	17.6.93	17.6.93	17.6.93	17.6.93	17.6.93
position	rim	rim	rim	rim	core	rim	rim	rim
SiO2	55,97	57,06	58,27	57,87	58,47	57,40	58,35	58,86
TiO2	0,03	0,02	0,01	0,01	0,01	0,07	0,02	0,18
Al2O3	11,20	11,35	11,65	11,66	11,75	11,74	11,81	11,57
Cr2O3	0,02	0,01	0,00	0,00	0,02	0,02	0,02	0,01
Fe2O3	5,46	2,73	1,39	1,27	1,12	1,38	1,42	1,32
FeO	3,89	5,56	6,94	8,10	7,54	8,58	6,58	6,46
MnO	0,06	0,01	0,05	0,00	0,04	0,00	0,03	0,02
MgO	11,79	11,82	11,16	10,51	10,79	10,20	11,31	11,59
CaO	1,97	1,88	0,92	0,88	0,64	1,05	0,77	0,64
ZnO	0,20	0,17	0,08	0,05	0,07	0,05	0,01	0,01
Na2O	5,85	6,36	7,08	7,15	7,27	7,06	7,16	7,32
K2O	0,21	0,06	0,03	0,03	0,03	0,04	0,05	0,02
H2O	2,18	2,19	2,20	2,19	2,21	2,19	2,21	2,22
total	98,84	99,22	99,78	99,73	99,96	99,77	99,74	100,21
normed on 23 oxygen, Fe3 over Si+Ti+Al+Fe+Mn+Mg+Ca+Zn = 15								
Si	7,712	7,815	7,925	7,914	7,946	7,876	7,921	7,947
Alt	0,288	0,185	0,075	0,086	0,054	0,124	0,079	0,053
	8,000	8,000	8,000	8,000	8,000	8,000	8,000	8,000
Alo	1,531	1,647	1,792	1,794	1,828	1,775	1,811	1,788
Fe3	0,566	0,282	0,142	0,131	0,115	0,143	0,145	0,134
Cr	0,002	0,001	0,000	0,000	0,002	0,002	0,002	0,001
Ti	0,003	0,002	0,001	0,001	0,001	0,005	0,001	0,013
Mg	2,421	2,413	2,262	2,142	2,186	2,086	2,289	2,332
Fe2	0,449	0,637	0,790	0,927	0,857	0,984	0,747	0,729
Mn	0,007	0,001	0,006	0,000	0,005	0,000	0,003	0,002
Zn	0,020	0,017	0,008	0,005	0,007	0,005	0,001	0,001
	5,000	5,000	5,000	5,000	5,000	5,000	5,000	5,000
Ca	0,291	0,276	0,134	0,129	0,093	0,154	0,112	0,093
Na	1,563	1,689	1,866	1,871	1,907	1,846	1,885	1,907
	1,854	1,965	2,000	2,000	2,000	2,000	2,000	2,000
Na	0,000	0,000	0,001	0,025	0,009	0,033	0,000	0,009
K	0,038	0,011	0,005	0,005	0,005	0,007	0,009	0,004
	0,038	0,011	0,006	0,030	0,014	0,040	0,009	0,012
sum	14,891	14,975	15,006	15,030	15,014	15,040	15,009	15,012
OH	2	2	2	2	2	2	2	2

position means analysis of: core is core position in a gln grain, rim is rim position in a gln grain

---

sample	Bk 10B	Bk 10B	Bk 10B	Bk 10B	Bk 10B	Bk 10B	Bk 10B	Bk 10B	Bk 10B	Bk 10B	Bk 10B
analysis	26	27	28	11	12	13	14	15	20	21	22
date	18.10.93	18.10.93	18.10.93	19.10.93a	19.10.93a	19.10.93a	19.10.93a	19.10.93a	19.10.93a	19.10.93a	19.10.93a
position	sympl	core	core	sympl	sympl	core	sympl	clz	sympl	core	clz
SiO2	38,60	39,19	39,15	37,80	37,91	38,08	37,63	38,34	38,06	38,27	38,40
Al2O3	25,52	29,13	29,21	26,21	28,46	28,09	26,04	29,48	26,81	27,62	28,17
Fe2O3	10,97	5,98	5,79	9,25	5,68	6,69	9,74	5,47	8,35	7,71	7,00
CaO	23,44	24,07	24,03	23,03	23,34	23,94	23,72	24,34	23,69	23,95	24,28
H2O	1,91	1,95	1,94	1,88	1,89	1,91	1,89	1,94	1,90	1,92	1,93
Total	98,53	98,37	98,18	96,29	95,39	96,80	97,13	97,63	96,91	97,55	97,85
normed on 8 kations, all iron assumed to be Fe3											
Si	3,026	3,020	3,021	3,014	3,011	2,990	2,979	2,970	3,005	2,993	2,986
Al	2,358	2,646	2,656	2,463	2,664	2,600	2,429	2,691	2,495	2,546	2,582
Fe3	0,647	0,347	0,336	0,555	0,339	0,395	0,580	0,319	0,496	0,454	0,410
	3,005	2,992	2,993	3,018	3,003	2,995	3,009	3,010	2,991	3,000	2,991
Ca	1,969	1,987	1,987	1,968	1,986	2,014	2,012	2,020	2,004	2,007	2,023
OH	1,000	1,000	1,000	1,000	1,000	1,000	1,000	1,000	1,000	1,000	1,000
XAl2Fe	0,644	0,349	0,339	0,545	0,338	0,397	0,575	0,316	0,501	0,454	0,413

position means analysis of: i(x), inclusion of czo in mineral x, core is core position in a czox grain, mineral x, rim position in czo grain in contact with mineral x, mineral x(i), czo at an inclusion of mineral x in czo

sample	Bk 10B	Bk 10B	Bk 10B	Bk 10B	Bk 10B	Bk 10B	Bk 10B	Bk 17	Bk 17	Bk 17	Bk 17
analysis	23	24	25	26	27	28	29	9	10	11	12
date	19.10.93a	19.10.93a	19.10.93a	19.10.93a	19.10.93a	19.10.93a	19.10.93a	25.7.94	25.7.94	25.7.94	25.7.94
position	core	amph	amph	core	core	clz	sympl	ab	clz	core	sympl
SiO2	38,44	38,80	38,26	38,54	38,28	38,34	38,48	37,77	38,27	38,10	38,19
Al2O3	28,92	25,62	27,48	29,12	27,65	28,86	28,29	25,83	27,59	26,18	26,18
Fe2O3	5,41	11,17	7,80	5,62	7,48	5,49	5,76	10,28	8,05	10,04	9,71
CaO	23,32	23,05	24,09	23,99	24,11	23,86	24,15	23,47	23,78	23,49	23,53
H2O	1,90	1,91	1,92	1,93	1,92	1,91	1,91	1,89	1,92	1,91	1,90
Total	96,09	98,64	97,63	97,27	97,52	96,55	96,68	97,35	97,69	97,81	97,61
normed on 8 kations, all iron assumed to be Fe3											
Si	3,027	3,040	2,991	2,999	2,993	3,006	3,017	2,989	2,992	2,998	3,008
Al	2,684	2,366	2,532	2,671	2,548	2,666	2,614	2,409	2,542	2,428	2,430
Fe3	0,321	0,659	0,459	0,329	0,440	0,324	0,340	0,612	0,473	0,594	0,576
	3,005	3,025	2,991	3,000	2,988	2,990	2,954	3,021	3,016	3,022	3,006
Ca	1,968	1,935	2,018	2,000	2,020	2,004	2,029	1,990	1,992	1,980	1,986
OH	1,000	1,000	1,000	1,000	1,000	1,000	1,000	1,000	1,000	1,000	1,000
XAl2Fe	0,319	0,643	0,463	0,329	0,445	0,327	0,356	0,599	0,466	0,581	0,572

sample	Bk 17	Bk 17	Bk 17	Bk 17	Bk 17	Bk 17	Bk 17	Bk 17	Bk 18	Bk 18	Bk 18
analysis	13	25	26	27	38	39	40	46	61	62	19
date	25.7.94	9.7.94	9.7.94	9.7.94	9.7.94	9.7.94	9.7.94	9.7.94	25.7.94	25.7.94	5.8.94
position	core	clz	ab	sympl	ab	clz	sympl	core	sympl	core	core
SiO2	37,94	38,09	37,57	37,78	37,89	38,89	38,47	38,16	38,16	37,99	38,17
Al2O3	27,30	25,65	24,84	25,36	25,47	26,75	25,25	27,00	29,35	28,97	27,50
Fe2O3	7,89	10,55	11,36	10,91	10,95	10,06	11,45	8,57	5,32	5,87	8,11
CaO	23,79	23,69	23,46	23,55	23,33	24,20	23,68	23,79	23,88	23,64	23,95
H2O	1,90	1,90	1,88	1,89	1,90	1,95	1,92	1,91	1,92	1,91	1,92
Total	96,92	97,98	97,23	97,60	97,64	99,90	98,85	97,52	96,71	96,47	97,73
normed on 8 kations, all iron assumed to be Fe3											
Si	2,989	2,998	2,990	2,989	2,997	2,994	3,011	2,995	2,983	2,983	2,984
Al	2,535	2,379	2,330	2,365	2,374	2,427	2,329	2,498	2,704	2,681	2,533
Fe3	0,468	0,625	0,680	0,650	0,652	0,583	0,674	0,506	0,313	0,347	0,477
	3,003	3,004	3,010	3,015	3,026	3,010	3,003	3,004	3,017	3,028	3,011
Ca	2,008	1,998	2,000	1,996	1,977	1,996	1,986	2,001	2,000	1,989	2,006
OH	1,000	1,000	1,000	1,000	1,000	1,000	1,000	1,000	1,000	1,000	1,000
XAl2Fe	0,467	0,622	0,673	0,640	0,635	0,577	0,672	0,504	0,308	0,337	0,472

sample	Bk 18	Bk 18	Bk 18	Bk 18	Bk 39	Bk 39	Bk 39	Bk 39	Bk 39	Bk 39	Bk 39
analysis	22	23	24	10	2	3	4	5	6	7	8
date	5.8.94	5.8.94	5.8.94	6.8.94	13.3.93	13.3.93	13.3.93	13.3.93	13.3.93	13.3.93	13.3.93
position	amph	core	par	rut	clz	sympl	core	clz	clz	clz	clz
SiO2	37,92	38,22	38,14	38,71	37,52	37,96	37,87	37,94	37,98	38,09	37,83
Al2O3	27,18	27,22	27,08	27,69	26,20	27,01	26,89	26,55	26,42	27,26	28,89
Fe2O3	8,76	8,46	8,60	8,36	9,21	8,17	8,41	8,86	9,01	8,45	5,76
CaO	23,75	23,77	23,76	23,59	24,18	24,00	23,59	23,83	23,73	23,62	23,26
H2O	1,91	1,91	1,91	1,93	1,90	1,90	1,90	1,90	1,90	1,91	1,90
Total	97,61	97,67	97,58	98,35	97,11	97,14	96,76	97,18	97,14	97,42	95,74
normed on 8 kations, all iron assumed to be Fe3											
Si	2,974	2,994	2,992	3,009	2,965	2,987	2,995	2,992	2,999	2,991	2,993
Al	2,513	2,513	2,504	2,537	2,440	2,505	2,506	2,468	2,458	2,523	2,693
Fe3	0,517	0,499	0,508	0,489	0,548	0,484	0,501	0,526	0,535	0,499	0,343
	3,030	3,011	3,011	3,026	2,988	2,989	3,007	2,994	2,994	3,022	3,036
Ca	1,996	1,995	1,997	1,965	2,047	2,024	1,999	2,014	2,007	1,987	1,971
OH	1,000	1,000	1,000	1,000	1,000	1,000	1,000	1,000	1,000	1,000	1,000
XAl2Fe	0,502	0,493	0,502	0,477	0,555	0,489	0,49	0,529	0,539	0,488	0,331

position means analysis of: i(x), inclusion of czo in mineral x, core is core position in a czo grain, mineral x, rim position in czo grain in contact with mineral x, mineral x(i), czo at an inclusion of mineral x in czo

sample	Bk 39	Bk 39	Bk 39	Bk 39	Bk 39	Bk 39	Bk 39	Bk 39	Bk 39	Bk 39	Bk 39
analysis	9	10	12	13	15	16	17	18	19	20	21
date	13.3.93	13.3.93	13.3.93	13.3.93	13.3.93	13.3.93	13.3.93	13.3.93	13.3.93	13.3.93	13.3.93
position	clz	clz	sympl	core	clz	clz	par	par	par	par	clz
SiO2	38,36	37,92	37,82	38,24	37,84	38,22	37,91	38,08	37,94	37,92	38,24
Al2O3	30,24	28,48	27,15	28,40	26,97	27,21	27,55	27,63	27,35	27,19	29,13
Fe2O3	4,69	6,29	8,24	6,51	8,76	8,42	7,70	7,79	8,41	8,27	5,68
CaO	24,05	23,73	23,76	23,63	23,64	24,04	23,71	23,93	23,99	23,74	23,81
H2O	1,94	1,90	1,90	1,91	1,90	1,92	1,90	1,91	1,92	1,90	1,92
Total	97,34	96,42	96,97	96,78	97,21	97,89	96,87	97,43	97,69	97,12	96,86
normed on 8 kations, all iron assumed to be Fe3											
Si	2,971	2,985	2,982	3,001	2,981	2,986	2,986	2,982	2,970	2,985	2,989
Al	2,760	2,642	2,523	2,627	2,504	2,506	2,557	2,550	2,523	2,523	2,683
Fe3	0,273	0,373	0,489	0,385	0,519	0,495	0,456	0,459	0,496	0,490	0,334
	3,034	3,014	3,011	3,012	3,023	3,001	3,014	3,010	3,019	3,013	3,017
Ca	1,996	2,001	2,007	1,987	1,995	2,013	2,001	2,008	2,012	2,002	1,994
OH	1,000	1,000	1,000	1,000	1,000	1,000	1,000	1,000	1,000	1,000	1,000
XAl2Fe	0,264	0,367	0,483	0,380	0,507	0,495	0,450	0,455	0,486	0,484	0,328

sample	Bk 39	Bk 39	Bk 39	Bk 39	Bk 39	Bk 39	Bk 39	Bk 39	Bk 39	Bk 39	Bk 39
analysis	22	23	24	9	17	20	21	22	35	36	42
date	13.3.93	13.3.93	13.3.93	24.6.92	24.6.92	24.6.92	24.6.92	24.6.92	24.6.92	24.6.92	24.6.92
position	clz	sympl	sympl	i (grt)	i (grt)	par	clz	core	par	clz	sympl
SiO2	38,21	38,28	38,03	37,31	37,96	37,25	37,28	37,51	37,75	38,02	37,17
Al2O3	29,00	28,15	27,16	28,94	28,42	26,47	27,77	26,57	27,42	28,83	25,86
Fe2O3	6,03	7,61	8,76	6,36	7,33	9,10	7,40	8,68	7,48	5,73	9,48
CaO	23,95	23,63	23,47	23,29	23,49	23,66	23,51	23,90	23,82	23,75	23,77
H2O	1,92	1,92	1,91	1,90	1,91	1,89	1,89	1,89	1,90	1,91	1,88
Total	97,19	97,67	97,42	95,90	97,20	96,48	95,96	96,66	96,47	96,33	96,28
normed on 8 kations, all iron assumed to be Fe3											
Si	2,980	2,988	2,989	2,951	2,973	2,961	2,960	2,972	2,984	2,989	2,966
Al	2,665	2,589	2,516	2,697	2,623	2,480	2,598	2,481	2,554	2,671	2,432
Fe3	0,354	0,447	0,518	0,378	0,432	0,544	0,442	0,518	0,445	0,339	0,569
	3,019	3,036	3,034	3,076	3,056	3,024	3,041	2,999	2,999	3,011	3,001
Ca	2,001	1,976	1,977	1,973	1,971	2,015	2,000	2,029	2,017	2,000	2,032
OH	1,000	1,000	1,000	1,000	1,000	1,000	1,000	1,000	1,000	1,000	1,000
XAl2Fe	0,347	0,431	0,501	0,352	0,409	0,532	0,425	0,518	0,445	0,336	0,568

sample	Bk 39	Bk 39	Bk 39	Bk 39	Bk 39	Bk 39	Bk 39	Bk 39	Bk 39	Bk 39	Bk 39
analysis	44	45	46	47	48	1	2	17	19	5,2	6,2
date	24.6.92	24.6.92	24.6.92	24.6.92	24.6.92	28.1.93	28.1.93	28.8.92	28.8.92	5.5.92	5.5.92
position	core	cpx	core	clz	par	i (grt)	i (grt)	cpx	cpx	cpx	core
SiO2	37,91	37,52	37,56	37,64	37,50	37,43	38,36	37,92	37,68	37,75	37,64
Al2O3	29,39	26,76	26,87	27,91	26,90	27,40	29,85	28,73	28,55	28,60	26,34
Fe2O3	5,46	8,81	8,62	6,91	8,39	7,86	4,63	6,89	7,22	5,69	8,75
CaO	23,97	23,75	23,47	23,74	23,57	23,12	23,46	23,92	24,21	23,90	23,79
H2O	1,92	1,90	1,89	1,90	1,89	1,88	1,91	1,92	1,92	1,90	1,89
Total	96,73	96,84	96,52	96,20	96,36	95,81	96,30	97,46	97,66	95,94	96,52
normed on 8 kations, all iron assumed to be Fe3											
Si	2,964	2,968	2,979	2,976	2,977	2,982	3,004	2,957	2,935	2,980	2,989
Al	2,708	2,495	2,512	2,601	2,517	2,573	2,755	2,640	2,621	2,661	2,465
Fe3	0,321	0,525	0,515	0,411	0,501	0,471	0,273	0,404	0,423	0,338	0,523
	3,029	3,019	3,026	3,012	3,018	3,044	3,028	3,045	3,044	2,999	2,987
Ca	2,008	2,013	1,994	2,011	2,005	1,974	1,968	1,998	2,021	2,021	2,024
OH	1,000	1,000	1,000	1,000	1,000	1,000	1,000	1,000	1,000	1,000	1,000
XAl2Fe	0,312	0,515	0,501	0,406	0,492	0,451	0,266	0,387	0,405	0,338	0,529

position means analysis of: i(x), inclusion of czo in mineral x, core is core position in a czo grain, mineral x, rim position in czo grain in contact with mineral x, mineral x(i), czo at an inclusion of mineral x in czo

sample	Bk 39	Bk 4	Bk 4	Bk 4	Bk 4	Bk 4	Bk 4	Bk 4	Bk 4	Bk 4	Bk 7
analysis	7,2	54	55	56	58	59	60	61	62	63	67
date	5.5.92	9.7.94	9.7.94	9.7.94	9.7.94	9.7.94	9.7.94	9.7.94	9.7.94	9.7.94	26.4.93
position	sympl	vein	vein	vein	vein	vein	vein	vein	vein	vein	i (grt)
SiO2	37,61	38,37	38,50	38,45	38,53	38,85	38,33	38,15	38,40	38,52	38,02
Al2O3	26,13	28,52	28,25	28,04	27,89	28,75	28,35	28,42	28,58	27,93	28,51
Fe2O3	8,48	6,33	6,81	7,45	6,99	6,50	6,48	5,93	6,35	6,98	6,93
CaO	23,94	23,87	24,10	23,83	24,01	23,80	23,62	23,76	23,65	23,85	23,52
H2O	1,88	1,92	1,93	1,92	1,92	1,93	1,91	1,90	1,92	1,92	1,91
Total	96,16	97,09	97,66	97,77	97,42	97,90	96,78	96,26	96,98	97,28	96,98
normed on 8 kations, all iron assumed to be Fe3											
Si	2,996	3,000	2,998	2,997	3,011	3,014	3,008	3,005	3,006	3,014	2,981
Al	2,453	2,628	2,592	2,576	2,568	2,629	2,623	2,638	2,637	2,576	2,634
Fe3	0,508	0,373	0,399	0,437	0,411	0,380	0,383	0,352	0,374	0,411	0,409
	2,961	3,001	2,992	3,013	2,979	3,008	3,005	2,990	3,011	2,987	3,044
Ca	2,043	2,000	2,011	1,990	2,010	1,978	1,986	2,005	1,984	1,999	1,976
OH	1,000	1,000	1,000	1,000	1,000	1,000	1,000	1,000	1,000	1,000	1,000
XAl2Fe	0,529	0,372	0,403	0,431	0,420	0,376	0,381	0,355	0,370	0,417	0,392

sample	Bk 7	Bk 7	Bk 7	Bk 7	Bk 7	Bk 7	Bk 7	Bk 7	Bk 7	Bk 7	Bk 7
analysis	68	69	70	9	10	11	12	13	14	20	21
date	26.4.93	26.4.93	26.4.93	27.8.92	27.8.92	27.8.92	27.8.92	27.8.92	27.8.92	27.8.92	27.8.92
position	i (grt)	i (grt)	i (grt)	amph	ap	cpx	core	cpx	par	par	par
SiO2	37,92	37,60	37,64	37,60	37,71	37,37	37,46	37,83	37,59	37,47	37,65
Al2O3	27,71	27,38	27,09	28,15	27,84	27,92	28,33	28,65	27,65	28,22	27,50
Fe2O3	7,45	8,20	8,76	6,81	6,99	7,12	6,48	6,06	7,28	6,67	7,91
CaO	23,23	23,51	23,35	23,99	23,47	23,52	23,81	24,37	23,59	23,64	24,07
H2O	1,89	1,90	1,90	1,90	1,89	1,89	1,90	1,92	1,89	1,89	1,91
Total	96,31	96,69	96,84	96,55	96,01	95,93	96,08	96,91	96,11	96,00	97,13
normed on 8 kations, all iron assumed to be Fe3											
Si	3,001	2,971	2,976	2,960	2,989	2,965	2,960	2,959	2,979	2,966	2,959
Al	2,585	2,550	2,525	2,612	2,601	2,611	2,639	2,641	2,583	2,632	2,547
Fe3	0,444	0,488	0,521	0,404	0,417	0,425	0,385	0,357	0,434	0,397	0,468
	3,029	3,038	3,046	3,016	3,018	3,036	3,024	2,998	3,017	3,030	3,015
Ca	1,970	1,991	1,978	2,024	1,993	1,999	2,016	2,043	2,003	2,005	2,027
OH	1,000	1,000	1,000	1,000	1,000	1,000	1,000	1,000	1,000	1,000	1,000
XAl2Fe	0,431	0,470	0,498	0,397	0,410	0,411	0,376	0,357	0,427	0,386	0,461

sample	Bk 7	Bk 7	Bk 7	Bk 7	Bk 7	Bk 7	Bk 7	Bk 7	Bk 8	Bk 8	Bk 8
analysis	22	14	15	16	17	52	53	54	2	3	4
date	27.8.92	7.7.92	7.7.92	7.7.92	7.7.92	7.7.92	7.7.92	7.7.92	14.3.93	14.3.93	14.3.93
position	cpx	ab	ab	clz	par	par	par	gnt	core	par	core
SiO2	37,50	37,28	37,46	37,51	37,00	37,23	37,38	37,66	38,42	37,87	38,13
Al2O3	28,12	27,56	27,31	27,82	28,63	26,79	27,19	27,33	28,57	27,98	28,49
Fe2O3	7,13	7,36	7,92	6,99	6,32	7,98	8,11	7,82	6,16	7,01	6,71
CaO	23,82	23,97	23,65	23,91	23,56	23,70	23,82	23,91	23,71	23,78	23,23
H2O	1,90	1,89	1,89	1,90	1,89	1,88	1,89	1,90	1,91	1,90	1,90
Total	96,57	96,17	96,34	96,23	95,51	95,70	96,50	96,72	96,86	96,64	96,56
normed on 8 kations, all iron assumed to be Fe3											
Si	2,955	2,953	2,969	2,966	2,938	2,972	2,959	2,972	3,010	2,982	3,001
Al	2,611	2,573	2,551	2,593	2,679	2,521	2,537	2,542	2,638	2,597	2,643
Fe3	0,423	0,439	0,473	0,416	0,378	0,479	0,483	0,465	0,363	0,416	0,398
	3,034	3,012	3,023	3,008	3,057	3,000	3,020	3,006	3,001	3,012	3,040
Ca	2,011	2,035	2,008	2,026	2,005	2,027	2,020	2,022	1,990	2,006	1,959
OH	1,000	1,000	1,000	1,000	1,000	1,000	1,000	1,000	1,000	1,000	1,000
XAl2Fe	0,409	0,433	0,462	0,412	0,357	0,479	0,474	0,462	0,363	0,411	0,382

position means analysis of: i(x), inclusion of czo in mineral x, core is core position in a czo grain, mineral x, rim position in czo grain in contact with mineral x, mineral x(i), czo at an inclusion of mineral x in czo

sample	Bk 8	Bk 8	Bk 8	Bk 8	Bk 8	Bk 8	Bk 8	Bk 9	Bk 9	Bk 9	Bk 9
analysis	5	8	9	10	11	21	22	1	2	3	28
date	14.3.93	14.3.93	14.3.93	14.3.93	14.3.93	14.3.93	14.3.93	2.7.94	2.7.94	2.7.94	2.7.94
position	clz	clz	par	clz	sympl	par	zoi	par	core	par	zoi
SiO2	37,67	38,10	37,83	38,04	37,75	38,12	38,25	38,14	38,50	38,16	38,15
Al2O3	27,48	27,65	28,26	28,02	27,07	29,38	29,41	27,60	29,25	27,66	28,16
Fe2O3	7,48	7,79	6,56	7,05	7,86	5,15	4,93	7,31	5,15	7,36	6,83
CaO	23,63	23,69	23,55	23,65	23,49	23,81	24,10	23,92	24,17	23,70	23,72
H2O	1,89	1,91	1,90	1,91	1,89	1,91	1,92	1,91	1,93	1,91	1,91
Total	96,26	97,23	96,20	96,76	96,17	96,46	96,69	96,97	97,07	96,88	96,86
normed on 8 kations, all iron assumed to be Fe3											
Si	2,984	2,990	2,987	2,992	2,998	2,986	2,987	2,997	2,998	3,002	2,995
Al	2,565	2,558	2,630	2,598	2,534	2,712	2,707	2,556	2,684	2,565	2,606
Fe3	0,446	0,460	0,390	0,417	0,470	0,303	0,290	0,432	0,301	0,436	0,404
	3,011	3,018	3,020	3,015	3,003	3,016	2,997	2,989	2,986	3,000	3,009
Ca	2,005	1,992	1,993	1,993	1,999	1,998	2,016	2,014	2,016	1,998	1,995
OH	1,000	1,000	1,000	1,000	1,000	1,000	1,000	1,000	1,000	1,000	1,000
XAl2Fe	0,441	0,452	0,382	0,411	0,468	0,299	0,291	0,437	0,306	0,435	0,400

sample	Bk 9	Bk 9	Bk 9	Bk 9	Bk 9	Bk 9	Bk 9	Bk 9	Bk 9	Bk 9	Bk 9
analysis	29	30	31	16	17	18	19	21	22	23	24
date	2.7.94	2.7.94	2.7.94	23.2.94	23.2.94	23.2.94	23.2.94	23.2.94	23.2.94	23.2.94	23.2.94
position	par	clz	sympl	par	core	core	amph	amph	ab	par	par
SiO2	38,32	38,67	37,67	38,04	37,96	38,39	38,48	38,22	38,22	37,96	38,12
Al2O3	26,66	29,67	25,57	27,56	27,59	29,93	29,16	29,07	28,91	27,29	28,75
Fe2O3	8,92	5,22	10,31	8,58	8,96	5,82	6,46	7,09	7,43	8,59	6,81
CaO	23,58	23,99	23,67	23,72	23,56	23,90	23,96	23,99	23,78	23,80	23,85
H2O	1,91	1,94	1,89	1,92	1,92	1,94	1,94	1,94	1,94	1,91	1,92
Total	97,48	97,55	97,22	97,90	98,06	98,04	98,05	98,37	98,35	97,64	97,54
normed on 8 kations, all iron assumed to be Fe3											
Si	3,014	2,996	2,986	2,972	2,964	2,963	2,978	2,954	2,958	2,974	2,970
Al	2,471	2,709	2,389	2,538	2,539	2,723	2,660	2,648	2,637	2,521	2,640
Fe3	0,528	0,304	0,615	0,504	0,526	0,338	0,376	0,412	0,433	0,507	0,399
	2,999	3,013	3,004	3,042	3,065	3,061	3,036	3,060	3,070	3,027	3,039
Ca	1,987	1,991	2,010	1,986	1,971	1,976	1,987	1,986	1,972	1,998	1,991
OH	1,000	1,000	1,000	1,000	1,000	1,000	1,000	1,000	1,000	1,000	1,000
XAl2Fe	0,529	0,300	0,613	0,484	0,494	0,319	0,363	0,389	0,405	0,493	0,384

sample	Bk 9	Bk 9	Bk 9	Bk 9	Bk 9	Bk 9	Bk 9	Bk 9	Bk 9	Bk 9	Bk 9
analysis	25	26	28	29	30	33	35	36	37	38	39
date	23.2.94	23.2.94	23.2.94	23.2.94	23.2.94	23.2.94	23.2.94	23.2.94	23.2.94	23.2.94	23.2.94
position	par	core	clz	core	par	par	clz	par	par	par	core
SiO2	38,32	38,07	38,33	38,58	37,73	38,28	38,38	38,34	38,38	38,21	38,43
Al2O3	28,45	28,50	29,01	30,32	27,99	29,19	28,45	28,81	29,29	28,09	29,49
Fe2O3	7,31	7,40	6,63	5,33	7,60	6,32	7,31	7,00	6,49	7,63	6,47
CaO	23,90	23,98	24,11	24,24	23,75	24,16	23,54	24,03	23,94	23,97	24,18
H2O	1,93	1,93	1,94	1,95	1,91	1,94	1,92	1,94	1,94	1,93	1,95
Total	97,98	97,96	98,08	98,48	97,07	97,95	97,68	98,18	98,10	97,91	98,56
normed on 8 kations, all iron assumed to be Fe3											
Si	2,977	2,959	2,967	2,959	2,963	2,964	2,991	2,969	2,968	2,975	2,957
Al	2,605	2,611	2,647	2,741	2,590	2,664	2,614	2,629	2,670	2,578	2,675
Fe3	0,428	0,433	0,386	0,308	0,449	0,368	0,429	0,408	0,378	0,447	0,375
	3,033	3,044	3,033	3,049	3,039	3,032	3,043	3,037	3,048	3,025	3,049
Ca	1,990	1,997	2,000	1,992	1,998	2,004	1,966	1,994	1,984	2,000	1,994
OH	1,000	1,000	1,000	1,000	1,000	1,000	1,000	1,000	1,000	1,000	1,000
XAl2Fe	0,414	0,415	0,374	0,294	0,432	0,357	0,411	0,393	0,361	0,436	0,357

position means analysis of: i(x), inclusion of czo in mineral x, core is core position in a czo grain, mineral x, rim position in czo grain in contact with mineral x, mineral x(i), czo at an inclusion of mineral x in czo

sample	Bk 9	Bk 9	Bk 9	Bk 9	Bk 9	Bk 9	Bk 9	Bk 9	Bk 9	Bk 9	Bk 9
analysis	8	9	10	11	12	13	69	74	75	76	4
date	24.2.94	24.2.94	24.2.94	24.2.94	24.2.94	24.2.94	24.2.94	24.2.94	24.2.94	24.2.94	4.3.94
position	chl	chl	chl	chl	chl	chl	chl	sympl	core	zoi	zoi
SiO2	38,21	38,30	38,09	38,03	38,32	37,37	38,22	37,85	38,20	38,07	39,27
Al2O3	29,60	29,42	28,86	28,45	29,58	25,49	30,00	26,72	28,34	29,24	29,31
Fe2O3	5,93	6,01	7,06	7,48	6,03	10,97	5,25	9,31	7,29	6,16	6,60
CaO	24,02	24,21	23,98	23,09	23,90	23,57	24,26	23,89	23,81	23,95	24,28
H2O	1,94	1,94	1,93	1,91	1,94	1,89	1,94	1,91	1,92	1,93	1,96
Total	97,77	97,94	97,99	97,05	97,83	97,40	97,73	97,77	97,64	97,42	99,46
normed on 8 kations, all iron assumed to be Fe3											
Si	2,959	2,962	2,956	2,985	2,967	2,962	2,954	2,970	2,979	2,962	2,998
Al	2,702	2,682	2,639	2,632	2,699	2,382	2,732	2,471	2,604	2,681	2,637
Fe3	0,346	0,350	0,412	0,442	0,352	0,654	0,305	0,550	0,428	0,360	0,379
	3,048	3,032	3,051	3,073	3,051	3,036	3,038	3,021	3,032	3,042	3,016
Ca	1,993	2,006	1,993	1,942	1,983	2,002	2,009	2,009	1,989	1,996	1,986
OH	1,000	1,000	1,000	1,000	1,000	1,000	1,000	1,000	1,000	1,000	1,000
XAl2Fe	0,330	0,339	0,392	0,412	0,335	0,632	0,294	0,539	0,414	0,346	0,373

sample	Bk 9	Bk 9	Bk 9	Bk 9	Cig 91-1	Cig 91-1	Cig 91-1
analysis	5	6	7	8	13	55	56
date	4.3.94	4.3.94	4.3.94	4.3.94	16.6.93	17.6.93	17.6.93
position	zoi	chl	chl	core	i (grt)	i (grt)	i (grt)
SiO2	39,23	39,18	38,92	38,85	38,06	38,43	38,49
Al2O3	29,34	29,56	28,74	29,25	26,63	28,57	28,48
Fe2O3	6,63	6,40	7,27	6,65	9,35	6,87	7,02
CaO	24,23	24,06	23,98	24,00	22,83	24,14	24,08
H2O	1,96	1,96	1,95	1,95	1,89	1,93	1,93
Total	99,43	99,20	98,91	98,75	96,87	98,01	98,07
normed on 8 kations, all iron assumed to be Fe3							
Si	2,996	2,996	2,995	2,987	3,016	2,981	2,985
Al	2,641	2,664	2,607	2,651	2,487	2,612	2,603
Fe3	0,381	0,368	0,421	0,385	0,557	0,401	0,410
	3,022	3,033	3,028	3,035	3,045	3,013	3,013
Ca	1,982	1,971	1,977	1,977	1,939	2,006	2,001
OH	1,000	1,000	1,000	1,000	1,000	1,000	1,000
XAl2Fe	0,373	0,357	0,410	0,371	0,533	0,396	0,405

sample	Bk 8	Bk 8	Bk 9	Bk 9	Bk 9	Bk 9	Bk 9	Bk 9	Bk 9	Bk 9	Bk 9
analysis	1	7	27	14	15	27	31	32	1	70	71
date	14.3.93	14.3.93	2.7.94	23.2.94	23.2.94	23.2.94	23.2.94	23.2.94	24.2.94	24.2.94	24.2.94
position	par(i)	core	par	par	core	core	core	par(i)	qtz(i)	core	qtz(i)
SiO2	39,05	38,35	39,46	39,41	38,74	39,30	38,77	39,02	38,97	38,78	39,29
Al2O3	31,86	31,14	31,53	32,79	31,94	32,81	32,33	32,89	32,48	32,25	33,10
Fe2O3	1,71	2,34	2,54	2,26	3,06	2,01	1,82	1,62	2,11	2,51	1,80
CaO	24,34	24,95	24,74	24,14	24,65	24,41	24,04	24,58	24,39	24,63	24,45
H2O	1,95	1,94	1,97	1,98	1,97	1,98	1,95	1,97	1,97	1,97	1,98
Total	96,96	96,78	98,27	98,59	98,39	98,53	96,96	98,12	97,95	98,17	98,64
normed on 8 kations, all iron assumed to be Fe3											
Si	3,005	2,963	3,005	2,985	2,949	2,976	2,982	2,964	2,970	2,953	2,969
Al	2,889	2,835	2,830	2,927	2,866	2,928	2,931	2,944	2,918	2,894	2,948
Fe3	0,099	0,136	0,146	0,129	0,175	0,115	0,105	0,093	0,121	0,144	0,102
	2,988	2,972	2,976	3,056	3,041	3,043	3,036	3,036	3,039	3,038	3,051
Ca	2,007	2,065	2,019	1,959	2,010	1,981	1,981	2,000	1,992	2,009	1,980
OH	1	1	1	1	1	1	1	1	1	1	1
XAl2Fe	0,10	0,14	0,15	0,12	0,17	0,11	0,10	0,09	0,12	0,14	0,10

position means analysis of: i(x), inclusion of czo/zoi in mineral x, core is core position in a czo/zoi grain, mineral x, rim position in czo/zoi grain in contact with mineral x, mineral x(i), czo/zoi at an inclusion of mineral x in czo/zoi

sample	Bk 9	Bk 9	Bk 9	Bk 9	Cig 90/40	Cig 90/40
analysis	72	73	1	2	10	11
date	24.2.94	24.2.94	4.3.94	4.3.94	1.6.91b	1.6.91b
position	core	core	clz	clz	core	clz
SiO2	39,06	38,94	40,08	39,87	38,89	39,14
Al2O3	32,93	32,47	32,73	32,21	31,44	31,47
Fe2O3	1,96	2,58	2,48	2,85	2,10	2,90
CaO	24,55	24,43	24,92	24,70	24,62	24,02
H2O	1,98	1,97	2,01	1,99	1,95	1,95
Total	98,50	98,41	100,21	99,63	97,05	97,53
normed on 8 kations, all iron assumed to be Fe3						
Si	2,958	2,958	2,990	2,997	2,994	3,006
Al	2,939	2,907	2,878	2,853	2,853	2,849
Fe3	0,111	0,147	0,139	0,161	0,122	0,168
	3,050	3,054	3,017	3,014	2,975	3,017
Ca	1,992	1,988	1,992	1,989	2,031	1,977
OH	1	1	1	1	1	1
XAl2Fe	0,11	0,14	0,14	0,16	0,12	0,16

position means analysis of: i(x), inclusion of zoi in mineral x, core is core position in a zoi grain, mineral x, rim position in zoi grain in contact with mineral x, mineral x(i), zoi at an inclusion of mineral x in zoi

sample	Bk 10B	Bk 18	Bk 18	Bk 18	Bk 39	Bk 39	Bk 39	Bk 39	Bk 39	Bk 39	Bk 39
analysis	21	15	16	17	1,2	2,2	41	42	43	45	47
date	19.10.93	6.8.94	6.8.94	6.8.94	13.3.93	13.3.93	13.3.93	13.3.93	13.3.93	13.3.93	13.3.93
SiO2	47,12	47,32	47,37	46,57	46,39	46,92	46,35	46,27	47,32	46,94	47,16
Al2O3	37,84	39,80	38,76	39,47	39,83	39,94	38,97	39,42	39,08	38,63	37,68
Fe2O3	1,07	0,46	0,57	0,42	0,30	0,49	0,48	0,54	0,42	0,42	0,48
MgO	0,67	0,18	0,25	0,15	0,14	0,17	0,22	0,32	0,47	0,42	0,24
CaO	0,13	0,21	0,17	0,20	0,15	0,25	0,15	0,18	0,31	0,17	0,19
Na2O	6,84	7,01	6,67	7,13	7,59	7,38	7,68	7,49	7,58	7,59	7,67
K2O	1,42	0,83	1,31	0,67	0,27	0,28	0,50	0,40	0,28	0,44	0,41
total	95,09	95,81	95,10	94,61	94,67	95,43	94,35	94,62	95,46	94,61	93,83
H2O	4,66	4,73	4,68	4,67	4,67	4,71	4,64	4,66	4,71	4,66	4,63
normed on 22 oxygen, all iron assumed to be Fe3											
Si	3,030	3,003	3,033	2,993	2,977	2,986	2,992	2,976	3,013	3,018	3,056
Alo	2,868	2,977	2,925	2,989	3,012	2,995	2,965	2,988	2,933	2,927	2,878
Fe3	0,052	0,022	0,027	0,020	0,014	0,023	0,023	0,026	0,020	0,020	0,023
	2,920	2,998	2,953	3,010	3,027	3,019	2,988	3,014	2,953	2,947	2,901
Mg	0,064	0,017	0,024	0,014	0,013	0,016	0,021	0,031	0,045	0,040	0,023
Ca	0,009	0,014	0,012	0,014	0,010	0,017	0,010	0,012	0,021	0,012	0,013
	0,073	0,031	0,036	0,028	0,024	0,033	0,032	0,043	0,066	0,052	0,036
Na	0,853	0,862	0,828	0,888	0,944	0,911	0,961	0,934	0,936	0,946	0,964
K	0,119	0,069	0,109	0,056	0,023	0,023	0,042	0,034	0,023	0,037	0,035
	0,972	0,931	0,937	0,944	0,967	0,934	1,003	0,968	0,959	0,983	0,998
sum	4,141	4,036	4,016	4,051	4,070	4,066	4,101	4,121	4,084	4,075	4,019
OH	2	2	2	2	2	2	2	2	2	2	2

sample	Bk 39	Bk 39	Bk 39	Bk 39	Bk 39	Bk 39	Bk 39	Bk 39	Bk 39	Bk 39	Bk 39
analysis	48	49	50	51	52	53	54	55	56	57	58
date	13.3.93	13.3.93	13.3.93	13.3.93	13.3.93	13.3.93	13.3.93	13.3.93	13.3.93	13.3.93	13.3.93
SiO2	46,62	46,45	47,11	46,43	46,75	46,85	46,66	46,61	46,80	46,93	46,80
Al2O3	40,01	39,85	39,66	40,00	39,33	39,50	39,90	39,49	39,15	39,47	39,60
Fe2O3	0,36	0,36	0,47	0,44	0,38	0,33	0,32	0,41	0,40	0,32	0,34
MgO	0,13	0,20	0,14	0,13	0,22	0,25	0,14	0,22	0,27	0,28	0,22
CaO	0,18	0,17	0,20	0,25	0,23	0,18	0,23	0,56	0,21	0,18	0,20
Na2O	7,08	7,40	6,96	7,03	7,38	7,41	7,08	7,36	7,20	6,97	7,40
K2O	0,33	0,35	0,57	0,33	0,55	0,74	0,55	0,59	0,71	0,90	0,65
total	94,71	94,78	95,11	94,61	94,84	95,26	94,88	95,24	94,74	95,05	95,21
H2O	4,68	4,68	4,70	4,68	4,68	4,69	4,69	4,69	4,67	4,69	4,69
normed on 22 oxygen, all iron assumed to be Fe3											
Si	2,984	2,977	3,006	2,977	2,998	2,994	2,986	2,982	3,005	3,002	2,991
Alo	3,019	3,010	2,982	3,023	2,972	2,975	3,009	2,977	2,962	2,976	2,982
Fe3	0,017	0,017	0,022	0,021	0,018	0,016	0,016	0,020	0,019	0,016	0,017
	3,036	3,027	3,005	3,044	2,991	2,991	3,025	2,997	2,982	2,991	2,999
Mg	0,012	0,019	0,013	0,012	0,021	0,024	0,013	0,021	0,026	0,027	0,021
Ca	0,012	0,012	0,014	0,017	0,016	0,012	0,016	0,038	0,014	0,012	0,014
	0,025	0,031	0,027	0,030	0,037	0,036	0,029	0,059	0,040	0,039	0,035
Na	0,879	0,920	0,861	0,874	0,918	0,918	0,878	0,913	0,896	0,864	0,917
K	0,028	0,029	0,047	0,028	0,046	0,062	0,046	0,049	0,059	0,075	0,054
	0,906	0,949	0,908	0,901	0,964	0,980	0,924	0,962	0,956	0,940	0,971
sum	4,026	4,072	4,012	4,048	4,064	4,075	4,038	4,118	4,057	4,040	4,072
OH	2	2	2	2	2	2	2	2	2	2	2

sample	Bk 39	Bk 39	Bk 39	Bk 39	Bk 39	Bk 39	Bk 39	Bk 39	Bk 39	Bk 39	Bk 39
analysis	10	23	24	25	30	31	32	33	49	50	51
date	24.6.92	24.6.92	24.6.92	24.6.92	24.6.92	24.6.92	24.6.92	24.6.92	24.6.92	24.6.92	24.6.92
SiO2	46,89	46,08	46,23	46,09	45,82	45,84	45,54	45,82	46,03	46,22	46,00
Al2O3	37,07	39,36	39,43	39,53	39,77	39,80	39,29	39,22	39,35	39,53	39,07
Fe2O3	1,30	0,36	0,33	0,32	0,30	0,26	0,32	0,46	0,32	0,38	0,47
MgO	0,83	0,25	0,26	0,15	0,08	0,12	0,15	0,15	0,22	0,19	0,24
CaO	0,09	0,19	0,17	0,22	0,21	0,19	0,18	0,16	0,17	0,17	0,13
Na2O	6,85	7,44	6,69	7,26	7,21	6,80	7,44	7,30	7,22	7,31	7,07
K2O	1,22	0,40	0,83	0,39	0,30	0,32	0,53	0,59	0,63	0,58	0,86
total	94,25	94,08	93,94	93,96	93,69	93,33	93,45	93,70	93,94	94,38	93,84
H2O	4,62	4,64	4,64	4,64	4,63	4,62	4,60	4,62	4,63	4,65	4,62
normed on 22 oxygen, all iron assumed to be Fe3											
Si	3,042	2,978	2,989	2,979	2,968	2,975	2,966	2,976	2,980	2,979	2,985
Alo	2,834	2,998	3,005	3,011	3,036	3,044	3,016	3,003	3,002	3,003	2,988
Fe3	0,063	0,017	0,016	0,016	0,015	0,012	0,016	0,022	0,016	0,018	0,023
	2,898	3,016	3,021	3,027	3,051	3,056	3,032	3,025	3,018	3,021	3,011
Mg	0,080	0,024	0,025	0,014	0,008	0,012	0,015	0,015	0,021	0,018	0,023
Ca	0,006	0,013	0,012	0,015	0,015	0,013	0,013	0,011	0,012	0,012	0,009
	0,087	0,037	0,037	0,030	0,022	0,025	0,027	0,026	0,033	0,030	0,032
Na	0,862	0,932	0,839	0,910	0,906	0,856	0,940	0,919	0,906	0,913	0,890
K	0,103	0,034	0,070	0,033	0,025	0,027	0,045	0,050	0,053	0,049	0,073
	0,965	0,966	0,909	0,943	0,931	0,883	0,985	0,969	0,959	0,962	0,962
sum	4,163	4,091	4,035	4,061	4,056	4,014	4,102	4,090	4,075	4,080	4,083
OH	2	2	2	2	2	2	2	2	2	2	2

sample	Bk 39	Bk 39	Bk 39	Bk 39	Bk 39	Bk 39	Bk 39	Bk 39	Bk 39	Bk 39	Bk 39
analysis	35	36	38	39	40	41	42	43	44	46	47
date	28.1.93	28.1.93	28.1.93	28.1.93	28.1.93	28.1.93	28.1.93	28.1.93	28.1.93	28.1.93	28.1.93
SiO2	47,25	47,38	46,51	46,70	47,48	45,74	45,94	46,38	46,37	46,95	46,63
Al2O3	38,56	38,10	39,21	38,58	38,26	39,33	39,29	38,73	39,70	38,25	39,07
Fe2O3	0,91	0,90	0,72	0,71	0,76	0,69	0,46	0,58	0,78	0,91	0,67
MgO	0,40	0,61	0,12	0,40	0,21	0,18	0,11	0,34	0,09	0,24	0,13
CaO	0,13	0,10	0,15	0,13	0,12	0,12	0,15	0,29	0,56	0,49	0,13
Na2O	7,50	7,46	7,39	7,32	7,36	7,43	7,03	7,39	7,47	7,44	7,40
K2O	0,26	0,17	0,18	0,21	0,94	0,93	0,49	0,16	0,41	0,10	0,60
total	95,01	94,72	94,28	94,05	95,13	94,42	93,47	93,87	95,38	94,38	94,63
H2O	4,68	4,67	4,66	4,64	4,68	4,63	4,62	4,63	4,69	4,65	4,66
normed on 22 oxygen, all iron assumed to be Fe3											
Si	3,024	3,039	2,996	3,015	3,043	2,960	2,985	3,002	2,965	3,025	3,000
Alo	2,909	2,880	2,977	2,936	2,890	2,999	3,008	2,954	2,992	2,905	2,962
Fe3	0,044	0,043	0,035	0,035	0,036	0,034	0,022	0,028	0,037	0,044	0,032
	2,952	2,924	3,012	2,970	2,926	3,033	3,031	2,982	3,029	2,949	2,995
Mg	0,038	0,058	0,012	0,038	0,020	0,017	0,011	0,033	0,009	0,023	0,012
Ca	0,009	0,007	0,010	0,009	0,008	0,008	0,010	0,020	0,038	0,034	0,009
	0,047	0,065	0,022	0,047	0,028	0,026	0,021	0,053	0,047	0,057	0,021
Na	0,931	0,928	0,923	0,916	0,915	0,932	0,886	0,927	0,926	0,930	0,923
K	0,022	0,014	0,015	0,018	0,079	0,078	0,041	0,013	0,034	0,008	0,050
	0,952	0,942	0,938	0,934	0,993	1,011	0,927	0,941	0,960	0,938	0,973
sum	4,087	4,083	4,063	4,068	4,049	4,162	4,045	4,085	4,158	4,089	4,075
OH	2	2	2	2	2	2	2	2	2	2	2

sample	Bk 39	Bk 39	Bk 39	Bk 39	Bk 39	Bk 39	Bk 39	Bk 39	Bk 39.1	Bk 39.1	Bk 39.1
analysis	48	49	50	3	5,2	7,2	12	13	20	22	23
date	28.1.93	28.1.93	28.1.93	4.5.92	5.5.92	5.5.92	5.5.92	5.5.92	28.8.92	28.8.92	28.8.92
SiO2	46,00	45,80	46,69	46,21	46,40	45,72	47,26	46,49	46,17	46,64	46,30
Al2O3	39,79	39,27	39,22	38,91	38,44	39,10	37,72	38,69	40,08	39,97	40,49
Fe2O3	0,53	0,59	0,92	0,50	0,41	0,40	0,53	0,44	0,56	0,56	0,31
MgO	0,09	0,13	0,12	0,15	0,14	0,11	0,12	0,18	0,06	0,16	0,08
CaO	0,19	0,15	0,25	0,21	0,16	0,21	0,38	0,17	0,16	0,20	0,27
Na2O	7,23	7,28	7,46	7,50	7,69	7,73	7,72	7,09	7,65	7,45	7,34
K2O	0,38	0,60	0,40	0,64	0,53	0,38	0,41	0,68	0,46	0,39	0,32
total	94,21	93,82	95,06	94,12	93,77	93,65	94,14	93,74	95,14	95,37	95,11
H2O	4,65	4,62	4,68	4,63	4,62	4,61	4,64	4,62	4,68	4,70	4,70
normed on 22 oxygen, all iron assumed to be Fe3											
Si	2,967	2,972	2,991	2,992	3,013	2,973	3,055	3,014	2,956	2,974	2,956
Alo	3,025	3,004	2,961	2,969	2,942	2,997	2,874	2,957	3,025	3,004	3,047
Fe3	0,026	0,029	0,044	0,024	0,020	0,020	0,026	0,022	0,027	0,027	0,015
	3,051	3,033	3,006	2,993	2,962	3,016	2,900	2,978	3,051	3,031	3,062
Mg	0,009	0,013	0,011	0,014	0,014	0,011	0,012	0,017	0,006	0,015	0,008
Ca	0,013	0,010	0,017	0,015	0,011	0,015	0,026	0,012	0,011	0,014	0,018
	0,022	0,023	0,029	0,029	0,025	0,025	0,038	0,029	0,017	0,029	0,026
Na	0,904	0,916	0,927	0,941	0,968	0,975	0,968	0,891	0,950	0,921	0,909
K	0,032	0,051	0,033	0,054	0,045	0,032	0,035	0,057	0,038	0,032	0,027
	0,936	0,967	0,960	0,995	1,013	1,007	1,002	0,949	0,988	0,954	0,935
sum	4,082	4,103	4,112	4,096	4,064	4,113	4,030	4,029	4,126	4,095	4,080
OH	2	2	2	2	2	2	2	2	2	2	2

sample	Bk 7	Bk 7	Bk 7	Bk 7	Bk 7	Bk 7	Bk 7	Bk 7	Bk 7	Bk 7	Bk 7
analysis	60	61	62	63	64	65	66	67	68	69	70
date	27.8.92	27.8.92	27.8.92	27.8.92	27.8.92	27.8.92	27.8.92	27.8.92	27.8.92	27.8.92	7.8.92
SiO2	46,33	46,70	46,66	46,18	46,91	46,72	46,32	46,29	46,54	46,12	46,45
Al2O3	39,96	39,97	40,30	39,54	39,76	40,01	40,26	40,19	40,12	39,77	40,24
Fe2O3	0,36	0,42	0,29	0,41	0,37	0,31	0,34	0,42	0,37	0,32	0,46
MgO	0,12	0,19	0,11	0,26	0,28	0,17	0,09	0,12	0,10	0,11	0,16
CaO	0,25	0,14	0,21	0,19	0,17	0,19	0,25	0,15	0,16	0,21	0,16
Na2O	7,28	6,64	7,25	6,80	6,61	6,92	6,84	6,49	6,84	6,75	6,49
K2O	0,48	0,84	0,55	1,12	1,03	0,67	0,51	0,67	0,60	0,46	0,82
total	94,78	94,90	95,37	94,50	95,13	94,99	94,61	94,33	94,73	93,74	94,78
H2O	4,68	4,69	4,71	4,65	4,69	4,69	4,68	4,67	4,68	4,64	4,68
normed on 22 oxygen, all iron assumed to be Fe3											
Si	2,971	2,987	2,973	2,977	2,997	2,986	2,970	2,975	2,980	2,982	2,974
Alo	3,020	3,013	3,026	3,004	2,993	3,014	3,042	3,044	3,028	3,030	3,037
Fe3	0,017	0,020	0,014	0,020	0,018	0,015	0,017	0,020	0,018	0,016	0,022
	3,038	3,034	3,040	3,024	3,011	3,028	3,059	3,064	3,046	3,046	3,059
Mg	0,011	0,018	0,010	0,025	0,027	0,016	0,009	0,011	0,010	0,011	0,015
Ca	0,017	0,010	0,014	0,013	0,012	0,013	0,017	0,010	0,011	0,015	0,011
	0,029	0,028	0,025	0,038	0,038	0,029	0,026	0,022	0,021	0,025	0,026
Na	0,905	0,824	0,896	0,850	0,819	0,857	0,850	0,809	0,849	0,846	0,806
K	0,040	0,070	0,046	0,094	0,086	0,056	0,043	0,056	0,050	0,039	0,068
	0,945	0,894	0,941	0,944	0,904	0,913	0,893	0,865	0,899	0,885	0,874
sum	4,074	4,023	4,058	4,084	4,027	4,030	4,037	4,014	4,022	4,013	4,029
OH	2	2	2	2	2	2	2	2	2	2	2

sample	Bk 7	Bk 7	Bk 8	Bk 8	Bk 8	Bk 8	Bk 8	Bk 8	Bk 9	Bk 9	Bk 9
analysis	62	68	23	46	47	48	49	50	34	35	40
date	7.7.92	7.7.92	14.3.93	14.3.93	14.3.93	14.3.93	14.3.93	14.3.93	2.7.94	2.7.94	23.2.94
SiO2	47,66	47,68	47,21	46,57	46,81	47,36	46,35	46,73	46,44	46,83	48,51
Al2O3	40,39	40,55	40,89	39,77	39,60	39,80	39,17	38,69	39,32	38,96	41,66
Fe2O3	0,91	0,67	0,57	0,51	0,44	0,43	0,30	0,83	0,48	0,28	0,41
MgO	0,51	0,30	0,13	0,13	0,25	0,14	0,12	0,35	0,13	0,21	0,16
CaO	0,23	0,15	0,20	0,22	0,18	0,24	0,34	0,52	0,25	0,21	0,27
Na2O	6,90	6,70	6,46	7,14	6,91	7,00	6,44	7,01	7,45	7,21	6,54
K2O	0,23	0,96	0,57	0,55	0,82	0,43	0,70	0,68	0,31	0,58	0,74
total	96,83	97,01	96,03	94,89	95,01	95,40	93,42	94,81	94,38	94,28	98,29
H2O	4,79	4,78	4,75	4,68	4,69	4,72	4,62	4,66	4,66	4,65	4,87
normed on 22 oxygen, all iron assumed to be Fe3											
Si	2,986	2,988	2,978	2,983	2,995	3,010	3,007	3,004	2,991	3,017	2,990
Alo	2,982	2,995	3,040	3,002	2,986	2,981	2,995	2,931	2,984	2,958	3,026
Fe3	0,043	0,031	0,027	0,025	0,021	0,021	0,015	0,040	0,023	0,013	0,019
	3,025	3,026	3,067	3,027	3,007	3,002	3,010	2,972	3,007	2,971	3,045
Mg	0,048	0,028	0,012	0,012	0,024	0,013	0,012	0,034	0,012	0,020	0,015
Ca	0,015	0,010	0,014	0,015	0,012	0,016	0,024	0,036	0,017	0,014	0,018
	0,063	0,038	0,026	0,028	0,036	0,030	0,035	0,069	0,030	0,035	0,033
Na	0,838	0,814	0,790	0,887	0,857	0,862	0,810	0,874	0,930	0,901	0,781
K	0,019	0,078	0,047	0,046	0,068	0,036	0,059	0,057	0,026	0,049	0,059
	0,857	0,892	0,837	0,933	0,926	0,898	0,869	0,931	0,956	0,949	0,841
sum	4,094	4,058	4,009	4,064	4,048	4,000	3,979	4,122	4,069	4,017	3,989
OH	2	2	2	2	2	2	2	2	2	2	2

sample	Bk 9	Bk 9	Bk 9	Bk 9	Bk 9	Bk 9	Bk 9	Bk 9	Bk 9	Bk 9	Bk 9
analysis	41	42	43	45	46	48	49	50	51	45	46
date	23.2.94	23.2.94	23.2.94	23.2.94	23.2.94	23.2.94	23.2.94	23.2.94	23.2.94	24.2.94	24.2.94
SiO2	47,83	48,14	47,21	47,12	47,37	48,33	47,44	47,38	47,80	47,38	47,67
Al2O3	41,33	41,86	41,96	41,36	41,17	41,38	41,73	41,33	41,64	40,73	40,87
Fe2O3	0,34	0,44	0,41	0,50	0,48	0,53	0,64	0,44	0,48	0,34	0,38
MgO	0,11	0,20	0,07	0,11	0,09	0,21	0,26	0,08	0,10	0,19	0,24
CaO	0,32	0,56	0,28	0,27	0,27	0,23	0,27	0,25	0,16	0,24	0,17
Na2O	6,99	6,51	6,82	6,86	7,12	6,28	6,84	6,98	6,70	7,15	7,00
K2O	0,52	0,94	0,27	0,24	0,32	0,90	0,34	0,43	0,51	0,37	0,73
total	97,44	98,65	97,02	96,46	96,82	97,86	97,52	96,89	97,39	96,40	97,06
H2O	4,82	4,87	4,80	4,78	4,79	4,84	4,82	4,79	4,82	4,77	4,79
normed on 22 oxygen, all iron assumed to be Fe3											
Si	2,977	2,965	2,946	2,959	2,967	2,993	2,950	2,965	2,972	2,980	2,982
Alo	3,032	3,038	3,086	3,061	3,040	3,020	3,058	3,049	3,052	3,020	3,014
Fe3	0,016	0,021	0,019	0,024	0,023	0,025	0,030	0,021	0,022	0,016	0,018
	3,048	3,059	3,106	3,084	3,062	3,045	3,088	3,069	3,074	3,036	3,031
Mg	0,010	0,018	0,007	0,010	0,008	0,019	0,024	0,007	0,009	0,018	0,022
Ca	0,021	0,037	0,019	0,018	0,018	0,015	0,018	0,017	0,011	0,016	0,011
	0,032	0,055	0,025	0,028	0,027	0,035	0,042	0,024	0,020	0,034	0,034
Na	0,844	0,777	0,825	0,835	0,865	0,754	0,825	0,847	0,808	0,872	0,849
K	0,042	0,075	0,022	0,020	0,026	0,073	0,028	0,035	0,041	0,030	0,060
	0,886	0,853	0,847	0,855	0,891	0,827	0,852	0,882	0,849	0,902	0,909
sum	4,029	4,064	4,042	4,043	4,051	3,990	4,085	4,042	4,008	4,039	4,043
OH	2	2	2	2	2	2	2	2	2	2	2

sample	Bk 9	Bk 9	Bk 9	Bk 9	Bk 9	Bk 9	Bk 9	Cig 91-1	Cig 91-1	Cig 91-1	Cig 91-1
analysis	47	48	52	32	33	34	35	27	31	35	36
date	24.2.94	24.2.94	24.2.94	30.6.94	30.6.94	30.6.94	30.6.94	17.6.93	17.6.93	17.6.93	17.6.93
SiO2	45,65	47,13	49,10	46,61	46,49	46,44	46,83	47,30	47,34	48,05	48,21
Al2O3	40,48	40,87	38,67	39,69	39,20	39,32	38,96	39,41	39,45	38,17	37,90
Fe2O3	0,57	0,41	0,48	0,36	0,36	0,48	0,28	1,00	1,07	1,12	1,07
MgO	0,07	0,09	0,13	0,13	0,17	0,13	0,21	0,27	0,34	0,79	0,88
CaO	0,21	0,23	0,24	0,24	0,21	0,25	0,21	0,11	0,16	0,14	0,13
Na2O	7,34	7,42	7,13	7,31	7,30	7,45	7,21	6,66	7,09	6,57	6,34
K2O	0,39	0,36	0,57	0,62	0,77	0,31	0,58	1,48	1,41	1,36	1,62
total	94,71	96,51	96,32	94,96	94,50	94,38	94,28	96,23	96,86	96,20	96,15
H2O	4,67	4,76	4,77	4,68	4,65	4,66	4,65	4,73	4,75	4,73	4,72
normed on 22 oxygen, all iron assumed to be Fe3											
Si	2,933	2,966	3,089	2,986	2,995	2,991	3,017	3,002	2,991	3,048	3,060
Alo	3,065	3,031	2,867	2,996	2,976	2,984	2,958	2,948	2,938	2,853	2,836
Fe3	0,027	0,019	0,023	0,017	0,017	0,023	0,013	0,048	0,051	0,054	0,051
	3,093	3,051	2,890	3,013	2,994	3,007	2,971	2,995	2,988	2,907	2,887
Mg	0,007	0,008	0,012	0,012	0,016	0,012	0,020	0,026	0,032	0,075	0,083
Ca	0,014	0,016	0,016	0,016	0,014	0,017	0,014	0,007	0,011	0,010	0,009
	0,021	0,024	0,028	0,029	0,031	0,030	0,035	0,033	0,043	0,084	0,092
Na	0,914	0,905	0,870	0,908	0,912	0,930	0,901	0,819	0,869	0,808	0,780
K	0,033	0,030	0,047	0,052	0,065	0,026	0,049	0,122	0,116	0,112	0,134
	0,947	0,935	0,916	0,960	0,977	0,956	0,949	0,942	0,985	0,920	0,914
sum	4,137	4,073	3,909	4,065	4,066	4,069	4,017	4,099	4,160	4,103	4,087
OH	2	2	2	2	2	2	2	2	2	2	2

sample	Bk 10B	Bk 10B	Bk 10B	Bk 10B	Bk 10B	Bk 10B	Bk 10B	Bk 7	Bk 7	Bk 7	Bk 7
analysis	63	64	27	31	32	33	34	45	46	48	50
date	18.10.93	18.10.93	19.10.93b	19.10.93b	19.10.93b	19.10.93b	19.10.93b	26.4.93	26.4.93	26.4.93	26.4.93
position	large core	large core	small	small	small	small	small	i (grt)	i (grt)	i (grt)	i (grt)
SiO2	51,72	52,23	50,12	49,21	49,27	49,35	49,18	48,56	48,22	48,89	49,21
TiO2	0,17	0,19	0,30	0,17	0,23	0,21	0,35	0,20	0,20	0,17	0,18
Al2O3	24,49	24,96	27,89	27,69	27,64	27,99	27,91	27,86	27,36	27,84	28,10
Fe2O3	1,13	1,16	1,52	1,92	1,83	1,89	1,65	2,62	3,41	1,88	2,70
FeO	0,68	0,73	0,19	0,16	0,00	0,00	0,02	0,00	0,00	0,52	0,00
MgO	4,59	4,56	3,58	3,33	3,48	3,46	3,42	3,26	3,72	2,99	3,17
Na2O	0,38	0,32	0,67	0,69	0,63	0,66	0,62	0,89	0,90	0,92	0,87
K2O	10,57	10,71	10,15	10,21	10,29	10,16	10,36	9,95	9,77	10,19	10,16
H2O	4,43	4,48	4,47	4,40	4,41	4,42	4,41	4,38	4,37	4,39	4,43
total	98,16	99,34	98,88	97,78	97,78	98,14	97,92	97,73	97,96	97,79	98,82
normed on 11 oxygen, Fe3 estimated over Fetot - (Si-Mg-3) iterativ											
Si	3,492	3,485	3,352	3,337	3,339	3,328	3,328	3,297	3,264	3,324	3,309
Alt	0,508	0,515	0,648	0,663	0,661	0,672	0,672	0,703	0,736	0,676	0,691
Alo	1,440	1,447	1,551	1,550	1,546	1,553	1,554	1,527	1,447	1,555	1,535
Ti	0,009	0,010	0,015	0,009	0,012	0,011	0,018	0,010	0,010	0,009	0,009
Fe3	0,058	0,058	0,076	0,098	0,094	0,096	0,084	0,134	0,174	0,096	0,137
	1,506	1,515	1,642	1,657	1,651	1,659	1,656	1,671	1,631	1,659	1,681
Fe2	0,038	0,041	0,010	0,009	0,000	0,000	0,001	0,000	0,000	0,030	0,000
Mg	0,462	0,453	0,357	0,337	0,351	0,348	0,345	0,330	0,375	0,303	0,318
	0,500	0,494	0,367	0,346	0,351	0,348	0,346	0,330	0,375	0,333	0,318
Na	0,050	0,041	0,087	0,091	0,083	0,086	0,081	0,117	0,118	0,121	0,113
K	0,930	0,931	0,885	0,902	0,909	0,893	0,914	0,881	0,862	0,903	0,890
	0,980	0,973	0,972	0,993	0,992	0,979	0,995	0,998	0,980	1,024	1,004
sum	6,987	6,982	6,981	6,995	6,994	6,986	6,997	6,998	6,987	7,016	7,002
OH	2	2	2	2	2	2	2	2	2	2	2
Mg/(Mg+Fe)	0,83	0,82	0,80	0,76	0,79	0,78	0,80	0,71	0,68	0,71	0,70
Na/(Na+K)	0,05	0,04	0,09	0,09	0,08	0,09	0,08	0,12	0,12	0,12	0,11

Position means analysis of: large core, core of large phengite; large rim, rim of large phengite: large c-r, undefined position in a large phengite; small, a small phengite; i(grt), phengite inclusion in garnet

sample	Bk 7	Bk 7	Bk 7	Cig 91-1	Cig 91-1	Cig 91-1	Cig 91-1	Cig 91-1	Cig 91-1	Cig 91-1	Cig 91-1
analysis	54	55	56	77	78	2	3	4	6	7	8
date	26.4.93	26.4.93	26.4.93	16.6.93	16.6.93	17.6.93	17.6.93	17.6.93	17.6.93	17.6.93	17.6.93
position	i (grt)	i (grt)	i (grt)	small	small	small c	small c	small c	small r	small	small
SiO2	49,33	49,74	48,60	49,89	50,56	52,31	51,97	52,80	48,99	49,58	50,13
TiO2	0,22	0,21	0,21	0,37	0,24	0,18	0,20	0,16	0,35	0,29	0,20
Al2O3	28,29	27,92	28,82	29,39	28,76	24,67	24,84	24,80	28,34	28,11	27,61
Fe2O3	2,20	1,61	2,04	2,45	2,13	0,96	1,17	0,63	2,86	2,26	2,42
FeO	0,35	0,56	0,00	0,28	0,37	0,76	0,60	1,25	0,41	0,24	0,10
MgO	3,02	3,21	2,95	2,93	3,21	4,63	4,56	4,50	2,84	3,22	3,50
Na2O	0,98	0,81	0,82	0,77	0,71	0,33	0,32	0,32	0,80	0,70	0,69
K2O	10,25	10,30	10,33	10,22	10,51	11,05	11,16	10,97	10,14	10,36	10,50
H2O	4,45	4,45	4,41	4,53	4,54	4,48	4,47	4,51	4,44	4,45	4,47
total	99,09	98,80	98,19	100,83	101,03	99,37	99,29	99,94	99,17	99,21	99,62
normed on 11 oxygen, Fe3 estimated over Fetot - (Si-Mg-3) iterativ											
Si	3,310	3,342	3,286	3,285	3,323	3,495	3,478	3,507	3,290	3,320	3,344
Alt	0,690	0,658	0,714	0,715	0,677	0,505	0,522	0,493	0,710	0,680	0,656
Alo	1,548	1,553	1,582	1,565	1,551	1,437	1,438	1,448	1,533	1,539	1,514
Ti	0,011	0,011	0,011	0,018	0,012	0,009	0,010	0,008	0,018	0,015	0,010
Fe3	0,111	0,081	0,104	0,122	0,105	0,048	0,059	0,032	0,145	0,114	0,121
	1,670	1,645	1,697	1,705	1,668	1,495	1,507	1,488	1,695	1,667	1,646
Fe2	0,020	0,031	0,000	0,016	0,020	0,043	0,033	0,070	0,023	0,013	0,006
Mg	0,302	0,321	0,297	0,288	0,314	0,461	0,455	0,446	0,284	0,321	0,348
	0,322	0,353	0,297	0,303	0,335	0,504	0,488	0,515	0,308	0,335	0,354
Na	0,128	0,106	0,107	0,098	0,090	0,043	0,042	0,041	0,104	0,091	0,089
K	0,897	0,902	0,910	0,877	0,900	0,962	0,973	0,950	0,887	0,904	0,913
	1,024	1,007	1,018	0,975	0,991	1,005	1,015	0,991	0,992	0,995	1,002
sum	7,016	7,005	7,012	6,984	6,994	7,003	7,010	6,994	6,994	6,997	7,001
OH	2	2	2	2	2	2	2	2	2	2	2
Mg/(Mg+Fe)	0,70	0,74	0,74	0,68	0,71	0,84	0,83	0,82	0,63	0,72	0,73
Na/(Na+K)	0,12	0,10	0,11	0,10	0,09	0,04	0,04	0,04	0,11	0,09	0,09

sample	Cig 91-1	Cig 91-1	Cig 91-1	Cig 91-1	Cig 91-1	Cig 91-1	Cig 91-1	Cig 91-1	Cig 91-1	Cig 91-1	Cig 91-1
analysis	9	10	11	12	13	14	15	19	20	21	22
date	17.6.93	17.6.93	17.6.93	17.6.93	17.6.93	17.6.93	17.6.93	17.6.93	17.6.93	17.6.93	17.6.93
position	small	small	small	small	small	small	small	small	small	large core	large core
SiO2	48,69	49,03	50,30	49,96	50,15	50,19	49,81	49,57	49,93	52,46	52,24
TiO2	0,35	0,26	0,22	0,21	0,28	0,19	0,18	0,26	0,29	0,21	0,26
Al2O3	28,91	28,52	28,40	27,81	28,09	27,65	28,04	27,79	28,71	25,15	24,72
Fe2O3	3,08	3,00	2,18	2,48	1,81	2,29	2,33	2,40	1,87	1,70	1,64
FeO	0,00	0,00	0,01	0,00	0,78	0,26	0,16	0,34	0,45	0,36	0,30
MgO	2,85	3,14	3,42	3,59	3,10	3,43	3,28	3,19	3,09	4,64	4,75
Na2O	1,01	0,86	0,85	0,81	0,70	0,70	0,84	0,76	0,63	0,27	0,32
K2O	10,35	10,54	10,41	10,45	10,66	10,54	10,44	10,50	10,49	11,31	11,26
H2O	4,45	4,46	4,51	4,48	4,49	4,47	4,47	4,45	4,49	4,52	4,49
total	99,69	99,81	100,30	99,78	100,06	99,72	99,54	99,26	99,96	100,62	99,98
normed on 11 oxygen, Fe3 estimated over Fetot - (Si-Mg-3) iterativ											
Si	3,255	3,272	3,327	3,325	3,337	3,346	3,326	3,325	3,317	3,467	3,474
Alt	0,745	0,728	0,673	0,675	0,663	0,654	0,674	0,675	0,683	0,533	0,526
Alo	1,533	1,515	1,541	1,506	1,540	1,518	1,533	1,522	1,564	1,425	1,412
Ti	0,018	0,013	0,011	0,011	0,014	0,010	0,009	0,013	0,014	0,010	0,013
Fe3	0,155	0,151	0,108	0,124	0,091	0,115	0,117	0,121	0,094	0,084	0,082
	1,705	1,678	1,660	1,640	1,644	1,643	1,659	1,656	1,672	1,520	1,507
Fe2	0,000	0,000	0,001	0,000	0,043	0,015	0,009	0,019	0,025	0,020	0,016
Mg	0,284	0,312	0,337	0,356	0,307	0,341	0,326	0,319	0,306	0,457	0,471
	0,284	0,312	0,338	0,356	0,351	0,355	0,335	0,338	0,331	0,477	0,487
Na	0,131	0,111	0,109	0,105	0,090	0,090	0,109	0,099	0,081	0,035	0,041
K	0,902	0,917	0,897	0,906	0,924	0,916	0,909	0,918	0,908	0,974	0,976
	1,033	1,028	1,006	1,011	1,015	1,006	1,017	1,017	0,989	1,009	1,017
sum	7,022	7,019	7,004	7,007	7,010	7,004	7,012	7,011	6,993	7,006	7,012
OH	2	2	2	2	2	2	2	2	2	2	2
Mg/(Mg+Fe)	0,65	0,67	0,76	0,74	0,70	0,72	0,72	0,69	0,72	0,81	0,83
Na/(Na+K)	0,13	0,11	0,11	0,10	0,09	0,09	0,11	0,10	0,08	0,03	0,04

Position means analysis of: large core, core of large phengite; large rim, rim of large phengite: large c-r, undefined position in a large phengite; small, a small phengite; i(grt), phengite inclusion in garnet

sample	Cig 91-1	Cig 91-1	Cig 91-1	Cig 91-1	Cig 91-1	Cig 91-1	Cig 91-1	Cig 91-1	Cig 91-1	Cig 91-1	Cig 91-1
analysis	23	24	25	26	29	30	42	13	14	15	16
date	17.6.93	17.6.93	17.6.93	17.6.93	17.6.93	17.6.93	17.6.93	28.11.93	28.11.93	28.11.93	28.11.93
position	large core	large core	large rim	large core	large rim	large rim	small	large rim	large rim	large core	large core
SiO2	52,52	52,35	49,96	52,33	48,62	49,48	50,35	50,58	49,27	51,71	51,43
TiO2	0,24	0,24	0,21	0,20	0,36	0,35	0,22	0,26	0,29	0,21	0,22
Al2O3	24,61	24,78	27,77	25,09	28,67	28,12	27,43	28,44	27,59	24,51	24,15
Fe2O3	0,98	1,38	1,89	0,80	2,69	1,94	1,76	1,41	1,19	0,66	0,78
FeO	0,86	0,50	0,27	1,00	0,07	0,58	0,46	0,72	0,93	1,26	0,94
MgO	4,63	4,70	3,40	4,41	2,89	3,06	3,49	3,22	3,07	4,32	4,50
Na2O	0,29	0,26	0,61	0,29	0,76	0,78	1,04	0,70	0,62	0,27	0,27
K2O	11,29	11,19	10,76	11,28	10,21	10,26	10,19	10,53	10,40	10,94	11,05
H2O	4,50	4,49	4,46	4,50	4,42	4,45	4,47	4,52	4,40	4,43	4,40
total	99,92	99,89	99,33	99,90	98,69	99,02	99,41	100,38	97,76	98,31	97,74
normed on 11 oxygen, Fe3 estimated over Fetot - (Si-Mg-3) iterativ											
Si	3,495	3,482	3,344	3,483	3,276	3,321	3,362	3,344	3,349	3,496	3,498
Alt	0,505	0,518	0,656	0,517	0,724	0,679	0,638	0,656	0,651	0,504	0,502
Alo	1,426	1,424	1,534	1,451	1,553	1,546	1,521	1,561	1,559	1,449	1,434
Ti	0,012	0,012	0,011	0,010	0,018	0,018	0,011	0,013	0,015	0,011	0,011
Fe3	0,049	0,069	0,095	0,040	0,136	0,098	0,088	0,070	0,061	0,034	0,040
	1,487	1,505	1,640	1,502	1,707	1,661	1,620	1,644	1,635	1,494	1,486
Fe2	0,048	0,028	0,015	0,056	0,004	0,033	0,026	0,040	0,053	0,071	0,053
Mg	0,459	0,466	0,339	0,438	0,290	0,306	0,347	0,317	0,311	0,435	0,456
	0,507	0,494	0,354	0,493	0,294	0,339	0,373	0,357	0,364	0,507	0,509
Na	0,037	0,034	0,079	0,037	0,099	0,102	0,135	0,090	0,082	0,035	0,036
K	0,979	0,970	0,939	0,979	0,897	0,898	0,887	0,907	0,921	0,964	0,980
	1,017	1,003	1,018	1,016	0,996	0,999	1,021	0,997	1,003	0,999	1,015
sum	7,011	7,002	7,012	7,011	6,997	6,999	7,014	6,998	7,002	7,000	7,010
OH	2	2	2	2	2	2	2	2	2	2	2
Mg/(Mg+Fe)	0,83	0,83	0,75	0,82	0,67	0,70	0,75	0,74	0,73	0,81	0,83
Na/(Na+K)	0,04	0,03	0,08	0,04	0,10	0,10	0,13	0,09	0,08	0,04	0,04

sample	Cig 91-1	Cig 91-1	Cig 91-1	Cig 91-1	Cig 91-1	Cig 91-1	Cig 91-1	Cig 91-1	Cig 91-1	Cig 91-1	Cig 91-1
analysis	17	18	19	20	22	23	24	25	26	28	30
date	28.11.93	28.11.93	28.11.93	28.11.93	28.11.93	28.11.93	28.11.93	28.11.93	28.11.93	28.11.93	28.11.93
position	large core	large core	large c-r	large c-r	large c-r	large c-r	large core	large core	large rim	large c-r	large core
SiO2	51,76	51,13	50,66	50,92	50,77	50,66	51,38	51,63	50,33	51,05	51,77
TiO2	0,19	0,18	0,22	0,30	0,24	0,18	0,18	0,21	0,20	0,19	0,21
Al2O3	24,25	24,38	25,56	25,14	25,40	26,02	24,43	24,19	26,73	25,89	24,29
Fe2O3	0,82	0,84	1,66	0,96	0,45	1,05	0,72	0,59	2,45	0,64	0,84
FeO	0,84	1,02	0,29	0,87	1,26	0,63	1,14	1,26	0,10	1,28	1,01
MgO	4,58	4,34	4,18	4,15	3,90	3,96	4,32	4,40	3,70	3,79	4,50
Na2O	0,32	0,32	0,43	0,42	0,45	0,40	0,39	0,25	1,31	0,62	0,24
K2O	11,14	10,63	10,75	10,82	10,76	10,84	10,71	10,91	10,28	10,53	11,00
H2O	4,43	4,38	4,42	4,41	4,40	4,42	4,40	4,41	4,46	4,44	4,43
total	98,33	97,22	98,17	97,99	97,64	98,17	97,67	97,85	99,57	98,43	98,29
normed on 11 oxygen, Fe3 estimated over Fetot - (Si-Mg-3) iterativ											
Si	3,499	3,490	3,427	3,454	3,455	3,426	3,493	3,506	3,364	3,444	3,500
Alt	0,501	0,510	0,573	0,546	0,545	0,574	0,507	0,494	0,636	0,556	0,500
Alo	1,432	1,452	1,465	1,463	1,492	1,500	1,451	1,443	1,470	1,502	1,436
Ti	0,010	0,009	0,011	0,015	0,012	0,009	0,009	0,011	0,010	0,010	0,011
Fe3	0,042	0,043	0,085	0,049	0,023	0,053	0,037	0,030	0,123	0,033	0,043
	1,483	1,504	1,561	1,527	1,528	1,562	1,497	1,483	1,604	1,544	1,489
Fe2	0,048	0,058	0,017	0,049	0,072	0,036	0,065	0,072	0,006	0,072	0,057
Mg	0,462	0,442	0,421	0,420	0,396	0,399	0,438	0,445	0,369	0,381	0,453
	0,509	0,500	0,438	0,469	0,467	0,435	0,503	0,517	0,374	0,453	0,511
Na	0,042	0,042	0,056	0,055	0,059	0,052	0,051	0,033	0,170	0,081	0,031
K	0,982	0,946	0,948	0,956	0,954	0,955	0,949	0,966	0,896	0,926	0,969
	1,024	0,988	1,004	1,012	1,014	1,008	1,000	0,999	1,065	1,007	1,001
sum	7,016	6,992	7,003	7,008	7,009	7,005	7,000	6,999	7,044	7,005	7,000
OH	2	2	2	2	2	2	2	2	2	2	2
Mg/(Mg+Fe)	0,84	0,81	0,81	0,81	0,81	0,82	0,81	0,81	0,74	0,78	0,82
Na/(Na+K)	0,04	0,04	0,06	0,05	0,06	0,05	0,05	0,03	0,16	0,08	0,03

Position means analysis of: large core, core of large phengite; large rim, rim of large phengite: large c-r, undefined position in a large phengite; small, a small phengite; i(grt), phengite inclusion in garnet

sample	Cig 91-1.2	Cig 91-1.2	Cig 91-1.2	Cig 91-1.2	Cig 91-1.2	Cig 91-1.2	Cig 91-1.2	Cig 91-1.2	Cig 91-1.2
analysis	54	55	1	2	3	4	5	6	7
date	2.7.94	2.7.94	3.7.94	3.7.94	3.7.94	3.7.94	3.7.94	3.7.94	3.7.94
position	large core	large rim	large rim	large c-r	large core	large core	large core	large core	large core
SiO2	51,99	49,52	50,60	51,89	52,01	52,24	51,19	52,02	51,65
TiO2	0,18	0,26	0,22	0,21	0,21	0,19	0,20	0,16	0,15
Al2O3	24,84	27,33	27,32	24,03	24,46	24,40	25,04	24,45	24,23
Fe2O3	0,90	1,71	1,31	0,75	0,69	0,85	1,24	0,51	0,76
FeO	0,81	0,45	0,84	0,96	0,74	0,73	0,78	1,22	1,08
MgO	4,52	3,38	3,49	4,66	4,70	4,73	4,26	4,47	4,46
Na2O	0,39	0,68	0,59	0,29	0,39	0,43	0,36	0,31	0,37
K2O	10,68	10,26	10,27	10,68	10,70	10,78	10,57	10,65	10,74
H2O	4,46	4,41	4,47	4,42	4,44	4,46	4,42	4,44	4,41
total	98,77	98,00	99,11	97,89	98,34	98,82	98,05	98,23	97,85
normed on 11 oxygen, Fe3 estimated over Fetot - (Si-Mg-3) iterativ									
Si	3,489	3,353	3,384	3,514	3,503	3,505	3,463	3,510	3,504
Alt	0,511	0,647	0,616	0,486	0,497	0,495	0,537	0,490	0,496
Alo	1,453	1,535	1,537	1,432	1,444	1,434	1,460	1,455	1,442
Ti	0,009	0,013	0,011	0,011	0,011	0,010	0,010	0,008	0,008
Fe3	0,045	0,087	0,066	0,038	0,035	0,043	0,063	0,026	0,039
	1,507	1,635	1,614	1,481	1,490	1,486	1,533	1,489	1,488
Fe2	0,046	0,025	0,047	0,055	0,042	0,041	0,044	0,069	0,061
Mg	0,452	0,341	0,348	0,470	0,472	0,473	0,430	0,450	0,451
	0,498	0,367	0,395	0,525	0,513	0,514	0,474	0,519	0,512
Na	0,051	0,089	0,077	0,038	0,051	0,056	0,047	0,041	0,049
K	0,934	0,906	0,895	0,943	0,939	0,943	0,932	0,937	0,950
	0,985	0,995	0,972	0,981	0,990	0,998	0,979	0,977	0,998
sum	6,990	6,997	6,981	6,987	6,993	6,999	6,986	6,985	6,999
OH	2	2	2	2	2	2	2	2	2
Mg/(Mg+Fe)	0,83	0,75	0,75	0,84	0,86	0,85	0,80	0,83	0,82
Na/(Na+K)	0,05	0,09	0,08	0,04	0,05	0,06	0,05	0,04	0,05

Position means analysis of: large core, core of large phengite; large rim, rim of large phengite: large c-r, undefined position in a large phengite; small, a small phengite; i(grt), phengite inclusion in garnet

Sample	Bk 10B	Bk 10B	Bk 18	Bk 39	Bk 39	Bk 39	Bk 39.1	Bk 39a	Bk 39a	Bk 7	Bk 7
Date	19.10.93	19.10.93	6.8.94	2.7.94	2.7.94	5.5.92	28.8.92	28.1.93	28.1.93	30.6.94	6.7.92
Nr	5	6	1	20	21	12	15	27	30	53	42
TiO2	97,00	98,83	99,70	97,87	98,09	98,09	99,02	98,62	98,57	98,23	98,5
Fe2O3	0,59	0,46	0,57	0,77	0,77	0,58	0,66	1,04	0,73	0,42	0,63
sum	97,59	99,29	100,27	98,64	98,86	98,67	99,68	99,66	99,30	98,65	99,13
normed on 1cation											
Ti	0,994	0,995	0,994	0,992	0,992	0,994	0,993	0,990	0,993	0,996	0,994
Fe3	0,006	0,005	0,006	0,008	0,008	0,006	0,007	0,010	0,007	0,004	0,006

Sample	Bk 7	Bk 8	Bk 8	Bk 8	Bk 8	Bk 8	Bk 8	Bk 9	Bk 9	Bk 9	Bk 9
Date	6.7.92	14.3.93	29.1.93	29.1.93	29.1.93	29.1.93	29.1.93	24.2.94	24.2.94	24.2.94	24.2.94
Nr	70	45	1	2	4,2	6,2	16,2	2	3	77	78
TiO2	98,17	97,12	97,72	98,05	97,36	96,6	98,42	98,4	96,6	97,41	99
Fe2O3	0,47	0,71	0,54	0,62	0,63	0,60	0,81	0,49	0,62	0,40	0,44
sum	98,64	97,83	98,26	98,67	97,99	97,20	99,23	98,89	97,22	97,81	99,44
normed on 1cation											
Ti	0,995	0,993	0,995	0,994	0,994	0,994	0,992	0,995	0,994	0,996	0,996
Fe3	0,005	0,007	0,005	0,006	0,006	0,006	0,008	0,005	0,006	0,004	0,004

Sample	Bk 9	Bk 9	Cig 91.1.2
Date	30.6.94	30.6.94	2.7.94
Nr	23	23	13
TiO2	98,24	98,29	98,89
Fe2O3	0,47	0,46	0,56
sum	98,71	98,75	99,45
normed on 1cation			
Ti	0,995	0,995	0,994
Fe3	0,005	0,005	0,006

sample	Bk7	Bk7	Bk7	Bk7	Bk7	Bk7	Bk7	Bk7	Bk7	Bk7	Bk7
analysis	5	6	9	10	11	12	23	24	59	60	6
date	26.4.93	26.4.93	26.4.93	26.4.93	26.4.93	26.4.93	26.4.93	26.4.93	26.4.93	26.4.93	6.7.92
Ca	29,67	29,90	29,32	33,34	29,95	30,34	29,61	29,51	29,45	29,46	33,90
Mg	15,69	15,98	15,43	13,18	15,68	15,43	14,62	15,75	15,53	16,04	17,40
Fe	7,79	7,59	7,81	6,91	8,04	7,60	8,55	7,96	7,92	7,56	8,34
Mn	0,40	0,41	0,47	0,56	0,54	0,51	0,40	0,41	0,54	0,43	0,56
sum	53,55	53,88	53,03	53,99	54,21	53,88	53,18	53,63	53,44	53,49	60,20
CO2	45,43	45,81	44,93	45,13	45,88	45,63	44,68	45,48	45,25	45,53	51,06
total	98,98	99,69	97,96	99,12	100,09	99,51	97,86	99,11	98,69	99,02	111,26
normed on 2 cations											
Ca	1,025	1,024	1,024	1,159	1,025	1,044	1,040	1,018	1,021	1,016	1,042
Mg	0,754	0,762	0,750	0,638	0,746	0,738	0,714	0,756	0,749	0,769	0,744
Fe	0,210	0,203	0,213	0,188	0,215	0,204	0,234	0,214	0,214	0,203	0,200
Mn	0,011	0,011	0,013	0,015	0,015	0,014	0,011	0,011	0,015	0,012	0,014
	0,975	0,976	0,976	0,841	0,975	0,956	0,960	0,982	0,979	0,984	0,958
CO3	2	2	2	2	2	2	2	2	2	2	2

sample	Bk7	Bk7
analysis	9	34
date	6.7.92	6.7.92
Ca	33,26	32,61
Mg	16,81	17,52
Fe	8,82	8,84
Mn	0,61	0,63
sum	59,50	59,60
CO2	50,24	50,52
total	109,74	110,12
normed on 2 cations		
Ca	1,039	1,013
Mg	0,731	0,757
Fe	0,215	0,214
Mn	0,015	0,015
	0,961	0,987
CO3	2	2

sample	Bk 7	Bk 7	Bk 7	Bk 7	Bk 7	Bk 7	Bk 7	Bk 7	Bk 7	Bk 7	Bk 7Th
analysis	7	8	21	22	63	64	2	4	10	33	3
date	26.4.93	26.4.93	26.4.93	26.4.93	26.4.93	26.4.93	6.7	6.7	6.7	6.7	11.6.94
CL colour	yellow	brown	yellow	yellow	yellow	yellow	yellow	yellow	orange	yellow	yellow
Ca	52,39	50,90	51,10	50,55	53,28	51,92	63,61	62,28	59,98	62,60	54,90
Mg	1,97	2,55	2,39	2,43	1,31	1,30	1,24	1,68	2,18	1,01	1,85
Fe	2,13	2,41	2,19	2,45	1,47	1,57	1,40	2,11	2,72	1,87	1,20
Mn	0,65	0,65	0,56	0,53	0,63	0,57	0,86	1,06	1,29	1,07	0,64
CO2	44,97	44,61	44,40	44,15	44,53	43,48	52,66	52,66	51,92	52,04	46,24
total	102,11	101,12	100,64	100,11	101,22	98,84	119,77	119,79	118,09	118,59	104,83
normed on 1cation											
Ca	0,914	0,895	0,903	0,898	0,939	0,937	0,948	0,928	0,907	0,944	0,932
Mg	0,048	0,062	0,059	0,060	0,032	0,033	0,026	0,035	0,046	0,021	0,044
Fe	0,029	0,033	0,030	0,034	0,020	0,022	0,016	0,025	0,032	0,022	0,016
Mn	0,009	0,009	0,008	0,007	0,009	0,008	0,010	0,012	0,015	0,013	0,009
CO3	1	1	1	1	1	1	1	1	1	1	1

sample	Bk 7Th	Bk 7Th	Bk 7Th	Bk 7Th	Bk 7Th	Bk 7Th	Bk 7Th	Bk 7Th	Bk 7Th	Bk 7Th	Bk 7Th
analysis	4	7	16	17	18	19	20	21	22	23	24
date	11.6.94	11.6.94	11.6.94	11.6.94	11.6.94	11.6.94	11.6.94	11.6.94	11.6.94	11.6.94	11.6.94
CL colour	yellow	orange	yellow	orange	orange	yellow	yellow	orange	orange	orange	yellow
Ca	54,28	53,65	51,42	51,38	52,79	51,54	52,91	49,87	50,59	50,05	50,21
Mg	1,77	1,97	1,75	1,83	1,96	1,30	1,26	1,66	1,62	1,70	1,41
Fe	1,54	1,85	1,43	2,12	2,52	1,77	1,73	1,96	1,90	1,80	1,79
Mn	0,68	0,73	0,50	0,96	0,82	0,72	0,71	0,74	0,68	0,69	0,54
CO2	45,90	45,84	43,45	44,21	45,62	43,40	44,40	42,61	43,06	42,66	42,37
total	104,17	104,04	98,55	100,50	103,71	98,73	101,01	96,84	97,85	96,90	96,32
normed on 1cation											
Ca	0,928	0,918	0,929	0,912	0,908	0,932	0,935	0,919	0,922	0,921	0,930
Mg	0,042	0,047	0,044	0,045	0,047	0,033	0,031	0,043	0,041	0,044	0,036
Fe	0,021	0,025	0,020	0,029	0,034	0,025	0,024	0,028	0,027	0,026	0,026
Mn	0,009	0,010	0,007	0,013	0,011	0,010	0,010	0,011	0,010	0,010	0,008
CO3	1	1	1	1	1	1	1	1	1	1	1

sample	Bk 7Th	Bk 7Th	Bk 7Th	Bk 7Th	Bk 7Th	Bk 7Th	Bk 7Th	Bk 7Th	Bk 7Th	Bk 7Th	Bk 7Th
analysis	25	26	28	29	30	31	33	34	33	34	36
date	11.6.94	11.6.94	11.6.94	11.6.94	11.6.94	11.6.94	11.6.94	11.6.94	11.6.94	11.6.94	11.6.94
CL colour	orange	yellow	orange	orange	yellow	orange	yellow	yellow	yellow	yellow	brown
Ca	49,40	51,13	49,92	50,64	50,64	50,92	50,63	52,62	50,63	52,62	50,98
Mg	1,69	1,34	1,76	1,71	1,75	1,38	1,50	1,05	1,50	1,05	1,60
Fe	1,98	1,57	2,27	1,94	2,13	1,97	2,02	1,60	2,02	1,60	1,94
Mn	0,74	0,59	0,62	0,70	0,67	0,60	0,46	0,55	0,46	0,55	0,70
CO2	42,29	42,92	42,87	43,23	43,37	43,05	42,89	43,76	42,89	43,76	43,38
total	96,10	97,55	97,44	98,22	98,56	97,92	97,50	99,58	97,50	99,58	98,60
normed on 1cation											
Ca	0,917	0,935	0,914	0,919	0,916	0,928	0,926	0,944	0,926	0,944	0,922
Mg	0,044	0,034	0,045	0,043	0,044	0,035	0,038	0,026	0,038	0,026	0,040
Fe	0,029	0,022	0,032	0,027	0,030	0,028	0,029	0,022	0,029	0,022	0,027
Mn	0,011	0,009	0,009	0,010	0,010	0,009	0,007	0,008	0,007	0,008	0,010
CO3	1	1	1	1	1	1	1	1	1	1	1

sample	Bk 7Th	Bk 7Th	Bk 7Th	Bk 7Th	Bk 7Th	Bk 7Th	Bk 7Th	Bk 7Th	Bk 7Th	Bk 7Th	Bk 7Th
analysis	37	38	40	41	42	43	44	45	46	47	48
date	11.6.94	11.6.94	11.6.94	11.6.94	11.6.94	11.6.94	11.6.94	11.6.94	11.6.94	11.6.94	11.6.94
CL colour	brown	brown	brown	yellow	yellow	yellow	yellow	yellow	yellow	yellow	yellow
Ca	50,37	50,52	51,27	53,03	52,14	53,13	51,72	52,47	52,24	53,38	51,47
Mg	1,64	1,60	1,51	0,72	0,98	0,71	1,33	1,22	1,00	0,72	1,60
Fe	1,79	1,93	1,69	0,75	0,97	0,73	0,93	0,98	0,87	0,92	1,45
Mn	0,66	0,60	0,68	0,69	0,65	0,62	0,55	0,75	0,58	0,56	0,70
CO2	42,83	42,95	43,34	43,29	42,99	43,30	42,95	43,58	42,98	43,59	43,46
total	97,29	97,60	98,49	98,48	97,73	98,49	97,48	99,00	97,67	99,17	98,68
normed on 1cation											
Ca	0,923	0,923	0,928	0,961	0,952	0,963	0,945	0,945	0,954	0,961	0,929
Mg	0,042	0,041	0,038	0,018	0,025	0,018	0,034	0,031	0,025	0,018	0,040
Fe	0,026	0,028	0,024	0,011	0,014	0,010	0,013	0,014	0,012	0,013	0,020
Mn	0,010	0,009	0,010	0,010	0,009	0,009	0,008	0,011	0,008	0,008	0,010
CO3	1	1	1	1	1	1	1	1	1	1	1

sample	Bk 7Th	Bk 7Th	Bk 7Th	Bk 7Th	Bk 9	Bk 9	Bk 9	Bk 9	Bk 9	Bk 9	Bk 9
analysis	49	50	51	52	52	30	31	32	4	35	36
date	11.6.94	11.6.94	11.6.94	11.6.94	23.2.94	24.2.94	24.2.94	24.2.94	24.2.94	24.2.94	24.2.94
CL colour	orange	orange	orange	orange							
Ca	51,19	52,24	51,58	52,05	64,32	63,38	64,31	62,37	62,15	63,08	61,35
Mg	1,52	1,43	1,41	1,40	0,79	0,22	0,18	0,74	0,64	0,28	0,43
Fe	1,29	1,46	1,19	1,16	0,63	0,76	0,65	1,17	1,14	0,66	0,66
Mn	0,71	0,64	0,52	0,64	0,30	0,28	0,25	0,51	0,44	0,37	0,24
CO2	43,06	43,85	43,07	43,48	51,91	50,62	51,22	50,79	50,44	50,44	49,17
total	97,77	99,62	97,77	98,73	117,95	115,26	116,61	115,58	114,81	114,83	111,85
normed on 1cation											
Ca	0,933	0,935	0,940	0,939	0,972	0,983	0,985	0,964	0,967	0,981	0,979
Mg	0,039	0,036	0,036	0,035	0,017	0,005	0,004	0,016	0,014	0,006	0,010
Fe	0,018	0,020	0,017	0,016	0,007	0,009	0,008	0,014	0,014	0,008	0,008
Mn	0,010	0,009	0,007	0,009	0,004	0,003	0,003	0,006	0,005	0,005	0,003
CO3	1	1	1	1	1	1	1	1	1	1	1

sample	Bk 9	Bk 9	Bk 9	Bk 9	Bk 97Th	Bk 97Th	Bk 97Th	Bk 97Th	Bk 97Th	Bk 97Th	Bk 97Th
analysis	14	15	17	18	54	55	56	57	58	59	60
date	4.3.94	4.3.94	4.3.94	4.3.94	11.6.94	11.6.94	11.6.94	11.6.94	11.6.94	11.6.94	11.6.94
CL colour					orange	orange	orange	brown	orange	yellow	yellow
Ca	63,48	63,99	65,16	65,04	57,01	54,98	54,81	53,11	54,26	53,71	54,35
Mg	0,60	0,44	0,89	0,78	0,38	0,37	0,29	0,75	0,19	0,24	0,28
Fe	0,67	0,65	1,31	1,28	0,43	0,54	0,39	0,64	0,45	0,38	0,40
Mn	0,34	0,37	0,37	0,41	0,41	0,48	0,43	0,41	0,41	0,41	0,33
CO2	51,09	51,33	53,14	52,93	45,67	44,18	43,84	43,14	43,32	42,90	43,41
total	116,18	116,78	120,87	120,44	103,90	100,55	99,76	98,05	98,63	97,64	98,77
normed on 1cation											
Ca	0,975	0,978	0,962	0,964	0,980	0,977	0,981	0,966	0,983	0,983	0,983
Mg	0,013	0,009	0,018	0,016	0,009	0,009	0,007	0,019	0,005	0,006	0,007
Fe	0,008	0,008	0,015	0,015	0,006	0,007	0,005	0,009	0,006	0,005	0,006
Mn	0,004	0,004	0,004	0,005	0,006	0,007	0,006	0,006	0,006	0,006	0,005
CO3	1	1	1	1	1	1	1	1	1	1	1

sample	Bk 97Th	Bk 97Th	Bk 97Th	Bk 97Th	Bk 97Th	Bk 97Th	Bk 97Th	Bk 97Th	Bk 97Th	Bk 97Th
analysis	61	62	63	64	65	66	67	68	69	70
date	11.6.94	11.6.94	11.6.94	11.6.94	11.6.94	11.6.94	11.6.94	11.6.94	11.6.94	11.6.94
CL colour	brown	brown	brown	brown	brown	brown	brown	orange	orange	yellow
Ca	53,72	53,40	53,77	53,34	53,50	53,59	54,46	53,35	54,10	53,85
Mg	0,46	0,34	0,33	0,62	0,51	0,32	0,53	0,26	0,25	0,26
Fe	0,54	0,55	0,55	0,85	0,61	0,79	0,57	0,50	0,49	0,39
Mn	0,35	0,35	0,35	0,57	0,40	0,48	0,26	0,38	0,37	0,41
CO2	43,21	42,83	43,11	43,41	43,16	43,19	43,83	42,69	43,26	43,04
total	98,28	97,47	98,11	98,79	98,18	98,37	99,65	97,18	98,47	97,95
normed on 1cation										
Ca	0,976	0,978	0,979	0,964	0,973	0,974	0,975	0,981	0,981	0,982
Mg	0,012	0,009	0,008	0,016	0,013	0,008	0,013	0,007	0,006	0,007
Fe	0,008	0,008	0,008	0,012	0,009	0,011	0,008	0,007	0,007	0,006
Mn	0,005	0,005	0,005	0,008	0,006	0,007	0,004	0,006	0,005	0,006
CO3	1	1	1	1	1	1	1	1	1	1

sample	Bk 10B	Bk 10B	Bk 10B	Bk 10B	Bk 17	Bk 17	Bk 17	Bk 17	Bk 17	Bk 17	Bk 17
analysis	5	13	45	32	39	41	42	43	44	46	56
date	18.10.93	18.10.93	18.10.93	19.10.93a	13.7.94	13.7.94	13.7.94	13.7.94	13.7.94	13.7.94	3.7.94
position	sympl	sympl	sympl	sympl	sympl	sympl	grt ps	grt ps	grt ps	sympl	sympl
SiO2	69,37	70,32	67,45	68,76	67,64	67,94	66,31	66,33	66,01	68,09	68,40
Al2O3	20,06	20,25	19,80	19,70	19,65	20,08	21,20	20,87	21,14	19,79	19,98
Fe2O3	0,26	0,23	0,18	0,44	0,04	0,08	0,10	0,07	0,03	0,12	0,21
CaO	0,50	0,19	0,68	0,56	0,22	0,62	1,93	1,72	1,97	0,67	0,50
BaO	0,03	0,00	1,31	0,01	0,03	0,00	0,03	0,00	0,00	0,00	0,18
Na2O	11,27	10,66	10,83	11,06	10,98	11,06	10,44	10,35	10,28	11,06	11,25
K2O	0,07	0,08	0,10	0,05	0,05	0,07	0,07	0,07	0,10	0,06	0,03
Total	101,56	101,73	100,35	100,58	98,61	99,85	100,08	99,41	99,53	99,79	100,55
normed on 8 oxygen, all Fe assumed Fe3											
Si	2,979	2,999	2,963	2,978	2,989	2,970	2,906	2,922	2,908	2,978	2,972
Al	1,015	1,018	1,025	1,006	1,023	1,035	1,095	1,083	1,098	1,020	1,023
Fe3	0,020	0,018	0,013	0,034	0,003	0,006	0,008	0,005	0,003	0,009	0,016
	4,014	4,036	4,002	4,018	4,016	4,011	4,008	4,010	4,008	4,007	4,011
Ca	0,023	0,009	0,032	0,026	0,010	0,029	0,091	0,081	0,093	0,031	0,023
Ba	0,001	0,000	0,023	0,000	0,001	0,000	0,001	0,000	0,000	0,000	0,003
Na	0,938	0,882	0,922	0,929	0,941	0,938	0,887	0,884	0,878	0,938	0,948
K	0,004	0,004	0,006	0,003	0,003	0,004	0,004	0,004	0,006	0,003	0,002
	0,966	0,895	0,983	0,958	0,955	0,971	0,982	0,969	0,977	0,973	0,976
sum	4,980	4,930	4,984	4,976	4,970	4,981	4,990	4,979	4,985	4,980	4,987
An%	2,382	0,970	3,257	2,713	1,091	2,992	9,226	8,376	9,519	3,228	2,385

sample	Bk 17	Bk 17	Bk 17	Bk 17	Bk 17	Bk 17	Bk 17	Bk 17	Bk 17	Bk 17	Bk 17
analysis	57	58	59	60	61	62	63	64	3	14	15
date	3.7.94	3.7.94	3.7.94	3.7.94	3.7.94	3.7.94	3.7.94	3.7.94	9.7.94	9.7.94	9.7.94
position	sympl	sympl	sympl	sympl	sympl	sympl	sympl	sympl	sympl	sympl	sympl
SiO2	67,89	67,69	66,34	68,14	66,13	68,16	68,25	68,28	66,93	68,74	68,34
Al2O3	19,72	19,70	20,65	19,82	20,49	19,62	19,53	19,63	20,33	19,76	19,95
Fe2O3	0,08	0,08	0,12	0,17	0,12	0,06	0,04	0,07	0,34	0,07	0,06
CaO	0,47	0,35	1,42	0,48	1,43	0,29	0,26	0,21	1,25	0,31	0,37
BaO	0,03	0,06	0,00	0,03	0,09	0,00	0,05	0,01	0,02	0,00	0,00
Na2O	10,78	11,32	10,20	11,17	10,46	11,19	11,36	11,15	10,79	11,38	11,28
K2O	0,05	0,06	0,05	0,04	0,06	0,06	0,03	0,05	0,03	0,05	0,02
Total	99,02	99,26	98,78	99,85	98,78	99,38	99,52	99,40	99,69	100,31	100,02
normed on 8 oxygen, all Fe assumed Fe3											
Si	2,987	2,979	2,934	2,978	2,931	2,991	2,992	2,993	2,935	2,989	2,981
Al	1,023	1,022	1,076	1,021	1,070	1,015	1,009	1,014	1,051	1,013	1,026
Fe3	0,006	0,006	0,009	0,013	0,009	0,004	0,003	0,005	0,026	0,005	0,004
	4,016	4,006	4,019	4,011	4,010	4,009	4,005	4,013	4,013	4,007	4,010
Ca	0,022	0,017	0,067	0,022	0,068	0,014	0,012	0,010	0,059	0,014	0,017
Ba	0,001	0,001	0,000	0,001	0,002	0,000	0,001	0,000	0,000	0,000	0,000
Na	0,920	0,966	0,875	0,946	0,899	0,952	0,966	0,948	0,918	0,960	0,954
K	0,003	0,003	0,003	0,002	0,003	0,003	0,002	0,003	0,002	0,003	0,001
	0,945	0,987	0,945	0,972	0,972	0,969	0,981	0,961	0,978	0,977	0,972
sum	4,961	4,993	4,964	4,983	4,982	4,978	4,986	4,973	4,991	4,984	4,983
An%	2,344	1,672	7,122	2,313	6,988	1,407	1,246	1,027	6,004	1,479	1,778

position: sympl is albite in symplectite, grt ps is albite in chlorite albite epidoze aggregates after garnet, vein is albite in veins

sample	Bk 17	Bk 17	Bk 17	Bk 17	Bk 17	Bk 17	Bk 17	Bk 17	Bk 17	Bk 17	Bk 18
analysis	16	17	18	19	20	21	22	23	52	53	17
date	9.7.94	9.7.94	9.7.94	9.7.94	9.7.94	9.7.94	9.7.94	9.7.94	9.7.94	9.7.94	5.8.94
position	vein	vein	vein	vein	vein	vein	sympl	sympl	sympl	sympl	sympl
SiO2	66,45	66,19	66,65	66,53	67,45	66,47	68,63	68,94	68,52	68,77	67,97
Al2O3	21,27	20,97	20,83	20,92	20,38	20,70	19,61	19,58	19,39	19,53	20,29
Fe2O3	0,08	0,08	0,08	0,11	0,13	0,14	0,21	0,09	0,10	0,20	0,13
CaO	1,82	1,82	1,65	1,67	1,22	1,67	0,11	0,05	0,09	0,13	0,84
BaO	0,00	0,00	0,00	0,05	0,01	0,00	0,00	0,00	0,00	0,00	0,00
Na2O	10,46	10,42	10,55	10,44	10,89	10,41	11,34	11,26	11,27	11,50	10,62
K2O	0,06	0,03	0,07	0,04	0,04	0,06	0,03	0,02	0,02	0,02	0,03
Total	100,14	99,51	99,83	99,76	100,12	99,45	99,93	99,94	99,39	100,15	99,88
normed on 8 oxygen, all Fe assumed Fe3											
Si	2,908	2,914	2,924	2,920	2,947	2,925	2,991	3,003	3,002	2,993	2,966
Al	1,097	1,088	1,077	1,082	1,049	1,074	1,007	1,005	1,001	1,002	1,044
Fe3	0,006	0,006	0,006	0,008	0,010	0,011	0,016	0,007	0,008	0,015	0,010
	4,011	4,008	4,007	4,011	4,006	4,010	4,015	4,015	4,011	4,010	4,020
Ca	0,085	0,086	0,078	0,079	0,057	0,079	0,005	0,002	0,004	0,006	0,039
Ba	0,000	0,000	0,000	0,001	0,000	0,000	0,000	0,000	0,000	0,000	0,000
Na	0,888	0,890	0,897	0,889	0,922	0,888	0,958	0,951	0,957	0,970	0,899
K	0,003	0,002	0,004	0,002	0,002	0,003	0,002	0,001	0,001	0,001	0,002
	0,976	0,977	0,979	0,970	0,982	0,970	0,965	0,954	0,963	0,978	0,940
sum	4,987	4,985	4,986	4,981	4,988	4,980	4,980	4,969	4,974	4,988	4,959
An%	8,741	8,787	7,923	8,095	5,815	8,114	0,532	0,244	0,439	0,620	4,180

sample	Bk 18	Bk 39	Bk 39	Bk 39	Bk 39	Bk 39	Bk 39	Bk 39	Bk 39.1	Bk 39.1	Bk 39.1
analysis	18	11	33	54	55	59	60	6	21	25	26
date	5.8.94	13.3.93	13.3.93	24.6.92	24.6.92	24.6.92	24.6.92	5.5.92	28.8.92	28.8.92	28.8.92
position	sympl	sympl	sympl	sympl	sympl	sympl	sympl	sympl	sympl	sympl	sympl
SiO2	68,68	69,02	67,82	69,13	68,22	68,38	66,69	67,24	67,28	68,80	69,21
Al2O3	20,08	20,10	19,44	20,08	19,85	20,23	20,61	19,35	19,88	19,75	20,76
Fe2O3	0,33	0,00	0,29	0,21	0,52	0,29	0,26	0,40	0,08	0,12	0,06
CaO	0,28	0,36	0,44	0,17	0,51	0,29	0,93	0,54	0,61	0,31	0,36
BaO	0,01	0,00	0,18	0,02	0,11	0,05	0,00	0,05	0,10	0,00	0,00
Na2O	10,90	11,50	11,57	11,16	10,57	11,27	10,83	11,26	11,46	11,46	10,58
K2O	0,11	0,02	0,03	0,01	0,02	0,02	0,02	0,02	0,00	0,03	0,03
Total	100,39	101,00	99,77	100,78	99,80	100,53	99,34	98,86	99,41	100,47	101,00
normed on 8 oxygen, all Fe assumed Fe3											
Si	2,977	2,983	2,974	2,985	2,973	2,966	2,933	2,970	2,963	2,987	2,978
Al	1,026	1,024	1,005	1,022	1,020	1,034	1,068	1,007	1,032	1,011	1,053
Fe3	0,026	0,000	0,022	0,016	0,040	0,022	0,019	0,030	0,006	0,009	0,004
	4,029	4,006	4,001	4,024	4,033	4,022	4,021	4,008	4,000	4,007	4,035
Ca	0,013	0,017	0,021	0,008	0,024	0,013	0,044	0,026	0,029	0,014	0,017
Ba	0,000	0,000	0,003	0,000	0,002	0,001	0,000	0,001	0,002	0,000	0,000
Na	0,916	0,964	0,984	0,934	0,893	0,948	0,923	0,964	0,978	0,965	0,883
K	0,006	0,001	0,002	0,001	0,001	0,001	0,001	0,001	0,000	0,002	0,002
	0,935	0,981	1,009	0,943	0,920	0,963	0,968	0,992	1,009	0,981	0,901
sum	4,964	4,988	5,010	4,967	4,953	4,985	4,989	4,999	5,009	4,988	4,936
An%	1,390	1,699	2,048	0,834	2,589	1,399	4,525	2,576	2,852	1,470	1,842

sample	Bk 39.1	Bk 7	Bk 7	Bk 8	Bk 8	Bk 9	Bk 9	Bk 9	Bk 9	Bk 9	Bk 9
analysis	45	27	36	13	60	25	26	17	18	19	20
date	28.8.92	27.8.92	27.8.92	14.3.93	14.3.93	2.7.94	2.7.94	24.2.94	24.2.94	24.2.94	24.2.94
position	sympl	sympl	sympl	sympl	sympl	sympl	sympl	sympl	sympl	sympl	sympl
SiO2	68,80	68,20	68,90	68,48	69,08	67,45	67,51	68,58	68,68	68,62	68,70
Al2O3	19,48	20,94	20,96	20,34	18,75	19,99	20,18	20,12	20,15	20,10	20,03
Fe2O3	0,93	0,22	0,09	0,58	0,78	0,07	0,09	0,22	0,28	0,10	0,21
CaO	0,84	0,44	0,54	0,87	0,74	0,70	0,91	0,48	0,23	0,25	0,27
BaO	0,00	0,05	0,00	0,00	0,03	0,00	0,00	0,01	0,09	0,05	0,00
Na2O	10,14	11,14	10,75	10,08	9,87	10,89	10,98	11,01	11,09	11,31	11,23
K2O	0,03	0,04	0,05	0,23	0,05	0,07	0,06	0,04	0,09	0,05	0,04
Total	100,22	101,03	101,29	100,58	99,30	99,17	99,73	100,46	100,61	100,48	100,48
normed on 8 oxygen, all Fe assumed Fe3											
Si	2,977	2,945	2,962	2,960	3,012	2,969	2,958	2,974	2,975	2,979	2,979
Al	0,993	1,066	1,062	1,036	0,964	1,037	1,042	1,029	1,029	1,028	1,024
Fe3	0,072	0,017	0,007	0,045	0,060	0,005	0,007	0,017	0,021	0,008	0,016
	4,042	4,028	4,031	4,041	4,035	4,011	4,007	4,020	4,025	4,015	4,019
Ca	0,039	0,020	0,025	0,040	0,035	0,033	0,043	0,022	0,011	0,012	0,013
Ba	0,000	0,001	0,000	0,000	0,001	0,000	0,000	0,000	0,002	0,001	0,000
Na	0,851	0,933	0,896	0,845	0,834	0,929	0,933	0,926	0,931	0,952	0,944
K	0,002	0,002	0,003	0,013	0,003	0,004	0,003	0,002	0,005	0,003	0,002
	0,891	0,956	0,924	0,898	0,872	0,966	0,979	0,951	0,949	0,967	0,959
sum	4,933	4,985	4,955	4,939	4,908	4,978	4,987	4,971	4,973	4,982	4,978
An%	4,369	2,129	2,693	4,487	3,963	3,416	4,364	2,346	1,125	1,202	1,308

position: sympl is albite in symplectite, grt ps is albite in chlorite albite epidoze aggregates after garnet, vein is albite in veins

sample	Bk 9	Bk 9	Bk 9	Cig91-1
analysis	21	22	23	34
date	24.2.94	24.2.94	24.2.94	17.6.93
position	sympl	sympl	sympl	sympl
SiO2	68,48	69,53	68,69	64,21
Al2O3	20,12	20,10	20,03	21,28
Fe2O3	0,26	0,19	0,17	3,03
CaO	0,41	0,15	0,24	0,85
BaO	0,00	0,00	0,10	0,00
Na2O	10,99	11,31	11,29	10,03
K2O	0,05	0,04	0,05	0,14
Total	100,30	101,32	100,57	99,54
normed on 8 oxygen, all Fe assumed Fe3				
Si	2,974	2,988	2,979	2,798
Al	1,030	1,018	1,024	1,093
Fe3	0,020	0,015	0,013	0,232
	4,023	4,020	4,016	4,123
Ca	0,019	0,007	0,011	0,040
Ba	0,000	0,000	0,002	0,000
Na	0,925	0,942	0,949	0,847
K	0,003	0,002	0,003	0,008
	0,947	0,951	0,965	0,895
sum	4,970	4,972	4,981	5,017
An%	2,014	0,726	1,156	4,434

position: sympl is albite in symplectite, grt ps is albite in chlorite albite epidoze aggregates after garnet, vein is albite in veins

---

sample	Bk 10 B	Bk 10 B	Bk 10 B	Bk 10 B	Bk 10 B	Bk 10 B	Bk 10 B	Bk 10 B	Bk 10 B	Bk 10 B	Bk 18
analysis	8	9	10	15	3	5	9	16	18	19	9
date	19.10.93b	19.10.93b	19.10.93b	19.10.93b	26.11.93	26.11.93	26.11.93	26.11.93	26.11.93	26.11.93	5.8.94
SiO2	41,31	40,90	39,39	41,24	38,38	41,53	41,47	39,94	41,35	38,30	41,16
TiO2	0,12	0,06	0,08	0,02	0,17	0,17	0,02	0,11	0,06	0,05	0,25
Al2O3	11,75	11,74	13,99	12,21	14,86	12,85	11,93	13,83	14,21	15,92	12,60
Cr2O3	0,00	0,02	0,00	0,02	0,00	0,01	0,00	0,00	0,02	0,01	0,02
Fe2O3	10,32	10,13	10,05	10,02	9,12	8,35	8,36	7,65	7,77	7,40	5,79
FeO	13,92	14,73	13,85	13,76	15,24	14,17	15,10	15,36	13,01	15,65	15,82
MnO	0,23	0,16	0,27	0,23	0,21	0,20	0,22	0,15	0,15	0,17	0,28
MgO	6,67	6,37	6,08	6,79	5,30	6,64	6,59	6,29	7,52	5,21	7,40
CaO	9,28	9,37	9,70	9,37	9,74	9,52	9,57	9,85	9,86	9,79	11,37
ZnO	0,27	0,18	0,33	0,04	0,25	0,19	0,17	0,00	0,22	0,17	0,29
Na2O	2,88	2,90	2,74	2,79	2,82	2,46	2,79	2,89	2,79	2,80	2,12
K2O	0,68	0,72	0,88	0,70	1,04	0,84	0,70	0,83	0,74	1,15	0,62
H2O	1,96	1,95	1,95	1,96	1,93	1,96	1,95	1,95	1,99	1,93	1,97
total	99,39	99,22	99,32	99,16	99,07	98,89	98,87	98,84	99,69	98,54	99,69
normed on 23 oxygens, Fe3 over Si+Ti+Al+Fe+Mn+Mg+Ca+Zn = 13											
Si	6,320	6,293	6,052	6,303	5,950	6,343	6,373	6,152	6,224	5,943	6,274
Alt	1,680	1,707	1,948	1,697	2,050	1,657	1,627	1,848	1,776	2,057	1,726
Alo	0,439	0,423	0,586	0,503	0,665	0,657	0,534	0,662	0,745	0,854	0,538
Fe3	1,189	1,173	1,162	1,153	1,064	0,959	0,967	0,887	0,880	0,864	0,664
Cr	0,000	0,002	0,000	0,002	0,000	0,001	0,000	0,000	0,002	0,001	0,002
Ti	0,010	0,005	0,007	0,002	0,014	0,014	0,002	0,009	0,005	0,004	0,029
Mg	1,521	1,461	1,392	1,547	1,225	1,512	1,509	1,444	1,687	1,205	1,681
Fe2	1,781	1,895	1,780	1,759	1,976	1,810	1,940	1,978	1,638	2,030	2,016
Mn	0,030	0,021	0,035	0,030	0,028	0,026	0,029	0,020	0,019	0,022	0,036
Zn	0,031	0,020	0,037	0,005	0,029	0,021	0,019	0,000	0,024	0,019	0,033
Ca	1,521	1,545	1,597	1,534	1,618	1,558	1,576	1,626	1,590	1,628	1,857
Na	0,479	0,455	0,403	0,466	0,382	0,442	0,424	0,374	0,410	0,372	0,143
	2,000	2,000	2,000	2,000	2,000	2,000	2,000	2,000	2,000	2,000	2,000
Na	0,376	0,410	0,413	0,361	0,465	0,286	0,407	0,489	0,404	0,470	0,484
K	0,136	0,144	0,176	0,139	0,210	0,167	0,140	0,167	0,145	0,233	0,123
	0,511	0,554	0,589	0,501	0,676	0,454	0,547	0,655	0,549	0,702	0,607
sum	15,511	15,554	15,589	15,501	15,676	15,454	15,547	15,655	15,549	15,702	15,607
OH	2	2	2	2	2	2	2	2	2	2	2
name	mag-hst-hbl	mag-hst-hbl	mag-has	mag-hst-hbl	mag-has	fer-act-hbl	mag-hst-hbl	mag-has	mag-has	mag-has	mag-hst-hbl

amphibole names after Leake (1978): ed-hbl is edenitic-hornblende, fer-act-hbl is ferro-actinolitic-hornblende, fer-par is ferroan-pargasite, fer-par-hbl is ferroan-pargasitic-hornblende, mag-has is magnesian-hastingite, mag-hst-hbl is magnesian-hastingitic-hornblende, tscherm is tschermakite

sample	Bk 18	Bk 39	Bk 39	Bk 39	Bk 7	Bk 7	Bk 7	Bk 7	Bk 7	Bk 8	Bk 8
analysis	12	21	22	24	25	11	13	7	8	24	25
date	5.8.94	23.3.92	23.3.92	23.3.92	6.7.92	7.7.92	7.7.92	7.8.92	7.8.92	14.3.93	14.3.93
SiO2	40,23	40,20	39,60	41,44	40,97	43,27	44,88	40,72	43,08	41,24	42,54
TiO2	0,22	0,03	0,06	0,22	0,08	0,10	0,10	0,05	0,10	0,07	0,00
Al2O3	12,54	13,06	13,67	14,91	15,73	13,96	12,35	15,48	14,67	15,32	13,46
Cr2O3	0,00	0,00	0,01	0,00	0,03	0,00	0,00	0,03	0,00	0,00	0,04
Fe2O3	13,20	5,49	6,78	2,74	3,69	3,00	4,11	5,58	4,15	4,66	5,54
FeO	8,65	13,63	12,92	12,76	11,85	14,11	12,81	10,90	10,44	13,49	13,62
MnO	0,22	0,21	0,21	0,12	0,21	0,20	0,13	0,21	0,16	0,28	0,28
MgO	8,66	8,58	8,45	9,04	9,31	8,19	9,45	9,58	10,14	7,72	7,79
CaO	10,30	9,65	9,68	9,04	10,10	8,68	8,68	10,07	9,43	9,38	9,08
ZnO	0,15	n.a	n.a	n.a	n.a	n.a	n.a	0,16	0,31	0,11	0,19
Na2O	1,74	4,29	4,20	4,49	3,74	4,16	4,17	4,00	3,89	3,84	3,81
K2O	0,51	0,34	0,40	0,47	0,41	0,47	0,31	0,31	0,44	0,43	0,23
H2O	1,97	1,94	1,95	1,97	1,99	1,99	2,02	2,00	2,02	1,98	1,98
total	98,40	97,42	97,93	97,19	98,11	98,13	99,01	99,09	98,83	98,52	98,57
normed on 23 oxygens, Fe3 over Si+Ti+Al+Fe+Mn+Mg+Ca+Zn = 13											
Si	6,113	6,214	6,097	6,306	6,170	6,525	6,669	6,091	6,382	6,238	6,431
Alt	1,887	1,786	1,903	1,694	1,830	1,475	1,331	1,909	1,618	1,762	1,569
Alo	0,359	0,593	0,578	0,979	0,963	1,006	0,831	0,821	0,943	0,969	0,830
Fe3	1,510	0,638	0,786	0,313	0,418	0,340	0,459	0,628	0,463	0,530	0,630
Cr	0,000	0,000	0,001	0,000	0,004	0,000	0,000	0,004	0,000	0,000	0,005
Ti	0,025	0,002	0,005	0,018	0,006	0,008	0,008	0,004	0,008	0,006	0,000
Mg	1,961	1,977	1,939	2,050	2,090	1,841	2,093	2,136	2,239	1,741	1,755
Fe2	1,099	1,762	1,664	1,623	1,492	1,780	1,592	1,364	1,293	1,706	1,723
Mn	0,028	0,027	0,027	0,015	0,027	0,026	0,016	0,027	0,020	0,036	0,036
Zn	0,017	-	-	-	-	-	-	0,018	0,034	0,012	0,021
Ca	1,677	1,598	1,597	1,474	1,630	1,402	1,382	1,614	1,497	1,520	1,471
Na	0,323	0,402	0,403	0,526	0,370	0,598	0,618	0,386	0,503	0,480	0,529
	2,000	2,000	2,000	2,000	2,000	2,000	2,000	2,000	2,000	2,000	2,000
Na	0,190	0,884	0,851	0,798	0,722	0,619	0,583	0,774	0,614	0,646	0,588
K	0,101	0,068	0,080	0,093	0,080	0,092	0,060	0,060	0,085	0,085	0,045
	0,291	0,952	0,931	0,892	0,802	0,711	0,643	0,835	0,699	0,731	0,633
sum	15,291	15,952	15,931	15,892	15,802	15,711	15,643	15,835	15,699	15,731	15,633
OH	2	2	2	2	2	2	2	2	2	2	2
name	tscherm	mag-has	mag-has	fer-par-hbl	fer-par	ed-hbl	ed-hbl	fer-par	fer-par-hbl	fer-par	fer-par-hbl

sample	Bk 8	Bk 8	Cig 91-1	Cig 91-1
analysis	28	29	68	69
date	14.3.93	14.3.93	17.6.93	17.6.93
SiO2	41,65	42,28	41,16	42,56
TiO2	0,08	0,07	0,08	0,06
Al2O3	14,58	13,96	18,38	17,09
Cr2O3	0,00	0,03	0,00	0,00
Fe2O3	6,55	6,43	1,95	3,03
FeO	13,09	12,86	14,52	13,48
MnO	0,32	0,22	0,17	0,13
MgO	7,42	7,94	7,18	7,85
CaO	9,09	8,79	9,07	8,76
ZnO	0,25	0,12	0,00	0,01
Na2O	3,77	4,07	4,42	4,36
K2O	0,33	0,30	0,61	0,55
H2O	1,99	1,99	2,01	2,03
total	99,12	99,06	99,55	99,92
normed on 23 oxygens, Fe3 over Si+Ti+Al+Fe+Mn+Mg+Ca+Zn = 13				
Si	6,277	6,355	6,128	6,280
Alt	1,723	1,645	1,872	1,720
Alo	0,866	0,828	1,353	1,251
Fe3	0,743	0,727	0,218	0,337
Cr	0,000	0,004	0,000	0,000
Ti	0,006	0,006	0,006	0,005
Mg	1,667	1,779	1,593	1,726
Fe2	1,649	1,616	1,807	1,663
Mn	0,041	0,028	0,021	0,016
Zn	0,028	0,013	0,000	0,001
Ca	1,468	1,416	1,447	1,385
Na	0,532	0,584	0,553	0,615
	2,000	2,000	2,000	2,000
Na	0,569	0,602	0,723	0,632
K	0,065	0,059	0,118	0,106
	0,634	0,660	0,841	0,738
sum	15,634	15,660	15,841	15,738
OH	2	2	2	2
name	fer-par-hbl	fer-par-hbl	fer-par	fer-par-hbl

amphibole names after Leake (1978): ed-hbl is edenitic-hornblende, fer-act-hbl is ferro-actinolitic-hornblende, fer-par is ferroan-pargasite, fer-par-hbl is ferroan-pargasitic-hornblende, mag-has is magnesian-hastingite, mag-hst-hbl is magnesian-hastingitic-hornblende, tscherm is tschermakite

sample	Bk 10 B	Bk 10 B	Bk 10 B	Bk 10 B	Bk 18	Bk 18	Bk 18	Bk 18	Bk 18	Bk 18	Bk 39
analysis	20	21	5	7	13	2	5	6	7	8	26
date	18.10.93	18.10.93	19.10.93b	19.10.93b	5.8.94	6.8.94	6.8.94	6.8.94	6.8.94	6.8.94	24.6.92
SiO2	49,60	50,50	46,96	46,55	49,31	52,00	49,18	48,84	48,97	51,25	45,40
TiO2	0,05	0,10	0,54	0,17	0,19	0,19	0,13	0,21	0,20	0,15	0,24
Al2O3	8,46	8,08	7,94	7,37	5,05	8,53	5,06	5,77	5,78	8,46	10,75
Cr2O3	0,00	0,00	0,01	0,02	0,00	0,00	0,01	0,00	0,03	0,03	0,03
Fe2O3	4,79	4,94	8,63	8,52	9,56	2,75	7,80	9,72	10,02	4,35	5,40
FeO	9,35	8,33	13,18	13,27	10,41	9,00	12,60	11,43	11,40	9,05	11,64
MnO	0,17	0,09	0,26	0,26	0,51	0,14	0,41	0,36	0,40	0,14	0,15
MgO	12,74	13,18	8,41	8,80	10,87	12,41	10,56	9,97	9,97	11,91	10,03
CaO	9,93	9,58	8,60	9,19	8,94	7,49	9,85	8,30	8,52	7,30	8,25
ZnO	0,37	0,16	0,21	0,27	0,20	0,20	0,15	0,18	0,27	0,05	n.a.
Na2O	2,41	2,18	2,45	2,28	2,10	3,44	1,78	2,67	2,52	3,52	4,17
K2O	0,26	0,22	0,29	0,30	0,18	0,14	0,16	0,20	0,22	0,13	0,32
H2O	2,09	2,09	2,01	1,99	2,03	2,09	2,03	2,03	2,04	2,08	2,01
total	100,22	99,45	99,49	98,99	99,35	98,37	99,72	99,67	100,34	98,42	98,39
normed on 23 oxygens, Fe3 over Si+Ti+Al+Fe+Mn+Mg+Ca+Zn = 13											
Si	7,131	7,246	7,013	7,005	7,277	7,465	7,277	7,218	7,199	7,394	6,776
Alt	0,869	0,754	0,987	0,995	0,723	0,535	0,723	0,782	0,801	0,606	1,224
Alo	0,564	0,612	0,411	0,313	0,156	0,909	0,160	0,223	0,200	0,832	0,667
Fe3	0,518	0,534	0,970	0,964	1,062	0,297	0,868	1,080	1,109	0,473	0,607
Cr	0,000	0,000	0,001	0,002	0,000	0,000	0,001	0,000	0,003	0,003	0,004
Ti	0,004	0,008	0,043	0,014	0,021	0,021	0,014	0,023	0,022	0,016	0,019
Mg	2,730	2,819	1,872	1,974	2,391	2,656	2,329	2,196	2,185	2,561	2,231
Fe2	1,124	1,000	1,646	1,670	1,285	1,080	1,560	1,412	1,402	1,092	1,453
Mn	0,021	0,011	0,033	0,033	0,064	0,017	0,051	0,045	0,050	0,017	0,019
Zn	0,039	0,017	0,023	0,030	0,022	0,021	0,016	0,020	0,029	0,005	-
Ca	1,530	1,473	1,376	1,482	1,414	1,152	1,562	1,314	1,342	1,128	1,319
Na	0,470	0,527	0,624	0,518	0,586	0,848	0,438	0,686	0,658	0,872	0,681
	2,000	2,000	2,000	2,000	2,000	2,000	2,000	2,000	2,000	2,000	2,000
Na	0,201	0,079	0,086	0,147	0,015	0,110	0,072	0,079	0,060	0,113	0,526
K	0,049	0,041	0,056	0,059	0,035	0,026	0,031	0,039	0,042	0,024	0,062
	0,250	0,120	0,142	0,206	0,049	0,136	0,103	0,118	0,102	0,137	0,588
sum	15,250	15,120	15,142	15,206	15,049	15,136	15,103	15,118	15,102	15,137	15,588
OH	2	2	2	2	2	2	2	2	2	2	2
name	mag-hbl	mag-hbl	mag-hbl	mag-hbl	ac-hbl	barr	ac-hbl	barr	mag-hbl	barr	mag-kat

sample	Bk 39	Bk 39	Bk 39	Bk 7	Bk 7	Bk 7	Bk 8	Bk 8	Bk 9	Bk 9	Bk 9
analysis	29	37	40	26	45	52	23	24	8	9	5
date	24.6.92	24.6.92	24.6.92	7.8.92	7.8.92	7.8.92	29.1.93b	29.1.93b	2.7.94	2.7.94	23.2.94
SiO2	49,33	50,48	46,85	50,38	47,59	52,27	48,78	48,09	50,67	48,96	47,33
TiO2	0,19	0,12	0,10	0,09	0,04	0,04	0,16	0,14	0,05	0,03	0,05
Al2O3	10,30	10,36	9,66	7,22	8,16	3,86	11,61	9,26	6,52	9,95	8,22
Cr2O3	0,05	0,02	0,02	0,02	0,01	0,06	0,01	0,01	0,00	0,00	0,04
Fe2O3	3,79	4,99	3,35	2,57	4,14	2,28	1,42	4,28	3,71	3,53	2,06
FeO	11,34	7,55	9,47	9,10	6,90	6,82	11,44	8,88	6,39	7,98	10,58
MnO	0,08	0,07	0,15	0,20	0,17	0,19	0,11	0,06	0,07	0,09	0,13
MgO	9,62	11,33	12,64	13,78	15,09	17,34	11,07	13,21	16,19	13,40	13,35
CaO	5,35	4,81	9,11	9,26	11,00	11,79	8,23	9,85	11,37	9,59	11,76
ZnO	n.a.	n.a.	n.a.	0,22	0,18	0,25	0,16	0,20	0,25	0,13	0,16
Na2O	5,33	5,46	3,81	3,15	2,59	1,52	4,03	3,04	1,74	2,89	1,69
K2O	0,18	0,13	0,23	0,17	0,15	0,09	0,29	0,31	0,17	0,19	0,23
H2O	2,04	2,07	2,02	2,06	2,05	2,09	2,07	2,07	2,10	2,08	2,02
total	97,60	97,39	97,41	98,22	98,06	98,60	99,39	99,40	99,23	98,82	97,62
normed on 23 oxygens, Fe3 over Si+Ti+Al+Fe+Mn+Mg+Ca+Zn = 13											
Si	7,258	7,309	6,944	7,329	6,960	7,509	7,053	6,976	7,246	7,057	7,023
Alt	0,742	0,691	1,056	0,671	1,040	0,491	0,947	1,024	0,754	0,943	0,977
Alo	1,044	1,077	0,631	0,567	0,367	0,162	1,032	0,559	0,345	0,748	0,461
Fe3	0,420	0,544	0,374	0,281	0,455	0,247	0,154	0,467	0,400	0,383	0,230
Cr	0,006	0,002	0,002	0,002	0,001	0,007	0,001	0,001	0,000	0,000	0,005
Ti	0,015	0,009	0,008	0,007	0,003	0,003	0,012	0,011	0,005	0,003	0,006
Mg	2,110	2,445	2,792	2,988	3,290	3,713	2,386	2,856	3,451	2,879	2,953
Fe2	1,395	0,914	1,173	1,107	0,844	0,819	1,384	1,077	0,764	0,962	1,312
Mn	0,010	0,009	0,019	0,025	0,021	0,023	0,013	0,007	0,008	0,011	0,016
Zn	-	-	-	0,024	0,019	0,027	0,017	0,021	0,026	0,014	0,018
Ca	0,843	0,746	1,447	1,443	1,724	1,815	1,275	1,531	1,742	1,481	1,870
Na	1,157	1,254	0,553	0,557	0,276	0,185	0,725	0,469	0,258	0,519	0,130
	2,000	2,000	2,000	2,000	2,000	2,000	2,000	2,000	2,000	2,000	2,000
Na	0,364	0,279	0,542	0,332	0,458	0,238	0,405	0,386	0,225	0,289	0,356
K	0,035	0,025	0,044	0,032	0,029	0,017	0,055	0,059	0,032	0,036	0,044
	0,398	0,303	0,586	0,364	0,487	0,255	0,459	0,444	0,256	0,324	0,400
sum	15,398	15,303	15,586	15,364	15,487	15,255	15,459	15,444	15,256	15,324	15,400
OH	2	2	2	2	2	2	2	2	2	2	2
name	barr	barr	ed	ac-hbl	mag-hbl	act	barr	mag-hbl	mag-hbl	mag-hbl	mag-hbl

amphibole names after Leake (1978): ac-hbl is actinolitic-hornblende, act is actinolite, barr is barroisite, ed is edenite, ed-hbl is edenitic-hornblende, mag-hbl is magnesio-hornblende, mag-kat is magnesio-katophorite

sample	Cig 91-1	Cig 91-1	Cig 91-1	Cig 91-1
analysis	31	76	77	78
date	16.6.93	17.6.93	17.6.93	17.6.93
SiO2	48,18	52,19	54,36	45,40
TiO2	0,12	0,14	0,07	0,26
Al2O3	14,00	10,82	12,01	11,95
Cr2O3	0,02	0,01	0,01	0,00
Fe2O3	4,12	1,80	0,99	2,02
FeO	11,10	8,99	10,41	11,21
MnO	0,07	0,08	0,05	0,13
MgO	8,89	12,02	9,84	11,96
CaO	5,85	5,83	2,94	10,71
ZnO	0,00	0,04	0,00	0,09
Na2O	5,19	5,16	6,46	3,12
K2O	0,35	0,20	0,09	0,39
H2O	2,09	2,12	2,14	2,04
total	99,98	99,40	99,37	99,28
normed on 23 oxygens, Fe3 over Si+Ti+Al+Fe+Mn+Mg+Ca+Zn = 13				
Si	6,924	7,382	7,622	6,667
Alt	1,076	0,618	0,378	1,333
Alo	1,296	1,185	1,606	0,735
Fe3	0,446	0,192	0,104	0,223
Cr	0,002	0,001	0,001	0,000
Ti	0,009	0,011	0,005	0,021
Mg	1,904	2,534	2,056	2,618
Fe2	1,334	1,063	1,221	1,377
Mn	0,009	0,010	0,006	0,016
Zn	0,000	0,004	0,000	0,010
Ca	0,901	0,883	0,442	1,685
Na	1,099	1,117	1,558	0,315
	2,000	2,000	2,000	2,000
Na	0,347	0,299	0,198	0,573
K	0,066	0,037	0,016	0,075
	0,413	0,335	0,214	0,648
sum	15,413	15,335	15,214	15,648
OH	2	2	2	2
name	barr	barr	gln	ed-hbl

sample	Bk 10 B	Bk 10 B	Bk 10 B	Bk 10 B	Bk 10 B	Bk 10 B	Bk 10 B	Bk 10 B	Bk 10 B	Bk 10 B	Bk 10 B
analysis	16	1 q	8 q	9 q	10 q	11 q	12 q	16	17	31 q	32 q
date	19.10.93	18.10.93	18.10.93	18.10.93	18.10.93	18.10.93	18.10.93	18.10.93	18.10.93	18.10.93	18.10.93
SiO2	51,55	54,79	55,51	52,29	55,60	54,22	53,64	51,72	53,18	54,41	54,56
TiO2	0,08	0,03	0,03	0,08	0,04	0,07	0,10	0,02	0,02	0,09	0,11
Al2O3	6,84	1,79	1,62	5,18	1,67	3,63	4,17	6,18	5,12	3,53	3,53
Cr2O3	0,05	0,08	0,00	0,03	0,20	0,00	0,00	0,02	0,00	0,18	0,11
Fe2O3	1,75	2,89	0,89	2,95	1,60	3,07	2,67	3,37	4,99	0,64	0,86
FeO	8,69	9,08	9,84	9,17	9,22	8,90	8,77	8,16	7,26	8,93	9,85
MnO	0,04	0,14	0,12	0,16	0,15	0,13	0,20	0,12	1,15	0,07	0,10
MgO	14,71	16,42	16,83	14,75	16,94	15,50	15,51	15,30	15,22	16,78	16,03
CaO	10,61	12,01	12,06	10,75	12,01	10,86	11,02	10,93	11,01	11,94	11,44
ZnO	0,15	0,35	0,19	0,18	0,16	0,35	0,00	0,20	0,26	0,06	0,31
Na2O	1,77	0,61	0,75	1,62	0,72	1,36	1,17	1,93	1,53	0,95	1,38
K2O	0,17	0,03	0,07	0,15	0,06	0,12	0,13	0,17	0,15	0,11	0,12
H2O	2,08	2,11	2,11	2,09	2,13	2,12	2,10	2,11	2,14	2,12	2,12
total	98,49	100,33	100,02	99,39	100,50	100,32	99,48	100,23	102,03	99,81	100,53
normed on 23 oxygens, Fe3 over Si+Ti+Al+Fe+Mn+Mg+Ca+Zn = 13											
Si	7,418	7,776	7,873	7,503	7,843	7,682	7,643	7,353	7,442	7,703	7,713
Alt	0,582	0,224	0,127	0,497	0,157	0,318	0,357	0,647	0,558	0,297	0,287
Alo	0,578	0,075	0,144	0,379	0,121	0,288	0,343	0,388	0,286	0,292	0,301
Fe3	0,189	0,309	0,095	0,318	0,169	0,327	0,286	0,360	0,526	0,069	0,092
Cr	0,006	0,009	0,000	0,003	0,022	0,000	0,000	0,002	0,000	0,020	0,012
Ti	0,006	0,002	0,002	0,006	0,003	0,005	0,008	0,002	0,002	0,007	0,008
Mg	3,155	3,473	3,558	3,155	3,562	3,273	3,294	3,242	3,174	3,541	3,378
Fe2	1,045	1,077	1,167	1,100	1,088	1,054	1,045	0,970	0,849	1,057	1,165
Mn	0,005	0,017	0,014	0,019	0,018	0,016	0,024	0,014	0,136	0,008	0,012
Zn	0,016	0,037	0,020	0,019	0,017	0,037	0,000	0,021	0,027	0,006	0,032
Ca	1,636	1,826	1,833	1,653	1,815	1,648	1,682	1,665	1,651	1,811	1,733
Na	0,364	0,168	0,167	0,347	0,185	0,352	0,318	0,335	0,349	0,189	0,267
	2,000	1,994	2,000	2,000	2,000	2,000	2,000	2,000	2,000	2,000	2,000
Na	0,130	0,000	0,039	0,103	0,012	0,022	0,006	0,197	0,066	0,072	0,111
K	0,032	0,006	0,013	0,028	0,011	0,022	0,024	0,031	0,027	0,020	0,022
	0,161	0,006	0,052	0,131	0,023	0,044	0,030	0,228	0,093	0,092	0,133
sum	15,161	15,006	15,052	15,131	15,023	15,044	15,030	15,228	15,093	15,092	15,133
OH	2	2	2	2	2	2	2	2	2	2	2
name	act-hbl	act	act	act	act	act	act	act-hbl	act-hbl	act	act

amphibole names after Leake (1978): ac-hbl is actinolitic-hornblende, act is actinolite, barr is barroisite, ed is edenite, ed-hbl is edenitic-hornblende, mag-hbl is magnesio-hornblende, mag-kat is magnesio-katophorite

sample	Bk 10 B	Bk 10 B	Bk 10 B	Bk 10 B	Bk 10 B	Bk 10 B	Bk 10 B	Bk 17	Bk 17	Bk 17	Bk 17
analysis	35 q	39 q	42	10 q	11 q	12	13	27 q	28 q	29	52
date	18.10.93	18.10.93	18.10.93	26.11.93	26.11.93	26.11.93	26.11.93	25.7.94	25.7.94	25.7.94	3.7.94
SiO2	55,66	53,50	51,84	54,85	54,29	51,71	49,99	51,72	52,21	52,44	47,42
TiO2	0,09	0,11	0,09	0,03	0,05	0,13	0,14	0,11	0,09	0,07	0,21
Al2O3	3,11	4,69	6,04	1,34	1,88	5,87	6,83	4,23	3,78	3,89	10,63
Cr2O3	0,20	0,22	0,06	0,00	0,06	0,04	0,02	0,04	0,02	0,01	0,01
Fe2O3	0,10	2,41	3,50	1,81	2,42	3,83	4,48	3,14	3,60	4,04	4,37
FeO	9,47	8,23	7,07	9,20	8,99	8,25	8,56	10,41	10,37	10,35	9,75
MnO	0,12	0,14	0,09	0,08	0,12	0,10	0,20	0,18	0,20	0,27	0,13
MgO	16,54	16,02	15,75	16,93	16,38	14,74	13,93	14,28	14,30	14,08	11,55
CaO	11,24	11,21	10,86	12,24	11,74	10,63	10,65	10,89	10,95	10,63	9,03
ZnO	0,02	0,20	0,10	0,38	0,30	0,18	0,16	0,01	0,00	0,02	0,06
Na2O	1,27	1,46	1,68	0,56	0,77	1,62	1,73	1,50	1,29	1,50	3,14
K2O	0,10	0,16	0,19	0,11	0,08	0,17	0,21	0,16	0,13	0,13	0,30
H2O	2,13	2,12	2,10	2,10	2,09	2,09	2,07	2,06	2,07	2,08	2,05
total	100,05	100,48	99,37	99,63	99,17	99,36	98,97	98,74	99,01	99,50	98,65
normed on 23 oxygens, Fe3 over Si+Ti+Al+Fe+Mn+Mg+Ca+Zn = 13											
Si	7,840	7,551	7,387	7,828	7,785	7,412	7,244	7,526	7,574	7,574	6,932
Alt	0,160	0,449	0,613	0,172	0,215	0,588	0,756	0,474	0,426	0,426	1,068
Alo	0,356	0,332	0,402	0,054	0,103	0,404	0,411	0,252	0,220	0,236	0,764
Fe3	0,011	0,256	0,375	0,194	0,262	0,413	0,488	0,344	0,393	0,439	0,480
Cr	0,022	0,025	0,007	0,000	0,007	0,005	0,002	0,005	0,002	0,001	0,001
Ti	0,007	0,008	0,007	0,002	0,004	0,010	0,011	0,012	0,010	0,008	0,023
Mg	3,472	3,370	3,345	3,602	3,501	3,149	3,009	3,097	3,092	3,031	2,517
Fe2	1,115	0,971	0,843	1,098	1,078	0,989	1,037	1,267	1,258	1,250	1,192
Mn	0,014	0,017	0,011	0,010	0,015	0,012	0,025	0,022	0,025	0,033	0,016
Zn	0,002	0,021	0,011	0,040	0,032	0,019	0,017	0,001	0,000	0,002	0,006
Ca	1,696	1,695	1,658	1,872	1,804	1,633	1,654	1,698	1,702	1,645	1,414
Na	0,304	0,305	0,342	0,128	0,196	0,367	0,346	0,302	0,298	0,355	0,586
	2,000	2,000	2,000	2,000	2,000	2,000	2,000	2,000	2,000	2,000	2,000
Na	0,043	0,095	0,122	0,027	0,018	0,083	0,140	0,121	0,065	0,065	0,304
K	0,018	0,029	0,035	0,020	0,015	0,032	0,040	0,030	0,025	0,024	0,057
	0,061	0,124	0,158	0,047	0,033	0,115	0,179	0,151	0,089	0,090	0,362
sum	15,061	15,124	15,158	15,047	15,033	15,115	15,179	15,151	15,089	15,090	15,362
OH	2	2	2	2	2	2	2	2	2	2	2
name	act	act	act-hbl	act	act	act-hbl	mag-hbl	act	act	act	mag-hbl

sample	Bk 17	Bk 17	Bk 17	Bk 17	Bk 17	Bk 17	Bk 17	Bk 17	Bk 17	Bk 17	Bk 17
analysis	53	54	55	4	6	7 q	8 q	10	42	50	51
date	3.7.94	3.7.94	3.7.94	9.7.94	9.7.94	9.7.94	9.7.94	9.7.94	9.7.94	9.7.94	9.7.94
SiO2	47,18	48,70	46,87	54,17	51,88	53,51	51,77	50,82	46,45	50,60	50,27
TiO2	0,20	0,16	0,25	0,07	0,12	0,06	0,12	0,15	0,25	0,14	0,16
Al2O3	10,35	7,68	9,16	2,85	5,41	2,50	4,02	6,73	10,09	6,68	7,38
Cr2O3	0,01	0,03	0,04	0,03	0,03	0,03	0,05	0,15	0,05	0,03	0,02
Fe2O3	4,36	5,94	6,07	3,37	5,08	2,38	5,27	5,29	6,18	4,31	4,87
FeO	9,61	9,77	10,13	9,56	8,89	10,85	11,10	9,05	11,22	10,42	9,39
MnO	0,14	0,30	0,32	0,24	0,29	0,26	0,21	0,21	0,15	0,44	0,32
MgO	11,96	12,31	11,01	15,05	13,62	14,68	12,95	12,96	10,42	12,53	12,89
CaO	9,25	9,72	9,17	10,49	9,56	10,97	10,00	9,15	9,30	9,39	9,46
ZnO	0,00	0,00	0,12	0,07	0,12	0,06	0,08	0,00	0,03	0,00	0,03
Na2O	3,21	2,47	2,75	1,44	2,08	1,16	1,79	2,47	2,85	2,55	2,56
K2O	0,32	0,26	0,33	0,07	0,14	0,09	0,17	0,16	0,39	0,19	0,20
H2O	2,05	2,06	2,02	2,09	2,08	2,07	2,06	2,08	2,04	2,07	2,08
total	98,63	99,40	98,25	99,50	99,30	98,61	99,60	99,22	99,42	99,35	99,63
normed on 23 oxygens, Fe3 over Si+Ti+Al+Fe+Mn+Mg+Ca+Zn = 13											
Si	6,907	7,102	6,948	7,754	7,472	7,769	7,525	7,338	6,840	7,341	7,251
Alt	1,093	0,898	1,052	0,246	0,528	0,231	0,475	0,662	1,160	0,659	0,749
Alo	0,693	0,422	0,548	0,235	0,390	0,197	0,214	0,484	0,591	0,483	0,506
Fe3	0,480	0,652	0,677	0,363	0,551	0,260	0,577	0,575	0,685	0,470	0,529
Cr	0,001	0,003	0,005	0,003	0,003	0,003	0,006	0,017	0,006	0,003	0,002
Ti	0,022	0,018	0,028	0,008	0,013	0,007	0,013	0,016	0,028	0,015	0,017
Mg	2,610	2,676	2,433	3,211	2,924	3,177	2,806	2,789	2,287	2,709	2,771
Fe2	1,176	1,192	1,256	1,144	1,071	1,317	1,350	1,093	1,382	1,265	1,132
Mn	0,017	0,037	0,040	0,029	0,035	0,032	0,026	0,026	0,019	0,054	0,039
Zn	0,000	0,000	0,013	0,007	0,013	0,006	0,009	0,000	0,003	0,000	0,003
Ca	1,451	1,519	1,456	1,609	1,475	1,707	1,557	1,416	1,467	1,460	1,462
Na	0,549	0,481	0,544	0,391	0,525	0,293	0,443	0,584	0,533	0,540	0,538
	2,000	2,000	2,000	2,000	2,000	2,000	2,000	2,000	2,000	2,000	2,000
Na	0,362	0,217	0,247	0,008	0,056	0,033	0,062	0,107	0,281	0,177	0,178
K	0,061	0,049	0,064	0,013	0,026	0,017	0,032	0,030	0,075	0,036	0,038
	0,423	0,267	0,310	0,021	0,082	0,050	0,094	0,137	0,356	0,213	0,216
sum	15,423	15,267	15,310	15,021	15,082	15,050	15,094	15,137	15,356	15,213	15,216
OH	2	2	2	2	2	2	2	2	2	2	2
name	mag-hbl	mag-hbl	mag-hbl	act	act-hbl	act	act	act-hbl	mag-hbl	act-hbl	act-hbl

analysis q is in contact with quartz, amphibole names after Leake (1978): ac-hbl is actinolitic-hornblende, act is actinolite, barr is barroisite, ed is edenite, ed-hbl is edenitic-hornblende, mag-hbl is magnesio-hornblende

sample	Bk 18	Bk 18	Bk 18	Bk 18	Bk 18	Bk 18	Bk 39	Bk 39	Bk 39	Bk 39	Bk 7
analysis	50 q	51	53	14	15	16 q	25	27	52	53	55
date	25.7.94	25.7.94	25.7.94	5.8.94	5.8.94	5.8.94	13.3.93	13.3.93	24.6.92	24.6.92	7.7.92
SiO2	52,36	50,25	51,68	49,65	52,58	53,16	50,53	51,45	49,03	49,01	46,90
TiO2	0,03	0,07	0,06	0,13	0,09	0,10	0,17	0,08	0,11	0,10	0,15
Al2O3	4,47	5,45	5,44	8,99	6,06	5,22	6,63	6,46	6,99	7,84	10,55
Cr2O3	0,07	0,02	0,07	0,11	0,08	0,05	0,02	0,02	0,03	0,00	0,04
Fe2O3	1,31	3,86	4,00	3,42	6,04	2,51	1,08	3,28	2,85	2,88	1,72
FeO	8,85	8,39	7,98	8,79	4,69	7,80	8,17	7,47	8,68	9,06	10,49
MnO	0,16	0,23	0,20	0,13	0,10	0,16	0,08	0,11	0,09	0,08	0,18
MgO	16,10	14,87	14,83	12,77	15,85	15,40	15,83	15,57	14,76	13,86	12,07
CaO	11,82	11,33	10,39	8,97	9,51	10,13	10,78	10,25	10,56	9,63	9,28
ZnO	0,22	0,30	0,21	0,21	0,23	0,19	0,11	0,21	0,00	0,00	0,00
Na2O	1,29	1,48	1,82	2,94	2,19	1,91	2,55	2,67	2,68	3,18	3,58
K2O	0,12	0,15	0,16	0,20	0,13	0,11	0,22	0,18	0,19	0,19	0,24
H2O	2,08	2,06	2,08	2,07	2,13	2,10	2,07	2,11	2,05	2,05	2,02
total	98,89	98,46	98,92	98,38	99,67	98,84	98,24	99,86	98,01	97,89	97,22
normed on 23 oxygens, Fe3 over Si+Ti+Al+Fe+Mn+Mg+Ca+Zn = 13											
Si	7,531	7,320	7,440	7,199	7,414	7,588	7,312	7,326	7,176	7,176	6,955
Alt	0,469	0,680	0,560	0,801	0,586	0,412	0,688	0,674	0,824	0,824	1,045
Alo	0,288	0,256	0,363	0,736	0,421	0,467	0,443	0,410	0,381	0,529	0,799
Fe3	0,142	0,423	0,434	0,373	0,641	0,270	0,117	0,352	0,314	0,318	0,192
Cr	0,008	0,002	0,008	0,013	0,009	0,006	0,002	0,002	0,003	0,000	0,005
Ti	0,003	0,008	0,006	0,014	0,010	0,011	0,013	0,006	0,009	0,008	0,012
Mg	3,451	3,229	3,182	2,760	3,331	3,277	3,414	3,304	3,220	3,025	2,668
Fe2	1,065	1,022	0,960	1,066	0,553	0,931	0,989	0,890	1,062	1,110	1,302
Mn	0,019	0,028	0,024	0,016	0,012	0,019	0,010	0,013	0,011	0,010	0,023
Zn	0,023	0,032	0,022	0,022	0,024	0,020	0,012	0,022	0,000	0,000	0,000
Ca	1,821	1,768	1,603	1,394	1,437	1,549	1,671	1,564	1,656	1,511	1,475
Na	0,179	0,232	0,397	0,606	0,563	0,451	0,329	0,436	0,344	0,489	0,525
	2,000	2,000	2,000	2,000	2,000	2,000	2,000	2,000	2,000	2,000	2,000
Na	0,181	0,186	0,111	0,220	0,035	0,078	0,387	0,301	0,416	0,414	0,504
K	0,022	0,028	0,030	0,038	0,024	0,020	0,041	0,033	0,036	0,036	0,046
	0,204	0,215	0,141	0,258	0,059	0,098	0,428	0,334	0,453	0,450	0,550
sum	15,204	15,215	15,141	15,258	15,059	15,098	15,428	15,334	15,453	15,450	15,550
OH	2	2	2	2	2	2	2	2	2	2	2
name	act	act-hbl	act-hbl	mag-hbl	act-hbl	act	act-hbl	act-hbl	mag-hbl	mag-hbl	edenite

sample	Bk 7	Bk 7	Bk 8	Bk 8	Bk 8	Bk 8	Bk 8	Bk 8	Bk 8	Bk 9	Bk 9
analysis	43	47	5	17	18	56 q	57 q	2 q	34 q	21	22
date	7.8.92	7.8.92	14.3.93	14.3.93	14.3.93	14.3.93	14.3.93	29.1.93b	29.1.93b	2.7.94	2.7.94
SiO2	46,57	47,26	49,98	51,23	48,24	54,68	54,97	53,11	54,38	50,13	50,37
TiO2	0,06	0,04	0,15	0,03	0,05	0,03	0,00	0,08	0,04	0,04	0,02
Al2O3	9,65	9,51	8,95	6,46	10,67	1,13	0,56	3,43	1,50	7,85	8,62
Cr2O3	0,03	0,00	0,08	0,00	0,00	0,02	0,00	0,06	0,04	0,07	0,04
Fe2O3	3,05	3,37	3,04	0,62	2,86	2,34	0,93	0,70	3,22	0,49	0,02
FeO	10,18	9,64	8,07	8,83	8,18	8,49	10,24	9,70	8,40	8,26	8,99
MnO	0,19	0,21	0,12	0,11	0,10	0,06	0,04	0,06	0,04	0,15	0,09
MgO	12,44	12,86	13,80	15,53	13,26	17,02	16,63	15,57	16,49	15,48	14,71
CaO	10,01	10,10	9,20	10,70	9,37	11,44	11,87	10,73	11,10	11,65	11,27
ZnO	0,20	0,15	0,16	0,19	0,23	0,18	0,23	0,18	0,26	0,14	0,21
Na2O	3,22	3,10	3,19	2,52	3,38	1,07	0,78	1,70	1,18	1,68	1,78
K2O	0,21	0,20	0,24	0,16	0,26	0,06	0,03	0,10	0,05	0,24	0,22
H2O	2,02	2,04	2,09	2,08	2,07	2,09	2,07	2,06	2,09	2,08	2,08
total	97,84	98,48	99,07	98,45	98,67	98,61	98,36	97,48	98,79	98,26	98,41
normed on 23 oxygens, Fe3 over Si+Ti+Al+Fe+Mn+Mg+Ca+Zn = 13											
Si	6,906	6,939	7,179	7,393	6,980	7,858	7,950	7,734	7,815	7,237	7,255
Alt	1,094	1,061	0,821	0,607	1,020	0,142	0,050	0,266	0,185	0,763	0,745
Alo	0,593	0,584	0,695	0,492	0,799	0,049	0,046	0,323	0,069	0,573	0,718
Fe3	0,341	0,372	0,329	0,067	0,311	0,253	0,101	0,077	0,348	0,054	0,002
Cr	0,004	0,000	0,009	0,000	0,000	0,002	0,000	0,007	0,005	0,008	0,005
Ti	0,005	0,003	0,012	0,002	0,004	0,002	0,000	0,006	0,003	0,004	0,002
Mg	2,750	2,814	2,955	3,340	2,860	3,646	3,585	3,379	3,532	3,331	3,158
Fe2	1,263	1,184	0,970	1,065	0,989	1,020	1,239	1,181	1,010	0,997	1,082
Mn	0,024	0,026	0,015	0,013	0,012	0,007	0,005	0,007	0,005	0,018	0,011
Zn	0,022	0,016	0,017	0,020	0,025	0,019	0,025	0,019	0,028	0,015	0,022
Ca	1,590	1,589	1,416	1,654	1,453	1,761	1,839	1,674	1,709	1,802	1,739
Na	0,410	0,411	0,584	0,346	0,547	0,239	0,161	0,326	0,291	0,198	0,261
	2,000	2,000	2,000	2,000	2,000	2,000	2,000	2,000	2,000	2,000	2,000
Na	0,516	0,471	0,304	0,359	0,401	0,060	0,058	0,154	0,038	0,272	0,236
K	0,041	0,038	0,045	0,030	0,049	0,011	0,006	0,019	0,009	0,045	0,041
	0,557	0,510	0,349	0,390	0,450	0,071	0,064	0,173	0,047	0,317	0,278
sum	15,557	15,510	15,349	15,390	15,450	15,071	15,064	15,173	15,047	15,317	15,278
OH	2	2	2	2	2	2	2	2	2	2	2
name	edenite	edenite	mag-hbl	act-hbl	mag-hbl	act	act	act	act	mag-hbl	act-hbl

analysis q is in contact with quartz, amphibole names after Leake (1978): ac-hbl is actinolitic-hornblende, act is actinolite, barr is barroisite, ed is edenite, ed-hbl is edenitic-hornblende, mag-hbl is magnesio-hornblende

sample	Bk 9	Bk 9	Bk 9	Bk 9	Bk 9	Bk 9	Bk 9	Bk 9	Cig 91-1	Cig 91-1
analysis	6 q	8	12 q	13	27	29	22	23	73	74
date	23.2.94	23.2.94	23.2.94	23.2.94	24.2.94	24.2.94	4.3.94	4.3.94	17.6.93	17.6.93
SiO2	52,04	51,45	53,63	50,36	49,40	49,44	48,77	48,77	47,67	45,18
TiO2	0,12	0,08	0,05	0,12	0,00	0,14	0,14	0,17	0,28	0,26
Al2O3	4,99	6,81	4,35	8,09	8,10	8,46	9,26	8,58	8,82	12,61
Cr2O3	0,04	0,00	0,04	0,03	0,06	0,00	0,05	0,00	0,00	0,02
Fe2O3	0,85	1,96	0,07	1,76	2,73	1,69	3,68	2,83	0,98	1,63
FeO	9,16	8,12	9,29	8,81	7,98	9,60	10,30	10,59	9,38	10,11
MnO	0,05	0,11	0,08	0,12	0,05	0,07	0,15	0,15	0,09	0,12
MgO	15,62	14,74	16,25	13,95	14,56	13,45	12,30	12,67	15,05	12,40
CaO	11,43	10,05	11,49	10,03	10,57	9,99	9,96	10,27	11,68	10,24
ZnO	0,19	0,14	0,11	0,23	0,11	0,12	0,20	0,16	0,00	0,00
Na2O	1,39	2,15	1,42	2,37	2,31	2,54	2,60	2,45	2,66	3,55
K2O	0,13	0,14	0,08	0,18	0,14	0,21	0,25	0,25	0,33	0,40
H2O	2,07	2,07	2,10	2,07	2,07	2,05	2,07	2,06	2,06	2,04
total	98,09	97,82	98,95	98,13	98,07	97,76	99,73	98,95	99,00	98,55
normed on 23 oxygens, Fe3 over Si+Ti+Al+Fe+Mn+Mg+Ca+Zn = 13										
Si	7,533	7,435	7,660	7,293	7,172	7,221	7,059	7,113	6,939	6,640
Alt	0,467	0,565	0,340	0,707	0,828	0,779	0,941	0,887	1,061	1,360
Alo	0,384	0,594	0,392	0,674	0,558	0,677	0,638	0,588	0,453	0,824
Fe3	0,093	0,213	0,007	0,192	0,298	0,186	0,401	0,311	0,108	0,180
Cr	0,005	0,000	0,005	0,003	0,007	0,000	0,006	0,000	0,000	0,002
Ti	0,013	0,009	0,005	0,013	0,000	0,015	0,015	0,019	0,022	0,021
Mg	3,370	3,175	3,460	3,011	3,151	2,928	2,654	2,754	3,265	2,716
Fe2	1,109	0,981	1,109	1,068	0,969	1,172	1,247	1,292	1,141	1,242
Mn	0,006	0,013	0,010	0,015	0,006	0,009	0,018	0,019	0,011	0,015
Zn	0,020	0,015	0,012	0,025	0,012	0,013	0,021	0,017	0,000	0,000
Ca	1,773	1,556	1,758	1,556	1,644	1,563	1,545	1,605	1,822	1,612
Na	0,227	0,444	0,242	0,444	0,356	0,437	0,455	0,395	0,178	0,388
	2,000	2,000	2,000	2,000	2,000	2,000	2,000	2,000	2,000	2,000
Na	0,163	0,158	0,152	0,222	0,294	0,282	0,274	0,298	0,572	0,624
K	0,025	0,026	0,015	0,034	0,026	0,040	0,047	0,048	0,063	0,077
	0,187	0,185	0,167	0,256	0,321	0,322	0,321	0,345	0,635	0,701
sum	15,187	15,185	15,167	15,256	15,321	15,322	15,321	15,345	15,635	15,701
OH	2	2	2	2	2	2	2	2	2	2
name	act	act-hbl	act	act-hbl	mag-hbl	mag-hbl	mag-hbl	mag-hbl	edenite	ed-hbl

analysis q is in contact with quartz, amphibole names after Leake (1978): ac-hbl is actinolitic-hornblende, act is actinolite, barr is barroisite, ed is edenite, ed-hbl is edenitic-hornblende, mag-hbl is magnesio-hornblende

---

sample	Bk 10B	Bk 10B	Bk 10B	Bk 10B	Bk 17	Bk 17	Bk 39	Bk 39	Bk 39	Bk 39	Bk 39
analysis	7	8	9	10	46	44	67	16	27	14	15
date	19.10.93a	19.10.93a	19.10.93a	19.10.93a	3.7.94	9.7.94	28.1.93	28.7.92	28.7.92	3.7.94	3.7.94
SiO2	30,75	29,89	30,02	30,42	30,19	30,53	29,98	29,70	30,20	30,30	30,40
TiO2	36,67	38,48	37,34	37,15	37,79	36,25	37,41	37,78	37,03	37,55	37,08
Al2O3	2,03	1,38	1,98	1,99	1,42	2,64	1,76	1,45	2,05	1,68	1,56
Fe2O3	0,47	0,30	0,31	0,27	0,47	0,66	0,52	0,43	0,20	0,31	0,27
CaO	28,90	28,60	29,09	28,80	28,60	28,83	28,77	28,75	29,29	28,64	28,80
total	98,82	98,65	98,74	98,63	98,47	98,91	98,44	98,11	98,77	98,48	98,11
F	0,51	0,00	0,01	0,00	0,27	0,33	0,53	0,37	0,79	0,12	0,25
H2O	0,32	0,52	0,72	0,72	0,33	0,72	0,24	0,26	0,02	0,52	0,35
normed on 3 kations											
Si	1,002	0,982	0,981	0,995	0,992	0,992	0,984	0,980	0,985	0,994	1,000
Ti	0,899	0,951	0,917	0,913	0,934	0,886	0,923	0,937	0,908	0,926	0,917
Al	0,078	0,053	0,076	0,077	0,055	0,101	0,068	0,056	0,079	0,065	0,060
Fe3	0,011	0,007	0,008	0,007	0,012	0,016	0,013	0,011	0,005	0,008	0,007
Ca	1,009	1,007	1,018	1,009	1,007	1,004	1,012	1,016	1,023	1,007	1,015
sum	3,000	3,000	3,000	3,000	3,000	3,000	3,000	3,000	3,000	3,000	3,000
F	0,053	0,000	0,001	0,000	0,028	0,034	0,055	0,039	0,081	0,012	0,026
OH	0,037	0,061	0,083	0,083	0,038	0,083	0,026	0,029	0,002	0,060	0,041

sample	Bk 39	Bk 39	Bk 39	Bk 39	Bk 39	Bk 39	Bk 39	Bk 39	Bk 39	Bk 39	Bk 39
analysis	16	17	18	19	29	30	32	33	37	38	39
date	3.7.94	3.7.94	3.7.94	3.7.94	3.7.94	3.7.94	3.7.94	3.7.94	3.7.94	3.7.94	3.7.94
SiO2	30,39	30,39	30,26	30,29	30,38	30,42	30,51	30,40	30,27	30,49	30,32
TiO2	38,44	37,64	37,83	38,73	38,16	38,46	38,51	37,91	37,16	38,70	37,81
Al2O3	1,18	1,53	1,13	1,02	1,30	1,08	1,01	1,39	1,87	1,04	1,40
Fe2O3	0,36	0,32	0,39	0,40	0,30	0,28	0,32	0,39	0,58	0,38	0,38
CaO	28,61	28,80	28,85	28,50	28,75	28,82	28,67	28,55	28,52	28,40	28,75
total	98,98	98,68	98,46	98,94	98,89	99,06	99,02	98,64	98,40	99,01	98,66
F	0,23	0,27	0,02	0,01	0,01	0,00	0,00	0,00	0,20	0,14	0,36
H2O	0,26	0,34	0,44	0,42	0,49	0,42	0,41	0,55	0,57	0,30	0,23
normed on 3 kations											
Si	0,995	0,995	0,995	0,994	0,995	0,995	0,999	0,997	0,993	0,999	0,994
Ti	0,947	0,927	0,935	0,955	0,939	0,946	0,948	0,935	0,917	0,954	0,932
Al	0,046	0,059	0,044	0,039	0,050	0,042	0,039	0,054	0,072	0,040	0,054
Fe3	0,009	0,008	0,010	0,010	0,007	0,007	0,008	0,010	0,014	0,009	0,009
Ca	1,004	1,011	1,016	1,002	1,008	1,010	1,006	1,004	1,003	0,997	1,010
sum	3,000	3,000	3,000	3,000	3,000	3,000	3,000	3,000	3,000	3,000	3,000
F	0,024	0,028	0,002	0,001	0,001	0,000	0,000	0,000	0,021	0,015	0,037
OH	0,030	0,039	0,051	0,048	0,057	0,048	0,047	0,063	0,066	0,035	0,026

---

sample	Bk 39	Bk 39	Bk 39	Bk 39	Bk 7	Bk 7	Bk 7	Bk 7	Bk 7	Bk 7	Bk 4
analysis	66	40	10,2	11,2	46	47	48	49	51	18	1
date	28.1.93	3.7.94	5.5.92	5.5.92	2.7.94	2.7.94	2.7.94	2.7.94	2.7.94	7.7.92	27.6.94
SiO2	29,13	30,14	29,49	30,16	29,80	30,14	30,24	30,34	30,21	29,75	30,26
TiO2	37,16	38,04	38,40	36,75	37,35	36,35	38,05	38,30	37,77	35,94	37,21
Al2O3	1,46	1,16	0,80	1,63	1,78	2,43	1,43	1,05	1,70	2,51	1,93
Fe2O3	0,48	0,39	0,32	0,50	0,36	0,27	0,18	0,30	0,22	0,20	0,22
CaO	28,57	28,67	28,56	28,84	28,78	28,54	28,99	28,76	28,71	29,07	29,02
total	96,80	98,40	97,57	97,88	98,07	97,73	98,89	98,75	98,61	97,47	98,64
F	0,00	0,11	0,02	0,27	0,26	0,26	0,21	0,15	0,29	0,65	0,18
H2O	0,62	0,37	0,34	0,43	0,44	0,63	0,33	0,28	0,35	0,32	0,53
normed on 3 kations											
Si	0,974	0,992	0,981	0,994	0,981	0,992	0,989	0,996	0,990	0,980	0,989
Ti	0,934	0,942	0,961	0,911	0,925	0,900	0,936	0,945	0,931	0,891	0,915
Al	0,058	0,045	0,031	0,063	0,069	0,094	0,055	0,041	0,066	0,097	0,074
Fe3	0,012	0,010	0,008	0,012	0,009	0,007	0,004	0,007	0,005	0,005	0,005
Ca	1,023	1,011	1,018	1,019	1,016	1,007	1,016	1,011	1,008	1,026	1,016
sum	3,000	3,000	3,000	3,000	3,000	3,000	3,000	3,000	3,000	3,000	3,000
F	0,000	0,011	0,002	0,028	0,027	0,027	0,022	0,016	0,030	0,068	0,019
OH	0,070	0,043	0,037	0,048	0,051	0,074	0,038	0,032	0,041	0,035	0,061

---

sample	Bk 4	Bk 4	Bk 4	Bk 4	Bk 4	Bk 4	Bk 4	Bk 4	Bk 4	Bk 4	Bk 4
analysis	2	3	4	5	6	7	8	9	10	11	64
date	27.6.94	27.6.94	27.6.94	27.6.94	27.6.94	27.6.94	27.6.94	27.6.94	27.6.94	27.6.94	9.7.94
SiO2	30,36	30,47	30,48	30,07	30,29	30,46	30,64	30,29	30,49	30,37	30,33
TiO2	37,22	37,28	37,42	36,65	37,28	37,44	37,36	38,27	37,28	37,87	39,91
Al2O3	1,95	2,10	2,00	2,03	1,98	2,06	1,93	1,44	2,12	1,66	0,18
Fe2O3	0,22	0,17	0,27	0,18	0,24	0,20	0,26	0,21	0,17	0,17	0,42
CaO	29,03	28,92	28,98	28,95	28,91	29,06	29,03	28,97	29,01	28,90	28,91
total	98,78	98,94	99,15	97,88	98,70	99,22	99,22	99,18	99,07	98,97	99,75
F	0,06	0,17	0,23	0,09	0,12	0,06	0,13	0,27	0,00	0,34	0,11
H2O	0,64	0,58	0,52	0,67	0,60	0,72	0,62	0,30	0,79	0,30	0,05
normed on 3 kations											
Si	0,991	0,993	0,991	0,989	0,990	0,990	0,996	0,988	0,992	0,991	0,991
Ti	0,914	0,913	0,915	0,907	0,916	0,915	0,913	0,939	0,912	0,930	0,980
Al	0,075	0,081	0,077	0,079	0,076	0,079	0,074	0,055	0,081	0,064	0,007
Fe3	0,005	0,004	0,007	0,004	0,006	0,005	0,006	0,005	0,004	0,004	0,010
Ca	1,015	1,009	1,010	1,021	1,012	1,012	1,011	1,013	1,011	1,011	1,012
sum	3,000	3,000	3,000	3,000	3,000	3,000	3,000	3,000	3,000	3,000	3,000
F	0,006	0,018	0,024	0,009	0,012	0,006	0,013	0,028	0,000	0,035	0,011
OH	0,074	0,067	0,060	0,074	0,070	0,078	0,067	0,033	0,085	0,033	0,006

sample	Bk 9	Bk 9	Bk 9	Bk 9	Bk 9	Bk 9
analysis	4	5	12	13	14	15
date	2.7.94	2.7.94	2.7.94	2.7.94	2.7.94	2.7.94
SiO2	30,06	30,07	30,15	29,41	30,31	30,24
TiO2	37,67	36,90	38,21	36,85	37,37	38,11
Al2O3	1,69	2,00	1,39	1,58	1,70	1,48
Fe2O3	0,26	0,26	0,34	0,28	0,31	0,21
CaO	28,59	28,91	28,42	29,47	28,83	28,56
total	98,27	98,14	98,51	97,59	98,52	98,60
F	0,09	0,23	0,16	0,35	0,41	0,36
H2O	0,54	0,52	0,39	0,27	0,27	0,22
normed on 3 kations						
Si	0,989	0,988	0,991	0,972	0,993	0,993
Ti	0,932	0,911	0,945	0,916	0,921	0,941
Al	0,066	0,077	0,054	0,062	0,066	0,057
Fe3	0,006	0,006	0,009	0,007	0,008	0,005
Ca	1,008	1,017	1,001	1,044	1,012	1,004
sum	3,000	3,000	3,000	3,000	3,000	3,000
F	0,009	0,024	0,017	0,037	0,042	0,037
OH	0,062	0,060	0,046	0,032	0,031	0,025

sample	Bk 7	Bk 39	Bk 39	Bk 39	Bk 39	Bk 39	Bk 39	Bk 39	Bk 39
date	30.6.94	2.7.94	2.7.94	2.7.94	2.7.94	2.7.94	2.7.94	2.7.94	2.7.94
analysis	52	23	24	26	27	34	36	41	42
position	rt	rt	grt	grt	grt	rt	rt	rt	rt
TiO2	52,06	50,32	50,02	55,26	50,54	53,11	51,55	56,73	51,14
FeO	43,88	44,15	44,34	38,37	42,66	44,43	45,2	37,91	44,54
Mn	1,19	2,04	3,06	5,48	5,06	1,4	1,92	1,79	2,08
total	97,13	96,51	97,42	99,11	98,26	98,94	98,67	96,43	97,76
normed on 2 kations									
Ti	1,019	0,989	0,973	1,062	0,975	1,020	0,992	1,124	0,993
Fe	0,955	0,965	0,960	0,820	0,915	0,949	0,967	0,836	0,962
Mn	0,026	0,045	0,067	0,119	0,110	0,030	0,042	0,040	0,045

position: grt is ilmenite in garnet, rt is ilmenite in contact with rutile

sample	Cig 91-1	Cig 91-1	Cig 91-1	Cig 91-1	Cig 91-1	Cig 91-1	Cig 91-1	Cig 91-1	Cig 91-1	Cig 91-1	Cig 91-1
analysis	41	81	80	79	76	75	74	73	58	57	51
date	17.6.93	16.6.93	16.6.93	16.6.93	16.6.93	16.6.93	16.6.93	16.6.93	16.6.93	16.6.93	16.6.93
SiO2	34,56	34,70	33,69	33,71	35,78	34,06	34,30	34,45	36,18	35,61	34,91
TiO2	0,47	0,17	0,51	0,50	0,37	0,06	0,49	0,39	0,09	0,13	0,04
Al2O3	19,72	20,77	20,10	19,42	18,64	20,05	19,93	20,61	20,23	19,20	20,16
FeO	16,85	17,48	18,52	18,77	19,10	19,50	19,44	19,72	15,75	18,36	19,12
MnO	0,07	0,13	0,14	0,07	0,10	0,16	0,15	0,09	0,13	0,09	0,12
MgO	12,13	11,02	10,84	10,92	9,91	9,48	9,92	10,12	12,38	11,35	10,27
Na2O	0,52	0,67	0,59	0,49	0,40	0,38	0,39	0,45	0,25	0,28	0,29
K2O	9,79	9,05	8,85	8,40	9,33	9,70	9,69	9,54	9,62	9,65	9,50
F	0,19	0,00	0,34	0,27	0,00	0,00	0,00	0,00	0,00	0,06	0,00
H2O	1,87	1,96	1,77	1,78	1,94	1,92	1,94	1,96	2,00	1,94	1,95
total	94,11	93,99	93,24	92,28	93,63	93,39	94,31	95,37	94,63	94,67	94,41
normed on 22 oxygens, all Fe assumed Fe2											
Si	2,647	2,651	2,618	2,644	2,768	2,659	2,653	2,631	2,717	2,716	2,678
Alt	1,338	1,337	1,346	1,339	1,308	1,335	1,337	1,342	1,321	1,321	1,330
	3,985	3,988	3,963	3,983	4,076	3,994	3,990	3,973	4,038	4,037	4,009
Alo	0,442	0,533	0,495	0,456	0,391	0,510	0,480	0,512	0,470	0,405	0,493
Ti	0,019	0,007	0,021	0,021	0,015	0,003	0,020	0,016	0,004	0,005	0,002
	0,461	0,540	0,516	0,477	0,407	0,512	0,500	0,528	0,474	0,410	0,494
Fe	1,079	1,117	1,203	1,231	1,236	1,273	1,257	1,259	0,989	1,171	1,227
Mg	1,385	1,255	1,255	1,276	1,143	1,103	1,144	1,152	1,386	1,290	1,174
Mn	0,005	0,008	0,009	0,005	0,007	0,011	0,010	0,006	0,008	0,006	0,008
	2,469	2,380	2,468	2,512	2,385	2,387	2,411	2,417	2,383	2,467	2,409
Na	0,077	0,099	0,089	0,075	0,060	0,058	0,058	0,067	0,036	0,041	0,043
K	0,977	0,901	0,896	0,859	0,941	0,987	0,977	0,949	0,942	0,959	0,950
	1,055	1,000	0,985	0,933	1,001	1,045	1,035	1,016	0,978	1,001	0,993
sum	7,970	7,908	7,933	7,904	7,868	7,938	7,936	7,934	7,873	7,916	7,905
F	0,092	0,000	0,167	0,134	0,000	0,000	0,000	0,000	0,000	0,029	0,000
OH	1,908	2,000	1,833	1,866	2,000	2,000	2,000	2,000	2,000	1,971	2,000
Mg/(Mg+Fe)	0,562	0,529	0,511	0,509	0,480	0,464	0,476	0,478	0,583	0,524	0,489

sample	Bk 9	Bk 9	Bk 9	Bk 9	Bk 9	Bk 9	Bk 10 B	Bk 10 B	Bk 10 B	Bk 10 B	Bk 10 B
analysis	20	14	15	16	25	26	33	34	49	50	52
date	23.2.94	24.2.94	24.2.94	24.2.94	24.2.94	24.2.94	18.10.93	18.10.93	18.10.93	18.10.93	18.10.93
SiO2	45,27	47,26	48,16	48,38	45,99	46,74	52,09	53,01	49,79	52,18	50,37
TiO2	0,15	0,30	0,28	0,40	0,22	0,04	0,07	0,11	0,10	0,10	0,08
Al2O3	11,04	10,26	9,90	8,34	10,27	9,89	5,49	5,00	6,99	5,46	6,49
Cr2O3	0,05	0,01	0,04	0,10	0,00	0,02	0,00	0,01	0,00	0,00	0,00
Fe2O3	4,43	3,22	3,22	3,25	3,41	3,30	3,32	0,91	3,30	4,37	4,61
FeO	10,62	10,05	9,99	9,75	11,11	10,47	6,71	8,83	8,73	7,09	8,98
MnO	0,17	0,09	0,14	0,12	0,14	0,11	0,00	0,00	0,00	0,11	0,10
MgO	11,04	12,03	11,79	12,90	11,46	12,04	16,12	15,97	14,53	15,72	14,18
CaO	10,02	9,72	9,04	10,25	10,16	10,18	10,82	11,18	11,06	10,97	11,08
ZnO	0,12	0,07	0,17	0,18	0,16	0,10	0,70	0,07	0,00	0,25	0,25
Na2O	2,77	2,81	3,03	2,27	2,78	2,68	1,93	1,53	1,66	1,51	1,58
K2O	0,28	0,26	0,23	0,23	0,29	0,28	0,17	0,14	0,30	0,22	0,30
H2O	2,01	2,04	2,04	2,04	2,02	2,02	2,10	2,10	2,07	2,11	2,09
total	97,97	98,13	98,03	98,21	98,01	97,88	99,52	98,86	98,53	100,10	100,11
normed on 23 oxygens, Fe3 over Si+Ti+Al+Fe+Mn+Mg+Ca+Zn = 13											
Si	6,739	6,944	7,061	7,095	6,838	6,921	7,420	7,580	7,228	7,404	7,238
Alt	1,261	1,056	0,939	0,905	1,162	1,079	0,580	0,420	0,772	0,596	0,762
Alo	0,676	0,721	0,772	0,536	0,637	0,647	0,342	0,422	0,424	0,317	0,337
Fe3	0,496	0,357	0,356	0,359	0,381	0,367	0,356	0,098	0,361	0,467	0,499
Cr	0,006	0,001	0,005	0,012	0,000	0,002	0,000	0,001	0,000	0,000	0,000
Ti	0,017	0,033	0,031	0,044	0,025	0,004	0,007	0,012	0,011	0,011	0,009
Mg	2,449	2,635	2,577	2,820	2,540	2,657	3,423	3,404	3,144	3,325	3,037
Fe2	1,322	1,235	1,225	1,195	1,382	1,297	0,799	1,056	1,060	0,842	1,079
Mn	0,021	0,011	0,017	0,015	0,018	0,014	0,000	0,000	0,000	0,013	0,012
Zn	0,013	0,008	0,018	0,019	0,018	0,011	0,074	0,007	0,000	0,026	0,027
Ca	1,598	1,530	1,420	1,610	1,619	1,615	1,651	1,713	1,720	1,668	1,706
Na	0,402	0,470	0,580	0,390	0,381	0,385	0,349	0,287	0,280	0,332	0,294
	2,000	2,000	2,000	2,000	2,000	2,000	2,000	2,000	2,000	2,000	2,000
Na	0,397	0,331	0,282	0,256	0,420	0,384	0,184	0,137	0,188	0,083	0,146
K	0,054	0,050	0,044	0,044	0,056	0,054	0,032	0,026	0,057	0,041	0,056
	0,452	0,380	0,325	0,300	0,476	0,438	0,216	0,163	0,244	0,124	0,202
sum	15,452	15,380	15,325	15,300	15,476	15,438	15,216	15,163	15,244	15,124	15,202
OH	2	2	2	2	2	2	2	2	2	2	2
name	mag-hbl	mag-hbl	mag-hbl	mag-hbl	mag-hbl	mag-hbl	act-hbl	act	mag-hbl	act-hbl	mag-hbl

sample	Bk 10 B	Bk 10 B	Bk 10 B	Bk 10 B	Bk 10 B	Bk 18	Bk 18	Bk 18	Bk 18	Bk 18	Bk 18
analysis	54	55	2	3	4	52	55	56	57	58	2
date	18.10.93	18.10.93	19.10.93a	19.10.93a	19.10.93a	25.7.94	25.7.94	25.7.94	25.7.94	25.7.94	6.8.94
SiO2	50,52	50,26	47,24	50,20	50,94	49,57	52,85	51,72	52,96	48,73	52,00
TiO2	0,03	0,05	0,02	0,05	0,06	0,04	0,05	0,07	0,05	0,06	0,19
Al2O3	6,70	7,06	9,24	5,58	5,32	8,16	4,97	6,72	5,66	7,14	8,53
Cr2O3	0,04	0,09	0,00	0,00	0,02	0,06	0,04	0,04	0,03	0,06	0,00
Fe2O3	4,80	2,72	6,93	4,17	5,70	4,40	4,05	5,35	2,41	3,91	2,75
FeO	7,47	9,24	7,11	8,03	6,79	8,68	7,93	7,71	6,72	8,97	9,00
MnO	0,13	0,08	0,00	0,15	0,24	0,24	0,23	0,29	0,11	0,22	0,14
MgO	14,65	14,55	13,57	15,06	15,43	13,15	14,74	13,38	15,83	13,75	12,41
CaO	10,82	11,18	10,78	11,26	11,31	9,69	9,92	8,71	9,87	10,88	7,49
ZnO	0,50	0,35	0,00	0,25	0,30	0,32	0,24	0,26	0,13	0,28	0,20
Na2O	1,71	1,97	1,83	1,50	1,24	2,58	1,83	2,56	2,09	1,94	3,44
K2O	0,25	0,29	0,37	0,27	0,23	0,25	0,13	0,15	0,12	0,18	0,14
H2O	2,09	2,09	2,07	2,06	2,09	2,07	2,09	2,09	2,10	2,04	2,09
total	99,71	99,92	99,16	98,58	99,67	99,21	99,07	99,05	98,08	98,16	98,37
normed on 23 oxygens, Fe3 over Si+Ti+Al+Fe+Mn+Mg+Ca+Zn = 13											
Si	7,245	7,222	6,859	7,298	7,304	7,170	7,567	7,423	7,573	7,152	7,465
Alt	0,755	0,778	1,141	0,702	0,696	0,830	0,433	0,577	0,427	0,848	0,535
Alo	0,378	0,418	0,440	0,254	0,203	0,561	0,406	0,560	0,527	0,387	0,909
Fe3	0,518	0,294	0,758	0,456	0,615	0,479	0,436	0,578	0,259	0,431	0,297
Cr	0,005	0,010	0,000	0,000	0,002	0,007	0,005	0,005	0,003	0,007	0,000
Ti	0,003	0,005	0,002	0,005	0,006	0,004	0,005	0,008	0,005	0,007	0,021
Mg	3,132	3,116	2,937	3,263	3,298	2,835	3,146	2,862	3,374	3,008	2,656
Fe2	0,896	1,110	0,864	0,976	0,815	1,050	0,949	0,925	0,804	1,102	1,080
Mn	0,016	0,010	0,000	0,018	0,029	0,029	0,028	0,035	0,013	0,027	0,017
Zn	0,053	0,037	0,000	0,027	0,032	0,034	0,025	0,028	0,014	0,030	0,021
Ca	1,663	1,721	1,677	1,754	1,738	1,502	1,522	1,339	1,512	1,711	1,152
Na	0,337	0,279	0,323	0,246	0,262	0,498	0,478	0,661	0,488	0,289	0,848
	2,000	2,000	2,000	2,000	2,000	2,000	2,000	2,000	2,000	2,000	2,000
Na	0,138	0,270	0,192	0,177	0,082	0,225	0,030	0,052	0,092	0,263	0,110
K	0,047	0,054	0,070	0,051	0,043	0,047	0,024	0,028	0,022	0,034	0,026
	0,185	0,324	0,262	0,228	0,125	0,272	0,054	0,080	0,114	0,297	0,136
sum	15,185	15,324	15,262	15,228	15,125	15,272	15,054	15,080	15,114	15,297	15,136
OH	2	2	2	2	2	2	2	2	2	2	2
name	mag-hbl	mag-hbl	mag-hbl	act-hbl	act-hbl	mag-hbl	act	act-hbl	act	mag-hbl	barr

analysis vein is amphibole from a vein, amphibole names after Leake (1978): ac-hbl is actinolitic-hornblende, act is actinolite, barr is barroisite, mag-hbl is magnesio-hornblende

sample	Bk 18	Bk 18	Bk 18	Bk 17	Bk 17	Bk 17	Bk 18	Bk 18	Bk 18
analysis	3	4	8	12 vein	13 vein	11 vein	38 vein	37 vein	36 vein
date	6.8.94	6.8.94	6.8.94	9.7.94	9.7.94	9.7.94	25.7.94	25.7.94	25.7.94
SiO2	47,39	52,95	51,25	50,79	51,96	52,26	51,85	53,10	52,08
TiO2	0,06	0,05	0,15	0,11	0,08	0,08	0,16	0,06	0,15
Al2O3	9,77	4,97	8,46	3,34	2,20	2,15	3,02	2,34	4,40
Cr2O3	0,00	0,00	0,03	0,00	0,00	0,06	0,05	0,02	0,00
Fe2O3	4,30	0,11	4,35	2,18	1,78	1,24	2,61	2,03	2,15
FeO	9,73	10,58	9,05	15,28	15,52	15,82	11,30	9,73	12,42
MnO	0,12	0,15	0,14	0,50	0,49	0,53	0,24	0,21	0,25
MgO	12,06	14,25	11,91	11,93	12,13	12,19	14,17	15,45	13,14
CaO	9,71	9,91	7,30	11,83	11,84	11,95	11,27	11,31	10,45
ZnO	0,18	0,18	0,05	0,07	0,04	0,10	0,00	0,05	0,00
Na2O	2,77	2,09	3,52	0,88	0,54	0,56	1,07	0,88	1,75
K2O	0,31	0,11	0,13	0,17	0,12	0,12	0,10	0,09	0,17
H2O	2,04	2,06	2,08	2,02	2,02	2,02	2,04	2,05	2,06
total	98,44	97,41	98,42	99,11	98,72	99,08	97,88	97,31	99,01
normed on 23 oxygens, Fe3 over Si+Ti+Al+Fe+Mn+Mg+Ca+Zn = 13									
Si	6,959	7,710	7,394	7,547	7,724	7,742	7,633	7,772	7,592
Alt	1,041	0,290	0,606	0,453	0,276	0,258	0,367	0,228	0,408
Alo	0,649	0,563	0,832	0,132	0,109	0,117	0,157	0,175	0,348
Fe3	0,476	0,012	0,473	0,244	0,199	0,138	0,289	0,223	0,236
Cr	0,000	0,000	0,003	0,000	0,000	0,007	0,006	0,002	0,000
Ti	0,007	0,005	0,016	0,012	0,009	0,009	0,018	0,007	0,016
Mg	2,639	3,093	2,561	2,642	2,688	2,692	3,109	3,370	2,855
Fe2	1,194	1,288	1,092	1,899	1,929	1,959	1,391	1,191	1,514
Mn	0,015	0,019	0,017	0,063	0,062	0,067	0,030	0,026	0,031
Zn	0,020	0,019	0,005	0,008	0,004	0,011	0,000	0,005	0,000
Ca	1,528	1,546	1,128	1,883	1,886	1,897	1,778	1,774	1,632
Na	0,472	0,454	0,872	0,117	0,114	0,103	0,222	0,226	0,368
	2,000	2,000	2,000	2,000	2,000	2,000	2,000	2,000	2,000
Na	0,316	0,136	0,113	0,137	0,041	0,058	0,083	0,023	0,127
K	0,059	0,021	0,024	0,033	0,023	0,023	0,019	0,017	0,032
	0,376	0,157	0,137	0,170	0,065	0,081	0,102	0,040	0,159
sum	15,376	15,157	15,137	15,170	15,065	15,081	15,102	15,040	15,159
OH	2	2	2	2	2	2	2	2	2
name	mag-hbl	barr	act	act	act	act	act	act	act

analysis vein is amphibole from a vein, amphibole names after Leake (1978): ac-hbl is actinolitic-hornblende, act is actinolite, barr is barroisite, mag-hbl is magnesio-hornblende

---

sample	Bk 10B	Bk 10B	Bk 10B	Bk 10B	Bk 10B	Bk 10B	Bk 10B	Bk 10B	Bk 10B	Bk 17	Bk 17
analysis	14	15	19	24	25	26	27	32	33	14	15
date	27.11.93	27.11.93	19.10.93b	19.10.93b	27.11.93	27.11.93	27.11.93	27.11.93	27.11.93	25.7.94	25.7.94
position	grt	grt	grt	grt	grt	grt	grt	grt	grt	?	?
SiO2	24,91	25,25	25,47	24,92	25,22	24,64	24,77	24,79	25,30	26,73	25,84
TiO2	0,04	0,01	0,02	0,03	0,08	0,07	0,11	0,05	0,10	0,06	0,05
Al2O3	19,88	19,90	18,95	19,31	20,13	20,25	19,50	20,28	20,04	19,91	19,84
Cr2O3	0,01	0,00	0,04	0,04	0,00	0,01	0,02	0,03	0,03	0,01	0,04
Fe2O3	6,16	6,07	5,69	6,00	5,68	6,06	5,76	5,80	5,55	5,55	5,96
FeO	20,65	20,37	21,73	21,16	21,39	21,59	22,19	21,59	21,06	18,13	18,01
MnO	0,18	0,23	0,21	0,25	0,18	0,24	0,22	0,22	0,19	0,19	0,37
MgO	15,25	15,51	14,74	14,90	14,15	14,06	13,70	13,70	14,21	17,32	17,20
H2O	11,32	11,38	11,24	11,22	11,28	11,24	11,13	11,20	11,26	11,66	11,53
total	98,40	98,72	98,10	97,83	98,11	98,16	97,39	97,66	97,75	99,56	98,85
normed on 28 oxygens, Fe3=Al(t)-Al(o)-Cr-2*Ti											
Si	5,278	5,320	5,433	5,328	5,362	5,257	5,341	5,309	5,390	5,497	5,374
Al t	2,722	2,680	2,567	2,672	2,638	2,743	2,659	2,691	2,610	2,503	2,626
	8,000	8,000	8,000	8,000	8,000	8,000	8,000	8,000	8,000	8,000	8,000
Alo	2,243	2,262	2,197	2,194	2,407	2,348	2,296	2,427	2,421	2,322	2,238
Cr	0,002	0,000	0,007	0,007	0,000	0,002	0,003	0,005	0,005	0,002	0,007
Ti	0,006	0,002	0,003	0,005	0,013	0,011	0,018	0,008	0,016	0,009	0,008
Fe3+	0,982	0,962	0,914	0,966	0,909	0,973	0,935	0,935	0,890	0,858	0,934
Fe2	3,659	3,589	3,876	3,783	3,803	3,852	4,000	3,866	3,753	3,118	3,133
Mg	4,816	4,871	4,686	4,748	4,484	4,471	4,403	4,373	4,512	5,309	5,332
Mn	0,032	0,041	0,038	0,045	0,032	0,043	0,040	0,040	0,034	0,033	0,065
	11,741	11,727	11,721	11,748	11,648	11,699	11,695	11,654	11,631	11,651	11,716
	19,741	19,727	19,721	19,748	19,648	19,699	19,695	19,654	19,631	19,651	19,716
OH	16	16	16	16	16	16	16	16	16	16	16
Mg/(Mg+Fe2)	0,568	0,576	0,547	0,557	0,541	0,537	0,524	0,531	0,546	0,630	0,630

position: grt is chlorite at garnet, pg is chlorite at paragonite, v is chlorite in vein, ? is chlorite at undetermined textural position

sample	Bk 17	Bk 17	Bk 17	Bk 17	Bk 17	Bk 17	Bk 17	Bk 17	Bk 17	Bk 17	Bk 17
analysis	16	17	18	19	20	21	22	23	24	25	26
date	25.7.94	25.7.94	25.7.94	25.7.94	25.7.94	25.7.94	25.7.94	25.7.94	25.7.94	25.7.94	25.7.94
position	?	?	?	?	?	?	?	?	?	v	v
SiO2	25,60	25,36	25,03	25,39	25,75	25,68	25,90	25,63	25,48	26,51	26,33
TiO2	0,06	0,07	0,08	0,09	0,10	0,07	0,05	0,06	0,07	0,05	0,12
Al2O3	19,96	20,40	19,77	20,64	20,00	20,44	19,72	20,33	20,03	19,13	19,25
Cr2O3	0,07	0,04	0,03	0,10	0,06	0,03	0,07	0,07	0,05	0,14	0,13
Fe2O3	5,77	6,05	5,98	6,13	5,96	5,80	5,77	6,13	6,01	5,51	5,57
FeO	18,05	18,06	19,29	17,81	18,32	17,78	18,17	18,61	18,52	17,19	17,88
MnO	0,41	0,30	0,46	0,32	0,41	0,37	0,28	0,31	0,45	0,32	0,35
MgO	16,49	16,63	15,70	16,82	16,86	16,59	16,91	16,75	16,51	17,83	17,34
H2O	11,41	11,47	11,29	11,54	11,53	11,49	11,48	11,57	11,46	11,52	11,51
total	97,83	98,38	97,63	98,84	98,99	98,25	98,36	99,46	98,58	98,21	98,48
normed on 28 oxygens, Fe3=Al(t)-Al(o)-Cr-2*Ti											
Si	5,381	5,303	5,316	5,278	5,357	5,362	5,413	5,313	5,332	5,518	5,485
Al t	2,619	2,697	2,684	2,722	2,643	2,638	2,587	2,687	2,668	2,482	2,515
	8,000	8,000	8,000	8,000	8,000	8,000	8,000	8,000	8,000	8,000	8,000
Alo	2,326	2,330	2,265	2,336	2,260	2,392	2,270	2,279	2,272	2,210	2,212
Cr	0,012	0,007	0,005	0,016	0,010	0,005	0,012	0,011	0,008	0,023	0,021
Ti	0,009	0,011	0,013	0,014	0,016	0,011	0,008	0,009	0,011	0,008	0,019
Fe3+	0,913	0,952	0,955	0,959	0,933	0,912	0,908	0,956	0,946	0,864	0,873
Fe2	3,174	3,158	3,426	3,097	3,186	3,104	3,176	3,226	3,242	2,992	3,115
Mg	5,167	5,183	4,970	5,212	5,228	5,163	5,267	5,175	5,150	5,531	5,384
Mn	0,073	0,053	0,083	0,056	0,072	0,065	0,050	0,054	0,080	0,056	0,062
	11,674	11,693	11,717	11,691	11,705	11,653	11,691	11,711	11,709	11,685	11,686
	19,674	19,693	19,717	19,691	19,705	19,653	19,691	19,711	19,709	19,685	19,686
OH	16	16	16	16	16	16	16	16	16	16	16
Mg/(Mg+Fe2)	0,619	0,621	0,592	0,627	0,621	0,625	0,624	0,616	0,614	0,649	0,633

---

sample	Bk 17	Bk 17	Bk 17	Bk 17	Bk 17	Bk 17	Bk 17	Bk 17	Bk 17	Bk 18	Bk 18
analysis	30	31	33	34	35	36	37	70	71	20	21
date	9.7.94	9.7.94	9.7.94	9.7.94	9.7.94	9.7.94	9.7.94	4.7.94	4.7.94	6.8.94	6.8.94
position	?	?	?	?	?	?	?	v	v	?	?
SiO2	25,87	25,89	25,76	26,32	26,07	26,13	26,31	25,91	25,96	25,15	25,58
TiO2	0,06	0,08	0,07	0,02	0,09	0,05	0,04	0,11	0,01	0,00	0,02
Al2O3	19,70	19,68	19,93	19,91	19,67	20,06	19,72	19,13	18,98	21,36	20,52
Cr2O3	0,00	0,00	0,00	0,00	0,00	0,00	0,00	0,15	0,11	0,00	0,00
Fe2O3	5,75	5,79	5,84	5,58	5,71	5,94	5,74	5,93	5,67	5,99	5,77
FeO	18,00	17,71	18,18	17,42	17,06	17,04	16,96	17,26	16,19	15,41	16,47
MnO	0,32	0,36	0,30	0,33	0,30	0,33	0,25	0,32	0,29	0,09	0,10
MgO	16,95	17,22	16,82	17,26	17,66	17,92	17,97	18,02	18,21	17,40	17,25
H2O	11,46	11,48	11,48	11,54	11,51	11,63	11,58	11,50	11,39	11,46	11,44
total	98,10	98,21	98,38	98,38	98,07	99,10	98,57	98,33	96,81	96,86	97,15
normed on 28 oxygens, Fe3=Al(t)-Al(o)-Cr-2*Ti											
Si	5,416	5,409	5,383	5,470	5,434	5,390	5,449	5,404	5,467	5,266	5,363
Al t	2,584	2,591	2,617	2,530	2,566	2,610	2,551	2,596	2,533	2,734	2,637
	8,000	8,000	8,000	8,000	8,000	8,000	8,000	8,000	8,000	8,000	8,000
Alo	2,278	2,256	2,292	2,346	2,265	2,266	2,262	2,107	2,179	2,537	2,434
Cr	0,000	0,000	0,000	0,000	0,000	0,000	0,000	0,025	0,018	0,000	0,000
Ti	0,009	0,013	0,011	0,003	0,014	0,008	0,006	0,017	0,002	0,000	0,003
Fe3+	0,906	0,911	0,919	0,872	0,896	0,922	0,894	0,931	0,899	0,944	0,911
Fe2	3,151	3,094	3,178	3,028	2,973	2,940	2,937	3,011	2,851	2,698	2,887
Mg	5,290	5,363	5,239	5,346	5,486	5,509	5,547	5,602	5,716	5,431	5,391
Mn	0,057	0,064	0,053	0,058	0,053	0,058	0,044	0,057	0,052	0,016	0,018
	11,691	11,699	11,692	11,653	11,688	11,703	11,691	11,749	11,717	11,626	11,643
	19,691	19,699	19,692	19,653	19,688	19,703	19,691	19,749	19,717	19,626	19,643
OH	16	16	16	16	16	16	16	16	16	16	16
Mg/(Mg+Fe2)	0,627	0,634	0,622	0,638	0,649	0,652	0,654	0,650	0,667	0,668	0,651

position: grt is chlorite at garnet, pg is chlorite at paragonite, v is chlorite in vein, ? is chlorite at undetermined textural position

sample	Bk 18	Bk 18	Bk 18	Bk 18	Bk 18	Bk 18	Bk 18	Bk 18	Bk 18	Bk 9	Bk 9
analysis	22	25	26	27	29	30	63	64	65	9	10
date	6.8.94	5.8.94	5.8.94	5.8.94	5.8.94	5.8.94	25.7.94	25.7.94	25.7.94	4.3.94	4.3.94
position	?	grt	grt	grt	pg	pg	?	?	?	?	?
SiO2	25,13	25,49	25,44	25,48	26,25	26,21	26,15	25,18	25,89	26,20	27,48
TiO2	0,01	0,07	0,07	0,06	0,00	0,00	0,03	0,09	0,10	0,06	0,16
Al2O3	21,12	20,60	20,04	19,88	21,45	21,27	20,17	21,24	21,17	20,15	20,22
Cr2O3	0,00	0,03	0,01	0,01	0,03	0,09	0,01	0,01	0,04	0,00	0,00
Fe2O3	5,98	5,73	5,62	5,81	6,05	5,98	5,80	5,87	5,88	5,78	4,96
FeO	16,36	21,67	21,00	21,62	12,34	12,07	15,71	15,77	16,21	16,28	15,97
MnO	0,13	0,34	0,38	0,33	0,25	0,22	0,22	0,21	0,25	0,09	0,14
MgO	16,93	14,01	14,39	14,55	20,20	20,27	18,41	17,06	17,54	18,21	18,14
H2O	11,43	11,42	11,32	11,38	11,82	11,77	11,59	11,43	11,65	11,61	11,74
total	97,09	99,36	98,27	99,12	98,39	97,88	98,09	96,86	98,73	98,37	98,82
normed on 28 oxygens, Fe3=Al(t)-Al(o)-Cr-2*Ti											
Si	5,275	5,354	5,392	5,372	5,329	5,342	5,411	5,282	5,332	5,415	5,614
Al t	2,725	2,646	2,608	2,628	2,671	2,658	2,589	2,718	2,668	2,585	2,386
	8,000	8,000	8,000	8,000	8,000	8,000	8,000	8,000	8,000	8,000	8,000
Alo	2,500	2,454	2,398	2,311	2,461	2,452	2,329	2,533	2,471	2,324	2,482
Cr	0,000	0,005	0,002	0,002	0,005	0,015	0,002	0,002	0,007	0,000	0,000
Ti	0,002	0,011	0,011	0,010	0,000	0,000	0,005	0,014	0,015	0,009	0,025
Fe3+	0,945	0,906	0,897	0,922	0,925	0,918	0,903	0,927	0,911	0,899	0,763
Fe2	2,872	3,807	3,723	3,811	2,095	2,057	2,718	2,766	2,793	2,814	2,729
Mg	5,297	4,386	4,546	4,572	6,112	6,158	5,678	5,334	5,384	5,610	5,523
Mn	0,023	0,060	0,068	0,059	0,043	0,038	0,039	0,037	0,044	0,016	0,024
	11,638	11,630	11,645	11,687	11,641	11,637	11,673	11,614	11,624	11,672	11,546
	19,638	19,630	19,645	19,687	19,641	19,637	19,673	19,614	19,624	19,672	19,546
OH	16	16	16	16	16	16	16	16	16	16	16
Mg/(Mg+Fe2)	0,648	0,535	0,550	0,545	0,745	0,750	0,676	0,659	0,658	0,666	0,669

---

sample	Bk 9	Bk 9	Bk 9	Bk 9	Bk 9	Bk 9	Bk 9	Bk 9	Bk 9	Bk 9	Bk 9
analysis	11	13	16	19	20	21	37	38	39	40	41
date	4.3.94	4.3.94	4.3.94	4.3.94	4.3.94	4.3.94	24.2.94	24.2.94	24.2.94	24.2.94	24.2.94
position	?	?	?	?	grt	grt	?	?	?	?	?
SiO2	27,63	26,59	25,31	27,26	24,61	25,59	26,10	26,13	25,60	25,82	25,31
TiO2	0,07	0,04	0,04	0,04	0,07	0,03	0,03	0,09	0,04	0,05	0,04
Al2O3	19,48	19,18	20,62	20,24	21,00	21,14	19,75	19,58	19,55	19,97	19,93
Cr2O3	0,03	0,00	0,00	0,04	0,05	0,04	0,05	0,09	0,10	0,02	0,03
Fe2O3	5,49	5,37	5,83	5,38	5,90	5,89	5,53	5,25	5,59	5,80	5,84
FeO	15,77	16,17	14,37	16,86	17,97	17,51	18,22	18,44	17,87	15,16	14,10
MnO	0,15	0,18	0,14	0,18	0,17	0,19	0,19	0,23	0,18	0,14	0,11
MgO	19,69	18,31	18,21	18,06	15,41	16,54	16,66	16,12	16,55	18,54	18,73
H2O	11,88	11,49	11,39	11,79	11,25	11,54	11,45	11,37	11,31	11,48	11,34
total	100,19	97,33	95,92	99,85	96,43	98,47	97,99	97,30	96,79	96,98	95,43
normed on 28 oxygens, Fe3=Al(t)-Al(o)-Cr-2*Ti											
Si	5,578	5,549	5,329	5,545	5,248	5,317	5,466	5,514	5,430	5,394	5,355
Al t	2,422	2,451	2,671	2,455	2,752	2,683	2,534	2,486	2,570	2,606	2,645
	8,000	8,000	8,000	8,000	8,000	8,000	8,000	8,000	8,000	8,000	8,000
Alo	2,213	2,266	2,445	2,397	2,525	2,494	2,341	2,383	2,317	2,312	2,324
Cr	0,005	0,000	0,000	0,006	0,008	0,007	0,008	0,015	0,017	0,003	0,005
Ti	0,011	0,006	0,006	0,006	0,011	0,005	0,005	0,014	0,006	0,008	0,006
Fe3+	0,834	0,844	0,924	0,823	0,946	0,921	0,872	0,834	0,892	0,912	0,930
Fe2	2,662	2,821	2,530	2,869	3,205	3,042	3,191	3,255	3,170	2,649	2,495
Mg	5,925	5,695	5,714	5,476	4,898	5,123	5,201	5,070	5,232	5,773	5,906
Mn	0,026	0,032	0,025	0,031	0,031	0,033	0,034	0,041	0,032	0,025	0,020
	11,675	11,664	11,645	11,608	11,625	11,625	11,651	11,613	11,666	11,682	11,687
	19,675	19,664	19,645	19,608	19,625	19,625	19,651	19,613	19,666	19,682	19,687
OH	16	16	16	16	16	16	16	16	16	16	16
Mg/(Mg+Fe2)	0,690	0,669	0,693	0,656	0,604	0,627	0,620	0,609	0,623	0,685	0,703

position: grt is chlorite at garnet, pg is chlorite at paragonite, v is chlorite in vein, ? is chlorite at undetermined textural position

sample	Bk 9	Bk 9	Bk 9	Bk 9	Bk 9	Bk 9	Bk 9	Bk 9	Bk 9	Bk 9	Bk 9
analysis	42	43	44	49	50	53	53	54	54	57	58
date	24.2.94	24.2.94	24.2.94	24.2.94	24.2.94	24.2.94	23.2.94	23.2.94	24.2.94	24.2.94	24.2.94
position	?	?	?	pg	pg	pg	pg	pg	pg	pg	pg
SiO2	25,97	25,39	25,71	26,04	26,24	26,21	26,21	26,15	25,76	25,78	25,22
TiO2	0,04	0,05	0,06	0,04	0,05	0,03	0,00	0,03	0,05	0,01	0,04
Al2O3	20,35	20,01	19,18	21,24	20,98	20,52	20,80	21,24	21,50	21,27	20,90
Cr2O3	0,01	0,01	0,03	0,03	0,06	0,08	0,04	0,02	0,04	0,00	0,11
Fe2O3	5,80	5,84	5,43	5,91	5,57	5,82	5,78	6,09	6,04	5,98	6,00
FeO	14,39	17,42	18,31	12,42	12,47	12,11	11,27	10,64	12,18	11,48	11,30
MnO	0,11	0,19	0,20	0,22	0,14	0,12	0,13	0,11	0,17	0,15	0,15
MgO	18,95	16,87	16,32	19,82	19,53	20,39	20,63	21,34	19,82	20,23	19,98
H2O	11,56	11,37	11,26	11,69	11,62	11,65	11,65	11,79	11,68	11,63	11,45
total	97,18	97,15	96,49	97,41	96,66	96,94	96,51	97,41	97,23	96,53	95,16
normed on 28 oxygens, Fe3=Al(t)-Al(o)-Cr-2*Ti											
Si	5,390	5,357	5,479	5,341	5,416	5,395	5,394	5,321	5,290	5,315	5,281
Al t	2,610	2,643	2,521	2,659	2,584	2,605	2,606	2,679	2,710	2,685	2,719
	8,000	8,000	8,000	8,000	8,000	8,000	8,000	8,000	8,000	8,000	8,000
Alo	2,368	2,333	2,297	2,476	2,519	2,373	2,440	2,416	2,495	2,484	2,439
Cr	0,002	0,002	0,005	0,005	0,010	0,013	0,007	0,003	0,006	0,000	0,018
Ti	0,006	0,008	0,010	0,006	0,008	0,005	0,000	0,005	0,008	0,002	0,006
Fe3+	0,906	0,927	0,870	0,912	0,865	0,902	0,895	0,933	0,933	0,927	0,946
Fe2	2,498	3,074	3,263	2,130	2,152	2,085	1,940	1,810	2,092	1,980	1,979
Mg	5,862	5,305	5,184	6,060	6,008	6,256	6,329	6,473	6,067	6,217	6,236
Mn	0,019	0,034	0,036	0,038	0,024	0,021	0,023	0,019	0,030	0,026	0,027
	11,661	11,683	11,665	11,627	11,587	11,654	11,632	11,659	11,630	11,635	11,651
	19,661	19,683	19,665	19,627	19,587	19,654	19,632	19,659	19,630	19,635	19,651
OH	16	16	16	16	16	16	16	16	16	16	16
Mg/(Mg+Fe2)	0,701	0,633	0,614	0,740	0,736	0,750	0,765	0,781	0,744	0,758	0,759

---

sample	Bk 9	Bk 9	Bk 9	Bk 9	Bk 9	Bk 9	Bk 9	Bk 9
analysis	59	60	61	62	63	64	65	66
date	24.2.94	24.2.94	24.2.94	24.2.94	24.2.94	24.2.94	24.2.94	24.2.94
position	pg	pg	pg	pg	pg	pg	pg	pg
SiO2	25,76	26,31	26,18	25,77	27,01	26,62	26,08	26,12
TiO2	0,07	0,11	0,02	0,06	0,09	0,05	0,04	0,09
Al2O3	21,66	21,27	20,77	21,45	19,67	19,97	20,95	22,04
Cr2O3	0,05	0,10	0,06	0,03	0,12	0,13	0,08	0,07
Fe2O3	5,98	6,05	5,76	5,96	5,27	5,53	6,04	6,12
FeO	11,12	10,89	11,66	10,87	11,31	11,08	10,76	10,23
MnO	0,15	0,10	0,13	0,08	0,09	0,11	0,12	0,08
MgO	20,26	21,30	20,37	20,50	21,06	21,10	21,23	21,25
H2O	11,68	11,85	11,64	11,65	11,65	11,64	11,73	11,88
total	96,73	97,97	96,60	96,37	96,26	96,22	97,03	97,88
normed on 28 oxygens, Fe3=Al(t)-Al(o)-Cr-2*Ti								
Si	5,290	5,328	5,393	5,305	5,563	5,488	5,333	5,276
Al t	2,710	2,672	2,607	2,695	2,437	2,512	2,667	2,724
	8,000	8,000	8,000	8,000	8,000	8,000	8,000	8,000
Alo	2,532	2,404	2,437	2,509	2,338	2,340	2,383	2,522
Cr	0,008	0,016	0,010	0,005	0,020	0,021	0,013	0,011
Ti	0,011	0,017	0,003	0,009	0,014	0,008	0,006	0,014
Fe3+	0,924	0,922	0,893	0,923	0,816	0,857	0,930	0,931
Fe2	1,909	1,844	2,010	1,871	1,949	1,910	1,841	1,728
Mg	6,201	6,429	6,255	6,290	6,465	6,484	6,471	6,397
Mn	0,026	0,017	0,023	0,014	0,016	0,019	0,021	0,014
	11,612	11,648	11,630	11,620	11,617	11,639	11,664	11,616
	19,612	19,648	19,630	19,620	19,617	19,639	19,664	19,616
OH	16	16	16	16	16	16	16	16
Mg/(Mg+Fe2)	0,765	0,777	0,757	0,771	0,768	0,772	0,779	0,787

position: grt is chlorite at garnet, pg is chlorite at paragonite, v is chlorite in vein, ? is chlorite at undetermined textural position

sample	Bk 17	Bk 17	Bk 17	Bk 17	Bk 17	Bk 17	Bk 17	Bk 17	Bk 17	Bk 17	Bk 17
analysis	48	50	1	2	3	4	5	6	7	8	28
date	2.7.94	2.7.94	25.7.94	25.7.94	25.7.94	25.7.94	25.7.94	25.7.94	25.7.94	25.7.94	9.7.94
position	grt	grt	grt	grt	grt	grt	grt	grt	grt	grt	grt
SiO2	37,40	37,85	37,14	37,75	37,67	37,42	37,67	37,83	37,81	37,56	36,86
Al2O3	24,63	25,29	23,81	24,96	24,78	24,76	24,34	25,27	26,17	24,70	24,12
Fe2O3	11,15	10,31	13,20	11,60	11,92	11,55	12,31	11,28	10,18	11,89	11,69
CaO	23,48	23,40	23,18	23,31	23,40	23,56	23,49	23,30	23,70	23,32	23,09
H2O	1,87	1,88	1,87	1,89	1,89	1,88	1,89	1,89	1,91	1,89	1,85
total	96,66	96,85	97,33	97,62	97,77	97,29	97,81	97,68	97,86	97,47	95,76
normed on 8 cations,all Fe assumed Fe3											
Si	2,993	3,013	2,972	2,994	2,986	2,978	2,990	2,994	2,974	2,987	2,984
Al	2,323	2,373	2,246	2,333	2,315	2,322	2,277	2,358	2,426	2,315	2,301
Fe3	0,671	0,618	0,795	0,692	0,711	0,691	0,735	0,672	0,603	0,712	0,712
	2,994	2,991	3,041	3,025	3,026	3,014	3,012	3,029	3,029	3,026	3,013
Ca	2,013	1,996	1,987	1,981	1,987	2,009	1,998	1,976	1,997	1,987	2,003
OH	1	1	1	1	1	1	1	1	1	1	1
X Al2Fe	0,68	0,62	0,76	0,68	0,69	0,68	0,73	0,65	0,59	0,69	0,70

sample	Bk 17	Bk 18	Bk 18	Bk 18	Bk 18	Bk 18	Bk 18	Bk 18	Bk 18	Bk 18
analysis	29	31	32	34	35	47	48	49	20	21
date	9.7.94	25.7.94	25.7.94	25.7.94	25.7.94	25.7.94	25.7.94	25.7.94	5.8.94	5.8.94
position	grt	vein	vein	vein	vein	vein	vein	vein	grt	grt
SiO2	37,48	38,04	38,04	37,48	36,90	37,62	38,02	37,74	37,35	37,56
Al2O3	23,34	26,48	26,50	26,81	25,44	25,82	25,93	25,79	24,40	23,68
Fe2O3	13,08	9,15	9,01	9,06	9,78	10,01	9,57	9,71	12,20	13,07
CaO	22,99	23,16	23,25	23,04	22,77	23,17	23,36	23,22	23,38	23,34
H2O	1,86	1,89	1,89	1,88	1,85	1,88	1,89	1,88	1,88	1,88
total	96,89	96,83	96,80	96,39	94,89	96,62	96,88	96,46	97,33	97,65
normed on 8 cations,all Fe assumed Fe3										
Si	3,015	3,015	3,014	2,981	2,993	2,997	3,017	3,009	2,978	2,995
Al	2,213	2,473	2,475	2,513	2,432	2,425	2,425	2,424	2,293	2,226
Fe3	0,792	0,545	0,537	0,542	0,597	0,600	0,571	0,583	0,732	0,784
	3,004	3,019	3,012	3,055	3,029	3,025	2,997	3,007	3,025	3,010
Ca	1,981	1,967	1,974	1,963	1,979	1,978	1,986	1,984	1,997	1,994
OH	1	1	1	1	1	1	1	1	1	1
X Al2Fe	0,79	0,54	0,53	0,51	0,58	0,59	0,57	0,58	0,71	0,78

position: grt is epidote in a chlorite, albite, epidote aggregate after garnet, vein is epidote in a vein